MINISTRY OF EDUCATION AND SCIENCE OF UKRAINE

NATIONAL TECHNICAL UNIVERSITY OF UKRAINE
"IGOR SIKORSKY KYIV POLYTECHNIC INSTITUTE"

Y. Poplavko, S. Voronov, Y. Yakymenko

FUNCTIONAL DIELECTRICS IN-DEPTH STUDY

Recommended by the Academic Council of the National Technical University of Ukraine "Igor Sikorsky KPI" as a textbook for bachelors / masters / doctors of philosophy in the educational program "Applied Physics" specialty 105 "Applied Physics and Nanomaterials"

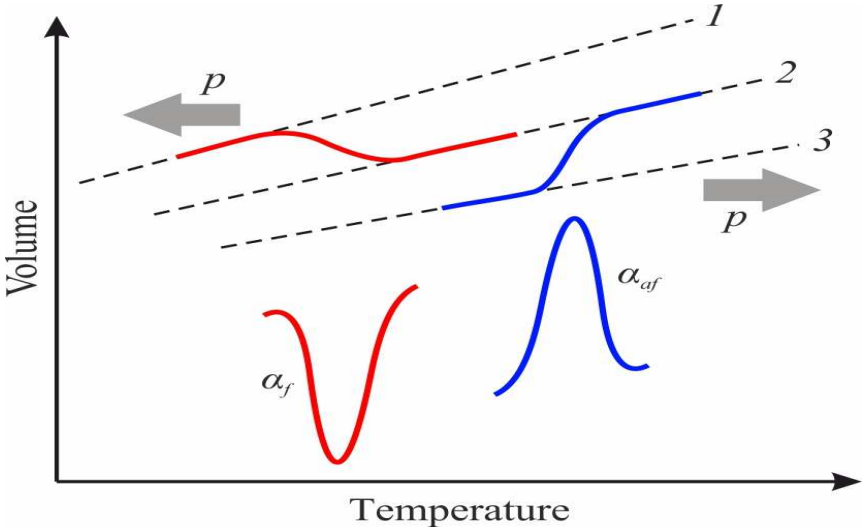

Kyiv
Igor Sikorsky KPI
2022

Reviewers:

O. Stronsky, Dr. Phys.-Math. Sciences, Professor,
Institute of Semiconductor Physics V.Y. Lashkareva
National Academy of Sciences of Ukraine;

V. Kotovsky, Dr. Technical Sciences, Professor,
Head of the Department of
General Physics and Solid State Physics
"Igor Sikorsky Kyiv Polytechnic Institute"

General Editor

S. Voronov, Dr. Technical Sciences, Professor,
Department of Applied Physics
"Igor Sikorsky Kyiv Polytechnic Institute"

The stamp was provided by the Methodical Council. Igor Sikorsky KPI
(protocol № 6 from 24.06.2022)
at the request of the Academic Council of the Educational and Scientific
Physical and Technical Institute
(protocol № 7 of 20.06.2022)

Educational edition

Y. Poplavko, Dr. Phys.-Mat. Sciences, Prof.,
S. Voronov, Dr. Tech. Sciences, Prof.,
Y. Yakymenko, Dr. Tech. Sciences, Prof., Academician of the National Academy of Sciences of Ukraine

FUNCTIONAL DIELECTRICS IN-DEPTH STUDY

Functional dielectrics in-depth study [Text]: textbook for students of specialty 105 "Applied Physics and Nanomaterials" / Y. Poplavko, S.Voronov, Y. Yakymenko."Igor Sikorsky KPI". – K.: "Igor Sikorsky KPI", 2022. – 304 p.

Abstract. The textbook discusses new developments, some methods for calculating parameters and practical application of functional dielectrics. Modern theoretical concepts, new experimental data main specifications of basic materials are considered. Provides basic data on the history of electronics, as well as the basic information about the materials used in electronics is given. The focus is on explaining the physical mechanisms of many effects used in modern electronics. The textbook is based on the authors' many years of experience in teaching physical materials science, intended for the students of higher educational institutions with specializations in the fields of "Applied Physics" and "Microelectronics and nanoelectronics". The book can also be used by the graduate students, engineers and researchers specializing in the materials science.

CONTENTS

Key features:

(1) Provides undergraduate and graduate students with new understanding of functional dielectrics theory and practical applications.

(2) Takes simplified mathematical approach to theories, discussing new effects and summarizes at the end of each chapters.

(3) Teaches practical training on the explaining and predicting new effects.

PREFACE

The purpose of this book is to introduce the undergraduate and graduate students to one field of modern materials science. For this purpose, the authors use the latest research in the field of functional dielectrics, partly those which are published in 2019 - 2921 and partly already accepted for publication but not yet published.

Since the book is a textbook intended to distinguish between established scientific phenomena and only developing scientific ideas, in almost every chapter, known data on the subject under consideration are preliminarily (in small print), and only then new ideas and facts are presented.

For the same purpose, the first two Chapters are devoted to the history of electronics as a scientific and technical direction, as wellas the main provisions of physical materials science, which give the student an introduction to this specialty. In order to deepen the cognitive process and instill practical skills in students, the last Chapter will include in detail examples of the study of one of new and promising phenomena for application. Thus, geven training course might be a key reference in the application of physics for advanced fundamental understanding of physical mechanisms in micro- and nanomaterials and their applications in electronics.

Recommendation for using the book

All Chapters *o*f this book are proposed for in-depth study of this subject, which primarily complement the official course published in the textbooks:

- Yu.M. Poplavko, Yu.I. Yakymenko. Functional dielectrics for electronics. Fundamentals of conversion properties. 2020, 294 pages. Edited by ELSEVIER, USA.
- Yu. M. Poplavko. Electronic materials. Principles and applied science. 2019, 683 pages. Edited by ELSEVIER, USA.
- Yu. M. Poplavko. Dielectric spectroscopy of electronic materials. Applied physics of dielectrics. 2021, 400 pages. Edited by ELSEVIER, USA.

The following selected chapters do not repeat, but complement the in-depth study of the physics of dielectrics.

1. Given chapters are not optional for all students: each student must study and complete a written review of several pages of only one of the chapters as an independent study and as a practical assignment.

2. Since the main emphasis is on new ideas and research results, each Chapter begins with short traditional description of description of a particular phenomenon, which can be consulted beforehand (these paragraphs are in small print)

3. The presented materials are new and modern, mostly not yet published, and each of the chapters can then serve as the basis not only for a bachelor's degree, but also a master's and even PhD dissertation (of course, with a more detailed elaboration with the original contribution of a dissertation candidate).

4. For students who are especially interested in science, it is advisable to read and think over two first Chapters, next five Chapters devoted to modern physics and last Chapter where training is given in practical calculations based on thermodynamics.

Рекомендації щодо користування книгою

Наступні вибрані глави не повторюють, а доповнюють поглиблене вивчення фізики функціональних діелектриків.

1. Наведені розділи не є обов’язковими для всіх студентів: кожен студент повинен вивчити та виконати письмовий рецензування кількох сторінок лише одного з розділів як самостійне дослідження та як практичне завдання.

2. Оскільки основний акцент робиться на нових ідеях та результатах дослідження, кожен розділ починається з короткого традиційного опису певного явища, з яким можна ознайомитися заздалегідь (ці абзаци написані дрібним шрифтом).

3. Представлені матеріали нові й сучасні, здебільшого ще не опубліковані, і кожен із розділів потім може послужити основою не лише для отримання ступеня бакалавра, а й для магістерської та навіть кандидатської дисертації (звісно, з більш детальною розробкою з оригінальним внеском кандидата дисертації).

4. Студентам, які особливо цікавляться природознавством, доцільно прочитати і подумати над двома першими розділами, наступними п'ятьма розділами, присвяченими сучасній фізиці, та останнім розділом, де дається навчання практичним розрахункам на основі термодинаміки. Всі розділи цієї книги пропонуються для поглибленого вивчення цього предмету, які в першу чергу доповнюють офіційний курс, опублікований у трьох англомовних підручниках.

INTRODUCTION

Modern education of students in the Technical university puts forward the requirement to teach not only characteristics of the profession but also the ability to work with scientific and technical literature, which is presented now mainly in English. Our practice shows that only a part of students are able to use technical English at their end in technical university study.

The contents of this book takes into account a rapid progress in the field of material sciences to reflect latest achievements. Below is a list of the modern advances in electronic materials science, presented in this book, that have not previously been described in the educational literature.

Chapter 1. Main stages of electronics development. In the development of the scientific and technical direction of electronics, four main stages are distinguished: vacuum tubes, semiconductors, microelectronics and nanoelectronics (future development of molectronics is also planned), Electronics technology use quite different materials: crystals, polycrystals (ceramics), glasses, composites, amorphous substances, liquid crystals and substances produced by the compaction of nano-crystalline structures. At the same time, at different stages of the development of this scientific and technical direction, the preference was given to different materials. The chapter is brief overview of development of electronics, indicating the predominantly used materials at different stages of electronics progress.

Chapter 2. Some physical aspects of electronic materials. For a more conscious study of the basics of materials science, it is advisable to dwell on the most important concepts and stages of epy development of physical science, which have become decisive for the creation of modern microelectronics and nanoelectronics. The study of the physical foundations of electronic material science is based on the main provisions of quantum mechanics, associated, for example, with discreteness of radiation and absorption of light, with the photoelectric effect, with the particle-wave dualism, with the uncertainty relation. The structure of the atom and atomic spectra are also important question as well as Pauli principle, structure of electronic shells and valence of atoms, the arrangement of atoms of chemical elements in periodic system of Mendeleev. Condensed Matter Physics, i.e., Solid State Physics and nanophysics use the knowledge gained in the previous sections of physics. Therefore, before getting acquainted with the physical effects that find

application in the microelectronics and nanoelectronics, it is necessary to pay some attention to comparing the basic concepts of classical mechanics about the structure of matter with a quantum mechanical approach to this issue.

Chapter 3. Electrical polarization and conductance relationship. It is shown that the conductivity arising instead of delayed polarization is not adequate to a classical understanding of this parameter and can only be considered only as the effective conductivity. In dielectrics and wide-gap semiconductors, the relaxation and resonant dispersion models (both leading to the appearance of effective conductivity) are considered separately. But in conductors, frequency dispersion of conductivity are observed as the relaxation and resonance phenomena simultaneously. It resulting in the negative effective permittivity that is obviously not adequate to usual understanding of this parameter and should be considered as effective ones. In some polar crystals, their electrical conductivity can change in thousands of times even with small change in temperature or under electrical or magnetic fields action. Appropriate materials are widely used as highly sensitive thermistors with positive or negative temperature coefficient, in the non-linear and field-controllable switching elements and in very susceptive sensors. It is argued that main reason for such properties is a finely balanced ionic-covalent polar inter-atomic bonding, arising due to difference in the electronegativity of neighboring ions. Complicated spatial distribution of internal polarity in the polar-neutral crystals explains the entanglement of charge carriers in the electrically alternating structure that contributes to formation of little mobile polarons and low electrical conductivity. In this case, the quasi-one-dimensional polar structure, which, in particular, can be induced by applied electrical field, has much lower resistance to the electrons transport as compared to complex multidimensional arrangement of polar bonds, which contribute to high electrical resistance by polarons formation. The alteration in the polar structure under external factors influence can lead to a large change in conductivity that is used in electronics.

Chapter 4. Polar-sensitive structures of non-centro symmetric crystals. To explain the unique properties of polar crystals, it is not necessary use the hypothesis of spontaneous polarization, which would have to be accompanied by some kind of "internal" electrical field, the existence of which is difficult to explain for thermodynamically equilibrium state of a crystal under conditions of inevitable presence of free charge carriers in it. The supposed reason of polar bonds existence in non-centrosymmetric crystal structures (as well as their formation) is the structural compensation of electronic states features of the ions making up polar structure, in particular, the difference in their electronegativity. Polar crystals are

characterized by finely balanced structure of their interatomic bonds, which makes these crystals highly sensitive to external influences. The mixed ionic-covalent polar-sensitive bonds is a main reason to generate electrical response of polar crystal onto non-electrical influences (thermal, mechanical, optical, etc.). That is why, exactly the uniform change in temperature is used here to determine experimentally the magnitude of own polarity; at that, in case of polar-neutral (piezoelectric) crystals, the method of partial limitation of thermal strain in the polar cut of crystal is applied.

Chapter 5. High-permittivity microwave dielectrics. Thermodynamic problem is considered regarding the mechanisms leading to the positive or negative value of temperature coefficient of permittivity. It is shown also that dielectric losses in the microwave dielectrics are due to the polar phase presence as in base material so in grain boundaries of ceramics. To improve properties of microwave high-permittivity dielectrics, three points are stated. First, high permittivity at microwaves can be obtained only in the crystals, possessing low frequency transverse optical lattice mode; as a rule, in the paraelectric-like materials. Second, small dielectric losses can be achived only in the monophase compositions based on "hard" paraelectric materials, in structure of which any internal polarity is absent for natural reasons. Third, thermal non-stability of the basic materials (oxigen-octahedral structures) can be suppressed by the imbedded between octahedrons foreign ions, including the paramagnetic components.

Chapter 6. Microwave absorption in shielding coatings. In order to select the optimal materials for microwave absorbing composites, various mechanisms of EM waves absorption in the main solid materials (fillers in composite) are considered. In the dielectrics possessing by electronic polarization only, any absorption is practically absent, but such polymers usually are good as the matrixes of composites. Metallic elements in the form of micro- and nano-particles have quite different properties than bulk metals, but can provide high microwave absorption. From dielectrics possessing ionic polarization, only ferroelectrics have big microwave absorption, increasing with frequency rise, that serves as benefit for shorter wavelength absorbers. Magnetic fillers can not provide in composite big permeability, yet they reducing microwaves reflection of from composite. Composite materials usually consist of two or more different substances with the interfaces between components. The constant interest in these materials is related to the fact that they represent a certain class of *artificial materials*, the properties of which can be deliberately set and vary within a very wide range by changing the matrix and filler materials, as well as by concentration and shape of inclusions. In

particular, by varying different components, it is possible to obtain a material with predetermined conductivity – from good dielectric to good conductor. The greatest heterogeneity of electrical properties can be created exactly when dielectric and conductor are mixed.

Chapter 7. Thermal diffusion and thermal deformation of polar crystals. In ferroelectrics, as well as in other dielectrics, in process of heat transfer the phonon mechanism dominates, at which the speed of short-wavelength longitudinal acoustic waves ("thermal phonons") is small as compared to long-wavelength "sound phonons". It is stated that in the case of polar crystals the phonon acoustic branch bends down while approaching to boundary of Brillouin zone. This effect is due to the acoustic-optical interaction, which reduces group velocity of phonons decreasing thermal conductivity. These effects are especially noticeable in the ferroelectrics near phase transitions, since in them the wavelength of thermal phonons becomes comparable with size of fluctuating polar clusters, whose activity, however, can be suppressed by the electrical field opening up the possibility of electrical control by heat flow. It has also been established that when studying heat transfer the thermal diffusion is a more sensitive factor than thermal conductivity. Indeed, in the ferroelectrics, phase transition point a sharp minimum of thermal diffusivity is found, which is due to the decrease in the wavelength of thermal phonons which are affected by polar bonds self-ordering increasing phonons scattering. On the contrary, in antiferroelectric phase transition, a sharp and big maximum of thermal diffusion is found, explained by the active participation of optical phonons in heat transfer in the vicinity of phase transition.

Chapter 8. Training in solving of applied problems. Practical skills in the calculations can be acquired by studying specific examples of the analysis and prediction of the properties of polar crystals. To this end, considering the thermodynamics of poezoelectrics and pyroelectrics and showing how on this basis it is possible to predict new effects on the example of quartz and gallium arsenide. A conception is discussed that any piezoelectric possesses an intra-crystalline polar moment, even though this crystal is not belongs to pyroelectric symmetry. In line with this assumption, an internal polarity of piezoelectric crystals is described by the different types of high-rank multiple moments. Octopole–sextuple–dipole moments correspond to three–two–one dimension arrangement of the intra-crystalline polarity. Dipole (1D) polarity is the pyroelectric spontaneous polarization that is a vector (first rank tensor). The 2D sextuple moment is arranged in a plane non-center symmetric configuration of three dipoles, and it is described by the second rank polar tensor. The octopole moment is the non-center symmetric spatial (3D) conformation

of four dipoles that is described by the third rank tensor. For technical application, it means that under the anisotropy of boundary conditions any high-gap $A^{III}B^{V}$ semiconductor-piezoelectric shows a behaviour of pyroelectric crystal. It is important that such a crystal might be used as far infrared sensor or as a volume-piezoeffect sensor integrated with amplifier in one $A^{III}B^{V}$ crystal. On the other hand, any device based on $A^{III}B^{V}$ semiconductor that has erroneous orientations of a crystal can generate polarization noises due to vibrations or thermal fluctuations.

CHAPTER 1. MAIN STAGES OF ELECTRONICS DEVELOPMENT

Contents

Electronics technology use quite different materials: crystals, polycrystals (ceramics), glasses, composites, amorphous substances, liquid crystals and substances produced by the compaction of nano-crystalline structures. At the same time, at different stages of the development of this scientific and technical direction, the preference was given to different materials. The following is a brief overview of the development of electronics, indicating the predominantly used materials at different stages of electronics progress.

Electronics is a branch of science and technology, in which the electronic phenomena in a matter are studied, and based on the results of these studies the ways for creating electronic devices, electronic circuits and systems are developed. Electronics can also be defined as the science of the interaction of electrons with electromagnetic fields in a material, as well as the methods of creating new materials and devices, in which this interaction is used to convert the electromagnetic energy for transmission, processing and store information. Theoretical problems of electronics are the study of electrons interaction both with the macroscopic fields in the working space of electronic device and with microscopic fields inside the crystal lattices, thin films, nano-particles and molecules. The practical tasks of electronics can be reduced to the development of different electronic devices, which perform various functions in the information conversion and transmission systems, in the controlling systems, in the computer technology, as well as in the power devices.

Currently electronics is one of the main sectors of the world economy. Moreover, the level of electronics development determines the type of modern civilization. The fact is that electronics is the basis of information technology, as well as the automation, telemechanics, computer technology, etc. Covering a wide

range of scientific, technical and industrial problems, electronics is based on the advances in various fields of knowledge, including the *physics of materials science.* At the same time, on the one hand, electronics poses challenges to other sciences and industry, stimulating their further development, and, on the other hand, equips them with qualitatively new technical means and research methods.

In the infinitely diverse fields of research and applications of electronics, the basic elements are the electronic amplifiers, converters and signal generators. The first electronic signal amplifier – the vacuum triode – was invented about a hundred years ago, and this date might be considered the beginning of electronics.

In its development, the electronics has gone through several stages:

- tube electronics;
- semiconductor electronics;
- ***microelectronics*** – integrated electronics;
- ***nanoelectronics*** –the modern, fourth stage of development of electronics;
- molecular electronics (?) – possible future direction.

Each of these types of electronics is originated in the depths of *physics, mathematics* and *chemistry*, while for the nanoelectronics and molecular electronics the advances in *biology* are also important.

It is difficult to pinpoint the date of the appearance of electronics, because many scientists and engineers were involved in the invention of different devices, the principle of which is based on the *control of the flow of electrons*. Undoubtedly, one of the most important discovery in this area was made by J.J. Thomson (Lord Kelvin), who used the vacuum tube to study so-called *cathode rays* and showed that these rays actually consist of negatively charged particles – electrons. More then hundred years ago, in 1906, for the discovery of electrons by J.J. Thomson received the Nobel Prize in Physics. However, it should be noted that this outstanding result was preceded by other inventions that contributed to the emergence of electronics. For example, in 1878, Crookes invented the early prototype of tube for "cathode rays"; in 1895 the *X*-rays created in such tubes, were designed to produce hard electromagnetic radiation. But *X*-ray tubes found practical application only after 1913 thanks to improvements made by Coolidge.

Of the many areas, in which electronics has developed, three should be noted: (1) the vacuum and semiconductor diodes; (2) the triodes and transistors; (3) the integrated circuits. The principle of operation of the vacuum diode was first patented by Edison, but suitable for practical applications vacuum diode was implemented by Fleming in 1904. The modern name of the diode appeared only in 1919: in Greek "di" means "two", and "ode" means "way". The most important for the birth of

electronics as scientific and technical direction can be considered the invention of the amplifying electronic device – a vacuum triode (De Forrest, 1906).

It is this invention could also be the basis of the "centenary of electronics".

1.1 First generation of electronics – vacuum tubes

It is based on the effect of emitting electrons from the heated cathode, and controlling the flow of these electrons in vacuum using the electrical field. Thermo-electronic emission was discovered by the American inventor Edison (1889) and studied by the English physicist Richardson (Nobel Prize in Physics, 1928). Based on this effect, an active circuit element was created – the radio lamp, which allows to rectify and amplify the electrical signal, as well as to generate electromagnetic oscillations. A radio lamp is the vacuum bulb (lamp) with two (cathode, anode) or a large number of electrodes. When heated, the cathode creates required concentration of electrons near its surface, and the field of a positively charged anode forms the anode current from these electrons. If a negative potential is applied to the anode, the anode current will be almost zero. Thus, the diode can serve as the AC rectifier.

Another electrode is added to the triode – a grid. With the help of an electrical potential applied to the grid it is possible to control the anode current, for example, to amplify it. This allows you to use the triode in electronic circuits as amplifier or signal generator. Therefore, the diode and triode are called *active* circuit elements. Resistor (electrical resistance), capacitor (capacitance), inductor are *passive* elements. The meaning of the term "triode" adopted for tube amplifier is obvious – it is a three-electrode device. Then the vacuum tetrode was invented (1926), then a pentode, and other, more complex, radio lamps were developed. The first electronic tubes designed to transmit and receive images (iconoscope and tube) were created in 1923 by Zvorykin. It is also interesting to note the relatively early invention of the first ultrahigh-frequency (microwave) vacuum generator – a magnetron (1921). Another type of microwave generator and amplifier – klystron – was invented only in 1938.

Materials. The development of electronics contributed to an in-depth study of the electrical and magnetic properties of materials – Solid state physics. Metals and alloys with the required emission, thermal and electrical properties were developed. Magnetic materials have been replenished with hundreds of ferrite grades with the required properties in various radio frequency ranges. Dielectric materials in the form of glasses, glass-ceramics, crystals, ceramics, polymers have been able to meet the needs of low and high power electronics.

Computer technology is the most important application of electronics. Before "electronic period" in computer technology, the mechanical devices were widely used: a calculator, arithmometers, etc. Mechanical engineering had low speed: for example, adding a unit to office accounts takes about a second. The speed of propagation of electromagnetic signals, which determines the speed limit of electronic computer systems, is at least tens of billions of times higher. It is obvious that speed of opearation is one of main reasons for need to switch from the mechanical computing devices to the electronic devices.

Electronic circuits of the first generation consisted of discrete (separate) *active* and *passive* circuit elements. Lamp discrete electronics were initially successfully used to create not very complex electronic circuits. However, demands of computer and military equipment in the 50s of XX century required the creation of very complex electronic systems, containing many tens of thousands of circuit elements. Problems arose before electronics: to increase the reliability of electronic systems many times over, significantly reduce their size, weight and energy consumption, as well as significantly reduce the cost of production of devices and to increase their performance.

Lamp electronics did not allow to radically solve any of these problems.

First, it was based on the use of only discrete elements made of different materials by the incompatible technologies. Under these conditions, it was impossible to significantly increase the productivity and reduce the cost of circuit elements.

Second, electronic circuits were assembled from many discrete elements by connecting them, for example, by the soldering conductors connecting individual elements. Interconnects were the most unreliable part of the scheme, and their creation could not be fully automated. So many connections were found in complex electronic systems that situation in electronics at the time was called the "tyranny of interconnections". It seemed impossible to increase significantly the reliability of complex electronic systems based on the tube electronics. For example, the first (1948) tubeless electronic computer (ENIAC, *Electronic Numerical Integrator and Computer*), with about 20.000 radio tubes and even more interconnections, could run for only a few hours. For comparison, modern integrated circuits containing up to a billion elements provide the computer with uninterrupted operation for a number of years.

Third, the principle of operation of radio lamps is such that it is almost impossible to significantly reduce their size, weight and energy consumption. Therefore, for example, the first ENIAC tube computer occupied an area of 200 m^2

and consumed about 200 kW of energy, although its capabilities were much inferior to modern personal computers. The described shortcoming of tube electronics did not allow, in particular, to create effective on-board electronic equipment, which was extremely necessary for military equipment.

Thus, by the fifties of the last century, the tube electronics has completely exhausted the ability to meet the demands of consumers of electronic equipment. But there was a fundamentally different electronics, based on the special properties of semiconductor structures.

1.2 Second generation of electronics – semiconductors

This stage of electronics is based on the semiconductor devices. The study of semiconductor structures began long ago by the German physicist Brown, who discovered in 1874 the effect of one-sided conductivity of metal-semiconductor contact. However, electrical characteristics of such structures were unstable, and, therefore, these structures could not be used to create electronic devices. Nevertheless, long studies performed by many scientists allowed until the middle of the XX century overcome this shortcoming. An outstanding step forward – to modern semiconductor electronics– was Bardin and Brattain's invention of the semiconductor transistor in 1947 (Nobel Prize in Physics, 1956). Like a triode, the transistor has 3 electrodes and can perform amplifying functions. In addition, the transistor can serve as electronic switch, and cascade of such switches is able to perform main logical functions. The modern design and theory of the transistor was developed by the USA physicist Shockley in 1951. The first transistors used crystalline germanium, only later it was found to use and after dominates the technology of more thermal stable *silicon*. Durable, small, do not require a vacuum glass bulb and are powered by low voltage, transistors have quickly replaced electronic lamps in most electronic circuits. It is interesting to note that for the first time the field-effect transistor as "electrical current control device" was patented by Lilienfeld in 1928. It proposed to use the Cu_2S semiconductor as a "working medium" and the Al_2O_3 dielectric as a "gate dielectric"; so for the first time in the past the modern terms "leak", "drain" and "shutter" were used. However, due to many technological difficulties, this invention has not found application. Only thirty years later, thanks to the use of modern silicon technology, it became possible to implement the proposed idea. Now such devices are called MDS transistors.

The semiconductor structure is the boundary between the regions of the semiconductor with special properties. If this boundary separates the layers of a

semiconductor with the hole and electronic type of electrical conductivity, it is called a *p-n* junction; the boundary of the layers of different compounds is called a hetero-junction. Structures including metal, dielectric and semiconductor layers are also used. In the MDS structure, the dielectric is usually a semiconductor oxide, such as silicon dioxide (SiO_2).

Materials. Although metals and dielectrics are also widely used in the semiconductor electronics, it is still based on the semiconductor materials. The basic principle of operation of the electronic devices, as noted above, is the electrical control of the flow of electrons (magnetic control is also used, but it is more inertial and technically more complex).

As is known, according to their electrical properties, that all materials are divided into metals, dielectrics and semiconductors. In metals, the mobility of electrons is high enough, but the electrical field in a metal is *screened* by the extremely high concentration of charge carriers. On the contrary, dielectrics could be defined as a substance, in which the electrical field (including control field) can exist, but the *mobility* of charge carriers in dielectrics is very low due to the polaron effect. It is in the semiconductors that electrons high mobility (necessary for controlled electronic flow) is successfully combined with the possibility of electrical control of this flow.

An extremely important feature of the semiconductors is the possibility of technological control (by doping the crystal) of most important electrical parameters of a material – conductivity and its thermal stability, as well as the sign and the mobility of charge carriers. Depending on the concentration of donors and acceptors, the conductivity of a semiconductor can be changed by a factor of millions, imitating in the extreme cases both a metal and a dielectric. Technological methods can be used to create both *p-n* and hetero-junctions in the structure of a semiconductor. And it is very important to be able to control the *lifetime* of charge carriers in the semiconductor by billion times, ensuring the operation of transistors up to the terahertz frequency range.

Thus, the lamp diode and triode were replaced by the crystal diode and transistor. Electronics based on the use of discrete semiconductor devices emerged. The reliability of electronic circuits and systems has increased significantly. Their dimensions, weight and energy consumption have significantly decreased. However, the "tyranny of interconnections" persisted so the cost of production also remained high. Therefore, electronics based on the discrete semiconductor devices did not last long.

1.3 Third generation of electronics – microelectronics

The further progress of electronics were the *integrated circuits*. Although the invention of the transistors has revolutionized electronics, their huge number in the computing devices (including other components of electronics – resistors, capacitors, inductors) has led to great difficulties in implementation of many interconnections. The solution to the problem was found by Kilby in 1958 at *Texas Instruments*, USA (Kilby received Nobel Prize for his invention in 2000). Transistors, diodes, resistors, capacitors and inductors – all main circuit elements together with their interconnections were implemented in one *monolithic* semiconductor block (the silicon was originally used). The process of manufacturing of such integrated circuits allowed the automation of their manufacture and a significant reduction in overall dimensions. The first application of the invention of Kilby were the miniature calculators.

Thus, the era of integrated semiconductor electronics – microelectronics (micron is equal to 10^{-6} m) began. The main element of complex electronic systems has become an integrated circuit (IC). An integrated circuit is a micro-miniature functional unit of the electronic equipment, in which the active, passive and connecting elements are manufactured in a *single* technological cycle on the surface or in the volume of a material and have a common shell. The manufacture of all elements of the chip in a single technological cycle and in one material allows you to use instead of sequential (individual for each element) technology wholesale technology, which is quite productive. The cost of production of complex electronic systems per one circuit element has decreased sharply.

The possibility of transition to the wholesale technology is due to the fact that the semiconductor structure has almost all the necessary circuit properties. Thus, a separate *p-n* junction can be used as a resistor, capacitor, diode, signal switch, voltage stabilizer, photosensitive element, LED, semiconductor laser, and in combination with other *p-n* junctions as the transistor, thyristor, etc. Therefore, forming on the semiconductor crystal in one technological cycle many *p-n* junctions, you can create a complex IC.

Summarizing many descriptions of microelectronics, we can conclude that:

(1) Microelectronics is a subsection of electronics related to the study and production of electronic components with geometric dimensions of characteristic elements of the order of a few micrometers or less. Such devices are usually made from the semiconductors and semiconductor compounds, using photolithography and doping. Most of the components of conventional electronics: resistors,

capacitors, inductors, diodes, transistors, insulators and conductors are also used in the microelectronics, but already in the form of miniature integrated devices.

(2) The digital integrated circuits use mostly transistors while the analog integrated circuits also contain the resistors and capacitors; the inductors are used in the circuits operating at high frequencies. With the development of technology, the size of components is constantly decreasing. With a very high degree of integration of components, and, consequently, with very small sizes of each component, the problem of inter-element interaction is very important (parasitic phenomena). That is why, one of the main tasks of designer is to compensate or minimize the effect of parasitic leaks.

(3) There are two main areas of microelectronics: *integral* and *functional*. The *microwave microelectronics*, which is engaged in the study and development of the microwave microcircuits, is of particular importance. As a rule, in such circuits, both hetero-junction and silicon chips are used, which are installed on the dielectric substrates with a passive film infrastructure (capacitors, resistors, etc.). In the *power* microwave electronics, the thick-film technologies based on the silk-screen printing method are actively used.

(4) Microelectronics is a subfield of electronics being the science and technology, involved in the making and using of very small electronic parts. Microelectronics relates to the study and micro-fabrication of very small electronic designs and components. These devices are typically made from semiconductor materials. Many components of normal electronic design are available in a microelectronic equivalent: these include transistors, capacitors, inductors, resistors, diodes, and naturally) insulators and conductors. As techniques have improved, the scale of microelectronic components has continued to decrease. At smaller scales, the relative impact of intrinsic circuit properties, such as interconnections, may become more significant. These are so-called parasitic effects, and goal of microelectronics design engineer is to find ways to compensate for or to minimize these effects, while delivering smaller, faster, and cheaper devices.

The development of solid-state integrated electronics (microelectronics) followed the path of reducing the size, increasing the speed, memory and reliability of electronic systems. It is in this way that methods of miniaturizing IC elements have been developed, which have opened up real possibilities for the transition to the nanoelectronics. In 1965, Gordon Moore observed that silicon transistors were undergoing a continual process of scaling downward, an observation which was later codified as Moore's law. Since his observation, the minimum feature size of transistor has decreased from 10 micrometers to 10 nanometers range as of 2019.

Continued realization of this law by using new methods and materials to build electronic devices is the aim of nanoelectronics enable the with sizes on nanoscale. Recent technology generation of silicon MOSFET (metal-oxide-semiconductor field-effect transistor, or MOS transistor) works already within this regime, including 22 nm CMOS (complementary MOS) nodes and succeeding 14 nm, 10 nm and even 7 nm FinFET (fin field-effect transistor).

1.4 Forth generation of electronics – nanoelectronics

Currently rapidly developing nanotechnology represents the further progress in the obtaining materials with new properties: they prepare real opportunities for the emergence of electronics of small elements. This progress is due to such changes in the structure of matter that affect its fundamental properties. Until now, main properties of materials have been determined mainly for the macroscopic objects. However, dimensional effects observed in thin films, in the properties of the surface of crystals and in very small particles of matter have long been known and now start to be used in engineering.

It is not easy to give an unambiguous definition of nanoelectronics, but it can be viewed from different angles.

(1) Nanoelectronics is a rapidly developing field of electronics, which is engaged in the development of technological and physical foundations for the construction of integrated electronic circuits with element sizes less than 100 nanometers. The term "nanoelectronics" itself reflects a transition from the microelectronics of modern semiconductors, where the dimensions of elements are measured in the units of micrometers, to the much smaller elements - with dimensions of tens of nanometers. With the transition to the nano-size elements, the *quantum effects* begin to dominate in the circuits, opening up many new properties, and, accordingly, signifying the prospects for their useful use.

(2) Nanoelectronics is a field of science and technology engaged in the creation, research and application of electronic devices with nanometer-sized elements, the functioning of which is based on epy quantum effects. There is no clear boundary between "nanoelectronics" and "microelectronics", since the specific micro-or-nano sizes are not decisive but are conditional. However, unlike the classical laws used in electronics and microelectronics, the basis for the operation of the nanoelectronic devices is the *quantum effects*: quantum capacity, kinetic inductance, quantum conductivity, plasmons, two-dimensional electron gas, and others. Due to this, not only a specific nomenclature of properties appears, but also

new prospects for their use. In particular, if in the the micro-size devices the quantum effects are largely undesirable (for example, in the operation of a classical transistor, when the size decreases, there is a size limitation due to the tunneling of charge carriers), then in nano-electronics the quantum effects are already the basis for the operation of some devices.

In this case, the main point is that it is possible to control the properties of matter by the changing its fragmentation. Due to the needs of technology, great progress has been made in the field of *nanophysics,* which is a new scientific field of physical materials science, associated with the creation and study of the structure and properties of materials condensed from very small crystals, clusters, fragments having a total volume of 10^3–10^6 atoms. In scientific terminology, term "nano" means 10^{-9}: one nanometer (nm) is equal to one thousandth of a micrometer ("micron"), or one millionth of a millimeter, or one billionth of a meter. An ultrathin microstructure having an average size of phases or granules (clusters), layers or filaments of the order of (or less) per 100 nm is considered nanostructured. Due to the small size of the blocks (particles, granules, phases), from which they are constructed, the nanomaterials demonstrate unique mechanical, optical, electrical and magnetic properties.

Polycrystalline fine-grained materials with an average grain size of 40 to 150 nm are sometimes called *microcrystalline*; and if the average grain size is less than 40 nm – *nanocrystalline*. It is known that in a polycrystalline substance, a decrease in the size of the "grains" of crystallites can lead to a significant change in its properties. Such changes become especially noticeable, when the average crystal grain size decreases to 100 nm, but the properties change greatly, when the grain size becomes less than 10 nm. In recent years, a new scientific and technical field is developing – magneto-electronics, or, as it is now called – "spintronics", engaged in the study and practical implementation of devices that use electron spins. Spintronics studies magnetic and magneto-optical interactions in metal and semiconductor structures, as well as quantum magnetic effects in nanometer-sized structures. Of particular importance for magnetoelectronics are modern nanotechnologies that allow the implementation of new advances in the field of nanophysics.

Thus, nanotechnology is a set of methods for the manufacture and processing of structures having a length of 1–100 nm (at least in one of the dimensions). It is generally accepted that nanotechnology is the most promising area of modern technology. It is believed that those who previously mastered nanotechnology will take a leading place in the technosphere of the XXI century. That is why economically developed countries allocate billions of dollars for the development of

nanotechnology. Currently, the world market already sells more than 3,000 products manufactured using nanotechnology. In the next 10 years, the global need for certified nanotechnology professionals will be in the millions; the value of the world market for nanotechnology products will be about 1 trillion US dollars. In recent years, more than tens of thousands of nanotechnology companies have been established, and their number is doubling every two years.

Nanosize materials in modern technologies. As the size of object decreases to micro- and, especially, nano-scale, the influence of the surface and shape on all its physical properties increases significantly in comparison with the influence of the bulk material of the object. From a thermodynamic point of view, this fact is explained by an increase and subsequent dominance of the *free surface energy*, which is determined by the shape of the object and its surface area ~ R^2, in comparison with the free volumetric energy of the sample, proportional to *R3*, with a decrease in its characteristic size *R*. Moreover, with a decrease sizes and shape factors below the "critical" ones, the physical properties of objects themselves can fundamentally change: the nano-objects and low-dimensional structures are characterized by the *size-induced* structural and phase transitions such as metal $\Rightarrow$ semiconductor $\Rightarrow$ dielectric or paramagnetic $\Rightarrow$ ferromagnetic $\Rightarrow$ antiferromagnetic ferroelectric $\Rightarrow$ paraelectric, elasticity $\Rightarrow$ plasticity and many others. These effects, predicted within the framework of phenomenological theories, have numerous experimental confirmations and are consistent with the modern quantum-mechanical microscopic calculations, proving fundamental changes in the band structure and symmetry of the unit cells, induced by the nanoscaling of the object. In this case, researchers are faced with nanomaterials, the physical properties of which may differ significantly from the "generating" bulk materials. For a number of properties of nano-scale objects, the nature of their material can play a secondary role in comparison with the primary role of shape (for example, a quantum dot, ellipsoid, sphere, tube, wire, or mono-layers), topological dimension (for example, ID, 2D, 3D confinement or fractal) and quantum size effect (in particular, the dimensions of the object are below or above the characteristic or critical dimensions).

The most technologically, advanced and promising nano-objects for the applications are the nanotubes, nanowires, graphene and clathrates, which clearly demonstrate the leading role of the *nanoscale* for the use of their physical characteristics in the modern submicronics and nanoelectronics, optoelectronics, data storage devices and computer memory, environmental energy and medicine.

Turning to specific examples, we note that, first of all, that nanoscale affects the electronic emission, electromechanical and thermoelectric properties of objects.

Single-wall nanotubes, synthesized from the semiconductors with different band gaps (carbon, silicon, boron nitride or zinc oxide) can have both low (up to the dielectric) and very high (up to the metallic) electrical conductivity, which can be easily controlled, even electrically. They are the objects with an almost ideal surface, since the existing defects, as a rule, affect only the structure of several nearby cells, but do not violate the structure of the tube of other nano-particle as a whole. Therefore, for the use of nanotubes as channels for field-effect transistors, their easily controllable electrical conductivity and extremely low wall roughness in comparison with conventional silicon channels play a decisive role. The result is the advanced scaling of gate and channel lengths down to a few nm, reduced channel scattering and, as a result, improved transistor performance.

[***Note.*** ***Many already implemented or promising applications of nanoelectrics are known:***

Memory storage. Electronic memory designs in the past have largely relied on the formation of transistors. However, research into crossbar switch based electronics have offered an alternative using reconfigurable interconnections between vertical and horizontal wiring arrays to create ultra high density memories. Some companies has proposed the use of *memristor* material as a future replacement of Flash memory. An example of such novel devices is based on *spintronics*. The dependence of the resistance of a material (due to the spin of the electrons) on the magnetic external field is called magneto-resistance. This effect can be significantly amplified (giant magneto-resistance) for the nanosized objects, for example when two ferromagnetic layers are separated by a nonmagnetic layer, which is several nanometers thick. This effect has led to a strong increase in the data storage density of hard disks and made the gigabyte range possible. Besides, the so-called tunneling magnetoresistance is very similar to giant magneto-resistance but is based on the spin-dependent tunneling of electrons through the adjacent ferromagnetic layers. Both effects are used to create the non-volatile main memory for computers, such as the so-called magnetic random access memory or MRAM.

Nano-modifications of carbon, especially the graphene and similar 2D (layered), 1D (tubes) and 0D (fullenes) materials are one of the main directions of nanophysics and nanoelectronics. Such materials, sometimes one atom thick, have remarkable properties that can be combined to create various electronic circuits. For example, technologies associated with probe microscopy make it possible to build various structures of individual atoms on the surface of a conductor in an ultrahigh vacuum, simply by rearranging them - this is the basis for creating monatomic electronic devices.

Optoelectronic devices. In the modern communication technology, the traditional analog electrical devices are increasingly replaced by the optical or optoelectronic devices due to their enormous bandwidth, capacity and respectively. Two promising examples are the photonic crystals and quantum dots. The photonic crystals are materials with a periodic variation in the refractive index with a lattice constant that is half the wavelength of the light used. They offer a selectable band gap for the propagation of a certain wavelength, thus they resemble a semiconductor, but using light or photons instead of electrons. Quantum dots are the nanoscaled

objects, which can be used, among many other things, for the construction of lasers. The advantage of a quantum dot laser over the traditional semiconductor laser is that their emitted wavelength depends on the *diameter* of the dot. Quantum dot lasers are cheaper and offer a higher beam quality than conventional laser diodes.

Displays. The production of displays with low energy consumption might be accomplished using carbon nanotubes (CNT) and/or silicon nanowires. Such nanostructures are electrically conductive and due to their small diameter of several nanometers, they can be used as field emitters with extremely high efficiency for field emission displays (FED). The principle of operation resembles that of the cathode ray tube, but on a much smaller length scale.

Quantum computers. Entirely new approaches for computing exploit the laws of quantum mechanics for novel quantum computers, which enable the use of fast quantum algorithms. The quantum computer has quantum bit memory space termed "Qubit" for several computations at the same time. This facility may improve the performance of the older systems.

Plasmatronics. Collective oscillations of free electrons inside a metal have the characteristic plasmon resonance with a wavelength of the order of hundreds of nanometers. Thus, it is possible to transmit the electromagnetic wave along a chain of metal nanoparticles, exciting the plasmon oscillations in them. This technology will allow the logical chains introducing into computer technology that can work much faster and transmit more information than traditional optical systems, and the size of such systems will be much smaller than the accepted optical ones.

Medical diagnostics. There is great interest in constructing nanoelectronic devices that could detect the concentrations of biomolecules in real time for use as medical diagnostics, thus falling into the category of nanomedicine. A parallel line of research seeks to create nanoelectronic devices which could interact with single cells for use in basic biological research. These devices are called nanosensors. Such miniaturization on nanoelectronics towards in vivo proteomic sensing should enable new approaches for health monitoring, surveillance, and defense technology.]

Another example is emitters from nanowires, multi-walled or single-walled nanotubes and their arrays, made of a wide variety of materials (carbon, silicon, gallium arsenide or boron nitride, coated with silver, titanium, platinum or gold, which are used in vacuum electronics as a new type of field cathodes. The main advantage of such emitters is the nanometer curvature of their tip. Due to the strong field concentration near the tops of the nanotubes or nanowires, the nanoscale provides the ultra-high field gains and ultra-low threshold voltages of the cathode. The use of empty nanotubes, inside which it is possible to move the metal nanoparticles and fix their position using electrical or magnetic pulses, will make it possible to achieve the ultra-high density of data recording. In this case, the material of the tube and the method of its manufacture do not play a noticeable role (which means that you can choose the cheapest one). The ultra-high density is achieved due to the fact that one nanotube is capable of fixing not only two positions of the nanoparticle (presence or absence), but much more positions of the particle (in fact, the coordinate of a particle in the tube).

Thermoelectric and electrocaloric properties of the fullerenes and clathrates (their high electrical conductivity combined with low thermal conductivity due to the dominant contribution of the ballistic mechanism of heat transfer) determine the high efficiency of fullerenes in the thermoelectric converters of a future. Due to the unique possibilities of storing and releasing other atoms and molecules (in particular hydrogen), fullerenes and clathrates may be of fundamental importance for the energy of the future. It turned out that the formation of fullerenes, clathrates and other very diverse supra-molecular ensembles is primarily determined not by the chemical nature of their constituent substances, but by their topological, geometric and charge correspondence.

The list of examples of unique properties that are "universal" for various nanomaterials and their use for the applications in various fields of science and technology is far from complete. It should be noted, however, that for the successful application of nanomaterials properties, it is necessary to develop new technologies such as the self-assembly; if possible, to use also the biochemical nano-assemblers and the "intelligent" molecular micro- and nano-machines, which will make it possible to synthesize sufficient quantities of identical units of nanomaterial and integrate them directly into circuits.

1.5 Moletronics (molecular electronics)

This could be a further perspective of electronics, and it distinguishes two main areas: the *macro*molecular electronics, or organic electronics, as well as the *micro*molecular electronics, abbreviated as moletronics. The size of electronic devices decreases with time exponentially, so that in the coming decades they will approach the size of molecules. Obviously, for this, the significant changes must occur both in the physical principles of creating such devices and in the methods of their industrial production. Thus, the field of electronics, which uses individual molecules of organic compounds as constituent elements of electronic circuits (diodes, transistors, memory elements), is usually called moleronics. The use of electronic devices based on molecular components marks the next important step in the development of microelectronics, which allows to achieve gains in increasing the density of elements, speed of response and lower energy consumption. Moletronics can also be used in solar energy, medicine and other fields of science and technology.

In a more specific definition, the moletronics is the application of molecular building blocks for IC fabrication for electronic components. The main idea here is

the size reduction of the conventional silicon fabrications. This can well be sought as a potential to extend Moore's Law beyond the limits of usual semiconductor circuits. Though molecular electronics spans over the disciplines of physics, chemistry and material science, the unifying feature is the molecular building blocks. Moletronics would not just help in size reduction of silicon chips but would also significantly increase data processing speeds by many times than the conventional chips. This technology can be further extended in the field of "nano-robotics" wherein the main aspect is minimum size.

Macromolecular electronics uses thin (20–200 nm) films of organic materials as the elements of electronic circuits. The plane of films in different devices can range from a few square micrometers (in transistors) to a few square centimeters (in photocells). The most widely used different polymers. They combine many electrical and optical properties of dielectrics, semiconductors and metals with the inherent lightness, ductility of polymers, simpler and cheaper technology. By doping, the electrical conductivity of polymers can vary from low electrical conductivity (dielectrics) to a fairly high electrical conductivity (high-conductivity metals). Conductive polymers are used in speaker membranes, for antistatic coatings, can be used for protection against electromagnetic radiation, are also used in lithography as components of resistors. Polymers (like polyaniline) have the ability to be doped electrochemically. Lightweight batteries can be made on their basis. Their electromotive force is about the same as that of lead batteries, but the current density is still an order of magnitude lower. Unalloyed polymers are usually dielectrics, but sometimes they have semiconductor properties. Different polymers can have both donor and acceptor properties.

On the basis of semiconductor polymers with the help of simple and cheap technology, the polymer transistors with an element size of ~ 5 μm were created. However, polymer transistors have low charge carrier mobility and are not suitable for use at frequencies above 100 kHz. Therefore, polymer integrated circuits cannot be used in computers (due to the low speed of information processing), but they are applicable in combination locks, electronic labels, etc., where they can successfully replace silicon chips. Polymers are increasingly used in the optoelectronics. The fully polymeric photodiodes and solar cells at polymer p-n junctions with a fairly high efficiency. Promising and fast-growing area is organic LEDs (light diods). The goal of many developments is to create cheap light sources, color flat displays and the most organic LEDs. The efficiency of organic converters of electric energy into light reaches the level of the best inorganic devices. The advantages of organic LEDs include low cost and the ability to obtain large surfaces, which is necessary, for

example, for lighting panels and walls. It is possible to use organic LEDs in the flat color displays, which might be thinner and cheaper than liquid crystal displays. Light road signs have already been developed, as well as flat displays used in various devices.

All fabrication techniques till today have the prime purpose to accommodate as many switches and also reduce their size. This simultaneously increased their speeds too. In moletronics, the above described transistor switches are made from molecules. This has a great advantage, as using an organic molecule reduces the size of the conventional switch to one-millionth size of a grain of sand and is 10 times faster than the traditional silicon-based switch. The organic molecule used was actually a thiol molecule, which is mixture of sulfur, carbon, and hydrogen. Several such thiol molecules were sandwiched between two gold plates to act as switches. These novel channels acted either insulators or conductors, as per the electric flow through them were generated. Further investigation in this field showed bafflingly results as the molecules could even amplify signals just like their conventional counterparts. This has further pushed the application of moletronics as logic gates. Conducting polymers such as polyacetylene, polypyrrole, and polyaniline have a linear-backbone and are the main classes of conducting polymers. These form the molecular building blocks in the field of moletronics. Poly (3- alkylthiophenes) is the archetypical materials for transistors. Along with these, the naturally available graphite too forms the raw material for moletronics. The Buckminster Fullerene or C-60 nanotubes are the final produce of graphite as an application in moletronics. While most of the conductive polymers have longed to find any large scale application, the nanostructured forms of these have provided a fresh look out to them.

Micromolecular electronics can use individual organic molecules or even their fragments as elements of microelectronic circuits. The ideas of molecular electronics (molectronics) was originated in the 70s of last century, but still many technological difficulties have not been overcome. Theoretically, it has been shown that different molecules can not only be insulators, but also conduct current, as well as act as diodes, memory cells and even transistors. However, experiments with individual molecules in recent years have been extremely difficult. Only in recent years has interest in molecular devices is grown. The reason for this is, firstly, that the limit of miniaturization of the technology of integrated circuits on silicon is approaching, so the search for new solutions that would lead to progress in microelectronics. Secondly, new experimental tools in nanotechnology have appeared, which make it possible to operate on individual molecules as well as to

make contacts with them. The idea to use organic molecules as an elemental base of microelectronics arose as a model of a rectifier (diode) consisting of one organic molecule. The two halves of this molecule have opposite properties with respect to the electron: one can only donate an electron (donor) and the other can only receive an electron (acceptor). If you place such an asymmetric molecule between two metal electrodes, the whole system will conduct current in only one direction. Interest in molecular electronics is due to the prospects that will open up if individual molecules can be used as basic elements of electronic circuits. There is a real possibility of creating 3D circuits with ultra-high element density, extremely high speed and low power consumption.

The basic working principle of moletronics is the same as the conventional silicon fabricated chips. The main difference is in the workability of the tthem. While conventional silicon chips have shown tremendous advancement throughout their development from the single transistor to the latest integrated circuits, the moletronics seems to the best bet when it comes to performance. Thus, moletronics uses the molecular blocks as a substitute to the traditional silicon. Everything else remains more and the same in the integrated circuits. Also, to use them as a switch only one electron is sufficient to either turn ON or OFF these molecular transistors.

An important step in the development of molecular circuitry was the abandonment of simple copying of semiconductor circuits with the replacement of conventional transistors with molecular ones. The fact is that there are many both natural and synthesized molecules, which in themselves can serve as logical elements. They are divided into two types. The first includes molecules having two stable states, which can be assigned the values "0" and "1". By learning to switch them from one state to another with the help of external influences, you can actually get a ready-made valve. Molecules of the second type contain fragments capable of acting as the above-mentioned control groups. One such molecule can work as a logically active element "NO - AND", "NO - OR", etc. (the control groups will serve as "inputs" of the element).

First main electronic component in moletronics is the molecular wire. Molecular wires can be infused as conductive polymers by enhancing their mechano-electric properties. Molecular wires have a repeating structure which can be either organic or inorganic in nature. These can conduct electricity. These typically have non-linear current-voltage characteristics and do not behave like ohmic conductors. These are also called as “nanowires” which should be able to self-assemble to be used in moletronics. They should have the ability to connect to

diverse metal surfaces such as gold which is extensively used in semiconductor fabrication industries to form the connection with the outside world.

Second important component of moletronics involves the molecular logic gate which is a molecule that is capable of doing the logical operations as its bulk electronic counterpart. Its operations are based on one or more physical or chemical inputs and a single output. These have advanced so far that now these are capable of computing combinational and sequential logical operations. One breakthrough in this technology is the use of these components as memory storage devices. Molecular logic gates work with input signals based on chemical processes and with electrical signals.

However, the key problem of molecular electronics is the integration of molecules into the circuit. The molecular device must be a complex branched chain of atomic groups. Approaches to the creation of basic elements of schemes are well developed, but the problem of their integration in the order that ensures the operation of the scheme is still far from being solved. If we use organic molecules as basic elements in the framework of traditional circuitry and technological techniques, the key problem is the problem of contacts. In any case, to design molecular devices it is necessary to know the electrical resistance of the contact "molecule-connecting conductor", the characteristics of molecules-diodes, triodes, switches. To experimentally determine these values, it is necessary to connect a current source, an ammeter, a voltmeter to the ends of an individual molecule. These problems are partially solved.

It should be noted that the importance of such research in the field of molecular electronics is growing, where quantum electronic devices are created from parts synthesized as a result of periodic chemical processes. These parts are then assembled into the required electronic circuits through self-assembly and self-sequencing processes. If the goal of molecular electronics - to assemble electronic circuits from individual molecules (switches) and carbon nanotubes (wires) - is achieved, then perhaps memory devices will appear with a recording density a million times higher than that of modern devices. In this case, the consumed electrical power will decrease by billions of times (compared, for example, with conventional semiconductor circuits on complementary MOS structures). Such a sharp increase in the amount of non-volatile memory in some cases could greatly simplify the work on the computer.

Moletronics might be seen as the next step in the world of microelectronics which can change the way chip fabrication works in this present era. Moletronics would have applications span over the various disciplines like physics, chemistry

and bio medicals to name a few. Scientists are particularly interested in the application of moletronics in Nano robotics. Nano robotics may necessarily use moletronics to use “molecular processors” as the central processing unit (CPU). Nano robotics is seen as the next big thing in the field of bio medical. But there are still some issues that need to be taken into consideration so as to practically implement this technology. Moletronics might have tremendous potential to rightly achieve another milestone in the fabrication industry.

1.6 Summary Chapter 1

Conclusions

The development of the now most important scientific and technical direction "***Electronics***" can be conditionally divided into four stages: vacuum tubes, semiconductors, microelectronics and nanoelectronics. These stages were accompanied by colossal changes in the mass and size parameters, as well as gigantic successes in increasing the reliability and speed of electronic devices. In addition, there are more and more works that can be attributed to the molectronics.

References

[1] *A brief history of communications*. IEEE edition, Piscutaway, 2002, 124
[2] Y.Y. Fedotov. *Semiconductors electronics*, Budapesht, Technical literature, 2001, 103.

Questions

1. Briefly describe the first two stages of electronics development
2. What are the features of microelectronics?
3. What is the main reason for the special properties of the nanomaterial?
4. What can we expect from moletronics?
5. What are the main materials used in microelectronics?
6. What are the main materials used in nanoelectronics?

CHAPTER 2. SOME PHYSICAL ASPECTS OF ELECTRONIC MATERIALS

Contents

The study of the physical foundations of electronic material science is based on the main provisions of quantum mechanics, associated, for example, with discreteness of radiation and absorption of light, with the photoelectric effect, with the particle-wave dualism, with the uncertainty relation. The structure of the atom and atomic spectra are also important question as well as Pauli principle, structure of electronic shells and valence of atoms, the arrangement of atoms of chemical elements in periodic system of Mendeleev. Condensed Matter Physics, i.e., Solid State Physics and nanophysics use the knowledge gained in the previous sections of physics. Therefore, before getting acquainted with the physical effects that find application in the microelectronics and nanoelectronics, it is necessary to pay some attention to comparing the basic concepts of classical mechanics about the structure of matter with a quantum mechanical approach to this issue.

For a more conscious study of the basics of materials science, it is advisable to dwell on the most important concepts and stages of epy development of physical science, which have become decisive for the creation of modern microelectronics and nanoelectronics.

2.1 Modern physical picture of the world

A restriction exclusively to the field of electronic materials science significantly narrows the horizons of the student's knowledge; therefore, it seems rather important to consider briefly what the general understanding of the physical picture of the Universe currently looks like. These representations are considered essential to broaden the horizons of the graduate student.

The place of material science, based on the solid state physics, in the general physics is close to the classical mechanics and quantum mechanics, as illustrated in Fig. 2.1. It is seen that the classical mechanics is a region of low velocities υ (in comparison with the speed of light c), and a region of small values of the ratio of the Planck constant $\hbar$ to the moment S of material particle movement.

It is pertinent to recall that first ideas about the quantum nature of microobjects and processes arose in the study of the laws of thermal radiation. It has been shown that the correct theory of thermal radiation, proved experimentally over the entire wavelength range, can be constructed only under the assumption that the light is emitted by a matter *discretely*, that is, by individual portions - quanta. This assumption is called the Planck's hypothesis: energy of light quantum E is proportional to its frequency ν, i.e., $E = h\nu$. For his work in the field of thermal radiation Planck was recognized worthy of the Nobel Prize (1918). Planck's constant h means: *energy* $\times$ *time* = *length* $\times$ *pulse* = *moment of movement*, and refers to the fundamental physical constants, as well as the Boltzmann constant k_B, the charge e and mass m_e of electron. Newton lows can always be done by the putting $h = 0$.

The dimension of the parameter S is same as the dimension of Planck constant h, and, therefore, both scales in Fig. 2.1 are *dimensionless*. The moment of movement S is a physical quantity equals to the product of energy over time; it is one of the most important dynamic characteristics of the motion of a particles and their systems, both in classical and quantum mechanics.

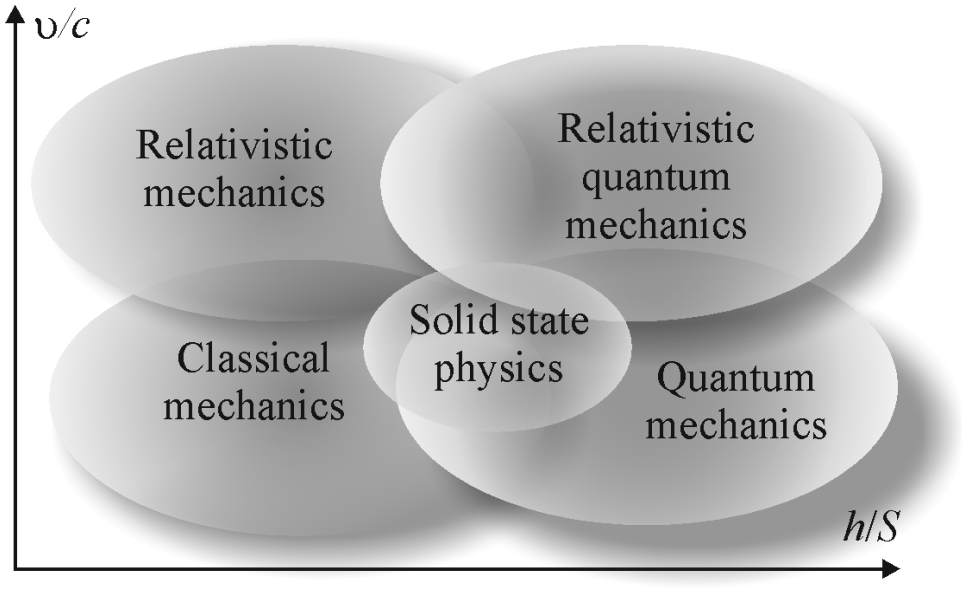

Fig. 2.1. Schematic representation of the connection of different fields of physics. Solid State Physics (or Condensed Matter Physics) is located mainly in the fields of classical and quantum mechanics, but in some sections (in particular, the physics of magnetism) is located on the border of quantum and relativistic quantum mechanics.

Thus, condensed matter physics of (in particular, the solid state physics) is based on the classical and quantum mechanics, Fig. 2.1. However, in describing one of the important sections of solid state physics (namely, the magnetism) we have to involve the concept of relativistic quantum mechanics. The magnetism, which in statics looks simply like the mechanical attraction or repulsion of substances in a magnetic field, has a rather complex physical nature. Classical physics cannot fundamentally explain magnetism; this quantum phenomenon by its nature is also relativistic. However, the relativistic quantum mechanics is necessary mainly to understand the elementary particle physics [1-3].

For a general idea, the more detailed relationship between various sections of fundamental physics is useful. Figure 2.2 shows the so-called "cube", representing modern perceptions of fundamental physics. As can be seen from this figure, that development of physics began with Newtonian mechanics. Then the fundamental gravitational constant γappeared in the Newton's theory of gravitation, but since the gravitational forces are billions of times weaker than electrical interactions, the gravitational forces can be neglected in the solid state physics.

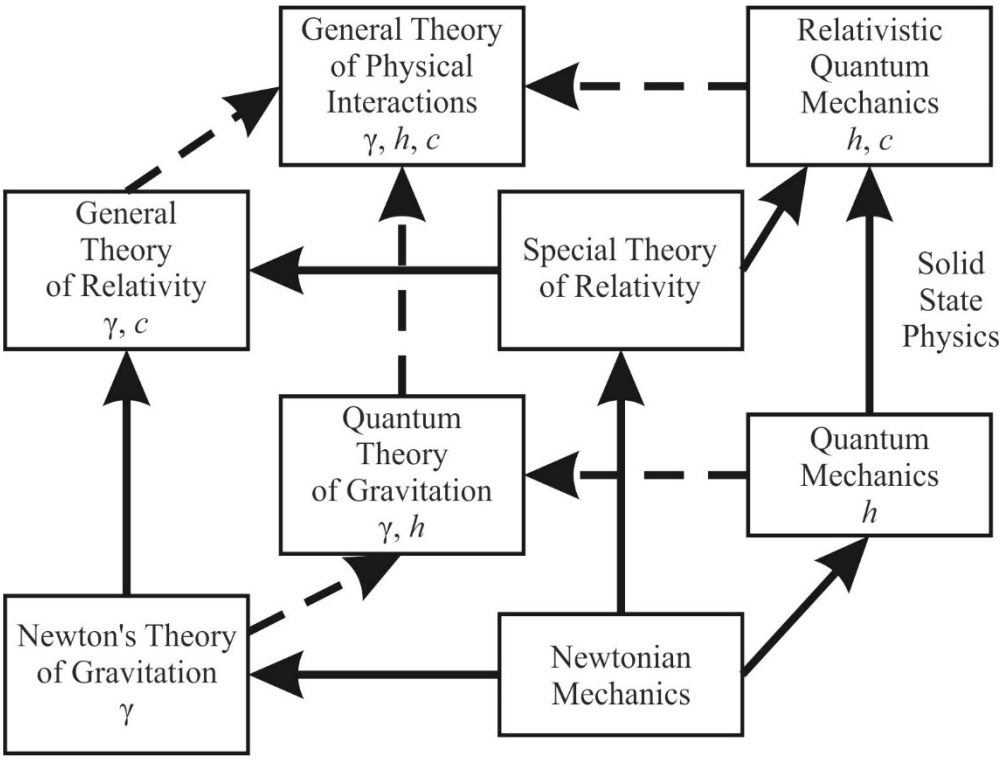

Fig. 2.2. The cube conditionally shows the connection of different areas of physics, and the arrows show the direction of development of these areas. Solid State Physics uses the methods and ideas of both classical and quantum physics, and the physics of magnetism as part of Solid State Physics "enters" the field of relativistic quantum mechanics.

In the Einstein's special theory of relativity another fundamental constant appeared: the speed of light in a vacuum c. This parameter is very important for the

solid state physics and materials science, because it is used to describe the interaction of crystals with electromagnetic waves. As already mentioned, the symbol of quantum mechanics is the Planck constant h. For the relativistic quantum mechanics, which is the result of a combination of the theory of relativity and quantum mechanics, both fundamental parameters are equally important: h and speed of light c.

Other areas of physics: General theory of relativity, Quantum theory of gravity and, especially, the expected in future General theory of physical interactions are apart from the Solid state physics, Fig. 2.2, on which electronics is based. Describing the properties of a matter, solid state physics operates not only with the fundamental constants h and c, but also with the parameters of electron: its charge e, the magnetic spin moment μ_B, and the mass m_e.

The division of physical constants into the fundamental and the derivative parameters is, in principle, arbitrary. Usually the fundamental constants are those which provide the simplest way to enter the formulas and have a *clear physical meaning*. It is noteworthy that all above constants (γ, h, c, e, m_e) have dimensions, which depends on the choice of the system of units and randomly selected standards (length, time, mass, charge, magnetic moment, etc.).

[***Note.*** The gravitational constant $\gamma = 6.67 \cdot 10^{-11}$ $m^3 \cdot s^{-2} \cdot kg^{-1}$ determines the force F of gravitational attraction between two masses m_1 and m_2, located at a distance r: $F = \gamma(m_1 \cdot m_2/r^2)$. The Planck constant (action quantum) $h = 6.6 \cdot 10^{-34}$ $kg \cdot m^2 \cdot s^{-1}$ (J·s) relates the amount of energy of a quantum of electromagnetic radiation to its frequency: $E = h\nu$. The speed of light in vacuum $c = 3 \cdot 10^8$ m/s. the charge of electron $e = 1.6 \cdot 10^{-19}$ C and the mass of electron $m_e = 9.1 \cdot 10^{-36}$ kg.]

However, physicists have long been interested in the possibility of describing the nature by some dimensionless parameters.

2.2 Dimensionless world constants

It is important to note that three fundamental parameters (electron's charge e, speed of light c and Planck's constant h) form a dimensionless combination:

$$\alpha = e^2/\hbar c = 1/137,$$

known in the quantum physics as "one hundred and thirty-seven" (also called the "constant of fine structure"). This name for the parameter α appeared due to the fact that the spectroscopic studies revealed a small split – "thin structure" in the hydrogen spectrum. At that, the ionization energy of hydrogen can be determined by the

relation: $R_\alpha = ½\alpha^2 mc^2$.

In the non-relativistic theory, the ionization energy does not depend on the speed of light. Thus, the parameter α is a *relativistic* relation for the basic structure of the energy levels – the ratio of the speed of an electron in its orbit to the speed of a light is taken into account: $v/c \sim \alpha$. Thus, the fine structure of hydrogen lines is the relativistic effect.

The parameter α is the dimensionless fundamental coupling constant between the *electromagnetic field* and the *elementary charge*. The fact that parameter $\alpha << 1$ physically means a weak connection between the particles and electromagnetic field. Only for this reason both particles and electromagnetic waves can be considered as some "basis", by means of which the quantum mechanics describes the phenomena in substances. It means that the atom is a "loosely bound" structure with "slow" (in relativistic terms) moving electron. For this reason, the non-relativistic theory of the atom is a good approximation: relativistic corrections have the order $(v/c)^2 \sim \alpha^2$.

However, the *constant of fine structure* also manifests itself in other aspects:

• Through α it is possible to *express* another world constant - the charge of electron e. Indeed, if one assumes that speed of light c and Planck constant ħ are the main physical parameters, describing the Universe ("world constants"), then the fine structure constant α can be really a measure of the electron's charge:

$$e = (\alpha\hbar c)^{1/2} = (\hbar c/137)^{1/2}.$$

• The constant of the fine structure allows you to *compare* important energy sources - electrostatic and magnetic. The magnetic energy of electrons interaction in the atom is estimated as $U_M \approx \mu_B^2/a^3$, where μ_B is the Bohr magneton, and a is the average distance between the electrons. The energy of electrostatic interaction of two electrons under the same conditions is equal to $U_{кул} = e^2/a$. If one estimates the ratio of these two energies, it can be obtained:

$$U_M/U_{кул} \approx (1/137)^2.$$

Thus, the magnetic interaction of electrons is much inferior to the electrostatic one.

• Parameter α is also important for the physics of magnetism, where fine-structure constant predicts a *small value* of magnetic susceptibility of the diamagnets. It can be shown that the *diamagnetic susceptibility*, with a good agreement with the experimental data, also can be estimated by the value of α:

$$\alpha^2 = (1/137)^2 \approx 5 \cdot 10^{-5}.$$

• A very important parameter in physics is the *size of an atom*; which can be again estimated through the constant of the fine structure

$$a_0 = \hbar^2/m_e c^2 = r_e/\alpha^2 = (137)^2 r_e,$$

where $r_e = e^2/m_e c^2 = 1.25 \cdot 10^{-13}$ cm is the radius of an electron. The size of the atom a_0 can be calculated, if the electrostatic energy of electronic radius r_e, which equals ~ e^2/r_e, equate to the calm-energy of the electron $m_e e^2$.

From listed above relations it can be stated that the dimensionless constant α is really very important. However, in the quantum physics, in addition to $e^2/\hbar c \approx 1/137$ there are other important dimensionless parameters, for example, the ratio of electron's mass to the proton mass: $m_e/m_p \approx 1/1840$, as well as the ratio $e^2/\gamma m_p^2 \approx 4.10^{42}$ (γ is the gravitational constant), and so on.

• Possibilities of applying quantum mechanics to describe the properties of microscopic objects can be evaluated in terms of a more general theory - the relativistic quantum mechanics. It turns out that high accuracy of quantum theory, which takes place when describing the properties of electrons in atoms, is due to the small size $\alpha = 1/137$. Otherwise, we could not talk about the permissible states in the atom. In particular, only due to the small size of α, the electron can be in the excited state for a relatively long time before moving to the lower energy state with the radiation of electromagnetic wave.

2.3 Evolution of the Universe

This problem follows from the physics sections described above in Fig. 2.2, gave rise to all the particles and fields of the interaction that arose in a process цршср obeys the only laws of nature. Figure 2.3 shows a *conditional* diagram of this evolution. The time *t* is plotted along the abscissa-axis from the moment of the origin of the Universe until our time (about 14 billion years). A conditional and compressed scale is used: first the time is given in fractions of a second, then in seconds, and finally in years. The scale is chosen so that it is convenient to explain what happened at different stages of the evolution. The size of Universe in meters is plotted on the ordinate-axis from point “0”. It is believed that the Universe has now expanded to the radius $R \approx 10^{26}$ m.

The continuous curves which have emerged since the birth of the Universe and have been drawn so far, depending on the size of the Universe (which is expanding), are arbitrary but correspond to *four* fundamental interactions known in

physics. The sequence of curves denoting *gravity* (1), *weak interaction* (2), *electromagnetic interaction* (3) and *strong interaction* (4) conditionally indicates the relative strength of these fundamental interactions.

The weakest interaction is the *gravitational* interaction: its constant is estimated to be ~ 10^{-39}, which is 10^{33} times less than the subsequent weak nuclear interaction with interaction constant ~ 10^{-14}. However, the gravitational interaction acts *everywhere*: its radius is infinite ($R_g = \infty$), while the radius of action of the weak interaction (characteristic of elementary particles) is extremely small: $R_w \sim 10^{-16}$ cm.

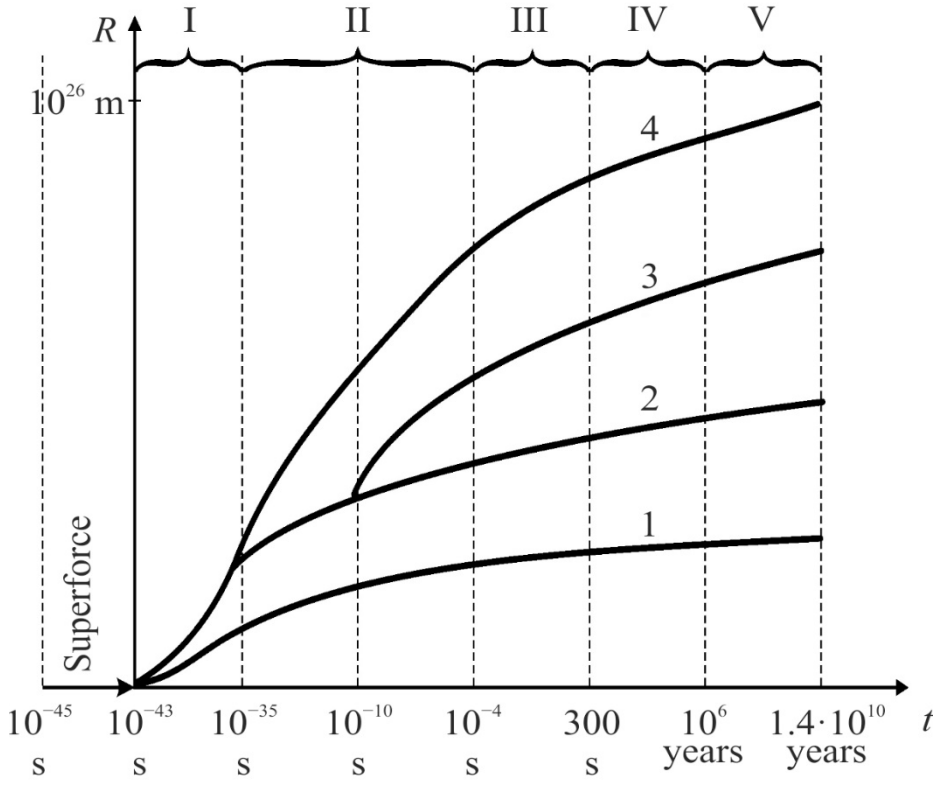

Fig. 2.3. Schematic representation of the evolution of the Universe: 1, 2, 3, 4 – basic interactions, I–V – periods of evolution.

The next strongest *electromagnetic* interaction with interaction constant ~10^{-2} much stronger than gravitational one and also has infinite radius *($R_{em} = \infty$).* However, this interaction is much inferior in strength to strong (nuclear) interaction, where the interaction constant is equal to 10, although the radius of the strong interaction is quite small: $R_w \sim 10^{-16}$ cm (as the size of atomic nuclea and the size of electron) Using the figure shown in Fig. 2.3 scheme, we can list the main stages of the evolution of the universe – according to the theory of the Big Bang. In this theory of "inflation" (expansion) of the Universe is associated with physical processes occurring in a vacuum, and the theory combines processes in the microworld and megaworld. According to nowadays ideas, a vacuum is a complex and ubiquitous

dynamic quantum mechanical system that constantly and everywhere generates the virtual particles and antiparticles. Quite complex processes in a vacuum, called "inflationary", underlie the birth of the Universe.

Our Universe originated about 14 billion years ago from an initially extremely small volume and began to expand very rapidly. This period in the history of the Universe is called the period of inflation. Before inflation, there was only one kind of fundamental interaction between the elementary particles that filled the Universe. This interaction is called "Superpower". At the time of 10^{-43} s, the gravity separated from the Superpower (curve 1 in Fig. 2.3). The era of inflation (period I) lasted a very short period of time: from 10^{-43} to 10^{-35} seconds; but the theory of this earliest stage of development of the Universe is not yet complete.

The Gravity exists as a separate fundamental force in our time.

Then, in addition to Gravity, there were three interactions: the Strong, the Electromagnetic and the Weak, and began a period that in the theory of the Big Bang received a strict theoretical justification. Thus, in the process of evolution of the Universe, a single interaction (Superpower) broke up into four fundamental interactions.

Then, in the process of evolution of the Universe, material structures of inorganic nature were formed.

In the period of ***inflation*** (10^{-43}–10^{-35} s, period I), there was only the root cause of the appearance of everything material in the future. At the time of inflation, the temperature of the universe was ~10^{30} K, so that matter could exist only in the form of the radiation, elementary particles and antiparticles. In the following stages of evolution, the particles and antiparticles were annihilated in pairs, turning into radiation. Only a certain number of particles survived (which is still quite a significant number: about 10^{80}). Note that research in the field of elementary particles is relevant: the 2008 Nobel Prize in Physics was awarded to J. Nambu, M. Kobayashi and T. Maskawa (scientists from the United States and Japan) for discovering a spontaneous violation of electrically weak symmetry and for explaining the causes. They proved the existence in nature of three varieties of quarks due to which, as the forces of interaction between particles increase, they jump into a new state – from non-mass to mass (particles gain mass).

In the period of 10^{-35}–10^{-4} s, the time of ***hadrons*** occurs (indicated in Fig. 2.3 by period II), and further expansion of the Universe continues according to the Big Bang theory. The temperature of the Universe decreases from 10^{28} K to 10^{12} K. At the end of this period of time, the quarks merged into hadrons, which include, in

particular, the protons and neutrons. Thus, the particles that make up the nuclei of atoms were formed. However, in the period of hadrons, the union of the neutrons and protons in the nuclei of atoms could not yet occur, because the temperature was still too high ($T > 10^{12}$ K).

During the ***lepton*** period (10^{-4}–300 s, period III), a reaction takes place between the protons and neutrons, as a result of which the ratio of the number of remaining neutrons to the number of protons became approximately 0.15. By 300 s, the temperature of the expanding universe had dropped to 10^9 K, and the conditions has formed for the formation of hydrogen (deuterium) and helium nuclei.

This was the beginning of the ***photons*** period, which lasted from about 300 s to 10^6 years (denoted by IV in Fig. 2.3), until the neutrons were spent entirely on the formation of helium nuclei (~25%), and the remaining protons later appeared as nuclei hydrogen atoms (~75%). Approximately the same ratio between the content of helium and hydrogen is preserved on average in the Universe today.

After the formation of the nuclei of light elements, the substance was ***plasma*** for a long time (~10^6 years). The high temperature did not allow neutral atoms to exist. Only after the temperature of the Universe dropped to about 4.000 K the electrons begin to stay close to the nuclei, forming the hydrogen and helium atoms. The activity of the interaction of photons with a matter has weakened, and the Universe, which was previously opaque, has become transparent. The period of ***matter*** (the period of stars) has begun, and continues today.

The above shows that in the periods of hadrons, leptons and photons, ie before the period of matter (V in Fig. 2.3), material systems became more complex and diverse by the combining elementary components into the increasingly complex structures. Substances (due to the gravitational forces) and huge condensations of a gas began to form around the initially rather weak inhomogeneities. Eventually, they turned into galaxies, which, in turn, disintegrated on the proto-stars. Compressing, the proto-stars heated to their own glow and thus became stars.

As a result, initially a continuous, almost homogeneous plasma medium of the Universe was transformed due to gravitational (and to a lesser extent – electromagnetic) interaction into the isolated star clusters – galaxies. There were new processes of the self-organization, which led first to the nuclear transformation of stellar hydrogen into a helium, as well as into the heavier elements (up to iron), and then into even heavier elements (up to uranium) – in the explosions of stars into metastable state ("supernova explosions"). Thus appeared the "building material" for the emergence of matter.

It is well known that main building material is the atom consisting of protons, neutrons and electrons.

[**Note.** When the *proton* is "far" from the nucleus (i.e., at a distance greater than 10^{-12} cm), it is possible to take into account only its electrical (Coulomb) repulsion from the nucleus. Therefore, a proton can approach the nucleus only, if it has a very high energy. For a *neutron*, there is no Coulomb repulsion, and it does not prevent its collision with the nucleus. When approaching the nucleus at a distance of about 10^{-13} cm, other, more powerful forces act on the protons and neutrons, which can overcome the mutual repulsion of protons. Thus, the electrical interactions in the nuclei are replaced by others – the nuclear interactions. It should be noted that nuclear forces do not act on the electrons.

Coulomb's law (slow decrease in electrical interaction with distance) is due to the *zero mass* of the photon. Nuclear forces (which hold *nucleons - protons and neutrons* in the nucleus) are characterized by the opposite case: these forces of interaction decrease with a distance much faster than the Coulomb forces. This *short-interaction* is due to the non-zero mass of particles which provide the binding of nucleons in the nucleus. It is convenient to approximate the rapid change of nuclear interactions with distance by "enhanced" Coulomb potential: the Yukawa potential: $U(r) = (q_1q_2/4\pi\varepsilon_0 r)\cdot\exp(-r/r_0)$, where is the radius of action $U(r)$. This radius is related by a simple relation to the mass of the particle: $r_0 = \hbar/me$. With strong interaction, the nuclear forces are two orders of magnitude larger than Coulomb forces, but act only at short distances: the radius of action of nuclear forces is $r_0 \sim 10^{-13}$ cm. Nuclear forces are provided by the particles called π-mesons (i.e., "intermediate"). This name is due to the fact that the mass of π-meson appears to be intermediate between the mass of electron me and the mass of proton m_r: $m_{mez} \sim \sqrt{m_e m_p} \sim 300\, m_e$. It should be noted that the same estimate of the mass of mesons is obtained using the formula $r_0 = \hbar/me$ under the assumption of $r_0 \sim 10^{-13}$ cm.

Three types of π-mesons have been experimentally identified: π^-, π^+ i π^0 – the upper index corresponds to the sign of the electrical charge of the meson. Thus, main carrier of the coupling forces between the nucleons can be both neutral and electrically charged. Charged mesons (π^- and π^+) can emit and absorb photons. The spin of all π-mesons is zero: unlike electrons, mesons are the Bose particles. As you know, particle physics deals with hundreds of different particles. However, they all arise and, as a rule, quickly disappear in the process of nuclear reactions and can be ignored when studying the problems of the physics of condensed matter. Thus, at distances of the order of 10^{-13} cm and less the *nuclear forces* operate. They bind nucleons (protons and neutrons). For nuclear forces, the neutron is "charged" and the electron is "neutral", i.e., the electron does not interact with the nucleon with nuclear forces, even if it approaches it at a distance of 10^{-13} cm. But the electron interacts with the proton by the electromagnetic field. The radius of the electron determined by the methods of classical physics is considered to be of the order of $r_e \sim 10^{-13}$ cm. This value is based on the assumption that the electron is a charged sphere and its electrostatic energy can be found: $U_{el} \sim e^2/r_e$. This assessment is not conclusive, because it is not clear whether Coulomb's law can operate at such a distance. In addition, since the electron is an elementary particle, the forces holding its charge are not clear.

It should be noted that in quantum theory one could also add the notion of ***fundamental length*** λ_0 and ***fundamental time interval*** $\tau_0 = \lambda_0/c$. In other words, in comparison with the classical

mechanics, where both *space* and *time* are *continuous,* the very structure of the space and the time is revised. The presence of a fundamental length λ_0 means the abandoning this continuity in favor of *discrete space-time*. From the set of experimental data, it follows that the fundamental length is of the order of $\lambda_0 \approx 10^{-13}$ cm. Note that this value corresponds to the assumed electron radius. Since the size of the atom ($a_0 \sim 10^{-8}$ cm) is 10^5 times larger than the size of both nucleus ($r_{\text{nucl}} \sim 10^{-13}$ cm) and electron ($r_e \sim 10^{-13}$ cm), then, from the point of view of classical mechanics, the atom may seem "empty".

However, in the study of solid state physics and nanophysics, in most cases it is enough to consider the space and the time as *continuous*, as well as the fact is that the crystal (and the nanoparticle) consists only of atoms (or ions) and "free" electrons (electromagnetic waves do not belong to this basis). It is known that when an excited atom appears in a solid body that "seeks" to go into a state with less energy, this transition is achieved by the emission of excess energy in the form of electromagnetic wave (light). However, this does not mean that the excited atom *contains* a light wave: last was created at the time of transition of an excited atom to the atom in a ground state. The wave whose length is 10^{-1}–10^{-4} cm cannot be “contained” in atom whose size is only ~ 10^{-8} cm.].

2.4 Particles, waves and their dualism

Thus, it has been established that solids consist of atoms, and atoms – of elementary particles: electrons, *protons* and *neutrons*. A particle is *elementary*, if it cannot be described as a complex system consisting of other, more elementary particles. If we do not take into account the hypothesis of "quarks", the components of the atom – electrons, protons and neutrons – are really elementary. All these particles that make up the atom have their own magnetic moment. Their properties are described by both classical and quantum mechanics.

Currently, especially in connection with annually emerging new data as to the structure of matter, obtained on the Large Hadron Collider[*)], there is increased interest in particle physics.

[Note. The Hadron Collider is the charged particle accelerator on oncoming beams, designed to disperse protons and heavy ions (lead ions), built in the research center of the European Council for Nuclear Research. Hadrons (from the Greek hadros – strong) is a class of elementary particles that interact strongly and are not truly elementary. Hadrons are divided into two main groups according to their quark compound: mesons consist of one quark and one anti-quark, and baryons consist of three quarks. The main part of matter observed by us is built of baryons: nucleons make up the nucleus of an atom and are represented by a proton and a neutron. Baryons also include numerous hyperons – heavier and unstable particles obtained on particle accelerators. The Hadron Collider will help confirm theories of the origin and structure of the universe.]

In classical mechanics, the basic object of study is a *material point* moving along a certain trajectory. It is given by the initial conditions (mass, coordinates, speed), as well as the forces acting on the material point. The atomic structure of a matter, at first glance, corresponds to this basic image of classical mechanics. Material points are *atoms, electrons and protons* – that is, those particles which should be considered elementary when considering an atom.

That is why, in classical physics, the properties of solids can be understood as the properties of sets of particles (material points) which interact with each other and move along certain trajectories. The forces of interaction between them must be known (note that quantum mechanics does not audit the existence of forces of interaction). Thus, the basis of the classical mechanical worldview is a material point – a particle, which can be said exactly where it is at a given time and how fast it moves. However, the classical worldview is not limited to the concept of a material point. The discovery of radio waves and the elucidation of the wave nature of light have shown that the matter exists not only in the form of particles, but also in the form of waves. A wave is a *space-time periodic process*.

The *spatial* characteristic of elementary wave is its *length* λ, measured in meters, [m]. The *time* characteristic of the wave is the *period* of oscillations T, measured in seconds, [s]. However, in the solid state physics, to characterize the wave the *inverse* of these dimensions are used: the circular frequency of the wave $\omega = 2\pi/T$ [radian·s^{-1}] and the wave vector $k = 2\pi/\lambda$ [m^{-1}]. In Fig. 2.4 the temporal and the spatial representations of this simplest one-dimensional wave are artificially separated.

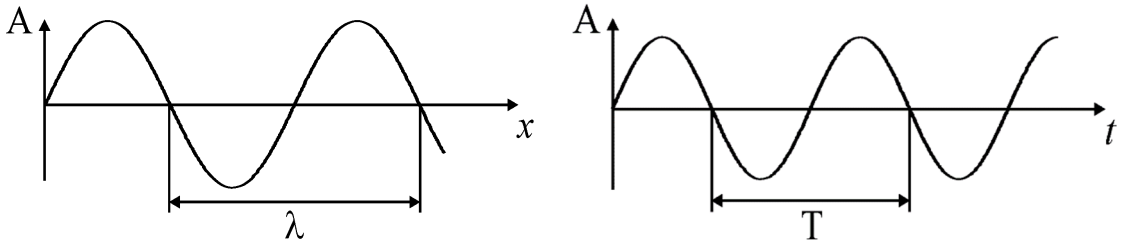

Fig. 2.4. Spatial A(x) and temporal A(t) representations of wave, A is amplitude of wave.

In the classical physics it is always clear what exactly fluctuates. In the case of ordinary mechanical oscillations (for example, sound waves) the oscillating motion is made by the particles of a matter (gas, liquid, solid). When it comes to the electromagnetic oscillations, the usual classical ideas are not suitable, because nothing that has no mass can oscillate. The electromagnetic wave (in its simplest form - a plane wave of a certain frequency) is another form of existence of matter -

the electromagnetic field. In this case, the elementary form from which all sorts of electromagnetic fields are constructed is an infinitely long wave in space and time.

The concept of *two velocities* is also connected with the wave. First, for the speed of movement of the wave is the phase speed $\upsilon_{phase} = \omega/k$ is used, which characterizes the structure of a wave, but does not directly determine the rate of energy transfer by wave. This is the second velocity $\upsilon_{group} = d\omega/dk$. which is called a group velocity because it is at this velocity that the *wave packet* (group of waves) propagates [4].

The equality of two velocities $\upsilon_{phase} = \upsilon_{group}$ means the absence of a *dispersion* in the medium where the wave propagates, i.e., the frequency is directly proportional to the wave vector.

This is exactly the situation with the propagation of electromagnetic waves in a vacuum: $\upsilon_{phase} = \upsilon_{group} = c = 3 \cdot 10^8$ m/s (c is the speed of light). If we go from the frequency to the wave energy $E = \hbar\omega$ and from the wave vector to the pulse $p = \hbar k$, we obtain the dependence of the energy of the "particle wave" on its pulse *E(p),* which is also called the *dispersion*, and it is the most important characteristic of the wave process.

Unlike a vacuum, the dispersion is inevitably observed when electromagnetic wave propagates in any solids which are partially transparent to it. Electromagnetic waves in solids, firstly, slow down: as υ_{group} *so* $\upsilon_{phase} < c$, and secondly, these velocities become dependent on the wave vector according to different functional laws. As a result, the dependence $\omega(k)$ becomes not directly proportional, i.e., there is a dispersion of the waves.

The slowing down of electromagnetic waves in the partially transparent solids is explained by the fact that these waves excite the oscillations of the bound electrical charges (electrons, ions), and such oscillations "carry" the electromagnetic wave.

But now the wave is accompanied by a spatial oscillating displacement of material particles with a certain inert mass (which was not in a vacuum), and this is what reduces the speed of the electromagnetic wave in the volume of a solid.

It is also interesting to note that the period of oscillation of the electromagnetic wave remains the same, but the speed decreases. This results in a reduction in the length of the electromagnetic wave as it propagates in the volume of a solid.

It is pertinent to note that at frequencies of 10^{16}–10^{17} Hz and above (*X-rays* and *gamma rays*) no electric charges due to their inertia can oscillate due to very large frequency of wave and, thus, solids become completely electromagnetically transparent.

At the first glance, the concepts of "wave" and "particle" are incompatible, mutually exclusive. Indeed, according to classical notions, a particle is something small that is in a certain place at any given time and moves at a certain speed. On the contrary, the wave is something common that fills the whole space. However, quantum mechanics for small particles, i.e., in the region of large relations $\hbar/S$ (Fig. 2.1) clearly indicates the *duality* (dualism) of the manifestation of the properties of both particles and waves [6-7].

In other words, micro-objects have the properties of both particles and waves. Next, it is considered the wave properties of particles. A strict explanation of the properties of micro-objects and their interactions is described in quantum mechanics exclusively by mathematics, and is usually not obvious. However, quantum (wave) mechanics allows us to preserve the idea of particles as the "clots" of matter, if we introduce them into the overall picture of waves, which corresponds to these "clots".

For example, the free motion of an electron in space can be imagined as the propagation of a wave packet, Fig. 2.5. At some point in the wave field is the electron itself, but where there is no wave, the probability of finding an electron is close to zero. The height of the wave (amplitude) characterizes the probability of finding a particle at a certain point, or more precisely - the probability is proportional to the square amplitude of the wave.

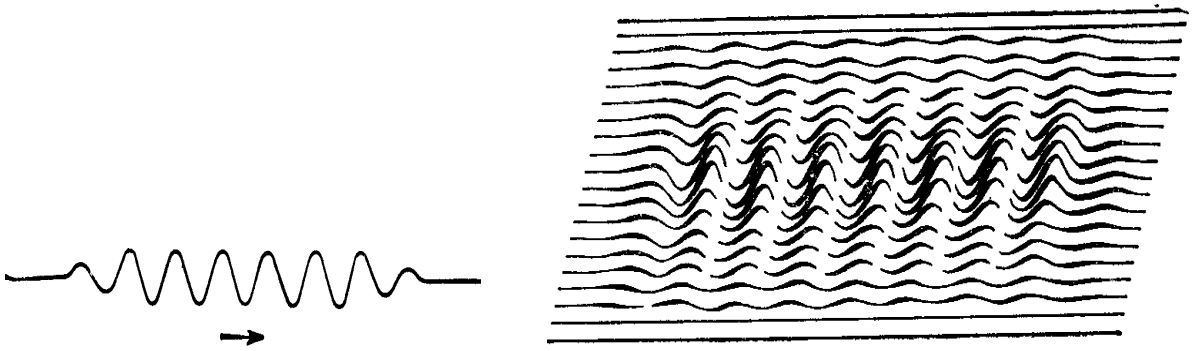

Fig. 2.5. Wave packet: one-dimensional (a) and two-dimensional (b) representation.

Such is the modern idea about the nature of waves which accompany particle. By calculating the probability waves for a given particle under different conditions, you can calculate the probability of finding a particle in the particular area of space. However, the wave packet generally characterizes only the free (or almost free) motion of the particle: for example, the motion of a "free" electron in a metal or semiconductor.

2.5 Quasiparticles in solids

Solid body is characterized by the mechanical strength, hardness and rigidity that seemingly exclude the possibility of any internal movement. However, there are many different types of the microscopic motions and displacements in the solids:

• The movement of structural defects is the displacement of interstitial atoms, dislocations, and vacancies. The fact is that the energy of a crystal is locally increased in the vicinity of defects, so that the defects move (very slowly) in order to find the energetically more favorable configuration.

• The diffusion transfer is a classic example of the motion of atoms in solids, which mechanism is the result of thermal fluctuations. Due to them, kinetic energy of some particles increases enough to overcome potential barrier, which separates one particle from another.

• The electrons and other charged particles (cations and anions) can move in solids, that determines many electrical and magnetic properties of a matter. At that, their directional movement is the conductivity. Compared with the high velocity of electrons, the velocity of ions is very slow, which makes it possible while investigations of the electrons motion consider the ions or atoms as the immobile particles. This is adiabatic approximation, the accuracy of which is determined by the parameter $(m_e/M)^{1/2}$ – the ratio of electron mass m_e to the mass of ion M.

1. Quasiparticles and collective motions. Next, the completely different movements in the crystals are considered. These include, for example, the microscopic oscillations and other excitations of the particles, which can exist and extend through a crystal in the form of *weakly interacting waves*. To explain the main characteristics of solids, it is generally considered that they contain some "hidden" states – the quasiparticles, which are the collective movement (e.i., local vibrations in the crystal lattice) of other many closely located atoms of solids. Many atoms are involved in each excitation; nevertheless, this movement has an *atomic* scale.

Thus, to explain very diverse characteristics of solids, it should be imagined that there are some other (not obvious) dynamic changes – quasiparticles – which resemble the properties of other aggregate states of matter and can behave *as a gas* (the vibrations of atoms in the lattice), as a *quantum fluid* (the electrons in metal), and even as the *plasma* (electron–hole clouds in semiconductors).

Formally, the quantum mechanics describe the microscopic objects only mathematically and, certainly, any simplified conventional model of the

quasiparticles is inadequate. Nevertheless, the quantum mechanics allows the retention of the idea of quasiparticles as some *mobile clusters* within a crystal; moreover, they might be described by the overall picture of waves that appear as the "wave-clots" or "wave-packets", Fig. 2.5).

For example, the free movement of electrons in a crystal can be imagined as the spreading of a wave packet. The actual electron might be located at any point within this packet, and the probability of finding the electron in any definite point is close to zero. In Fig. 2.5, the wave amplitude describes only the *probability* of finding a particle at some point; more precisely, this probability is proportional to the square of the amplitude of a wave. This simple model only promotes the understanding that moving quasiparticle is accompanied by a wave.

The quasiparticle might be interpreted both as the *collective motions* of some particles in a solid or as *the local vibrations* of some atomic group in a crystal lattice. Although this oscillation involves many atoms, this movement nonetheless has the *atomic scale*, because the average energy of each oscillation (phonons) equals approximately k_BT. Another example of collective motion is the electronic excitation of atoms or molecules that, for example, arises when the crystal lattice absorbs photons. This collective excitation is not localized within a particular cell of the crystal, but moves from cell to cell in the form of *exciton*. The average energy of excitons has the same order of magnitude as the energy of the excited state of *individual atoms*. At that, there are some phenomena in solids that involve *several* quasiparticles. For description of the magnetic properties in the ordered magnetics, the magnons are used with the assumption that the magnon is the quantum fluctuation of electronic spins. Another example is that electrical charge transfer is described mostly by the electrons (in dielectrics – by *polarons*), whereas the heat transfer can be attributed to the phonons, electrons and magnons.

In accordance with classic laws, the average energy of thermal motion of particles equals k_BT and, therefore, the internal heat in a solid is $E \sim N \cdot k_BT$, where N is the number of particles. However, with decreasing temperature, this simple linear dependence of energy on temperature $E(T)$ is violated, because the internal energy of solids tends to become zero much faster than it would occur linearly. This fact can be explained by a discrete (quantum) nature of the energy spectrum of solids. Thus, with decreasing temperature, a part of the collective excitations of atoms (or ions) freezes out. This process is initiated near the Debye temperature, usually $\theta_D \sim 100–300$ *K*, however, in some crystals, the nonlinearity in the $E(T)$ dependence is observed at much higher temperatures. The greater the difference between the energy levels, the higher the temperature of freezing out of the appropriate motion.

Therefore, the quantum motion in solids may occur at different temperatures. With the exception of electrons, phonons, excitons, and magnons, the quanta of electromagnetic field – photons – can be excited and may spread in solid dielectrics and semiconductors.

In *summary*, it can be concluded that:

• In fact, the materials consist only of *three kinds* of elementary particles: electrons, protons, and neutrons. The quasiparticles represent just the convenient theoretical model of solids that is used to explain the majority of crystals properties; it is obvious that quasiparticles can exist only inside a solid.

• Internal movements in solids might be very complicated; as example, the simple classic motion in solids exists as the transfer of structural defects, the diffusion of atoms and ions, and the movement of electrons. However, only these cases are insufficient to describe many electrical and thermal properties of solids, because the more complicated collective movements need to be considered. This is precisely the motivation for the concept of quasiparticles and collective excitations. Thus the complicated motion of actual particles in solids can be artificially described by a simple motion of *imagined* quasiparticles, which behave more like the non-interacting particles.

• Strictly stated, the elementary excitations might be regarded as the "*quasiparticles*", if they are the *fermions*, and as the "*collective excitations*", if they are the bosons. However, in further discussions, both are united under the term "quasiparticle" without any precise distinction. For example, the free electron is a particle with a definite value of weight (rest mass), but in a crystal it behaves as if it has another "effective mass", because it is affected by the environment; in both cases, the electron always is the fermion. Another example is the phonon that characterizes the oscillatory motions of neighboring atoms in a crystal; it is the collective excitation in a lattice because it has no "rest mass", being the boson.

• The quasiparticles are a mathematical tool for simplifying the description of many properties of solids. Instead of inconceivable difficult account of "how a large number of electrons and atoms moves in a specific coordinated way", the simplified concept of the quasiparticles is used.

• In most solids, the elementary excitations (quasiparticles) are treated as free (independent) but, in reality, they are only very close to being understood as independent. In many cases, it is necessary to take into account their *interaction*, for example, when explaining the electrical resistance by the electrons scattering on the phonons or the thermal resistance by the phonon-to-phonon scattering.

• Using the concept of "quasiparticles/collective excitations," it is possible to deal only with a handful of somewhat-independent elementary excitations, instead of analyzing the interactions of a very large amount of particles in solids (~10^{23} cm^{-3}). Therefore, this is a very effective approach to simplify many-body problems in quantum mechanics.

• The *electron* in solids is a quasiparticle, because it is affected by the forces and interactions. The "quasiparticle-electron" has the same charge and same spin as the "elementary particle-electron", and both are fermions. However, in a crystal, the mass of the "quasiparticle-electron" can differ substantially from a normal electron: it has an effective mass that might even be anisotropic.

• The *hole* is a quasiparticle consisting of a lack of electron in a crystal cell; the hole has an opposite sign of its charge to the electron, also has an effective mass and belongs to the classification of fermions. This concept is commonly used in the context of empty states in the valence band of a semiconductor.

• The *exciton* is a complex of electron and hole bound together.

• The *polaron* is a quasiparticle that describes electron's interacting with surrounding ions by local polarization of a dielectric; polarons have increased effective mass and belong to the class of fermions.

• The *phonon* is a collective excitation associated with collective oscillation of atoms (or ions) in a crystalline structure. It is a quantum of the elastic wave and belongs to bosons, with a rest mass of zero.

• The *magnon* is a collective excitation associated with electronic spin structure in the ordered magnetic lattice. It is the quantum of a spin wave; its rest mass is zero; and it belongs to the classification of bosons.

• The *photon* inside a crystal is a quasiparticle, because it is dependent on interactions with material. In particular, the "photon-quasiparticle" has a modified relation between energy and impulse (dispersion relation) that is described by the index of refraction of a material.

• The *polariton* is a special form of the photon in crystal, especially seen near its resonance with the lattice vibrational mode. For example, the excited polariton is a superposition of photon on phonon.

• The plasmon is a collective excitation that is the quantum of the plasma-type oscillations (wherein electrons simultaneously oscillate with respect to the ionic lattice).

2. Heisenberg's uncertainty principle and Pauli's principle are purely quantum phenomena and have no analogy in the classical mechanics.

The wave properties of micro-particles make it impossible to describe their behavior by simultaneously setting exact values of *coordinates* x and *velocities* (momentums p). This fact is mathematically described by ratios of Heisenberg uncertainties (Nobel Prize, 1932). The uncertainty principle states that products $\Delta p_x \cdot \Delta x \geq h/2$, $\Delta p_y \cdot \Delta y \geq h/2$ and $\Delta p_z \cdot \Delta z \geq h/2$; where the Δp_x, Δp_y *and* Δp_z are the uncertainties of the components of the particle momentum along the *x*, y and *z* axes, respectively, while the Δx, Δy and Δz are the uncertainties of the values of the particle coordinates at the same time. Thus, the wave properties of microparticles make it impossible to describe their behavior by the simultaneously setting the exact values of coordinates and velocities.

It is interesting to note that for combinations such as $\Delta p_x \cdot \Delta y$, $\Delta p_y \cdot \Delta x$, $\Delta p_z \cdot \Delta y$, etc. the uncertainty ratio does not work - the uncertainties of the values of unconjugated coordinates and components of the momentums can independently have any values. This feature of the uncertainty ratio is of great importance in the analysis of the behavior of electrons in the *nanoscale structures*.

The uncertainty relation also holds for energy and time variables: $\Delta E \cdot \Delta t \geq h/2$, where ΔE is the uncertainty of energy of a system in the considered quantum state, and Δt is the time the system is in this state.

The ratio of uncertainties refers to the fundamental provisions of physics; it has comprehensive experimental confirmation.

It has already been pointed out that the transition to classical mechanics can always be performed if $h = 0$. According to Heisenberg's principle, the uncertainties of both the coordinate (Δx) and the momentum (Δp) can be zero at the same time, so the fraction can have defined trajectory. The principle of uncertainty does not impose the restrictions on the motion of the macroscopic bodies.

When logically substantiating the uncertainty ratio, we can conclude that it has a wave origin. Indeed, a relationship of this type takes place in the wave optics. As already mentioned, a flat wave fills the entire space. However, it is known that the electromagnetic field can be concentrated in a limited (and even quite small) area of a space. Only for this purpose it is necessary to use a large number of waves: some of them amplify each other, others, thanks to interference, extinguish each other.

A possible "construction" of waves (wave packet) has already been considered in connection with Fig. 2.4B. The wave packet can be described by the interval of wave numbers Δk required for the concentration of the electromagnetic field in the region of space Δx. The set of wave vectors is the wider, the smaller the size Δx of the packet in space. There is a purely wave relation: $\Delta x \cdot \Delta k \geq 1$, where Δx is the size of the wave packet in space (“uncertainty” of the coordinate), and Δk is

the uncertainty of the wave vector in the wave packet. By comparing this inequality with the uncertainty relation $\Delta x \cdot \Delta p \geq \frac{1}{2}\hbar$, we can obtain the de Broglie relation: $p = \hbar \cdot k$.

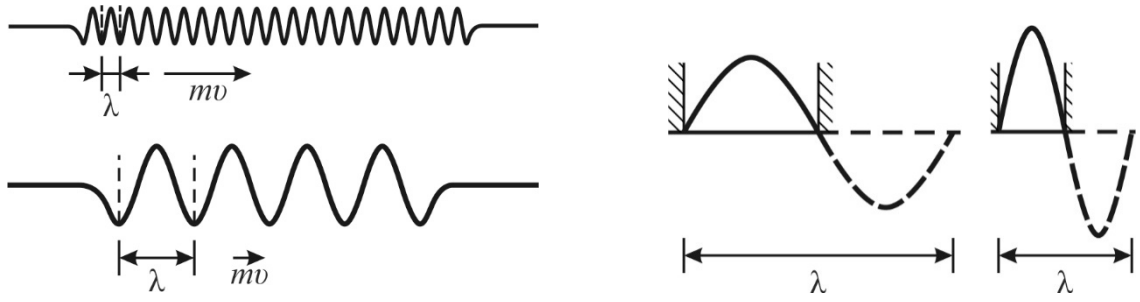

a b

Fig. 2.6. To uncertainty principle: a – wavelength λ and momentum mυ for fast and slow particles; b – reducing the space available for a particle requires reducing its wavelength.

Proposed for the first time by de Broglie, this important ratio of the wave mechanics relates the velocity of a particle to its wavelength. It is stated that p (the momentum of a particle) is inversely proportional to λ (its wavelength): $k = 2\pi/\lambda$. The momentum of particle is equal to product mass of particle by its velocity: p = mυ. Thus, according to the above ratio, the faster the particle moves, the shorter is its wavelength. In other words, the probability waves of a fast-moving electron and slow-moving electron will be significantly different, as schematically shown in Fig. 2.6a.

Based, first, on the relationship between the probability of a particle at a given point in a space and the square of the amplitude of its wave at a given point and, second, on the relationship between the velocity of a particle and its wavelength, we can establish the basic laws for atoms. The behavior of electrons in an atom is described as follows: if the electron is forced to be in a small volume of space, then its wavelength must be short, so that it "fits" in the allotted volume, Fig. 2.6b. But if the wavelength is small, then due to the de Broglie ratio, the velocity of the particle (electron) must be large. It follows that there must be a large kinetic energy of the electron, which is proportional to the square velocity of the particle.

Thus, the uncertainty principle means the recognition of particle wave properties. The alternative of the terms "wave" and "particle" (or wave or particle) is violated on two sides. Both on the part of the particles that have acquired wave properties and on the part of the waves, they have acquired corpuscular properties. The wave properties of particles, as well as the corpuscular properties of waves, have been repeatedly confirmed experimentally. It has been shown, for example, that an

electron behaves like a particle in some cases and like a wave in others. For example, the corpuscular properties of wave motion are manifested in the fact that the energy E of waves with frequency ω is equal to the integer number of energy quanta $\hbar\omega$ ($E = n\hbar\omega$, де $n = 1, 2, 3, ...$), and the momentum $\boldsymbol{p}$ is equal to $n\hbar\boldsymbol{k}$.

For solid state physics and, especially for the nanophysics, an important consequence of the uncertainty principle is that the motion of a quantum particle (electron, ion, atom), which is localized in a limited volume of space, cannot stop even at the lowest temperatures: stopping the thermal motion of an atom , ion, etc. at a temperature $T \to 0$ would mean that its momentum $p = 0$ (and, as a consequence, $\Delta p = 0$). This contradicts Heisenberg's principle because it requires complete delocalization of the particle ($\Delta x = \infty$). Thus, even near absolute zero temperature in crystals, there is an irresistible quantum motion, which is called "zero oscillations".

Thus, if the absolute temperature $T = 0$ K was achievable, then in this case the atoms in the solid would make "zero oscillations". For this reason, in particular, helium at normal pressure, even at the lowest achievable temperature of ~ 10^{-6} K, cannot crystallize (“freeze”) - it remains a liquid. For the same reason, for example, spontaneous polarization cannot occur in the paraelectrics such as strontium titanate or potassium tantalate. Spontaneous polarization would mean a spontaneous shift from the center of electrical symmetry of the active ions and their fixation in the crystal lattice, as this is hindered by quantum "zero oscillations".

The uncertainty ratio is a natural consequence of the corpuscular-wave model of micro-particles, which is based on quantum mechanics.

Quantum mechanics also explains why all atoms of the same substance (for example, hydrogen) are the same: because they are all in the same (ground) state. But this fact is not enough to explain the periodic Mendeleev's law, that is, to substantiate both the similarities and differences in the physicochemical properties of atoms of different elements. The explanation of these and many other properties of atomic objects is given by the *Pauli principle*. The ordinal number of the element Z corresponds to the number of electrons in its atom. But the fact that different atoms have different numbers of electrons is not enough to understand the properties of chemical elements.

As shown above, the nucleus of an atom together with the electrons creates some electrical field, and each electron moves in it. There are the "allowed" states in this field, and the lowest among them. It would seem that it should contain all the electrons. But in this case, the addition of another electron does little to change, especially if the number Z is large. However, this picture is very different from the reality: it is enough to compare the properties of argon Ar and potassium K, i.e., inert

gas and alkali metal, in which the number of electrons (atomic numbers) differ by only one. Quantum mechanics, to explain the properties of elements and many other laws of microscopic physics, must use, in addition to the principle of uncertainty, another principle of prohibition, formulated by Pauli.

This principle forbids two (or more) electrons to be in the same state. That is, each electron *must have its own state*. Sometimes two states are combined into one and the formulation of the Pauli principle is changed accordingly: one state for two electrons (however, not all particles in nature obey the Pauli principle).

This prohibition is so strict that it cannot be overcome by the natural desire of any physical system for a particle to occupy a state with the lowest energy. The periodic law finds its explanation in the arrangement of electrons of atoms by states, taking into account the Pauli principle. Thus, quantum mechanics is the basis not only of physics but also of chemistry.

The study of the electrical and magnetic properties of a matter makes it possible to better understand the nature of interactions. The electrical fields of atomic nuclei are large and they are determined by the number of protons in the nucleus. In this case, the nuclear magnetism is three orders of magnitude smaller than electronic magnetism, and, therefore, the properties of nuclei could not be taken into account in the electronic materials science when studying electronic magnetism. It should be noted, however, that the method of nuclear magnetic resonance "on protons" is used in physics and medicine to diagnose the structure of matter.

Thus, the electronic materials science and especially nanophysics sometimes have to take into account the more "subtle" structure of a matter. The main "structural elements", in addition to electrons "e", are the protons "p" and neutrons "n". The atomic number of chemical element corresponds to the number of electrons in the neutral atom and this number is equal to the number of protons in the nucleus (the "*principle of electrical neutrality*" is observed). However, when determining the mass of the atom, electrons can be ignored: the electron is ~1840 times lighter than the proton or neutron (however, this number "1840" cannot be obtained from the fundamental constants). As the experiment shows, the size of the atomic nucleus is of the order of 10^{-13} cm, which is negligible compared to the size of the atom (10^{-8} cm). Since the mass of nuclei is four orders of magnitude larger than the mass of electrons, the nucleus can be considered "infinitely heavy" when considering electronic processes, which is used in condensed matter physics to substantiate the band theory of electronic spectra ("adiabatic hypothesis").

Comparative parameters of the electron, neutron and proton are given in the table, in which the charge of a particle is given in units of charge of the electron, and

the mass of the particles is given in units of electron mass, the magnetic moment of the electron is taken as 1.

Table 2.1

Parameters of some elementary particles

	Charge	**Mass**	**Spin**	**Magnetic moment**
e	–1	1	½	1
n	0	1840	½	1,9/1838
p	+1	1838	½	2,89/1838

All the particles listed in the table are fermions, because their spin is equal to ½, i.e. is "half-integer". The magnetic moment of a neutron, despite the lack of electric charge, is almost 2 times greater than that of an electron. A proton is characterized by a slightly higher magnetic moment than a neutron.

3. Photons. In addition to particles, which have a certain charge, mass and spin (electrons, protons and neutrons), the wave nature of which is manifested in the description of solids and nanostructures properties, the photons - quantums of the electromagnetic field energy - play an important role. In constructing the theory of external photoeffect, Einstein showed that light is not only emitted and absorbed by quanta, but also *propagates* as a stream of special particles (photons) carrying a discrete portion of energy equal to $h\nu$ ($\nu = \omega/2\pi$ - wave frequency in *Hz*). On the basis of quantum ideas about light, Einstein explained not only the photo effect, but also other physical phenomena that could not be described in terms of wave (electromagnetic) theory of light (Nobel Prize, 1921).

It should be noted that the duality of the nature of a light was proved much earlier than the wave properties of the electron were discovered. The first assumptions about the discrete structure of light were formulated not only because it corresponded to experimental facts, but also because for several centuries there was a debate among physicists between supporters of the corpuscular theory of light and supporters of the wave theory of light. Finally, wave theory was able to explain both the rectilinear propagation of light and the laws of its refraction and reflection. Experiments on interference and diffraction testified in favor of the wave theory. After the creation of the theory of electromagnetism, all doubts about the wave nature of light disappeared.

However, the only possible explanation for the laws of radiation of an absolutely black body (as well as the photo effect) was the recognition of the corpuscular properties of light waves - photons, unusual particles that have no rest mass. It can be shown that Coulomb's law - a relatively slow decrease in the electrical interaction with distance - is due to the *zero rest mass* of the photon.

It is known that the electrostatic (Coulomb) interaction of charged particles leads to the quite large forces (compared to the gravitational interaction). Consider the interaction between two charged particles q_1 and q_2. If the second particle is removed "to infinity", then the first particle creates an electrical field around itself, the potential of which is proportional to q_1/r. If we approach the removed particle with charge q_2 to the distance $_r$, it will be affected by a force proportional to q_1q_2/r^2 directed from q_1 if the charges are of the same sign, or to q_1 if the charges are of different signs.

The electric field is introduced by the concept of "potential". The existence of the field is indicated by the fact that at the point where the electrical charge is, there is a feature. In a fundamental explanation of the problem of interactions of electrical charges, we can prove that the concept of "field" should be introduced in *order to reconcile the interaction of charges* with the maximum possible speed of propagation of any excitations and avoid contradictions with the theory of relativity.

The formula for the Coulomb force*:* $F = q_1q_2/(4\pi\varepsilon_0r^2)$ (where $4\pi\varepsilon_0$ is the coefficient that will match the dimensions of the quantities in the CI system) corresponds to the fact that the speed of light c is the maximum speed for any "signal". If the force is depended simply on the distance between the charged particles, then the shift of one of the particles (in this case, the charge q_2) would have to "instantly" affect the state of other particle (q_1). However, this contradicts the fundamental principle of the theory of relativity: the limited speed of signal propagation.

According to the physical meaning of the term "field", a charged particle located at a given point in space is subjected to a force corresponding to the electric field strength at this point. If one of the charges that create the field moves, then the field near it will change, and a perturbation wave will run from it, which will reach the second charge only after time r / s. In this way, the electromagnetic field provides the near-effect observed in nature.

According to the physical meaning of the term "field", a charged particle, located at a given point in space, is subjected to the force corresponding to the electrical field strength at this point. If one of the charges which creates the field moves, then the field near it will change, and a perturbation wave will run from it,

which will reach the second charge only after time r/c. In this way, the electromagnetic field provides the **near-effect** observed in the nature.

In the classical physics, the interaction of charged particles is carried out according to the scheme:

$$\text{particle} \Rightarrow \text{electromagnetic field} \Rightarrow \text{particle}.$$

The corresponding quantum scheme is as follows:

$$\text{particle} \Rightarrow \text{photon} \Rightarrow \text{particle},$$

that is, a charged particle during its movement gives birth to a photon, which is absorbed by another particle, which determines the strength of the interaction of particles.

It is also interesting to note that the Coulomb's law (which states that the force of the interaction of charges is inversely proportional to the square distance between charged particles) is a *consequence* of the fact that the mass of a photon is zero. And precisely because the rest mass of the photon is zero ($m_f = 0$) its speed is equal to the speed of a light.

Photon as an *electromagnetic wave* - reveals in some cases the properties of a particle. The characteristic of the corpuscular properties of an object is the *momentum p* while the wave properties are the *wave vector k*. They are related by the de Broglie relation: $p = \hbar k$, and this relation can be read both on the right and on the left: $\hbar k = p$. The corpuscular properties of a wave are manifested, for example, in the fact that a wave with frequency ω cannot have energy less than $\hbar\omega$ (according to the classical notion, the energy of a wave is proportional to the square of its amplitude and can be arbitrarily small).

A photon is an *electrically and magnetically neutral particle*; it is impossible to change its energy or trajectory by the electrical and magnetic fields in a vacuum. In other words, a photon can be either "born" (heated body radiation, luminescence, etc.) or "killed" (when absorbed). Photons do not interact with each other. This makes it possible to create monochromatic rays of any density (example is laser beams).

The *spin* of a photon is *integer*, it is equal to 1, so that a photon (as opposed to an electron) according to the law of energy distribution refers to *bosons* (named after the Indian physicist Bose). In this case, the photon can be in only two spin states: ± 1. Two spin states of a photon mean the right and left circular polarization of a wave, which is of great importance for understanding magneto-optical effects.

The energy of a photon is greater the greater its momentum p, i.e., the smaller the length of the electromagnetic wave λ because the momentum $p = \hbar k = 2\pi\hbar/\lambda = h/\lambda$. As already indicated, the dispersion law for a photon, ie, the relationship

between its energy and momentum, is expressed by a simple formula: $E = cp = hc/\lambda$. This fact, from the point of view of classical physics, fundamentally distinguishes a photon from a particle with the rest mass m (for which the dispersion law is $E = p^2/2m$). However, it follows from the relativistic formula for the energy $E^2 = c^2p^2 + m^2c^4$ that for large pulses (i.e., when $p >> mc$), as for any particle moving at the speed of light, the energy $E \approx cp$. Therefore, the photon is similar to a particle, but not to an ordinary one ("slow") but to a *relativistic* one.

The experimental foundations of electromagnetic theory are indisputable, so that the wave theory of light remains unshakable. It was only supplemented by a convincingly substantiated quantum theory of light. Thus, it is recognized that light has a dual (corpuscular-wave) nature. The value of k, defined in classical mechanics as a wave vector, is widely used in the quantum mechanics. The direction of the wave vector coincides with the direction of the momentum vector p of the photon, i.e., the wave vector is directed towards the propagation of the light wave. The modulus of the wave vector k is also called the wave number.

De Broglie showed that wave properties are inherent not only in photons, but also in any particle of a matter. The wavelength λ, which corresponds to the particle (proper wavelength), is called the de Broglie wave and is determined by the formula: $\lambda = h/p = h/m\upsilon$, where m is the mass of the particle, υ is its velocity. The hypothesis of corpuscular-wave dualism became universal and was used by Schrödinger to get basic equation of quantum mechanics – Schrödinger equation (Nobel Prize, 1933).

4. Electrons. When a particle is forced to be in a limited space (such as an electron in an atom), its wave properties are described slightly differently. In this case, the concept of a *steady state* is introduced – a state in which the particle is, if the quantum system (e.g., atom) as a whole remains unchanged over time. If a particle (for example, an electron in an atom) is in a steady state, i.e., does not lose or receive energy, then its wavelength and shape do not change over time. Therefore, the possible values of the total energy of the particle are not arbitrary. So an electron contained, for example, in an atom by the force of its attraction to the nucleus, can have an energy value only from a certain set.

On the contrary, according to classical mechanics, an electron, orbiting a nucleus, can have any energy, and therefore an arbitrary (including arbitrarily small) radius of rotation. But when the radius of rotation decreases, the moment of momentum decreases, and with it the orbital magnetic moment. Hence, it could be assumed that the orbital magnetic moment can be arbitrary, which is not true. In addition, different atoms of the same element could be different from each other,

and they are indistinguishable. For this and other reasons, the classical laws of motion are not applicable to the description of the properties of elementary particles.

In the simplest Bohr model, it is believed that an electron is forced to move in a circle around an atom. For an electron, all parts of such a circle are the same, and all that is known is that it is on the perimeter of the circle; more detailed localization of the electron is not determined. In this case, the probability wave of the electron must remain the same shape around the circle. To do this, by passing the entire circle, the wave must continuously pass into itself – that is, embedded on the length of the circle an integer number of times, as shown in Fig. 2.6, *a* and *b*. It is these allowed states that lead to a certain set of admissible values of the electron velocity, ie to a set of values of its energy.

Bohr model, Fig. 2.7, is the simplest assumption of wave mechanics about the location of electrons in an atom. A more accurate analysis shows that the electron can be located not only on the perimeter of a circle, but also in the entire space of the atom - also with some probability. Because the electron has a negative electric charge, it is attracted to the positively charged nucleus of the atom, so the probability that the electron is near the nucleus at some point in time is higher than the probability of finding it at a considerable distance from the nucleus.

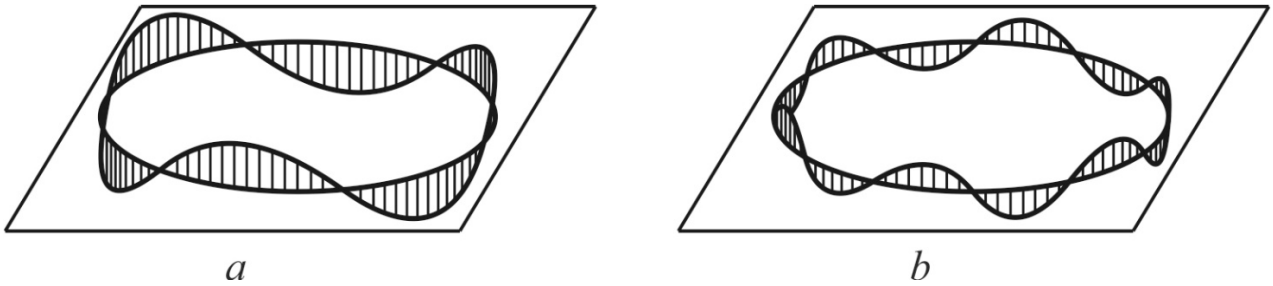

Fig. 2.7. Particle moving in a circle: a and b are allowed waves.

The amplitude of the wave probability of the electron is shown in Fig. 2.7, with a maximum near the nucleus. For clarity, we can assume that the electron moves rapidly along this stationary wave, and its amplitude indicates the relative intervals of time that it spends in one place or another. The square of the amplitude of the wave probability function – the wave density of the probability of the electron – is shown in Fig. 2.8. Quantum mechanics does not set the task of determining the trajectory of an electron: only the formula for the wave function and for the probability wave and the means for its use are given.

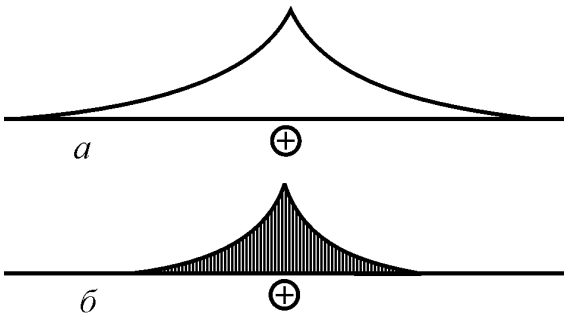

Fig. 2.8. Amplitude (*a*) and wave function (*b* – probability density of electron) in hydrogen atom

Thus, the real picture of the state of the electron in the atom is more complex than a simple rotation of it in well-defined orbit around the nucleus, as shown earlier in Fig. 2.6. Instead, the position of electron in atom is described by the probability wave which is concentrated near the nucleus and does not change over time. Thus explains the fact that the electron in the atom does not emit its energy in the form of electromagnetic waves - the fact that the wave density of the probability of the electron in the atom is stationary, constant over time.

One could create some clarity for the formal description of the properties of particles in quantum mechanics – this is done with the help of a complex wave function Ψ. This function is not a field, that is, if the Ψ-function is nonzero at some point, it does not mean that some force acts on some other particle at this point. In general, there is no simple interpretation of the Ψ-function (such, for example, interpretation as the electric field potential φ, the gradient of which is the electric field strength). However, the square of the modulus of the wave function $\Psi^*\Psi = |\Psi|^2$ is well interpreted – it is the probability of finding a particle at one point or another in space, and, most importantly, this probability can be determined experimentally. In general, the form of the Ψ-function is ambiguous, its reliability is determined by the correspondence of $|\Psi|^2$ to the results of the experimental measurement.

The probabilistic meaning of the wave function changes the style of describing "interactions" in quantum mechanics in comparison with classical mechanics, where the definition of initial conditions and forces determines the exact calculation of the evolution of the system. In quantum mechanics, the state of a system is described in completely different terms. Due to the uncertainty ratio or, similarly, due to the wave properties of the particles, the state of the system cannot be described with the degree of accuracy that is in principle possible in classical mechanics. All results of wave mechanics are formulated in probabilistic terms, and this is due to the uncertainty ratio.

5. Spin. In addition to charge and mass, the particles have their own mechanical magnetic and magnetic moments – spin (in English, the word "spin" means "rotation" or "spindle"). Thus, the particles – electron, proton and neutron - cannot be imagined simply as "fixed balls". If we use the "classical" representations, then these particles would be "forever rotating balls", Fig. 2.8. In this case, the speed of their rotation cannot be changed, because what is simply interpreted as "rotation" is an intrinsic property of the particles themselves. Thr electron or proton cannot change either the magnitude of its spin, or the magnitude of its mass, or the magnitude of its charge. This reveals the elementary nature of these particles (although they can participate in transformations).

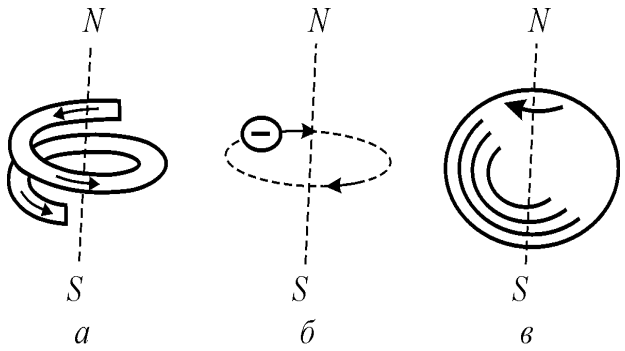

Fig. 2.9. Interpretation of magnetic moment of electron as magnetic moment of ring current: a – solenoid coil (current coil); b – charged particle moving in circular orbit; c – rotating charged ball.

Shown in Fig. 2.8 "classical" ideas about spin are an extreme simplification, for example, they contradict the theory of relativity. In fact, spin is not a consequence of spatial rotation, but some property of an elementary particle, which determines, in particular, its behavior in the "team" of surrounding particles. The spin moment projections for some particles can be only whole, and for others - only half-whole. Zero spin is counted as whole spins.

The "rotation" of the particles must be associated with the mechanical momentum *S*. Quantum mechanics gives the exact expression for it: $S = [s(s + 1)]^{1/2}\hbar$, where s is the spin number or just spin. All fundamental particles electrons, protons, neutrons have a spin equal to ½. *A* simple calculation for these particles gives the value of the mechanical moment $S \approx 0.86\hbar$.

As Dirac showed, a particle with spin ½, electric charge *e*, mass *m* has a magnetic moment: $\mu_B == e\hbar/2m_e$. This value is called the "Boron magneton" and for an electron it is equal to $9{,}3\cdot10^{-24}$ J/T. To have a magnetic moment means to be a source of a magnetic field. Since the electron has an electric charge, it is a source of

electrical field. Due to the "rotation" of a charged electron (which in the conventional language of classical physics can be considered a "ring current"), the electron is also a source of magnetic field. This is another evidence of the unity of electrical and magnetic fields. The law of interaction of two microscopic magnets is the same as for ordinary, macroscopic magnets and is a formal analogue of the interaction of electric charges. Provided that the magnetic dipoles μ_1 and μ_2 are spaced apart (large compared to their size), the force *FM* acting between two magnets (magnetic dipoles) is inversely proportional to the fourth power of the distance between them and is directly proportional to the product of the magnetic moments: $F_M \sim \mu_1\mu_2/r^4$.

For simplicity, the interaction of only two electrons in an atom is considered below, and it is assumed that the magnetic moment of atomic nucleus is much smaller (~ 1000 times), so it can be neglected. For electrons, the magnetic moments $\mu_1 = \mu_2 = \mu_B$. In this case, the strength of the magnetic interaction $F_M \approx \mu_B^2/r^4$. The sign of this approximate equality means that the force of F_M depends not only on the distance but also on the mutual orientation of the magnetic dipoles. The distance between the electrons in the atom is equal to the size of the atom a, and, therefore, the strength of the magnetic interaction is $F_M \approx \mu_B^2/a^4$, while the strength of the Coulomb interaction of the same electrons is estimated by the value $F_{Cul} = e^2/a^2$.

If we take into account the formula for the Bohr magneton $\mu_Б = e\hbar/2m_e$, as well as the formula for the size of the atom $a = \hbar^2/m_e e^2$, we can see that the magnetic forces are really much smaller than the electrostatic: $F_M/F_{Cul} \approx (e^2/\hbar)^2 = (1/137)^2 << 1$. This inequality is the reason that in an approximate description of the atom by magnetic interactions can be neglected. However, in many phenomena, including the description of magnetism in solids, the magnetic forces play a significant role.

Solid state physics studies rather complex spatial lattices consisting of microscopic particles — atoms, ions, or molecules. In this case, the forces acting between these particles are mainly of either electrostatic (ionic bond) or quantum "exchange" (covalent bond) origin. In the formation of a solid body, when atoms converge, the charges of different names are attracted, and charges of the same name are repelled. The force acting between atoms is the difference between the forces of attraction and repulsion. The effect that one atom has on the motion of electrons in another atom is such that the resultant force is always attraction.

The attraction of atoms (ions, molecules) acting at a distance is the cause of the formation and existence of solids. However, the attraction dominates until the atoms get so close that they almost collide. Then their repulsion begins to prevail - these forces are close-acting. Finally, at some distance the repulsive force becomes

equal to the force of attraction; then a molecule is formed from two atoms or ions, and a solid body from their set.

For solid state physics, it is important to explain the nature of *repulsiv*e forces. Since the size of an electron is one hundred thousand times smaller than the size of an atom (as well as the small size of the atomic nucleus), from the point of view of "classical" mechanics it turns out that the atom consists mainly of "voids" – so only a little space is occupied by electrons and nucleus. However, in the solid state physics (and especially in its important section – crystallography) a well-founded assumption is used that the atom behaves like a "solid ball". The concept of atomic or ionic radius is used in FTT - these data for atoms and ions of various chemical elements are given in reference tables. That is, the crystal can be represented as a regular lattice of properly packed "solid" balls (ions, atoms or molecules).

The high spatial and temporal stability of the structure formed by "empty" ball atoms in quantum mechanics is explained by the fact that when atoms converge, the possible space for the electrons bound in them decreases, i.e., the uncertainty of coordinates decreases. According to the Heisenberg uncertainty ratio, this leads to an increase in the uncertainty of the momentum, and thus to an increase in the magnitude of the momentum. As a result, the kinetic energy of motion of electrons increases, and with it the total energy. This increase in energy when particles come together leads to their repulsion, because the electrons of neighboring atoms are more common. As a result, an energetically advantageous position for atoms is their spaced position. Thus, the repulsive force that provides equilibrium in the structure of a rigid body has a quantum nature.

Returning to the magnetic properties of solids, it should be noted that the electronic magnetic moment is an unusual vector, because it can be oriented in space in only two ways: either in the field or against it. Accordingly, the moment of electron motion is always oriented $g = 2s + 1$ ways; with a spin equal to $s = ½$, these methods are only two. The most important consequence of Dirac's theory was the conclusion about the existence of *antiparticles*. For all particles there are antiparticles which are identical in all respects except the charge (it is inverse) and the magnetic moment (it is also inverse). For an electron, the antiparticle is a positron. Particle and antiparticle, colliding, disappear (annihilate), generating quanta of light. Conversely, a quantum of light can create two particles – an electron and a positron. For solid state physics, this fact is important because a number of experiments use the irradiation of crystals with positrons and investigate the resulting physical effects.

Electrons, protons and neutrons are called fermions (named Enrico Fermi).

This class includes all particles with a half-spin. Particles with a solid or zero spin are called bosons. This difference between the particles (whole or semi-whole spin) leads to a radical difference in the behavior of the system of a large number of fermions from the system of bosons. Only fermions obey the principle Pauli (there can be no more than two electrons in the system with the same energy). This prohibition does not apply to bosons. Moreover, bosons "try" to collectivize – to gather (condense) in one state (bose - condensation). This property is the basis of quantum light generators (lasers), as well as the cause of such phenomena as superfluidity and superconductivity.

2.6 Electrons in atoms and in crystals

Electronic states consideration in crystals is started from the electronic spectra of atoms. Atoms can be characterized by two complementary models: *spatial* model and *energy* model. The spatial model of atom reflects its volumetric three-dimensional structure, and, within this structure, electrons location in atom is described by the probability density. The electrons which are distributed near the nucleus form the electronic cloud. In the simplest case, this cloud is spherical (as in hydrogen atom in its non-excited state), but in most cases electronic clouds have complex configuration.

Conventional image of the external shape of electronic cloud is known for different quantum states. Schrödinger's equation gives the opportunity to perform rigorous mathematical description of electronic clouds: their geometric features in atoms and ions. However, sometimes, their visual representation is impossible, since to find the probability of electrons distribution in a cloud might be quite difficult. Therefore, to describe the configuration of atom, simplified model is often used – the model of Bohr. This model allows represent atom as a central positively charged nucleus and electrons moving in the orbits around it.

The number of electrons determines position of atom in Periodic Mendeleev Table, and it is exactly equal to the number of protons in nucleus of an atom. From experiments and theory, it is known that radius of atom equals $a \approx 10^{-8}$ cm. At that, the radius of nucleus is estimated by the size $\sim 10^{-13}$ cm, and roughly same is the size of electron; thus, the size of atoms in hundred thousand times greater than size of its nucleus. Therefore, on the face of it, the volume of atom looks like "empty", but in the solid state physics and materials science atom usually is represented by a solid

ball, and this is “good working" model. The question is that this “ball” is “filled” by a very strong electromagnetic field.

1. Electrons in atoms. To simplify further consideration, the simplest atom is discussed; namely, the hydrogen atom consisting of one proton and one electron. In this atom, the positively charged nucleus holds the negatively charged electron by the Coulomb force of attraction:

$$F_{\text{Coul}} = e^2/a,$$

where e is electron’s charge (same charge has the proton). To ensure the stability of atom, the force of attraction must be balanced by the repulsion force. This force is the centrifugal force:

$$F_{\text{centr}} = m\upsilon^2/a,$$

where m is the mass of electron and υ is its velocity. The equality of F_{Coul} and F_{centr} makes possible to determine the velocity of electron’s movement on its circular orbit:

$$\upsilon = (e^2/ma)^{1/2}.$$

As the charge e so the mass m of an electron are fundamental constants. By substituting the values of these constants in a given formula, it is possible to find the elocity of electron’s rotation in its orbit: $\upsilon = 10^8$ cm/s. In these calculation, the relativistic effects is negligible, because $\upsilon/c \approx 1/300$. However, if the atom would have size close to its nucleus (10^{-13} cm), the velocity of electron’s rotation would be close to the velocity of light (obviously, this is impossible).

Total energy of electron in the field of nucleus (sum of its kinetic and potential energy) is:

$$E = -e^2/2a.$$

Sign "minus" means that for zero energy such electron should be taken that is sent away on “infinite” distance from the nucleus (with decreasing distance energy decreases).

Accordingly to a simple model, the electron moves in atom with the velocity of $\upsilon \approx 10^8$ *cm/s* on a circle, so the vector of the velocity constantly changes its direction. It is reasonably to believe that $\Delta\upsilon \approx \upsilon$: this means that the uncertainty of velocity $\Delta\upsilon$ equals to the velocity. From the indeterminacy principle (in other words, uncertainty relation) it follows that $\Delta x \cdot \Delta p \geq \frac{1}{2}\hbar$. Taking into account that the impulse is $p = m\upsilon$, the uncertainty in electron’s coordinates is $\Delta x \geq \hbar/2m\upsilon$. From the mass of electron $m \approx 10^{-27}$ *g*, its velocity ~10^8 cm/s and using Plank constant ħ, it is possible

to find the uncertainty of electron location $\Delta x \geq 10^{-8}$ *cm* that exactly corresponds to the size of atom.

This means that the sphere of radius a represents the volume containing electron; however, to clarify its position in this volume is impossible. Quantum indeterminacy principle (Heisenberg principle) allows estimate the size of atom, namely, the atomic radius is determined by the uncertainty of orbital electrons position: $a \approx \Delta x \approx \hbar/m\upsilon$. Using this expression for the orbital velocity of an electron: $\upsilon = (e^2/ma)^{1/2}$, it is possible to get:

$$a = a_0 = \hbar^2/me^2.$$

Thus, the atomic radius a_0 can be expressed through the fundamental parameters: Planck constant $\hbar$, mass of electron m and charge of electron *e*. This radius approximately equals to $0.5 \cdot 10^{-8}$ *cm*, and it is the *Bohr radius*; it coincides with radius of hydrogen atom in its ground state.

According to the quantum mechanics, not all states are allowed but only the states with a certain energy; at that, there is one state (ground state), in which electron *does not radiate energy*. In addition, besides the ground state with the Bohr radius a_0, there are also a number of excited states; emerging the *transitions* between them, which result in the emission (or absorption) of the light quanta.

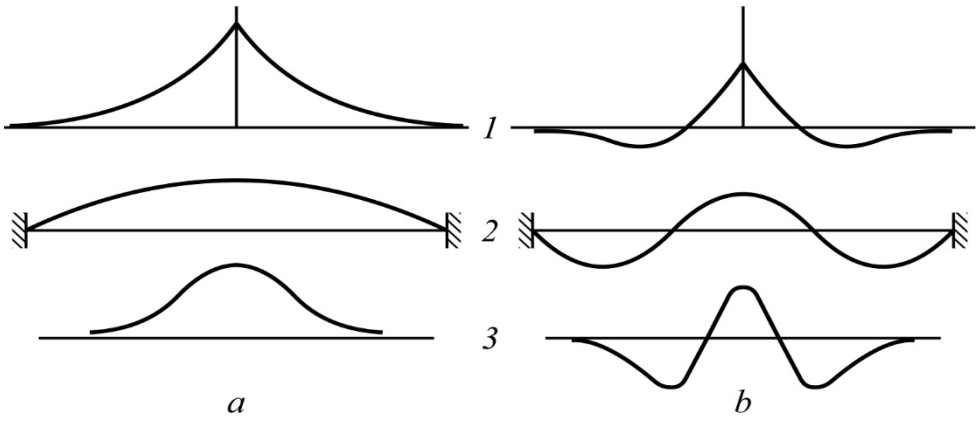

Fig. 2.10. Waveform probabilities for two allowed states electrons in atoms (1); for particle that moves in straight line (2), and for harmonic oscillator (3).

Inasmuch as electronic waves in atom propagate in three dimensions, it is possible to depict them graphically through intersections, Fig. 2.10. These sections show two types of permitted waves (a and b) in three quantum systems: electron in the hydrogen atom (1), the one-dimensional particle in a limited space (2) and the quantum oscillator (3).

It is a fact that all electronic waves in atom have the "tails" that extends to the large distance (infinitely); at that, Fig. 2.10 shows that the electron can have some little chance to attend in a big distance, but still most likely is its location near the nucleus. At that, the energy levels of electron which correspond to its possible natural waves in the hydrogen atom (Fig. 2.10 shows only two of them) can be placed in a series that converges, shown in Fig. 2.11b.

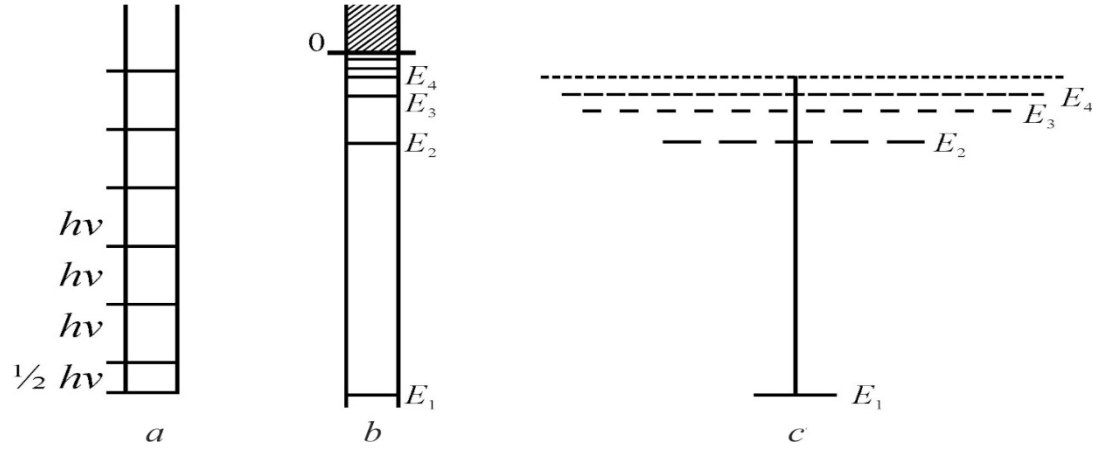

Fig. 2.11. Energy spectrum of the quantum oscillator and hydrogen atom: a – allowed energy levels of quantum oscillator; b – allowed energy levels of electron in hydrogen atom; c – correspondent to levels permitted states (number of strokes).

Unlike the energy levels in the quantum oscillator, which distance from each other is always $h\nu$, the distance between the electron's energy levels in atom *decreases* with energy increase. Therefore, by getting enough energy, the electron can finally leave the atom, and next its energy changes continuously, as it is shown in the top of Fig. 2.11*b* by the continuous energy spectrum. As "*zero point*" of energy exactly such state is selected, at which electron is found very far away from nucleus. When approach to each other, the electrons fall into influence of electromagnetic field of adjacent electrons (without outside electromagnetic field). Therefore, electrons interact with each other such as if they were two small interacting magnets. The Pauli principle proclaims: if two electrons are in one of stationary states (for example, on one orbit), they can not have spins, oriented in one direction, but necessarily must orient their spins in the opposite direction.

When approach to each other, the electrons fall into the influence of electromagnetic field of adjacent electrons (without outside electromagnetic field). Therefore, electrons interact with each other such as if they were two small interacting magnets. The Pauli principle proclaims: if two electrons are in one of stationary states (for example, on one orbit), they can not have spins, oriented in one

direction, but necessarily must orient their spins in the opposite direction. For example, in the helium atom, both electrons at normal conditions are authorized by a state with the lowest energy. Because both of them are in same state, their spins, according to Pauli principle, are opposed and form complete s-shell.

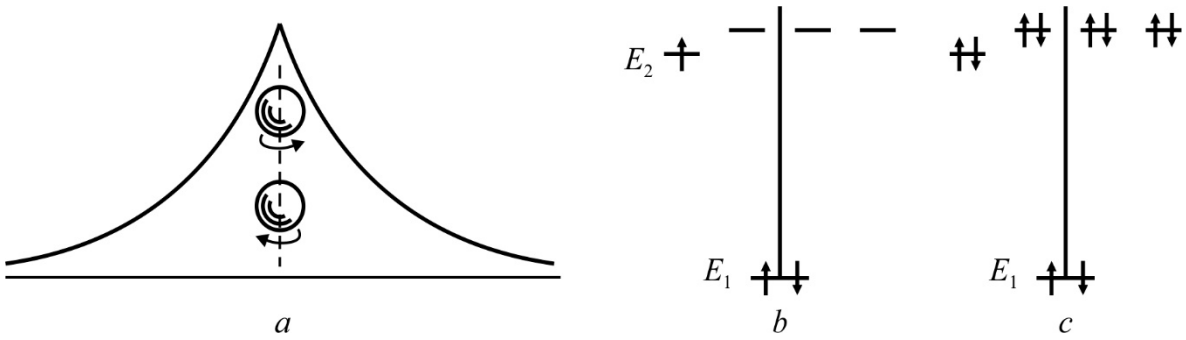

Fig. 2.12. Electrons and their spins in atoms: a – wave function for two electrons with opposite spins in helium; b – basic (E_1 and E_2) levels in lithium atom (dotted line shows next higher allowed states); c – five levels in atom of neon, occupied by electrons.

The lithium atom has three electrons; two of them choose the complete s-shell, while third electron would also acquire condition with minimal energy. However, this case is prohibited by the Pauli principle, since main (*s*-) state is already fully occupied by two electrons with opposite directions of spins. Therefore,n the third electron in Li atom reluctantly takes one of four following states, characterized by the higher energy than s-state.

The condition of electrons in atoms of any given element determines its physical and chemical properties. For example, chemically neutral inert gas argon has 18 electrons, but adding only one electron to a shell (and one proton to nucleus) transforms the inert argon atom into chemically very active potassium atom. Lithium starts a new row of elements in the Mendeleev Periodic System. The state which had to take his third electron is one of four possible levels in the electronic *p*-shell, following the *s*-shell, Fig. 2.12*b*. Each item in this series can be filled by electrons, and number of electrons in p-state district might be eight. They are all completely filled in the neon atom, Fig. 2.12*c*: electrons occupy all four levels that are in the *p*-shell, and each of them contains two electrons with the oppositely directed spins.

2. Electrons in crystals. Energy model of crystal will be considered below at elementary level and in close connection with above explained concepts of energy spectrum of atom (see Fig. 2.12 and 2.13). Without knowledge of main features of energy spectrum of electrons in a crystal, it is impossible to understand the principles of microelectronic devices operation (most of them are based on semiconductors).

Electronic energy spectrum of crystal is directly related to the energy spectrum of atoms, incoming to crystal structure. Specific examples of energy bands formation as well as the overlapping areas creation are considered below with relatively simple case – metallic sodium. The energy diagram of sodium atom that has 11 orbital electrons (balancing same number of positive charge in nucleus) is shown in Fig. 2.9. First two electrons occupy lowest level of energy 1*s* in the *K*-shell. Next, third and fourth electrons occupy lowest energy level 2*s* (shell L_I), fifth electron is located in the lowest remaining level (shell L_{II}), and so on. From Fig. 2.9 one may conclude that on the third level six electrons are set. However, there are three levels that differ only by a little energy (this is peculiar in atoms with low atomic number), so they can not be depicted with boundaries.

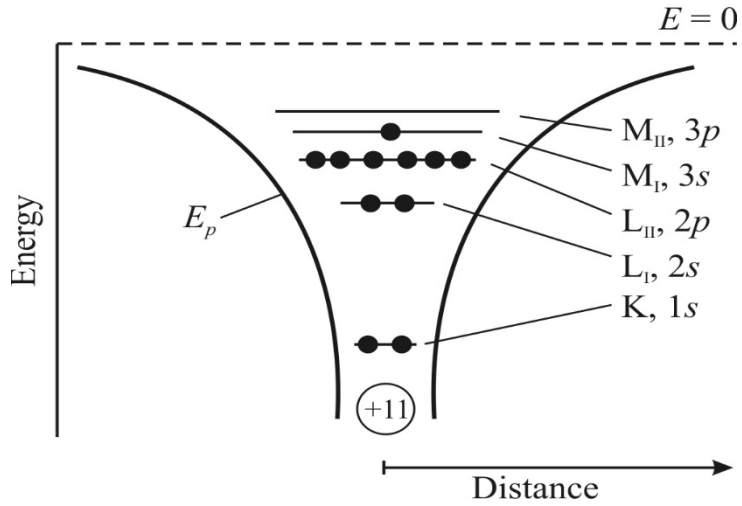

Fig. 2.13. Electronic arrangement in sodium atom: valence electron is located on level 3s in M_1 shell; K, L, M – designations of electronic shells, E_p – potential energy.

Correspondent energy levels for all 11 electrons are shown as characteristic of neutral atom of sodium. With addition of each subsequent electron the form of potential energy curve E_p changes, Fig. 2.13, while the location of energy levels becomes different. Each outer electron can approach to atom with lower velocity, because it is subjected not only by the attraction from nucleus, but by the repulsion from others, more deep electronic shells. At highest occupied level M_I, Fig. 2.13, the non-excited sodium atom has only one valence electron (in the state 3*s*), and just this electron determines most of chemical, electrical and optical properties of a sodium. Remaining 10 electrons are located so deep in the well of the potential energy so that they *can not participate* in the chemical, electrical or thermal processes.

In case of solid state formation from the individual atoms, the energy picture in first approximation is need: for constructing potential energy curves for series of atoms, located in distance equal to crystal lattice constant, Fig. 2.13. Because atoms

in crystal lattice are located close to each other, the potential curve between them can not rise to the level $E = 0$, as it happens in atom located out of crystal, Fig. 2.13. The maxims of potential energy between atoms cannot reach even the energy of single valence electron of atom. Therefore, nothing prevents the valence electrons (which originally belong to the atom) to leave its atom and to start free moving through a crystal under the influence of heat or other impacts.

As shown in the simplified diagram in Fig. 2.14, the valence electrons belong to *whole crystal* and have *same energy*. At the first glance, this contradicts to the Pauli principle. However, experiments show that the emission spectra of metals are not discrete (as it is seen for the atomic spectra), but they are continuous.

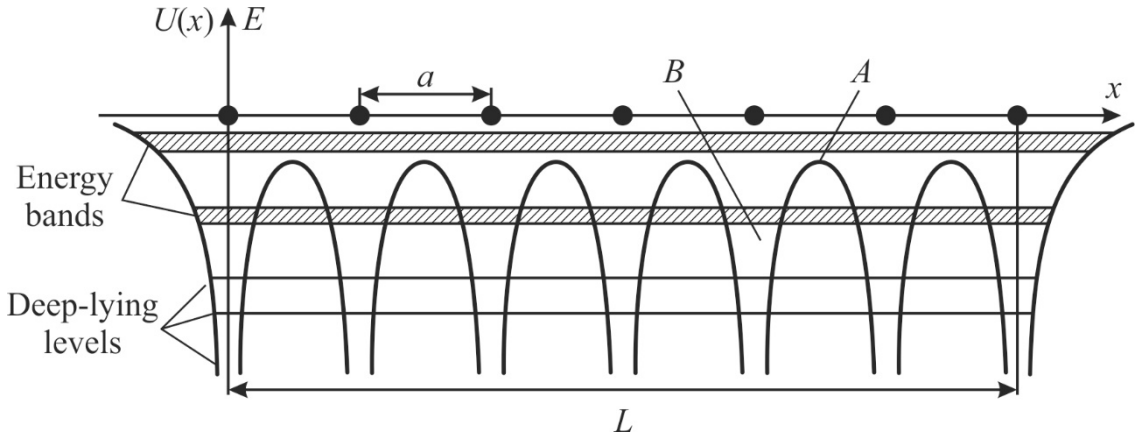

Fig. 2.14. One-dimensional energy model of crystal: a is inter-atomic distance; L is overall size of crystal; A is potential barrier that limits electrons transition from one atom to neighbour; *B* is potential well.

The point is that the discrete energy levels of atoms become split, and they form the *band* (or zone) consisting of same number of separated levels as there are atoms in crystal. It is expected that crystal is characterized by so many energy bands as many energy levels has isolated atom of substance. In this example in one cubic centimetre of sodium crystal the number of electronic levels in any band equals $3 \cdot 10^{22}$, at that, all valence electrons occupy different levels, but in the same area 3*s*.

As can be seen from Fig. 2.15, the valence band holds N narrowly located energy levels; in accordance with the Pauli principle, this band can accommodate *2N* electrons. Therefore, the levels in valence band are only *half filled*, since separated sodium atom has only one valence electron. In addition, specifically for sodium, the width of the highly placed bands corresponds to the number of 3*s* and 3*p* levels which overlap each other. As a result, some electrons move out from the 3*s* zone to lower levels of 3*p* zone, so both zones are filled together until entire stock of electrons will be exhausted (other energy bands, located above areas that overlaps,

are not shown in Fig. 2.15 in order to simplify the figure). Thus, the valence band of sodium crystal is not fully occupied by electrons. The top energy level, that in metals is occupied by electrons at temperatures $T = 0$, is the *Fermi level,* E_F.

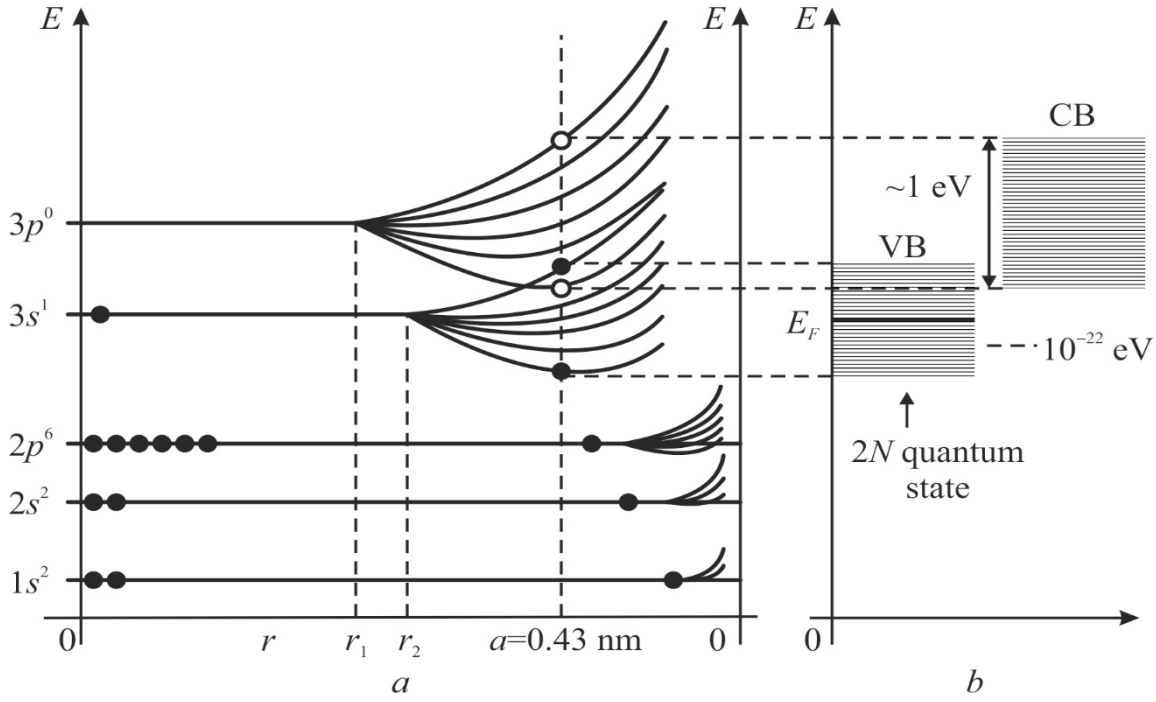

Fig. 2.15. Electronic energy spectra of system of N atoms of sodium (Na) depending on distance between them; CB – conduction band; VB – valence band, E_F – Fermi level

Valence electrons of metal are not located near their individual atoms, but they move freely around a crystal similar to the gas molecules in a certain vessel. This system of electrons in metals is the *electronic gas* (or quantum *electronic liquid*). Fermi level in metal plays for "electronic liquid" the same role, as the level of fluid in the communicating vessels. If two crystals with different Fermi levels would touch each other, the electrons will "flow" from one crystal to another one until their Fermi levels will be aligned. More clear definition of Fermi level position is given in thermodynamics.

If the electrical field is applied to a metal, the electrons can easily change their energy states, going from one level to another (located very close). Electrons, in addition to their random thermal motion, move in opposite direction to the electrical field that causes electrical current. The mono-valence metal sodium is a simplest case of electronic levels location in the energy spectrum of metals. Sodium demonstrates purely electronic conductivity that is verified experimentally by the Hall's effect study and by the definition of a sign of thermo-electromotive effect.

Electronic spectrum of a *copper* is not so simple then in the sodium (but, however, it is not so complicated, as the spectra of some rare earth metals). However,

already in the case of a copper, the contribution to conductivity is made not only by free electrons, but also by the *electronic vacancies – holes*. The energy diagram of copper crystal is shown in Fig. 2.16 where not only the band diagram with overlapping energy levels is shown, but also the formation of energy bands in case of individual atoms touching.

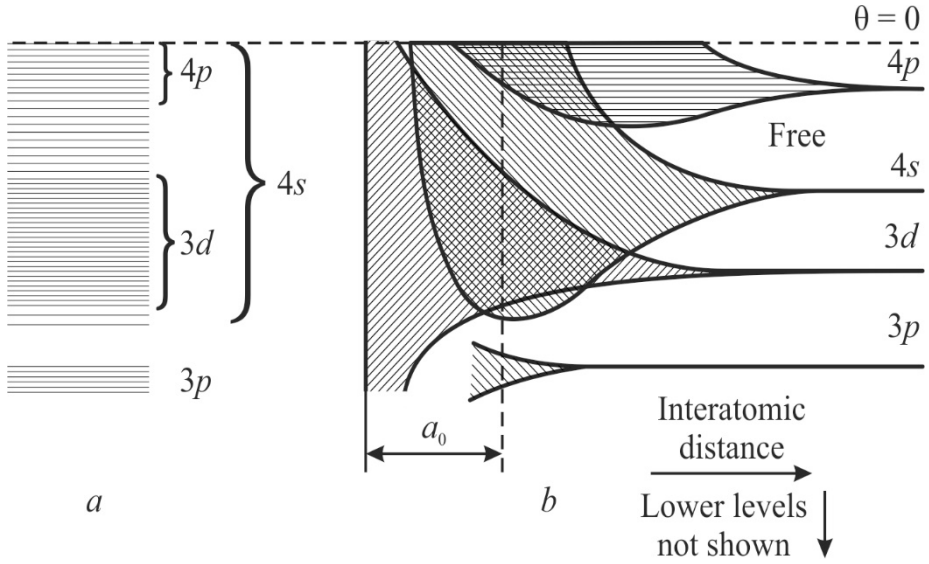

Fig. 2.16. Energy bands of copper: the overlap (a) and the splitting of energy levels in case of atoms touching (b); a_0 – lattice constant (bands are arbitrary shading, lower levels not shown).

Energy levels of the distant atoms in Fig. 2.16*b* look as discrete and narrow. However, as atoms converge, the interaction between electrons of outer shells starts, and overall energy levels become split, creating the *band*. With subsequent convergence of atoms the splitting amplifies, and the energy levels become deeper. When inter-atomic distance of copper becomes equal to lattice constant a_0, the bands 3*d*, 4*s* and 4*p* become such extended that they overlap each other, as it is shown in Fig. 2.16a. Deeper energy bands (only 3*p* level is shown) expand considerably less. In the case of entirely separated copper atom its energy levels are completely filled up to the 3*d* level, while on the 4*s* level (which can accommodate two electrons) the only one valence electron of each atom is located. In the copper crystal three top areas are united and completed.

In the above considered cases, the valence band is found as being partially filled with electrons (Na), or having some overlapping energy bands with a formation of broader band of levels that remains partially unfilled (Cu). In the metals that can be characterized by above shown energy diagrams, the electrons are free, so these materials are good conductors of electrical current.

The interaction of atoms in a crystal significantly changes the electronic energy spectrum. Highly located discrete energy levels of isolated atoms are

changed into the wide energy bands (zones), when atoms connected together in a crystal. The dependence of potential energy on coordinates *U(x,y,z)* radically changes: it becomes *periodic*. Neighbouring atoms of crystal change each other potential by such a way that it turns into the periodical set of potential barriers and potential wells, Fig. 2.15. The interaction between atoms also changes the initial position of discrete quantum states, and splits them into the separate closely located energy bands. Allowed band, in which the valence electrons are located, is the *valence band*. In sodium crystal this band is formed as a result of 3*s*-level splitting.

Consequently, when crystal lattice formation, all peculiar for a given type of atoms electronic levels (as filled by electrons, so unfilled) are displaced as a result of neighbouring atoms influence on each other. Due to the convergence of atoms electronic energy levels of individual atoms become separated into the bands of energy levels of electrons.

2.7 Metals, dielectrics and semiconductors

The above analysis of electrons behavior in simple monatomic crystals opens a possibility to draw preliminary conclusion as to cardinal types of solids. The fact is that features of energy electronic spectrum cause large difference in the electrical, optical, thermal and mechanical properties of materials.

Metals and dielectrics, due to fundamental distinction in nature of their atomic connections, differ significantly from each other as in electrical and optical properties so in their thermal and mechanical properties.

[**Note.** However, it should be noted that, very seldom, it is possible to meet crystals in which energy barrier between dielectric and metallic states is not big, and these materials can exist in both states. Moreover, some of solid materials undergo to phase transition of "dielectric-metal" type. At these transitions conductivity jumps in thousands and millions times, that is used in electronic devices].

Initially, it is better to compare *electrical properties*: conduction and polarization. Temperature dependences of conductivity σ in dielectrics and metals are opposite: while in the dielectrics σ increases with temperature rise accordingly exponential law (since thermal motion in crystal generates new charge carriers), in the metals, owing to charge carriers scattering on the thermal vibrations of crystal lattice, the conductivity decreases approximately as *1/T*. Therefore, when metal is cooled to low temperature, its conductivity greatly increases tending to infinity

(superconductors really have $\sigma = \infty$). In the dielectrics, on the contrary, at very low temperatures σ-value is close to zero, because free charge carriers in dielectrics are not generated, if intensity of thermal motion is small (and no radiation exposure). Just like in dielectrics, the conductivity of semiconductors at low temperatures also tends to zero.

Electrical polarization (which is most important phenomenon for dielectrics) does not occur in metals due to high concentration of free electrons, which form almost free "electronic gas" around positively charged ions. Electronic gas in metals gives rise to almost complete screening of electrical field. Only at very high frequencies, much higher than frequency of visible light (i.e., more than 10^{16} Hz) electronic gas in metals demonstrates its sluggishness: it has no time to interact with extremely fast change of electromagnetic field, and $\sigma \Rightarrow 0$. Thereby, it is possible to notice polarization of deep electronic shells which are located more close to ions nuclei. Such polarization, occurring at frequencies, higher than optical range, determines certain permittivity in metals.

Comparing *optical properties* of metals and dielectrics, it should be noted that free electrons in metals cause almost complete reflection of electromagnetic waves from the surface of metals that explains metallic shine. In contrast, electromagnetic waves of optical frequency can easily penetrate into dielectric, and majority of them are optically transparent (colour and opacity of some of them is due to impurities presence that absorb or scatter light by inhomogeneous structure).

Significant discrepancy between dielectrics and semiconductors can be seen in frequency dependence of electromagnetic waves absorption in these materials. Dielectrics are transparent in optical wavelength range: fundamental absorption in them is observed solely in ultraviolet wavelength region. Only at a very high frequency (10^{16} Hz) the energy of photons exceeds the band gap in electronic spectrum of dielectric, whereby photoconductivity and light absorption appears. In semiconductors electromagnetic wave absorption and reflection started at about 10^{14} Hz (in near infrared region), however, semiconductors, unlike dielectrics, have good transparency in the far infrared wavelength range.

Thermal properties of dielectrics and metals differ mainly in the value of thermal conductivity. Very big thermal conductivity of metals is due to free electrons participation in the heat transfer, whereas in solid dielectrics heat passes mainly by crystal lattice vibrations (phonons). The magnitude of thermal expansion and heat capacity of metals and dielectrics are not very different: due to quantum effects specific heat of electronic gas in metals is very small as compared with specific heat conditioned by the lattice vibrations.

In *mechanical properties* crystalline dielectrics are more fragile, while metals are usually pliant. This is also due to impact of free electrons on the properties of metals that crystallize in simple, densely packed lattices, where overwhelming strength of interaction is metallic bond (other types of electrical bonds between atoms in metals are shielded by free electrons). By contrast, dielectrics have complicated polyatomic structures with different physical nature of interaction in structural elements.

Many investigations of dielectrics and metals show that main differences in their properties are conditioned by the presence of free electrons in metals and complicated atomic bonding in dielectrics. More rigorous deduction as to difference between metals and dielectrics properties is explained on the base of energy-band theory.

Energy *band structure* of electrons in crystalline dielectrics and metals are qualitatively different. As atoms approach to each other and formed crystal, many of electronic energy levels appear. Due to electrons interaction the splitting of energy levels takes place, forming zones (bands), Fig. 2.14 and 2.15. This cleavage occurs mainly in those energy levels that correspond to the outer (valence) electrons as they are much stronger interact with each other than electrons of deep shells of atom. The type of electronic spectra of crystals depends on peculiarities of atomic wave functions and on degree of these functions overlap when atoms approach during crystal formation.

In theory of electronic energy spectra the one-electron approximation is typically used: it is assumed that each electron moves in a force field of ions and electrons, while individual (pair) interactions are not taken into account even between nearest neighbouring electrons. The interactions are taken into account as so-cold middle field. In this case the solution of Schrödinger equation in periodic potential of crystal lattice is Bloch functions, and eigenvalues spectrum of electrons forms the energy bands like in Fig. 2.14 and 2.15.

The number of levels in each band is determined by the number of atoms in lattice, thereby forming quasi-continuous energy bands. According to Pauli principle, only two electrons (with opposite spin values) can coexist in each level of zone, at $T = 0\ K$ electrons occupy states with minimal energy in each energy band.

Electronic energy spectrum of crystals, i.e., electrons energy distribution in allowed bands, is usually described in the quasi-momentum space, that is, in reciprocal lattice. The dispersion law W(p) for free electrons is the dependence of electrons energy W from their momentum $p = \hbar k$, where k is wave number. In case of free electrons, function W(p) is simple parabolic function:

$$W = \frac{\hbar^2 k^2}{2m} = \frac{p^2}{2m},$$

where m is mass of electron. Accounting for periodic potential of crystal lattice (Bloch method) complicates this relationship, resulting in breaches of parabolic dependence *W(p)* in the area of forbidden energy band, Fig. 2.17. The function *W(p)* is continuous only in definite intervals of momentum space, namely, in the Brillouin zones (first zone corresponds to $\pi/a \le k \le \pi/a$). During transition from one to other Brillouin zone this function is terminated.

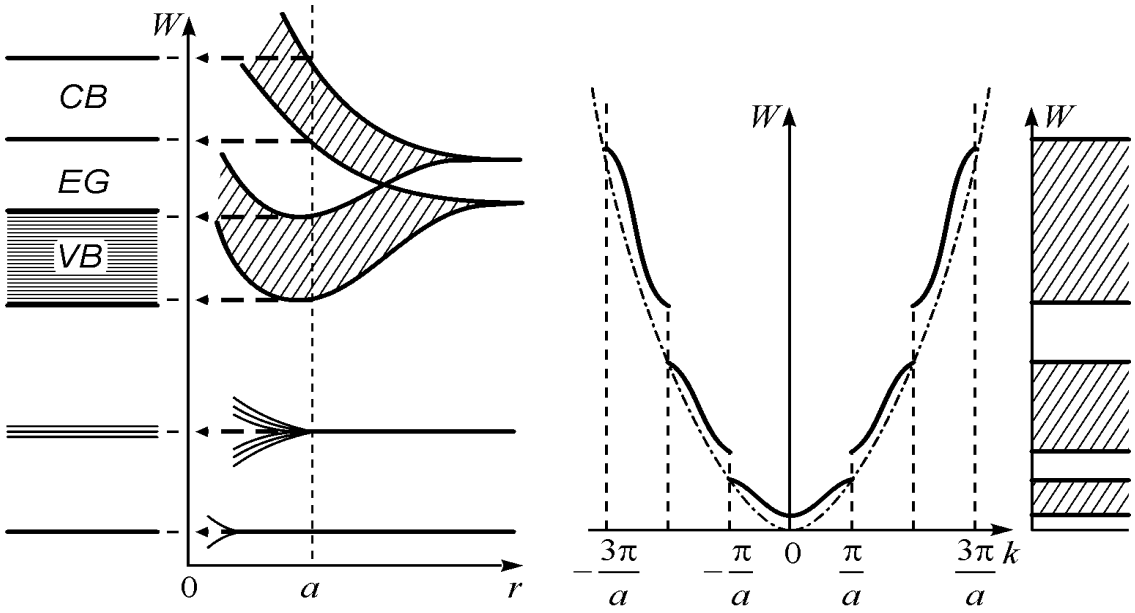

Fig. 2.17. Splitting of energy levels of electrons of isolated atoms, energy bands formation due to atoms convergence: *CB* – conduction band; EG – energy gap; *VB* – valence band; *a* – lattice constant; *W* – electrons energy; *r* – distance between atoms

One-electron band theory with Bloch wave functions perfectly agrees and justified in the crystals with *s*- and p-electrons that have big orbital space with significant overlap. In the crystals with *d*- and f-orbitals band theory might be applied with caution.

Energy-band structure of electronic spectrum allows construct models of different variants of electronic spectra of crystals. There are three main cases:

1. *Energy bands of electronic spectrum do not overlap,* Fig. 2.18*a* and *b.*

1a. Crystals with an odd number of electrons per unit cell of crystal have upper energy band filled with exactly half, Fig. 2.18*a*. These crystals are metals; in each energy level two electrons can be placed (according to exclusions principle). Thus, energy band has *2N* vacancies, half of which is occupied by electrons: electrons occupy the lowest energy levels. In the ground state (when *T = 0 K*), the boundary of filling that separates in the impulse space filled part from unfilled part of valence

band is the Fermi level F (in tree-dimensional model F corresponds to Fermi surface). If $T > 0$ *K*, the boundary of Fermi surface becomes smeared as a result of thermal perturbations (phonons), and part of electrons goes on to levels above F (as a result, some of levels below F is released). Since distance between levels in band is extremely small (~ 10^{-23} eV), even very small external electric field can increase energy of electrons and cause electrical conduction in metals (that is limited only by electrons scattering on the lattice vibrations). With decreasing temperature conductivity of metals increases: if temperature $T \to 0$ conductivity $\sigma \to \infty$.

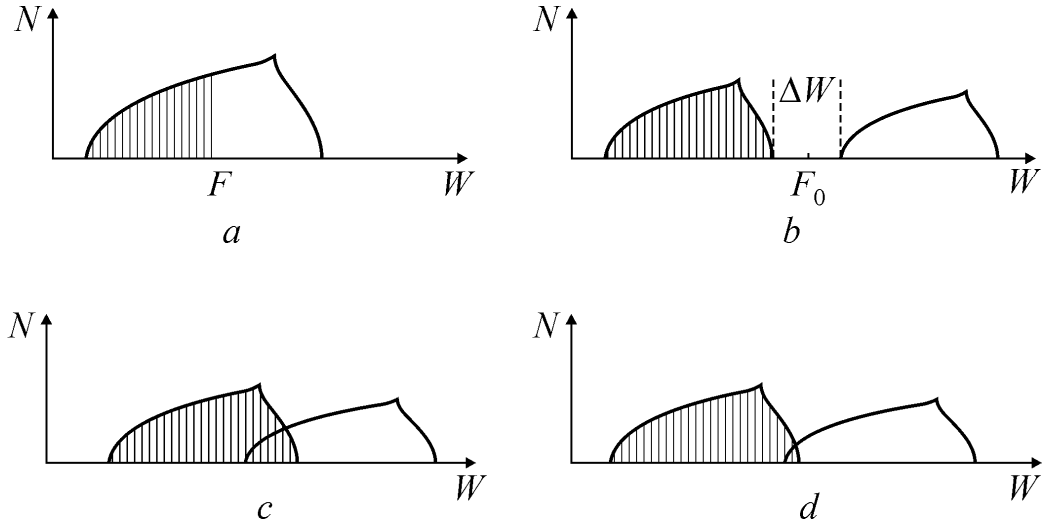

Fig. 2.18. Electronic levels in spectra (filled levels are shaded): *a* – "true" metal with odd number of electrons in unit cell; *b* – dielectric or semiconductor with gap ΔW between valence band and conduction band; *c* – metal with even number of electrons in unit cell; *d* – semimetal

1b. Crystals with the even number of electrons per unit cell are dielectrics or semiconductors (Fig. 2.18*b*). In the ground state (at $T = 0$ *K*) their energy bands are completely filled or empty. Therefore, electrical field can not change energy of electrons in the filled bands (since all levels are filled), while in the empty bands there are no charge carriers. Consequently, if temperature is critically reduced ($T \to 0$ *K*) in dielectrics or semiconductors conductivity is absent ($\sigma \to 0$). Upper filled band (valence) and nearest empty band (conduction band) are separated by the energy gap ΔW (forbidden band, Fig. 2.18*b*).

In crystals with energy gap the Fermi surface in electronic spectrum is absent, but in the middle of a gap (when there are no impurities and local levels) these is the Fermi level F_0 (Fig. 2.18*b*). To excite electrical conductivity in these crystals by thermal vibrations or by other factors, it needs that valence band would be partially released from electrons (holes mechanism of electrical conductivity) or conduction band would be partially filled by electrons (electronic conductivity mechanism).

2. Bands of electronic spectrum overlap, Fig. 2.18, *c* and *d*).

Such crystals, as with even so with odd numbers of electrons per lattice site, refer to metals. Significant overlap of two bans (Fig. 2.18*c*) results in a situation that is not very different from the case shown in Fig. 2.18*a*. In the event of small overlap of bands crystals belong to semimetals, Fig. 2.18*d*. Fermi surface for semimetals has discontinuities, and their conductivity by several orders of magnitude is lower than conductivity of metals. For example, in semimetal bismuth number of filled states in conduction band in 10^4 times smaller than in conventional metals, and, consequently, bismuth shows much lower conductivity. Other examples of semi-metals are antimony and graphite.

3. Bands of energy spectrum are in a contact without overlapping.

Crystals of this rare class are the gapless semiconductors. Fermi surface of such semiconductors is a line or a point in impulse space (whereas in semiconductors such surface does not exist and in semimetals this surface has discontinuities). In the semimetal under the influence of electrical field, electrons move within their area, but lower density of states reduces their mobility. In the gapless semiconductor electrons relatively easily (as compared with conventional semiconductor) comes into conduction band, but dynamic properties of charge carriers in these materials are significantly modified.

So, the crystals that in ground state have no partially filled bands belong to dielectrics or semiconductors. The metals and semimetals, by contrast, are characterized by electron spectrum with partially filled bands.

Electronic spectra of metals, semi-metals, semiconductors and dielectrics comparison is shown in Fig. 2.19, demonstrating energy spectra of electrons in these materials. In metals there is no energy gap between valence band and conduction band, so that electrons easily change their energy, moving from level to level, so they are free. Electrons in metal are not localized – they belong to the entire crystal and do not form spatially-directed bonds between ions.

Electronic spectra of metals, semi-metals, semiconductors and dielectrics comparison is shown in Fig. 2.19, demonstrating energy spectra of electrons in these materials. In metals there is no energy gap between valence band and conduction band, so that electrons easily change their energy, moving from level to level, so they are free. Electrons in metal are not localized – they belong to the entire crystal and do not form spatially-directed bonds between ions.

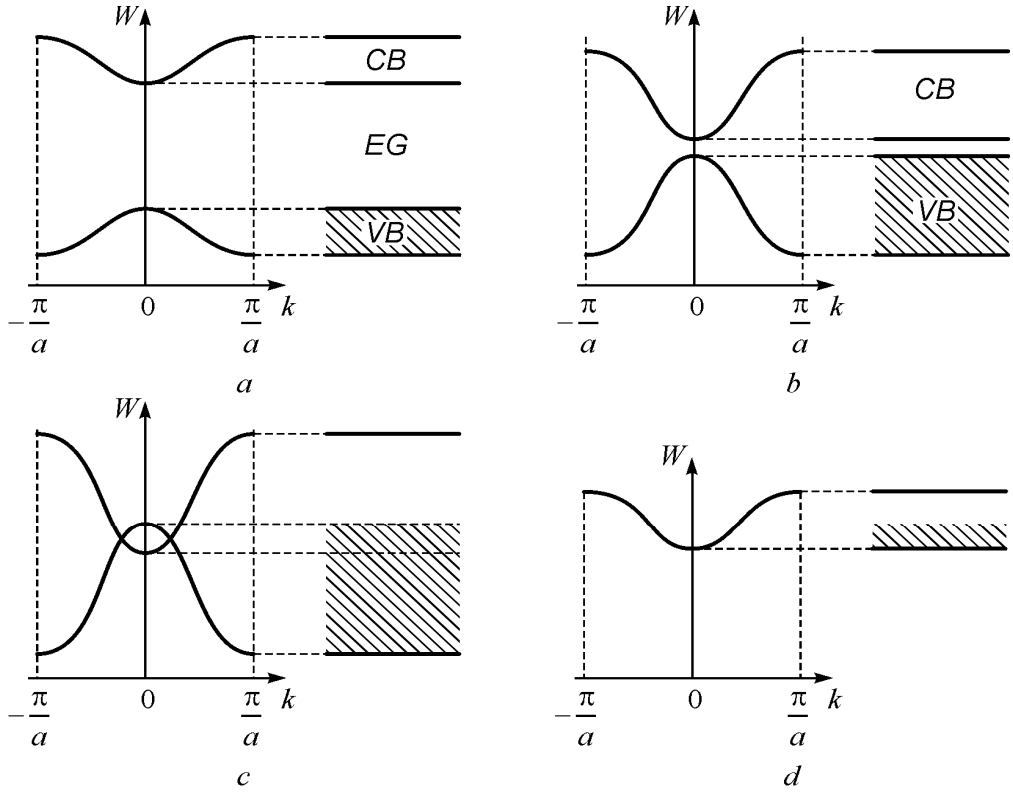

Fig. 2.19. Comparison of energy bands: *a* – dielectric, *b* – semiconductor, *c* – semimetal, *d* – metal: CB – conduction band, VB – valence band; *EG* – energy gap

In all other crystals most of electrons to some extent are localized. In the semimetals, however, excitation energy is almost zero, so even at temperature $T \to 0\ K$ mobile electrons exist and can provide essential conductivity. However, some of electrons in semimetals are localized between atoms and form spatially directed linkages.

Valence electrons in semiconductors (that are mainly covalent crystals) form the directed orbitals to link atoms, and their excitation energy (energy gap ΔW) usually exceeds thermal energy ($\Delta W > k_B T$). However, in semiconductors this energy gap is smaller than the energy of visible light ($\Delta W < 3\ eV$).

Valence electrons in dielectrics (that are mainly ionic and molecular crystals) are localized much stronger than in semiconductors. At that, they are localized not at the bonds between atoms (as in case of semiconductors) but near individual molecules or anions. The binding energy of electrons in dielectrics far exceeds not only thermal energy ($\Delta W >> k_B T$), but also the energy of visible light quantum: $\Delta W > \hbar\nu$. Therefore, probability of electrons excitation in dielectrics by thermal motion and even by light is very small. Moreover, small curvature of bands frontiers in the vicinity of their extremes in dielectrics (Fig. 2.20*a*) gives rise to increased effective masses of charge carriers, that results in low mobility of electrons.

Dielectrics and semiconductors are qualitatively similar: they both have energy gap in spectrum of electronic states. However, in semiconductors this band-gap is much smaller. Therefore, conductivity in semiconductors takes a wide interval, separating the value of conductivity of metals and dielectrics. For example, pure lead at temperature of 300 K has conductivity $\sigma = 5 \cdot 10^6$ *S/m* while in pure germanium conductivity is $\sigma = 2.5$ *S/m*. That is, conductivity of semiconductors is about a million times lower than conductivity of metals, but it is about same time semiconductors conductivity greater than in insulators.

In semiconductors the $\sigma(T)$ dependence can acquire "metallic character" only in the exceptional cases and in narrow temperature range; in general, temperature dependence of conductivity in semiconductors and dielectrics is similar. The width of energy gap of germanium is *0.72 eV*, in silicon it is *1.12 eV*, while in diamond (dielectric of same crystal structure as silicon and germanium) energy gap is about *5 eV*. If band-gap $\Delta W \leq 3$ *eV*, crystal can be regarded as semiconductor, while for larger values of ΔW it is dielectric.

The qualitative difference in the band gap and conductivity results in a significant differences between the optical, magnetic and electrical properties of dielectrics and semiconductors. In visible optical range dielectrics are light transparent and only a few reflect the light, while semiconductors have almost metallic reflection but dingy sheen. The reason for this lies in the fact that narrow energy gap of semiconductors allows light quanta with energy of about 2.5 eV excite free electrons that results in light reflection. In dielectrics such reflection is possible only in eye-invisible ultraviolet part of spectrum.

However, covalent crystals of semiconductors (such as silicon), in contrast to ionic dielectrics, are good transparent in the infrared region of spectrum, as energy of photons of this frequency (10^{12}...10^{14} Hz) is not sufficient to excite free electrons. Therefore, in the far infrared electronic devices the silicon and germanium can be used as transparent material of optical elements (lenses). Consequently, typical Si and Ge semiconductors at far infrared range play the role of “perfect dielectrics”. At the same time, glasses and ionic crystals, commonly used in the visible optics, can not be used in the far infrared range because they strongly absorb and intensively reflect these electromagnetic waves. The point is that just in far infrared range own oscillation frequencies of ionic crystal lattice are located, and this caused absorption of these waves.

Thus, it would not only roughly divide materials on dielectrics and semiconductors, but rather will distinguish semiconducting and dielectric properties of crystals that have energy gap in the spectrum of electronic states.

2.8 Summary Chapter 2

Conclusions

This chapter is devoted to general issues of applied solid state physics based on the main provisions of quantum mechanics with the particle-wave dualism and correspondent uncertainty relation. Materials science as part of solid state physics and nanophysics use the knowledge about structure of the atom and atomic spectra as well as Pauli principle, structure of electronic shells and valence of atoms. Before getting acquainted with the physical effects that find application in the microelectronics and nanoelectronics, it is necessary to pay some attention to comparing the basic concepts of classical mechanics about the structure of matter with a quantum mechanical approach to this issue.

References

[1] L.H. Van Vlack, Materials science for engineers, Addison-Wesley Publishing Co., 1975.
[2] C. Kittel, Introduction to solid state physics, fifth ed., John Willey, New York, 1976.
[3] N.W. Ashcroft, N.D. Mermin, Solid state physics, Holt and Winston, New York, 1976.
[4] Y.M. Poplavko, Polar crystals: physical nature and new effects, Lambert Academic Publishing, Saarbrucken, 2014.
[5] S.A. Voronov, Y.I, Yakymenko, L.P. Pereverzeva, Y.M. Poplavko, Materials science physics, Kiev Polytechnic Institute Ed., 2004.
[6] R. Waser (Ed.), Nanoelectronics and information technology: Advanced electronic materials and novel devices, Weinheim: Wiley-VCH, 2005.
[7] H.S. Nalva (Ed.), Nanostructured materials and nanotechnology, Academic Press, New York, 2002.

Questions

1. Describe the place of materials science in general physics
2. At what stage of the Universe's development did electromagnetism arise, and how do you think it affected the formation of atoms and solids?
3. How do you evaluate the idea of a dimensionless constant fine structure when describing the magnetic properties of matter?
4. What is the difference between the state of electrons in an atom and a crystal, and what is the role of spin?
5. In what other way can the zone theory be presented?
6. What are semi-metals and how do they differ from non-gap semiconductors?

CHAPTER 3. ELECTRICAL POLARIZATION AND CONDUCTANCE RELATIONSHIP

Contents

Electrical polarization and conductance can be considered separately only at a constant voltage, while in the alternating electrical field they are two sides of same process – forced by electrical field inertial motion of bound and relatively free charged particles. At that, to describe this process, the complex permittivity $\varepsilon^*(\omega) = \varepsilon'(\omega) - i\varepsilon''(\omega)$ and the complex conductivity $\sigma^*(\omega) = \sigma'(\omega) + i\sigma''(\omega)$ can be used equally that is shown by the examples of dielectrics, semiconductors and metals. As frequency increases, the delay of polarization leads to increase in conductivity, while the delay in electronic conductivity of metal can be described by the negative permittivity. The physical mechanisms of these transformations are explained.

In some non-centrosymmetric crystals, their internal polarity can essentially affect the electrical charge transfer. Inherent in polar crystals mixed ion-covalent bonds sometimes can be too finely balanced, so external influences (temperature, electrical field, etc.), lead to the great changing in electrical conductivity. This phenomenon manifests itself differently in the ordinary and strong electrical fields. In some polar crystals, the violation of their unbalanced structure can generate critical temperature change of resistivity, seen in the critistors and posistors; besides, such polar structure underlies the field-controllable switching elements and varistors. Used in based on polar nanostructures sensors, large sensitivity of conductivity to the external conditions, as well as the colossal magneto-resistance of certain compositions, also has to do with an unbalance of electrical polarity. Given representation of internal polarity impact on electrical charges transfer in the polar structures might be important for improving of relevant materials parameters.

Before considering effect of the interaction between the conduction and polarization, it is advisable to recall traditional concepts about these phenomena in the first two paragraphs.

3.1. Basic concepts of electrical conduction

Different responses of substance onto applied electrical field are listed symbolically in Fig. 3.1*a*. Several reversible and irreversible physical phenomena are seen – not only of *electrical* nature but also the *mechanical* and *thermal* responses. Among them are not only electrical responses – electrical induction $D(E)$ and current $j(E)$, but also the mechanical effects: electrostriction $x(E^2)$ and piezoelectric effect $x(E)$ as well as the thermal effects: Joule heat from dielectric losses $\delta Q(E^2)$ and heat or cold from the electrocaloric effect $\delta Q(E)$.

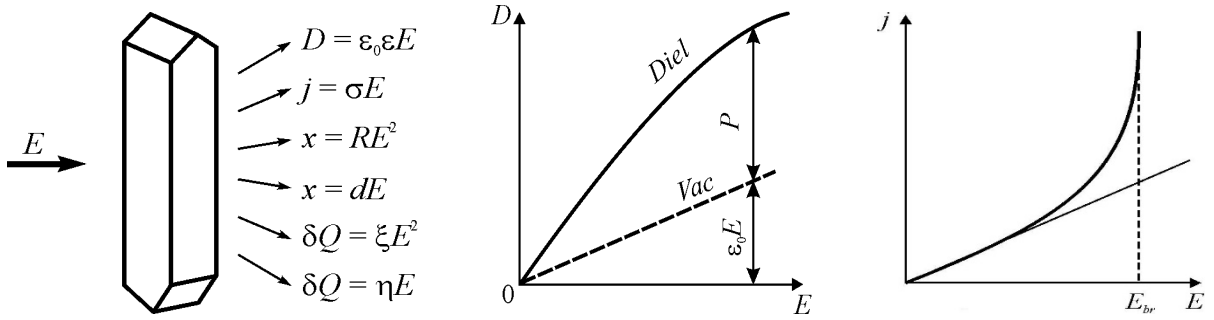

a *b* *c*

Fig. 3.1. Classification of polar crystal responses on electrical field influence: *a* – classification of electrical (*D, j*), mechanical (strain *x*) and thermal (δQ heat) effects (ε is permittivity, σ is conductivity, *R* is electrostriction coefficient, *d* is piezoelectric module, ξ is generalized loss factor, η is electrocaloric coefficient; *b* – electrical induction dependence on electrical field in dielectric compared with vacuum; *c* – electrical current density *j* dependence on electrical field *E*

However, only the *electrical conduction* is are discussed below, while next paragraph 3.2 is devoted to polarization.

The conduction, Fig. 3.1*c*, is an important phenomenon which arises in a material under the action of electrical field. If this field is not very big, then the current density, according to the Ohm's law, is proportional to voltage: $j = \sigma E$, where σ is the *specific conductivity* (otherwise called simply conductivity). However, in the strong electrical fields, the Ohm's law in dielectrics is violated, resulting in the *nonlinear* conductivity, so that $\sigma = \sigma(E)$, Fig. 3.1*c*. The increase in conductivity of dielectrics in a strong electrical field plays the decisive role in their *electrical*

durability (the steady state with small and time-independent conductivity). In the strong electrical field the conductivity increases with voltage growing, and becomes so big that the phenomenon of *electrical breakdown* occurs. Just before breakdown, the electrical current increases sharply due to the ionization effect, when the electrons moving in the electrical field interact with molecules, ions or atoms, adding them a sufficient energy to generate new electrons.

The electrical conductivity depends also on temperature, since the thermal motion of atoms and molecules leads to the activation of new free charge carriers, so that $\sigma = \sigma(T)$. In most dielectrics, a frequency dependence of conductivity is also observed: $\sigma = \sigma(\omega)$. This dependence can be absent only in those cases, when the electrical current is carried by the untied electrons – particles with a very high mobility. However, electronic conductivity in dielectrics, predominantly, has the hopping (polaron) character, when charge carriers have large effective mass and, hence, a low mobility. In the case of ionic conduction, as well as in the case of charge transfer by the micro-particles (molions), charge carriers have rather big inertia; consequently, the frequency dependence of electrical conductivity becomes evident. Thus, the bulk specific conductivity of dielectrics, as well as permittivity, is dependent not only on temperature but also on the electrical field intensity and frequency: $\sigma = \sigma(\omega, E, T)$.

Because of variety types of charged particles, quite different mechanisms of their generation (excitation) and different mechanisms of charges movement, electrical current in dielectrics, sometimes, might be rather complicated physical phenomenon. Dielectrics conduction classification, first of all, starts from the nature of charge carriers; in this case, there are several possible contributions to conductivity, which are listed in Fig. 3.2.

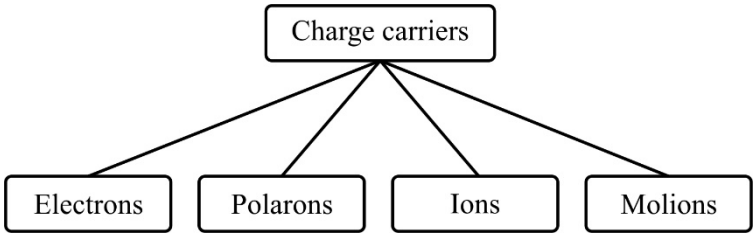

Fig. 3.2. Charge carriers classification in dielectrics

In the event of *electronic* conduction, current may consist of negatively charged electrons and positively charged electronic vacancies – holes. In dielectrics and some semiconductors, a polaron type charge carries is also possible, when electrons or holes are more or less associated with crystal lattice, and, therefore, they have relatively low mobility. *Ionic* charge transfer is typical for dielectrics. This

mechanism of conduction is defined by the flow of positively charged cations or negatively charged anions, as well as by charged ionic vacancies of the opposite polarity. In direct electrical field, the ionic conduction represents not only a charge transfer but also a matter transfer – electrolysis. Liquid dielectrics, except electronic and ionic conduction, can have so cold “mole-ionic” conduction, at which charge carriers constitute charged atomic groups or charged molecules – relatively large particles (electrophoresis). In the case of a positive charge, this electro-migration results in the cataphoresis, while in the case of their negative charge leads to anaphoresis.

Previously it was thought that dielectric (insulator) is a matter that characterized by predominantly ionic conduction; to emphasize this fact, in the early literature dielectrics were even called *electrolytes*. It should be noted that in solid electrolytes conductivity changes with time even at constant voltage, because of "exhaustion" of free charge carriers: quantity of free ions in dielectric is limited, so in the case of DC these charge carriers migrate gradually to the electrodes and accumulate there. In this regard, an ionic conduction is one of the causes of electrical insulators aging (this is the change in properties with time under the influence of electrical field). However, in an alternating electric field, ions do not have time to accumulate at the electrodes, so in the alternating field ionic conduction of dielectrics looks like a time-constant (stationary) process, as electronic conduction.

Electronic conduction, as confirmed by studies in recent years, plays a very important role in the electrical charge transfer of in dielectrics. As already noted, electronic charge transfer (in contrast to ionic and mole-ionic mechanisms) is a stationary process not only in alternating but in direct electric fields, and as between dielectric and electrodes there is an interchange by charge carriers of same physical nature (electrons). Two important properties of dielectrics – polarization and very low conduction – are largely interdependent. Electrons or holes, appearing in dielectrics as a result of various activation processes, may become less active, because they polarize by their field some surrounding area of dielectric, so they are forced to move with these polarized nano-regions (polarons). Consequently, even those small amount of free electrons which occur in the dielectric because of thermal activation of impurities, may not cause any appreciable charge transfer, just because *local polarization* around charge carriers exists, which reduces their mobility in an electrical field.

In turn, low concentration of charge carriers and their low mobility are responsible for electrostatic field long existence in the dielectrics. In conductors this field is screened by free charge carriers (in metals, for example, screening radius is

approximately equal to interatomic distance). Thus, electrical polarization contributes to the emergence and existence in dielectrics of a relatively stable state with extremely low electronic conduction. However, this stability may be broken in dielectric by heating of by high intensity irradiation, particularly, by coherent optical (laser) radiation. Then the charge carriers are generated in high concentrations, and they shield the electrical field, so dielectric is converted into a conductive medium. Stability of non-conducting state of dielectrics may be compromised by a strong electrical field, which accelerates the freed electrons (or holes) up to the energy, at which they can no longer be "captured" by polarization of dielectric surroundings and acquire a "slow-moving" state. These *fast electrons* cause percussive ionization in dielectric, resulting in rise in a number of free electrons, which ultimately gives rise to the electrical breakdown, and insulator changes into a conductor.

In some especial cases, the stability of non-conducting state of dielectrics may be compromised even in weak electrical fields and without their strong heating or irradiation. The reason is the change in the structure, associated with mutual arrangement of particles, and, hence, the change in symmetry of crystal. In such peculiar cases, even a small change in external conditions (pressure, temperature, magnetic field or electrical field) can lead to spasmodic increase (in 10^3...10^9 times) in conductivity, i.e. the insulator turns into a conductive state. Such discontinuity in the conductivity might be a result of phase transition (PT), wherein, on account of changes in the external conditions (field, temperature, pressure), some of electrons free themselves from their polarized surroundings and, in turn, shield an electrical field. For example, such phase transitions are observed in the oxides of transition metals, as well as in low- dimension systems and in "super-ionic" conductors. Unlike irreversible effects (electrical breakdown) these phase transitions from an insulating state to a conducting state are reversible, because dielectric do not undergo to destruction as it happens in the case of an electrical breakdown.

Charge carriers generation. Electrical conduction of dielectrics and semiconductors is always conditioned by the activation processes, charge carriers arise because of different mechanisms that causes their appearance, Fig. 3.3.

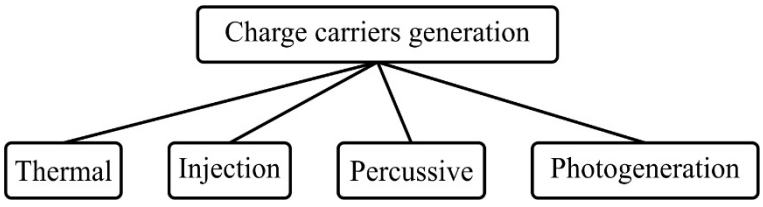

Fig. 3.3. Mechanisms of charge generation in dielectrics

The most universal and, therefore, the most important process is the *thermal activation* – a permanent mechanism for the appearance of the charge carriers in dielectrics and semiconductors. At normal and elevated temperatures thermal generation of charge carriers in dielectrics gives the main contribution to their conductivity; at that, in characterisation of dielectrics, not only thermal generation of electrons and holes are important, but also the generation of mobile ions. In addition to process of thermal generation of mobile electrons and ions, there exists and constantly going on the process of *recombination*, at which electron and hole (or ion and ionic vacancy) combines in a neutral structure, and as two type of carriers "cancel out each other." In dielectrics (as in semiconductors) between heat generation and recombination of carriers a *dynamic equilibrium* is established, which depends on energy levels and on temperature. Charge carriers produced by thermal activation are called as *balanced* (equilibrium) charge carriers. It is important to note that only those charge carriers are balanced, which formed by thermal excitation and relaxation, while other mechanisms for the charge carriers generation, listed in the Fig. 3.3, result in only to non-equilibrium charge carriers.

Injection of electrons or holes in the dielectric (or semiconductor) is executed from metal electrodes; those charge carriers, which are introduced into the crystal by this way, are always non-equilibrium. *Photo-generation* of charges in dielectric is caused due to various type of irradiation, at that mechanism the charge carries are also non- equilibrium. Finally, the *ionization by collision* occurs in the strong electrical fields, and it also leads to generation of non-equilibrium carriers: owing to this ionization, charge carriers concentration increases up to electronic avalanche that can cause the electrical breakdown.

Mechanisms of charge carries transport are another important aspect of the electrical conduction of dielectrics, Fig. 3.4. Transfer mechanism is called as *drift,* if upon chaotic (thermal) motion of charge carriers their directed movement (drift) in electrical field is imposed. In this movement charge carriers spent most of their time, while much less time they spend for collisions, captures and scattering on other particles. In the small electric fields, the drift velocity of charged particles is much less than the velocity of their chaotic movement.

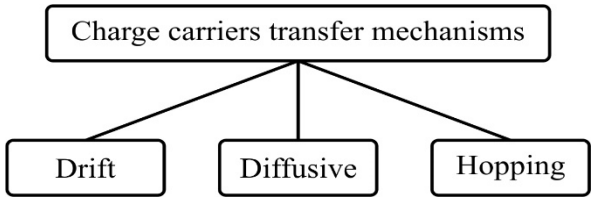

Fig. 3.4. Mechanisms of charge transfer in dielectrics

Very important for dielectrics is the mechanism of charge transfer that is considered as a *hopping* mechanism; it is peculiar as for ionic so for polaronic types of conduction. According to this mechanism, charge carriers most of time spent in the localized state, and only very short time expend for movement which is jump to a nearby centre of localization in crystal lattice. It should be noted that the jump itself is a change of quantum state, and it occurs almost instantaneously, but the number of jumps per unit time (their frequency) is limited.

As in semiconductors so in dielectrics, the *diffusive* mechanism of charge transfer is also possible, when in different places of sample the concentration of charged carriers is different, and, due to particles disordered (random) motion, the concentration of carriers in dielectric (or semi-conductor) is aligned. Charge carriers are gradually moving from the place of their higher concentration to the region of lower concentration. Diffusion current can be observed in the absence of an external electrical field.

3.2. Basic concepts of electrical polarization

The *electrical polarization*, among many others phenomena, should be noted as the first, as shown in Fig. 3.1. In dielectrics, the electrical *displacement D* (otherwise known as electrical *induction* (measured in [D] = C/m^2) appears which is greater than in vacuum owing to the electrical *polarization P*. Indeed, if there is no dielectric between metallic electrodes of capacitor (the case of a vacuum), the value of electrical induction equals $D = \varepsilon_0 E$, where $\varepsilon_0 = 8.854 \cdot 10^{-12}$ F/m is the electrical constant ([F] = *C/V* is the farad, unit of electrical capacitance *C* measure). Parameter ε_0 in SI agrees the units of *D* and *E*, characterizing the *absolute permittivity* of vacuum. The electrical polarization is most important property of dielectrics. In active dielectrics polarization is induced not only the externally applied electric field, but it can be spontaneous due to intracrystalline electrical moment. In the non centre symmetric dielectrics polarization can be induced by the mechanical action. In this chapter the only polarization induced by the external electrical field is discussed. Electrical charges in the dielectric structure are bound very tightly, therefore, the concentration of free charge carriers, causing an electrical conductivity in dielectrics, is usually very small. In this connection, in further consideration of the dielectric polarization it is assumed for simplicity the complete lack of electrical conductivity: $\sigma = 0$.

When dielectric is placed between the electrodes of a capacitor, then under the action of electrical field, bounded positive and negative charges of atoms, ions

and molecules of a material becomes slightly shifted relatively to each other, creating the overall electrical moment. The *specific electrical moment* (i.e., the moment per unit of volume) is the *polarization* P. The stronger electrical field the larger is the value of P, Fig. 3.1*b*. The *electrical displacement* D (otherwise called induction) is the sum, determined as $D = \varepsilon_0 E + P$. The ability of dielectric to polarization in electrical field is characterized by the *relative permittivity* ε (commonly referred to as dielectric constant), which shows how much more the electrical induction in a dielectric is greater than in vacuum: $D = \varepsilon_0 \varepsilon E$. It should be noted, however, that in the strong electrical field a deviation from this linear dependence of $D(E)$ can be observed, shown in Fig. 1B. This dielectric *nonlinearity* usually is bigger in the dielectrics possessing high permittivity, which in this case depends on the magnitude of electrical field: $\varepsilon = \varepsilon(E)$. As a matter of fact, the temperature usually affects the polarization process that results in the temperature dependence of permittivity: $\varepsilon = \varepsilon(T)$. Furthermore, when dielectric is studied at the AC voltage, the permittivity can vary with frequency, so $\varepsilon = \varepsilon(\omega)$. Thus, very important for dielectrics parameter can be a function of several external influences: $\varepsilon = \varepsilon(\omega, E, T)$.

Microscopic conception of the polarization mechanisms can be reduced to a few relatively simple models of the electrical moment appearance and changes in the electrical field. Since the quantum-mechanical calculations of the atomic electronic shells interaction with the nuclei are difficult even for some simple molecules, then to describe the polarization in the bodies consisting of a set of atoms, ions and molecules it is useful to consider the simple models of the polarization on the basis of classical concepts. Under electrical field applied to dielectric, the electrically connected charges are displaced relatively to each other, whereby the dielectric becomes polarized. As already mentioned, the external electric field induces in a dielectric the *elementary* electrical moments $p = qx$, where q is the shifting electrical charges and x is their mutual displacement.

Field-induced electric moment may get contribution from:

- *electrons*, displacing from their equilibrium positions in atoms;
- *ions,* deviating from the equilibrium state in the crystal lattice;
- *dipoles* (polar molecules), changing their orientation in the electrical field;
- *macro-dipoles* (electrically charged particles or complexes in an inhomogeneous structures (ferroelectrics, piezoceramics).

Electrons, ions and dipoles (including macro-dipoles) can form an electrical moment (i.e., the polarized state) through various mechanisms. If these particles are bound to the structure elastically and relatively rigid, the external electrical field or

other exposure (in piezoelectric – mechanical) can lead only to a very small (even compared with atomic dimensions) deviations from the unpolarized equilibrium state. However, since in the process of polarization involves all particles of the dielectric, even these small relative displacements of charges cause significant integral effect – the polarization. Such a mechanism is called the *elastic polarization*.

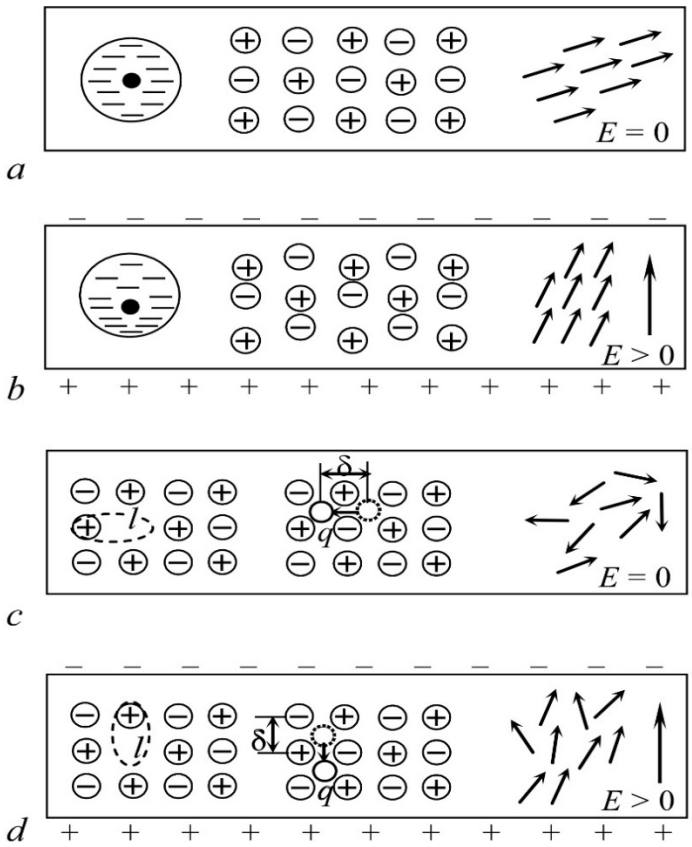

Fig. 3.5. Microscopic mechanisms of polarization: *a, b* – three mechanisms of elastic polarization: fragments of dielectric in absence of electric field *E* and when it is applied; *c, d* – three mechanisms of thermal polarization: fragments of dielectric in electric field *E* absence, and when it is applied

The basic physical mechanisms of elastic polarization are shown schematically in Fig. 3.5, *a* and *b*. In an unpolarized state ($E = 0$), the electronic shells of atoms are symmetrical with respect to the nuclei (Fig. 3.5*a*, the left-hand fragment), so that the effective centre of the negative charge coincides with the positively charged nucleus. Accordingly, the elemental dipole moment is zero ($p = 0$), since it is determined by the product of $qx = p$, and the relative displacement of the charges q^+ и q^- is absent, i.e., $x = 0$. If the electric field is applied (Fig. 3.5*b*) in the each atom, molecule or ion, their electronic shells become distorted and displaced with the respect to the nuclei, whereby the centre of negative charge shifts

relatively to the positively charged nucleus, so that a elementary polar moment appears as $p = qx > 0$. This is the mechanism of the ***electronic elastic*** polarization.

In an ionic crystal, in the absence of an externally applied electric field (see Fig. 3.5*a*, the central fragment), there are cations and anions in the crystal lattice sites. The system of charges is electrically neutral, and it does not form any electrical moments (polarization). But in an external electric field (Fig. 3.5*b*), the cations and anions are displaced under the influence of Coulomb forces, forming the polar lattice of q^+—q^- with the elementary electric moments $p = qx > 0$. By these way in the ***ionic elastic*** polarization arises that for ionic dielectrics is of great importance. The energy characteristics of the elastic polarization process are shown in Fig. 3.6*a*. The elastic energy of bound particles (ions in crystal, electrons in atom, dipole in lattice) is given by the equation $U = ½\ cx^2$, where c is the elastic coupling coefficient and x is elastic displacement from the equilibrium position.

In the absence of external influences $x = 0$, and the particle is localized in the bottom of the parabolic potential well. Under applied electric field the particle acquires extra energy $U = ½\ cx^2 - qxE$. That energy gain is added to elastic energy, so the minimum of energy shifts to the position of $x > 0$ (Fig. 3.5*a*) in which the particles already have elementary electrical momentum $p = qx$ and contribute to the polarization. Shutting the field leads to a rapid establishment of former equilibrium position when $x = 0$, and the elastic polarization disappears.

On the right-hand fragments of Fig. 3.5, *a* and *b*, the third elastic mechanism of polarization is shown, namely, the elastic rotation of the dipoles. It is possible only in the case of own polarity of dielectric (existing in the absence of an external field) that is observed in many active dielectrics. The dipoles ordering in such a polar lattice is conditioned by the internal interaction (usually, by the mixed ionic-covalent bonding) and spontaneously oriented by the intracrystalline field, which they themselves created. The external electric field alters the orientation of all dipoles of entire structure, thereby electrical field changes the electrical dipole moment, i.e., its new orientation induced the polarization (Fig. 3.5*b,* right-hand fragments). This is the mechanism of the *dipole elastic* polarization.

By switching off externally applied field, all the above said mechanisms of polarization disappear very rapidly: dielectric returns to its equilibrium (unpolarized) state. Electrons occupy electrically symmetrical position relatively to the nuclei due to Coulomb forces of attraction, cations and anions will return to their stable (equilibrium) position in the crystal lattice sites by the forces of repulsion of the electron shells of the ions. The area of coordinated dipole polarization returns to its original position (in which energy of oriented dipoles system is minimal). But

sometimes – in the ferroelectrics – there are the areas called the domains that can remain in the rotated state.

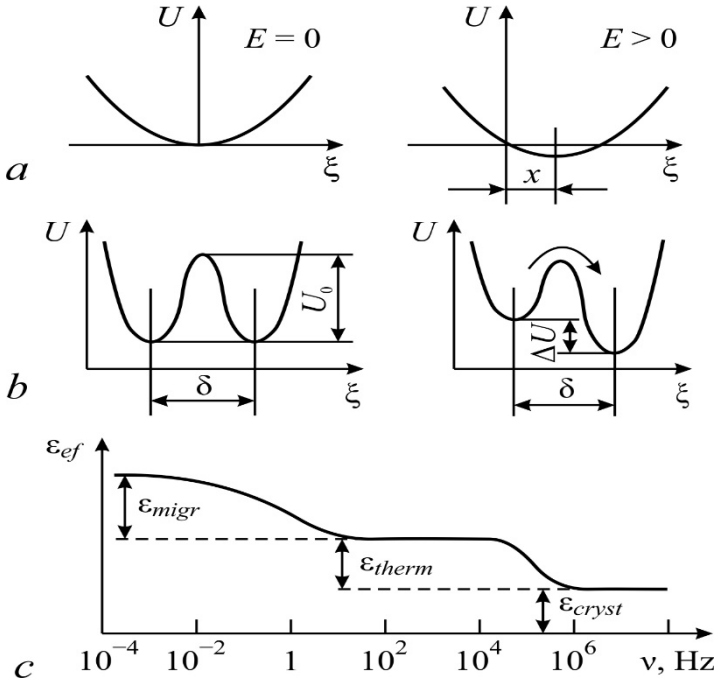

Fig. 3.6. To different polarization mechanisms explanation of: *a* – elastic energy change at deformation mechanism; *b* – change in thermal energy (relaxation mechanism); *c* – frequency dependences of the dielectric contributions from migratory, thermal and fundamental (lattice) polarization.

Besides the elastic (deformation) polarization, the electrons, ions and dipoles (macro-dipoles) may also participate in the mechanisms of both *thermal* and *migratory* polarization.

In the case of weak bonding in the structure, some electrons, ions and dipoles are significantly affected by the thermal (chaotic) motion of particles in a dielectric structure, and this may have an influence on the polarization, Fig. 3.5, *c* and *d*. These pictures show that such particles (usually impurities) are isolated in the local (nano-scale) areas, so they are not the main structural elements of the dielectric. Electrically charged impurities relatively loosely bound in the crystal lattice, but they are forced to be localized in the vicinity of the structural defects in the dielectric.

Remaining localized in the nano-volumes, these particles, under the influence of the thermal motion, perform the thermally activated jumps, moving over distances of atomic dimensions order. Therefore, their abrupt displacement in 10^4...10^6 times exceeds the value of small elastic displacements of the main structural units of the crystal (that produce elastic polarization). That is why these jumps can have a significant effect on the dielectric constant.

Electronic thermal polarization is due to the weakly bounded electrons, for example, the electrons, compensating the structural defects. These defects, for example, include the anion vacancies (lack of negative ions), as it is shown in Fig. 3.5*c*, the left-hand fragment. Charge compensation occurs because the crystal lattice always should be electrically neutral: that is, the number of negative charges in it equals to the number of positive charges. The electron, which charge compensates the charge of wanting anion, is localized near one of the surrounding position cations; at that, the orbital of this electron is strongly deformed: it is stretched out to an anion vacancy to compensate the absent charge, Fig. 2.3, *c,* left-hand. This leads to the spontaneous formation a local electrical moment $p_0 = ql_0$, where l_0 corresponds approximately to the lattice constant (~ 0.2 nm). The magnitude of this moment is not determined by the external electric field; while such "own" dipole moment p_0 thousands of times higher than possible electric moment induced by the external field elastic polarization ($p = qx$, where x is induced elastic displacement, has the order of 10^{-6} nm).

Weakly bonded electron (that is localized near the anion vacancy) even in the absence of an external field, from time to time, under the influence of thermal chaotic motion jumps from one of neighbouring cation to another, overcoming the energy barrier U_0 (Fig. 3.5*b*). At that, the direction of inserted dipole moment p_0 should be changed. Despite the fact that the quantity of these defective places in the real dielectric is rather big ($10^{24}...10^{26}$ m^{-3}, as compared with concentration of basic structural units of the crystal ~10^{28} m^{-3}), the macroscopic polarization in the crystal does not arise because all "own" dipoles are oriented randomly at any time.

Externally applied electric field reduces the potential barrier (Fig. 3.6*b*) that lead to excessive orientation of "electron-cation" dipoles in accordance with the applied field (Fig. 3.5 *d*, left-hand fragment). Such is, in general terms, the mechanism of the electronic thermal polarization. This polarization is called as “thermal” because the electron jumps between cations due to the thermal energy of the crystal. The electric field, that has low impact energy $\Delta U < k_B T$ (Fig. 3.6*b*), leads only to a certain redistribution of local electrical moments p_0 orientation.

Ionic thermal polarization mechanism (Fig. 3.5, *c* and *d*, the middle fragments) is largely similar to the thermal electronic mechanism. It is assumed that in the crystal lattice the impurity (embedded) ions are present that usually have small ionic radius (some of positive ions). This model is close to the ionic crystals doped with lithium ions or protons (one of experimental example). It is assumed that the impurity cations are located in the interstices of the structure, and their charge compensation is carried out due to the increased charge of one of the neighbouring

anions. In the vicinity of such anion, the impurity ion makes thermally induced jumps. These jumps are hampered by a potential barrier (Fig. 3.6*b*), because for change in its localization the impurity ions need to overcome the repulsive forces of the electron shells of the neighbouring ions. Dipole moment p_0 is created between the jumping impurity ion and the fixed charge-compensating anion (that has larger radius).

When the impurity ion makes hopping in the vicinity of its localization, changing the direction, the electrical moment with the anion is formed. In the absence of an external field, the set of such polar defects are reoriented chaotically, that usually do not lead to an integral polar moment – polarization. (However, there are some uncommon examples when interaction between such polar defects leads to the spontaneous polarization – artificial ferroelectricity).

In the externally applied electrical field E (Fig. 3.5*d*) along hopping direction the asymmetry appears, and thereby a macroscopic polarization arises (in this case – the thermal ionic polarization). After the switching off the electrical field, due to the disorienting effect of thermal chaotic motion, electrically induces thermal polarization gradually disappears. The energy barrier U_0, which should be overcame by the impurity ion (Fig. 3. *b*), is much greater than the energy of thermal motion of the particles in a dielectric: $U_0 >> k_B T$. However, the probability of thermal hopping of electrons or ions (as well as the likelihood of thermal reorientation of dipoles) increases with increasing temperature. These thermally activated jumps occur at a distance δ which is defined by the features of the crystal structure and defects, but does not depend on the external field E (as opposed to elastic polarization, when the polarization is determined by the size of displacement: $x \sim E$). In case of thermal polarization, the external electrical field only *changes the probability* of hopping over barrier particles. One of the potential wells, as compared to the other, becomes deeper on $\Delta U << U_0$. This value depends on the applied field: $\Delta U = q\delta E$, that is the contribution of the electrical energy at a distance of thermal hopping.

Dipole thermal polarization in crystals and textures can be approximately characterized by the model shown in the right-hand part of Fig. 3.5, *c* and *d*. In the absence of an external field, the "hard" dipoles already exist, but they are distributed randomly. Externally applied electrical field results in preferential orientation of the dipoles in the system, i.e., the bulk electrical moment appears. In reality, the possibility of thermal dipole polarization in the active dielectrics is limited to a certain number of stable dipole orientations (in accordance with the symmetry of crystal or texture). In the absence of an external field, the dipoles are oriented

uniformly in all permitted directions; after electrical field is switching on the likelihood of dipole orientation in a favourable direction increases.

It is obvious, that thermal polarization mechanisms are much slower in comparison with the elastic polarization. In the case of elastic polarization, the polarized system of elastically bounded charges, after electric field removal, returns to its equilibrium (non-polarized) state in a very short time $10^{-12}…10^{-16}$ s. On the contrary, in the case the thermally activated polarization, the thermo-electro-diffusion occurs for "semi-free" electrons or ions through the potential barriers. It is obvious that such a process is relatively slow: it needs time of about $10^{-2}…10^{-9}$ s. At that, the time of thermal relaxation is strongly dependent on temperature, which characterizes the intensity of thermal motion.

Migratory polarization, which might be peculiar for certain active dielectrics (polarized textures) is the slowest mechanism, Fig. 3.6*c*. When it happens, the related charges move at the highest (almost macroscopic) distance. In this case, the accumulation of electric charges takes place on the boundaries of the irregularities (between-crystallite layers, interstices, large defects) determines the *space-charged polarization*. This mechanism significantly increases the low frequency capacitance of electrical capacitor containing heterogeneous dielectrics. Migratory (space-charged) polarization can not be attributed to the microscopic mechanisms of polarization and, therefore, the dielectric constant calculated by the geometric dimensions and capacity of the capacitor, in the case of migratory polarization is called as "effective" ε_{ef}.

In the piezoelectric and pyroelectric textures (ceramics), the large dipole groups are involved to migratory polarization (by orientations of different sizes domains) that also should be described by the ε_{ef}. In the frequency dependence of permittivity, the contributions of migratory polarization ($\varepsilon_{ef} = \varepsilon_{migr}$) and thermal (relaxation) polarization ($\varepsilon = \varepsilon_{therm}$) are shown in Fig. 3.6*c*. In the case of a high concentration of the charged structural defects, these dielectric contributions may be much larger than the dielectric constant of pure (ideal) crystal ε_{cryst}. However, at higher frequencies (starting from the acoustic frequency range) there is no time to accumulate and dissipate the space charge; as a result, the migratory polarization is late, i.e., the ε_{migr} experiences a dispersion. In the frequency range of dielectric constant dispersion, the maximum of dielectric losses (tan δ) is also observed.

Microscopic structural defects that are resulting in the thermal polarization ε_{therm} give rise to the dielectric contribution at the frequencies below $10^5…10^9$ Hz, depending on the temperature and the type of defects. The dispersion (frequency

dependence) of ε_{therm} is also accompanied by a maximum of dielectric loss. Different inertia of various mechanisms of the induced polarization allows the experimental selection of their dielectric contributions if the properties of dielectrics are studied in a wide range of frequencies. This method of dielectric spectroscopy is not only suitable for the detection of the contributions in the ε_{migr} (space-charge polarization or domain reorientation in the textures and composites), also for the study of crystals with perfect structure, where the impurities, defects and space charges do not affect the ε-value.

3.3 Permittivity and conductivity interchangeability

Formal relationship between dynamically changing processes of polarization and electric charge transfer can be established on the basis of Lorentz-Maxwell's equations. The interaction of electrical and magnetic fields E and H in a matter is described as:

$$\text{rot } E = -\partial B/\partial t, \quad \text{rot } H = j + \partial D/\partial t, \quad \text{div } D = \rho, \quad \text{div } B = 0, \qquad (1)$$

where B is the magnetic induction, j is the current density, $D = \varepsilon_0 \varepsilon E$ is the dielectric displacement, and ρ is the density of electrical charges. The relationship between magnetic field H and magnetic induction B is defined as $B = \mu_0 \mu^* H$, where μ_0 is the magnetic permeability of vacuum, while $\mu^* = \mu' - i\mu''$ is the complex magnetic permeability denote the real and the loss part. In the case under consideration, i.e., for the diamagnetics and weak paramagnetics, it can be set $\mu^* = \mu' = 1$ and $\mu'' = 0$; therefore, any magnetic processes are no longer taken into account in future considerations [1].

Therefore, next only the electrical polarization and the electrical conduction will be considered. Both of these processes occur due to electrical field effect on the movement of charged particles in a substance, so in AC polarization and conduction are usually interdependent. To be described in the sinusoidal electrical field: $E(\omega) = E_0 \exp(i\omega t)$, both the dielectric displacement and the conduction should be represented by complex parameters. In the Maxwell-Lorentz equations (1), the second one (rot $H = j + \partial D/\partial t$) shows that the current density j and the time derivative of electrical displacement $\partial D/\partial t$ are additive quantities. That is why, current density $j = \sigma^* E$ and derivative $\partial D/\partial t = i\omega\varepsilon_0\varepsilon^* E$ would be represented as equivalent functions, if the complex values will be used to describe them. When these functions are presented by real and imaginary parts, complex conductivity $\sigma^*(\omega)$ is connected to complex permittivity $\varepsilon^*(\omega)$:

$$\sigma^*(\omega) = \sigma'(\omega) + i\sigma''(\omega) = i\omega\varepsilon_0\varepsilon^*(\omega), \qquad \varepsilon^*(\omega) = \varepsilon'(\omega) - i\varepsilon''(\omega), \quad (2)$$

where ε_0 is the dielectric permittivity of vacuum. Hence, in the sinusoidal electrical field, the complex conductivity and complex dielectric function are interconnected. It follows that the real and imaginary part of dielectric permittivity can be expressed through the components of complex conductivity:

$$\varepsilon'(\omega) = \sigma''(\omega)/(\varepsilon_0\omega); \qquad \varepsilon''(\omega) = \sigma'(\omega)/(\varepsilon_0\omega) \quad (3)$$

Similarly, the real and imaginary part of complex conductivity can be expressed through the components of complex permittivity:

$$\sigma'(\omega) = \varepsilon_0\omega\varepsilon''(\omega); \qquad \sigma''(\omega) = \varepsilon_0\omega\varepsilon'(\omega) \quad (4)$$

It should be noted that formally established connections between $\sigma^*(\omega)$ and $\varepsilon^*(\omega)$ is expedient to be explained by the microscopic mechanisms of substance responses, as from the side of polarization processes, which means the separation of bound electrical charges, so from the side of electrical conduction that means a transfer of non-bound charges [4].

In principle, any of aforementioned complex parameters can describe completely the frequency dependence of electrical response of a substance to the alternating voltage. Nevertheless, exactly the frequency dependence of permittivity is traditionally represented in most researches. However, it should be noted that in some cases, while obtained experimentally data processing, the more informative parameter is turned out the frequency dependence of conductivity*;* for example, to determine accurately the natural frequency of a damped oscillator: it corresponds exactly to the $\sigma'(\omega)$ maximum as will be shown below.

3.4 Inertia of electrical polarization mechanisms

All physical processes are limited by a speed of their completion. As for the electrical polarization, which is described by the permittivity, the least inertial is the elastic displacement of electronic shells relative to cores (~ 10^{-16} s), more inertial is the ionic lattice polarization (~ 10^{-13} s) but much more inertial are various mechanisms of thermally activated (relaxation) polarization (10^{-4}–10^{-9} s). In all cases, a mutually conditioned changes in the permittivity and electrical absorption (characterized by effective conductivity) is observed. At that, relaxation and resonant changes of electrical response parameters with increasing frequency are inevitable processes due to inertia of particles involved in polarization (at that, it is assumed that constant voltage conductivity is so small that it can be neglected). The delay of polarization mechanisms looks like the electrical charge transfer, i.e., as if the

effective conductivity appearance. It can both increase or decrease during frequency growth in accordance with the physical nature of polarization and depending on the properties of dielectric.

Relaxation polarization is described here by the idealized physical model of electrical response, characterizing gradual establishing balance in a system of dipoles perturbed by the electrical field in the condition of thermal chaotic motion. Main parameters of this model are its contribution to the permittivity ($\Delta\varepsilon$) and the relaxation time (τ). If constant electrical field $E = E_0$ acts on polar dielectric, then it contributes the orientation of some part of dipoles, creating induced electrical polarization $P = P_0$, Fig. 3.7*a*, where switching on moment of electrical field is not considered.

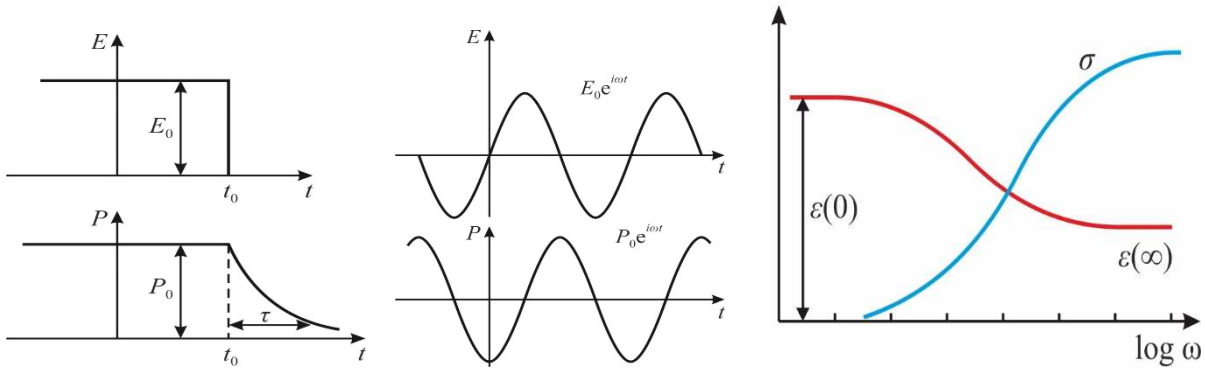

Fig. 3.7 Relaxation polarization: *a, b* – time-dependence of dipoles system polarization *P* under influence of constant (*a*) and alternating (*b*) electrical field *E; c* – permittivity $\varepsilon(\omega)$ and effective conductivity $\sigma(\omega)$

In the applied electrical field E_0, a lot of dipoles of dielectric are continuously orienting and disorienting, however, in average, the polarized state with value P_0 remains thermodynamically stable. Suppose that at the moment $t = t_0$ the electrical field is turned off; as a result, the chaotic thermal motion leads to a gradual depolarization of dielectric. At that, a new equilibrium state (not disturbed by the electrical field) will be already non-polarized. The principle of thermodynamics states that *rate of recovery of equilibrium state is proportional to magnitude of deviation from this state*, i.e., $dP/dt = -kP$. The dimension of proportionality coefficient k is inverse to time, so it can be denoted as $k = \tau^{-1}$. Therefore, differential equation, describing gradual decrease of polarization when it approaches to equilibrium state, is $dP/dt = -(1/\tau)P$. The solution of this equation results in description of time-dependent gradual decay of polarization: $dP/P = -dt/\tau$, so $P(t) = P_0 e^{-t/\tau}$. Frequency dependent dielectric permittivity can be found, if the *alternating* electrical field $E(\omega)$ acts on the model under consideration (system of non-

interacting dipoles), taking into account the definition of permittivity as the proportionality coefficient between electrical displacement D and electrical field E: $D = \varepsilon_0\varepsilon E = \varepsilon_0 E + P$; $\varepsilon = 1 + P/\varepsilon_0 E$, where ε_0 is electrical constant used in SI system.

To determine the permittivity, one need to find ratio $P/\varepsilon_0 E$. For this purpose, as shown in Fig. 3,7*b*, the sinusoidal (harmonic) dependence of electrical field on frequency should be used; $E(\omega) = E_0\exp(i\omega t)$, which in the *linear* case (correspondent to weak electrical field) leads to similar dependence of induced polarization $P(\omega) = P_0\exp(i\omega t)$. To find frequency dependence of permittivity, it is necessary to solve first-order inhomogeneous differential equation: $dP/dt = \tau^{-1}P = gE_0e^{i\omega\tau}$, where coefficient g is reactive conductivity $g = n_0\alpha_T$ determined by dipoles concentration n_0 and their polarizability α_T.. When solving this equation, the transient processes are not considered, so by substituting $P(\omega) = P_0\exp(i\omega t)$ it is possible to get the complex permittivity consisting of real $\varepsilon'(\omega)$ and imaginary $\varepsilon''(\omega)$ parts:

$$\varepsilon^*(\omega) = \varepsilon(\infty) + \frac{\varepsilon(0) - \varepsilon(\infty)}{1 + i\omega\tau} \quad (5)$$

The numerator $\varepsilon(0) - \varepsilon(\infty) = \Delta\varepsilon$ is the dielectric contribution of relaxation process. From this expression the main formulas describing frequency dependence of $\varepsilon'(\omega)$ and $\varepsilon''(\omega)$ as well as the effective conductivity $\sigma(\omega)$ follow:

$$\varepsilon'(\omega) = \varepsilon(\infty) + \frac{\varepsilon(0) - \varepsilon(\infty)}{1 + \omega^2\tau^2}; \qquad \varepsilon''(\omega) = \frac{\left[\varepsilon(0) - \varepsilon(\infty)\right]\omega\tau}{1 + \omega^2\tau^2}.$$

$$\sigma'(\omega) = \varepsilon_0\omega\varepsilon''(\omega) = \varepsilon_0\tau\omega^2[\varepsilon(0) - \varepsilon(\infty)]/(1 + \omega^2\tau^2)$$

Eventually, effective conductivity gradually reaches constant value $\sigma'_{ef} = \varepsilon_0\Delta\varepsilon/\tau$. This dependence of effective conductivity in dielectrics and wide-gap semiconductors are observed usually in a broad frequency range (10^{-4}–10^8 Hz), being typical for quite different structures and various chemical compositions [4]. This means that directed by electrical field thermally activated motion of partially bound charged particles (whose localization are determined by a set of potential barriers) gives rise to both the polarization and effective conduction.

Resonant dispersion of permittivity is described by the oscillator model. Compared to relatively "slow" processes of relaxation polarization, the establishing of quasi-elastic polarization occurs almost instantly. That is why, in equations describing thermal relaxation polarization the dielectric contribution of these fast processes to the value of permittivity was taken into account as the $\varepsilon(\infty)$, and it was assumed that in a

very broad frequency range this value remains constant, while dielectric losses and effective conductivity are attributed only to the slow polarization processes.

In the case of considered quasi-elastic polarization losses and effective conductivity arise at much higher frequencies; nevertheless, in some ferroelectrics already at microwaves the losses from soft modes of ionic polarization is significant. In case of ionic lattice polarization, this loss factor gradually increases with frequency grows but fully manifests itself in the far infrared frequency range (and in the ultraviolet range for electronic polarization). In case of the quasi-elastic polarization, at which the electrical field acts on ions (bound in crystal lattice) or electrons (bound in atom), they only slightly displace and the returning force arises, which is proportional to ions or electrons shifting from their equilibrium positions. It should be expected the appearance of oscillations of particles forcibly deviating by the applied field from their equilibrium position. The elastic polarization is distinguished by linear dependence of restoring force on displacement x induced by external field: $f = -cx$. At that, the polarizability is calculated $\alpha_{elas} = q^2/c$, where the elastic force cx resists to the displacement x of charge q.

Suppose that in the unit volume of dielectric n elastically bound charged particles are displacing that define the induced polarization $P = nqx$, where q is the charge shifting on distance x. Each of particles is characterized by mass m, coefficient elasticity c and damping factor λ' of oscillation. If the constant electrical field $E = E_0$ acts on such dielectric, then it forces charged particles to be displaced, i.e., constant shift x_0 for each charges is induced, resulting in polarization $P_0 = nqx_0$ (at that, initial time of electrical field switching on is not considered).

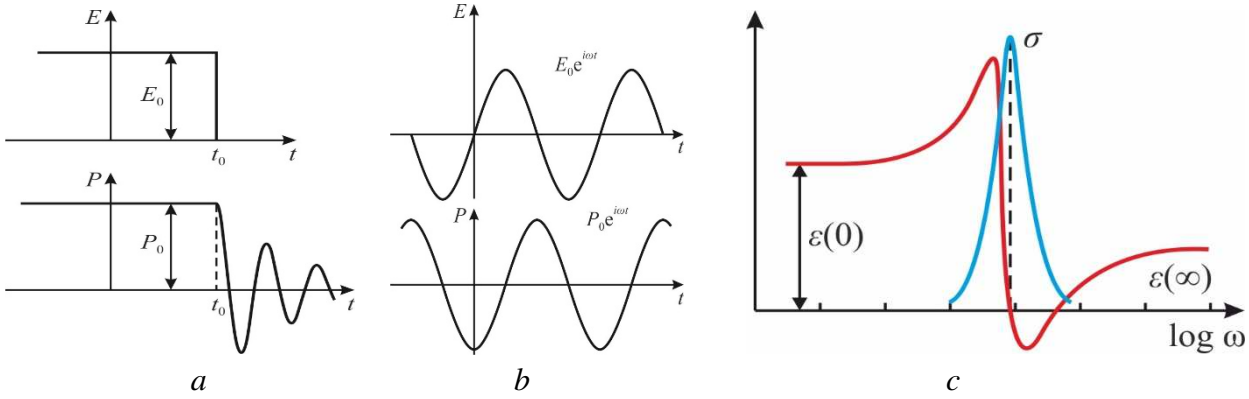

Fig. 3.8. Time-dependent polarization $P(t)$ of oscillators system under the influence of constant (a) and alternating (b) electrical field $E(t)$: c - frequency dependence of permittivity and effective conductivity for resonance polarization dispersion

Suppose also that in some moment $t = t_0$ the applied electrical field E_0 is turned off, Fig. 3.8a, so elastic forces seeks to return the non-polarized (equilibrium) state of dielectric. This process occurs with damped oscillations and can be

described by differential equation: $m(d^2x/dt^2) + \lambda'(dx/dt) + cx = 0$, in which $m(d^2x/dt^2)$ is the inertia force, $\lambda'(dx/dt)$ is the friction force, and cx is the elastic returning force. Dividing all members of this equality by m and taking into account the fact that $c/m = \omega_0^2$ is the oscillation frequency (if neglect friction), from above equation it is possible to get second order differential equation: $d^2x/dt^2 + \lambda(dx/dt) + \omega_0^2 x = 0$, where the damping coefficient is $\lambda = \lambda'/m$. Taking into account that $P = nqx$, received equation of oscillations can be rewritten for *polarization*: $d^2P/dt^2 + \lambda(dP/dt) + \omega_0^2 P = 0$, which characterizes damped oscillations of polarization around fast established non-polarized state with $P = 0$, as shown in Fig. 3.8*a*. Dielectric dispersion oscillator is described by resonant frequency ω_0, the wave vector $k = 2\pi/\lambda$ and relative damping factor Γ. Scattering of energy of oscillations is taken into account by introducing coefficient λ' at derivative dx/dt, i.e., representing a kind of "friction".

The frequency dependence of permittivity in the oscillatory model of electrical polarization can be found on the base of above equations, if one add the alternating electrical force $qE_0e^{i\omega t}$ acting on the oscillator:

$$m(d^2x/dt^2) + \lambda'(dx/dt) + cx = qE_0e^{i\omega t}.$$

The displacement x of charged particles in the electrical field ultimately determines polarization of dielectric, if n particles in unit volume are shifted in same way: $P = nqx$. Therefore, above equation can be rewritten for polarization:

$$P(\omega) = P_0 e^{i\omega t} = \frac{\frac{nq^2}{m} E_0 e^{i\omega t}}{\omega_0^2 - \omega^2 + i\lambda\omega}.$$

This formula shows that in the alternating electrical field $E_0e^{i\omega t}$ polarization varies with same frequency, but polarization turns out to be *complex parameter* having another phase in comparison with exciting electrical field. At last, at higher frequencies, the elastic polarization does not have time to be established, which leads to permittivity dispersion, while the presence of "friction coefficient" λ results in dielectric losses. The frequency dependent dielectric permittivity can be found from a definition of permittivity as the proportionality coefficient between electrical displacement and electrical field: $D = \varepsilon_0\varepsilon E = \varepsilon_0 E + P$, from which $\varepsilon = 1 + P/\varepsilon_0 E$. Thus, to determine permittivity, it is necessary to find the ratio $P/\varepsilon_0 E$, i.e., to get from above formula the complex parameter $\varepsilon^*(\omega) = 1 + nq^2/[\varepsilon_0 m(\omega_0^2 - \omega^2 + i\lambda\omega]$. To simplify this equation, the ideas of "*dielectric strength*" of oscillator $\varepsilon_q = nq^2/\varepsilon_0 m$ and *relative attenuation* $\Gamma = \lambda/\omega_0$ should be used. Suppose also that some different

processes of elastic polarization occur in a dielectric, due, for example, to the rapid displacement of valence electrons and other higher modes of ionic oscillations, etc.

To describe the permittivity dispersion in the simplest (cubic) ionic crystal by above formula, it needs to highlight the contribution of electronic polarization $\varepsilon_{el} = \varepsilon_{opt} = \varepsilon(\infty)$ from above sum. Then, for ionic polarization of crystal lattice the frequency dependence of permittivity can be described by following expression

$$\varepsilon^* = \varepsilon' - i\varepsilon'' = \varepsilon(\infty) + \frac{\varepsilon(0) - \varepsilon(\infty)}{1 - \left(\frac{\omega}{\omega_{TO}}\right)^2 + i\Gamma\frac{\omega}{\omega_{TO}}},$$

where ω_{TO} is the transverse optical frequency, Γ is the relative attenuation and the difference $\varepsilon(0) - \varepsilon(\infty)$ characterizes dielectric contribution of ionic polarization mechanism. This equation, which is usually called Drude–Lorentz equation, describes the resonance spectrum of permittivity dispersion. Turning to the analysis of frequency dependence of ε' and ε'', it is necessary in the above equation to separate the real and imaginary parts of complex permittivity:

$$\varepsilon'(\omega) = \varepsilon(\infty) + \frac{\left[\varepsilon(0) - \varepsilon(\infty)\right]\left(1 - \frac{\omega^2}{\omega_{TO}^2}\right)}{\left(1 - \frac{\omega^2}{\omega_{TO}^2}\right)^2 + \Gamma^2\frac{\omega^2}{\omega_{TO}^2}}; \quad \varepsilon''(\omega) = \frac{\left[\varepsilon(0) - \varepsilon(\infty)\right]\Gamma\frac{\omega}{\omega_{TO}}}{\left(1 - \frac{\omega^2}{\omega_{TO}^2}\right)^2 + \Gamma^2\frac{\omega^2}{\omega_{TO}^2}};$$

$$\sigma(\omega) = \frac{\left[\varepsilon(0) - \varepsilon(\infty)\right]\omega_0\varepsilon_0}{\Gamma}\frac{\Gamma^2\left(\frac{\omega}{\omega_0}\right)^2}{\left[1 - \left(\frac{\omega}{\omega_0}\right)^2\right]^2 + \Gamma^2\left(\frac{\omega}{\omega_0}\right)^2}$$

from which follows the presence a maximum $\sigma'_{max} = \varepsilon_0\Delta\varepsilon\omega_0/\Gamma$, locating exactly at the resonance frequency ω_0 of the oscillator describing this dispersion, where Γ is the relative damping factor and $\Delta\varepsilon = \varepsilon(0) - \varepsilon(\infty)$ is the dielectric contribution of resonant polarization mechanism.

Summing up, it should be noted that in case of gradual increase of frequency (that means more rapid changing of electrical field) the lag in displacement of bound charges and the inertia of free charge carriers begins to affect, so at sufficiently high frequencies their usual mode of movement becomes impossible. When frequency increases, the electrically induced displacement of bound charges, which at lower frequencies contributes to the polarization, in higher frequencies is converted into effective conduction. In dielectrics and wide-gap semiconductors, the relaxation and

resonant dispersion models (both leading to the appearance of effective conductivity) are considered separately. However, when ttudy conductivity dispersion in metals, resulting in the negative effective permittivity, the relaxation and resonance phenomena should be considered simultaneously that complicates a problem.

When discussing various aspects of conduction, it should be noted that the time-lag of electronic conductivity does not seen any noticeably even in the infrared frequency range. Thus, normal (described by zone theory) electronic charge transfer in the metals and alloyed semiconductors does not lead to any frequency dependence of conductivity over all frequency range used in the electronics (up to terahertz). Nevertheless, when the frequency of electromagnetic field extremely increases, the movement of electrons also manifests their inertia, and frequency dependence of electronic conductivity becomes seen in the optical frequency range as in the metals so in other conductors (allayed semiconductors, graphite, nanotubes, graphene, etc.).

However, the dispersion of electronic conductivity in the conductors has quite another character as compared to the effective conductivity conditioned by the delayed of polarization in dielectrics. In the above discussed cases (Fig. 1), the increase of effective $\sigma(\omega)$ was explained by the time-delay of different mechanisms of polarization. Eventually, this effective conductivity decreases in proportion to the increasing frequency. In what follows, the quite another mechanisms of $\sigma(\omega)$ decrease will be discussed, which become apparent, as a rule, in the highest frequency region. In this case, the inertia of free charge carriers begins to affect, that is why, their movement in phase with rapidly changing electrical field becomes no longer possible. At that, highly mobile electrons in metals and semiconductors, being exposure by a very high-frequency electrical field, demonstrate the plasma resonance and conductivity dispersion caused by the electronic gas. In the metals, it is seen in the ultraviolet frequency range, while in the semiconductors the less dense electronic plasma leads to the resonance phenomena and conductivity dispersion in the optical frequencies.

When charge carries show their inertia, the gradual decrease of conductivity is seen in ultraviolet wavelength range (above 10^{16} Hz) that is confirmed by the reflection coefficient frequency dependence. Eventually, shielding effect of polarization by free electrons gradually disappears, so the electronic shells of cantions lattice in metal lattice becomes noticeable as a contribution to permittivity.

Simplified model can describe the dispersion of conductivity from the point of view of relaxation processes. In the absence of external field, all chaotic motions of electrons are equally probable, and there is no electrical current; but in the case of $E > 0$, some average directed velocity of electrons appears. The equation of such motion of electronic

"gas" should describe the drift velocity υ dependence on electrical field under conditions of electrons collisions which slow down the charge transfer. If density of electrons is n, than the induced current is $j = -ne\upsilon = \sigma E$. Therefore, by drift velocity determination, it is possible to find the regularities for conductivity.

Suppose that under the action of a constant electrical field E_0 the average drift velocity $\langle \upsilon \rangle_0$ establishes in time, Fig. 3*a*. This velocity depends on the average free path l of electrons (dependent on crystal lattice perfection). In any case, the drift velocity in metals is small ($\upsilon < 1$ m/s) in comparison with Fermi speed of electrons chaotic movement (v ~ 10^6 m/s). Although the motion of individual electron is difficult to trace analytically, the derivation of equation for the "average" electron motion can be made, if consider the movement of electron in small time interval dt, where t is the time after last collision of electron. At initial moment, the speed of electron is υ_0, but after that, under the action of force eE, during a free path time τ it acquires the additional velocity $\upsilon = -eE\tau/m$, which is proportional to the applied field: $\upsilon = \mu E$ where u is mobility of drifting electrons. Because acceleration $a = eE/m$ works over a time interval τ, so the increment in velocity is $a \cdot \tau$, i.e., a desired value. Since many electrons after their collisions have arbitrarily directed velocity υ_0, they does not contribute to the average drift velocity:

$$\upsilon = -eE\tau/m; \quad j = \sigma E = ne\upsilon = neuE = (ne^2\tau/m)E; \quad \sigma = ne^2\tau/m, \quad u = e\tau/m$$

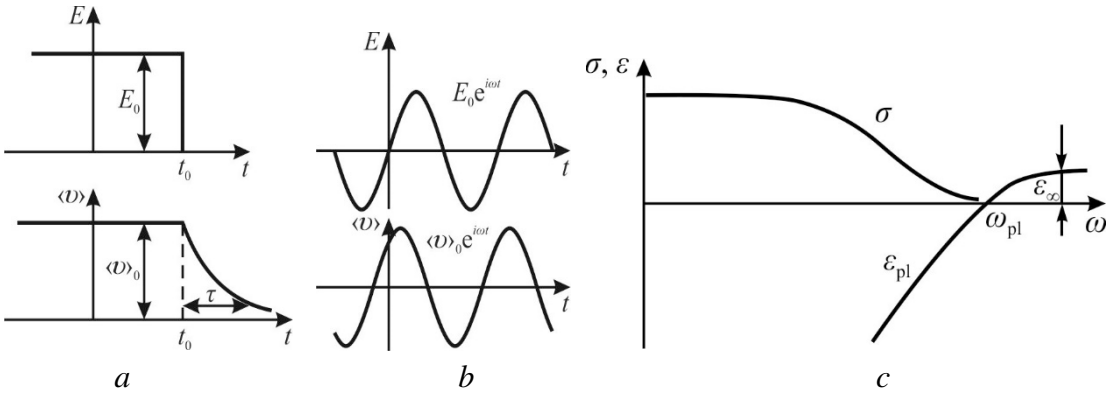

Fig. 3.9. Time-dependence of free electrons gas drift velocity under influence of constant (*a*) and alternating (*b*) electrical field E; *c* – frequency dependence of conductivity

As seen, the formula for conductivity includes all known quantities except τ; therefore, by measuring conductivity, one can find the relaxation time of electronic gas in a metal. At normal temperatures for metals parameter $\tau \sim 10^{-14}$s. The average free path of electrons l (a distance between their collisions) is defined as $l = \upsilon_0 \cdot \tau$; at that, by considering that average speed of the chaotic motion of electrons is ~10^6 m/s, the free length is estimated at ~10 microns, i.e., thousands of times higher than

crystal lattice parameter. Relations (1) describe the charge transfer in a conductor without taking into account the dynamics of this process, but this is very important in the case of rapidly changing electromagnetic field $E(t)$. The point is that due to the collisions a part of electrical energy, acquired by electron during its free path, is converted into the thermal energy of lattice vibrations and slows down the electrons reaction to $E(t)$. It should be noted that when free electron moves in electrical field, its acceleration is proportional to the field. However, in the case of electrons drift movement, not the acceleration, but the velocity is proportional to applied electrical field. That is why, conductivity is proportional to electron's charge not to its first power ($\sigma \sim e$) but to its square ($\sigma \sim e^2$),

Next suppose that at the moment $t = t_0$ the electrical field is turned off, Fig. 3.9*a*; as a result, the collisions of electrons leads to decrease of their drift velocity $\langle \upsilon \rangle(t) \to 0$. In means that in a new dynamic equilibrium state (not disturbed by external field) any drift of electrons is absent. The principle of non-equilibrium thermodynamics states that the rate of recovery of any equilibrium state is proportional to the magnitude of deviation from this state, i.e., $\mathrm{d}\upsilon/\mathrm{d}t = -k\upsilon$. The dimension of proportionality coefficient k is a value inverse to time, so it can be denoted as $k = \tau^{-1}$, i.e., the relaxation time, which in metal is very small ($\tau \approx 10^{-14}$ s) and during electrical field switching it is difficult to notice it. However, despite extreme smallness of the response time, the dynamics of almost free movement of electrons still can be estimated by the indirect measurement of τ. In this case, one needs to explore metals behaviour at a very high frequencies, as already shown in Fig. 3.9*c*: by studying of $\sigma(\omega)$ variance, i.e., frequency dependence of conductivity, it is possible experimentally evaluate τ for different metals.

The differential equation, describing gradual decrease of drift velocity when approaching to the equilibrium state is $\mathrm{d}\upsilon(t)/\mathrm{d}t = -(1/\tau)\upsilon(t)$. The solution of this equation results in the description of time-dependent gradual decay of drift velocity:

$$\mathrm{d}\upsilon(t)/\mathrm{d}t = -\upsilon(t)/\tau; \quad \mathrm{d}\upsilon(t)/\upsilon(t) = -\mathrm{d}t/\tau; \quad \upsilon(t) = \upsilon_0 \exp(-t/\tau),$$

which depicts the relaxation-type decrease of electrons drift velocity, and, accordingly, the electronic conductivity: $\sigma \sim \langle \upsilon \rangle$, caused by the collisions of electrons (at first approximation, without taking into account the inertia of this process due to a small but finite mass of moving electrons).

The frequency dependence of conductivity $\sigma(\omega)$ can be found, if the alternating electrical field $E(\omega) = E_0 \exp(i\omega t)$ acts in a model under consideration (the system of electrons, fast moving chaotically with collisions, at that slowly drifting under the external influence). The drift velocity forcedly have similar to the

driving field time-dependence: $\upsilon(\omega) = \upsilon_0 \exp(i\omega t)$, while the conductivity is determined by a ratio $\upsilon(t)/E(t)$ as it is determined by formula $\sigma = ne\upsilon/E$. To find the frequency dependence of conductivity, it is necessary to solve the first-order inhomogeneous differential equation, obtained when considering the mechanism of electrons drift, assuming that the acting force eE is the alternating electrical field:

$$m\{\mathrm{d}\upsilon(t)/\mathrm{d}t\} = -m\upsilon(t)/\tau + eE_0 \exp(i\omega t),$$

where all three components have the dimension of a force. Considering only the stationary solution of this equation (excluding transient solutions), obtain:

$$(1 + i\omega\tau) m\upsilon_0 = e\tau E_0,$$

insofar as $\sigma = ne\upsilon_0/E_0$; the final result is:

$$\sigma^*(\omega) = \sigma(0)/(1 + i\omega\tau),$$

The fact that conductivity is a complex value follows from the considered model. The real and imaginary parts of a conductivity $\sigma^*(\omega) = \sigma'(\omega) + i\sigma''(\omega)$ is determined as follows:

$$\sigma'(\omega) = \sigma(0)/(1 + \omega^2\tau^2); \quad \sigma''(\omega) = -\sigma(0)\omega\tau/(1 + \omega^2\tau^2), \quad \sigma(0) = ne^2\tau/m. \qquad (7)$$

In the dispersion region, the conductivity decreases with frequency, Fig. 1*c*; this drop in conductance also means the increase in losses, since the resistivity increases. Far from the region of a dispersion, when $\omega\tau << 1$, the real part of conductivity $\sigma'(\omega) \approx \sigma(0)$ remains practically constant, while its imaginary part, remaining rather small, yet increases linearly with frequency: $|\sigma''(\omega)| \approx \sigma(0)\omega\tau$. Reflection coefficient study in the terahertz frequency range (below plasma frequency) shows that a negative permittivity of highly conductive metals is close to several thousands, while in the lower-conductive (usually magnetic) metals it equals several hundreds.

Obtained relations (7) allow not only to explain the decrease of conductivity with frequency rise, but also to describe the frequency dependence of effective permittivity, which, as can be seen from Fig. 3.9*c,* takes a negative value in dispersion region and in lower frequencies:

$$\varepsilon'(\omega) = \sigma''(\omega)/(\varepsilon_0\omega) = -\sigma(0)\tau/[\varepsilon_0(1 + \omega^2\tau^2)]; \quad (8)$$

$$\varepsilon''(\omega) = \sigma'(\omega)/(\varepsilon_0\omega) = \sigma(0)/[\varepsilon_0\omega\,(1 + \omega^2\tau^2)]$$

Seen in Fig. 3*b* changing in real part of effective permittivity and its negative sign: $\varepsilon'(\omega) = -\sigma''(\omega)/(\varepsilon_0\omega)$ is due to the delay in electrons drift motion. During electron moving in their free path (between the collisions), very high frequency field changes its direction, and the electron, without experienced collision, is forced to change the direction of its movement during its free run. At the same time, the phase of its movement always lags behind the phase of changing field (this peculiarity is

also a consequence of spatial dispersion, at which the length of EM wave in conductor becomes commensurate with the free path of electrons).

Electronic plasma concept expands the understanding of conductivity dispersion in terms of some resonance process. Plasma can be considered as a subsystem, which interacts with crystal lattice that facilitates plasma properties. It is pertinent to note that plasma is made up of positive and negative charge carriers; at that, plasma can be charged (like electronic plasma in metals) or neutral (like electron-hole plasma in semiconductors). The density of electrons in charged plasma usually is close to 10^{22} cm^{-3}, while in neutral plasma charge carries density might be 10^{15}–10^{18} cm^{-3}. A characteristic property of plasma is the collective excitations (plasma oscillations), which, at sufficiently high frequency, lags behind the rapidly changing external field, which leads to the dispersion of conductivity. Plasma frequency (ω_{pl}) of electrons in the conductors (which determines the quasi-particle plasmon) is important parameter for metals and semiconductors; it characterizes dynamic properties of almost-free gas of electrons. It is generally accepted that at plasma frequency permittivity vanishes ($\varepsilon'(\omega) = 0$) crossing abscissa axis, but next increases reaching a value ε_∞ (in different metals $\varepsilon_\infty = 4$–8). Exactly this behavior of free electrons gas in the metals in very high-frequency EM field requires the introduction of plasma frequency concept.

To estimate plasma frequency, the spatial dispersion can be considered, but a simpler model can also be applied. Suppose that a returning force $\delta F = exE$ arises, when group of n electrons shifts from their equilibrium position on some distance x relatively to positively charged "non-moving" ionic lattice; in particular, this displacement can be induced by the external electrical field eE/ε_0. At that, the force of inertia $F_{in} = Ma = nm\mathrm{d}x^2/\mathrm{d}t^2$ opposes disturbing electrical force $F_{el} = -nex \cdot eE/\varepsilon_0$. The solution of this differential equation $F_{in} + F_{el} = 0$ leads to plasma oscillations frequency: $\omega_{pl} = (ne^2/m\varepsilon_0)^{1/2}$. Therefore, the returning force by its acting on the displaced electrons causes their oscillations around equilibrium position. Experiment indicates that the electronic gas in metals really demonstrates its inertia at frequencies near 10^{16} Hz: at the higher frequencies electrons have no time to follow fast change of electromagnetic field. The frequency dispersion of the complex conductivity can be expressed in terms of the plasma frequency:

$$\sigma^*(\omega) = \sigma(0)/(1 + i\omega\tau). \text{ where } \sigma(0) = ne^2\tau/m = \omega_{pl}^2\tau. \quad (9)$$

Thus, the conductivity $\sigma(\omega)$ of metals looks like practically constant value $\sigma(0)$, Fig. 3*a,* which defines the ohmic losses of a conductor in the broad frequency range including the terahertz range. With further increase in frequency, a smooth

decrease of conductivity up to zero is observed, accompanied by the negative effective permittivity. Above the plasma frequency (in the ultraviolet range) a positive permittivity $\varepsilon_{uv} = \varepsilon_{\infty}$ is determined, which is due to the elastic displacement of non-collectivized electrons (bound electronic shells inside ionic cores).

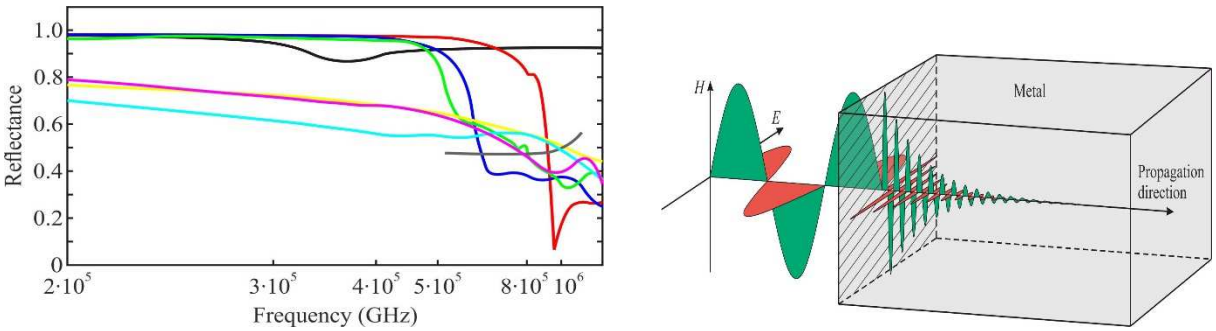

a b

Fig. 3.10. EM wave interaction with metal: a – reflectance spectra of metals: aluminum (black), silver (red), gold (blue), copper (green), beryllium (grey), cobalt (yellow), iron (cyan) and nickel (magenta) b – wavelength reduction and attenuation in metal

The existence of plasma oscillations is confirmed by the study of metals reflection spectra, Fig. 3.10a, [5]. These investigations indicates that the process of $\sigma(\omega)$ dispersion not nearly as simple as elementary theory predicts, because the manifestation of resonance processes is obvious. It is possible that the electron shells of different cations affect the spectrum in a different way (Au^{+1} repeats Rn shell, Cu^{+2} – Kr shell, Ag^{+1} – Xe shell, and Al^{+3} – Ar shell). But in the 3d and 4f metals, the electronic configurations of ions contain the uncompensated spins, which by their magnetic moment affect the dynamics of a drift motion of electronic gas. That is why, the EM waves reflection and conductivity of ferromagnetics much less than in the high conductivity metals.

EM waves in metal, in the ideal case of a superconductor, cannot propagate and they are completely reflected. But in the optical range, any superconductivity no longer manifests itself, because the photons energy is much higher than the energy of Cooper pairs. Therefore, in a real metal, despite the dominant reflection of the EM wave, it nevertheless partially penetrates into the conductor. From the microscopic point of view, the absorption of part of incident EM radiation occurs mainly because the electrons of metal, exciting by the EM radiation as during their transition to the higher energy levels above the Fermi level so at their subsequent return in the equilibrium state (accompanied by secondary emission of EM waves) interact with the ionic lattice exciting its oscillations, i.e., convert some of EM energy into a heat.

From the macroscopic point of view, the phase velocity of EM wave,

penetrating into a conductor, is greatly reduced in comparison with its velocity in a vacuum, so much so that the length of EM wave in the conductor becomes hundreds of times shorter than in vacuum, Fig. 3.10b. The reduction of EM wavelength in a substance occurs in $|\varepsilon^*|^{1/2}$ times, therefore this occurs due to large effective permittivity that in electrodynamics corresponds to the large conductivity dispersion. Without a doubt, due to the huge step in the impedance of "vacuum-metal" interface, as well as through a very small phase velocity of EM wave in a conductor, any EM wave falling on the conductor (even in case of grazing incidence) refracts practically in the direction perpendicular to conductor's surface. At that, transmittance of a part of incident on conductor EM radiation is possible only in the case of a very thin metal layer. Analysis shows that intensity of incident wave decreases exponentially while it propagates through a metal, Fig. 3.10b, that leads to much lower intensity of transmitting wave. This happens because the metal strongly damp the initial intensity of TM wave.

Thus, the frequency dispersion of the electronic conductivity of conductors has both relaxational and plasma-resonant natures, and leads to a negative effective permittivity.

3.5 Polar structure and conductivity anomalies

It is normally accepted to leave materials' electrical conductivity beyond consideration to simplify study of electrical polarization mechanisms in the dielectrics (including the piezoelectrics, pyroelectrics and ferroelectrics). Similarly, electrical polarization gets little attention during study of different processes, conditioned by the electrical conductivity in semiconductors and conductors. In most cases, these assumptions are justified; however, there are rare but nonetheless important cases, when the interdependence of crystal intrinsic polarity and its conductivity becomes an essential physical phenomenon. For example, in classification of the semiconductors one should not neglect intrinsic polarity: the non-polar crystals, such as Si or Ge, are characterized by the indirect band gap in electronic energy spectrum, while the polar semiconductors, such as $A^{III}B^{V}$ crystals (possessing piezoelectric symmetry) and $A^{II}B^{VI}$ crystals (with pyroelectric symmetry) are crystals characterized by the direct band gap [6].

Defining properties of dielectrics, namely the pronounced polarization and low conductivity, are tightly interdependent. To analyze the reasons for such behavior in some crystals, it is necessary to point out significant difference in the

inter-atomic bonds of solids, which can affect the electronic conductivity in different ways.

Firstly, in the dielectrics, possessing predominantly ionic bonds, Fig. 1*a*, where electrons or holes are generated as a result of various activation processes, electrons usually become very low mobile, because their own electrical field polarizes the surrounding nano-size areas in dielectric by displacing nearby ions, so electrons are forced to move together with these polarized regions (transforming into polarons). Consequently, even a small amount of free electrons, which appear in a dielectric due to thermal activation of impurities, may not cause any appreciable charge transfer just because the local polarization arises around charge carriers, which reduce their mobility. Thus, the stable ionic inter-atomic bonds suppress the electronic conduction, so that electrons mobility has order of magnitude only (1–10) $cm^2V^{-1}s^{-1}$.

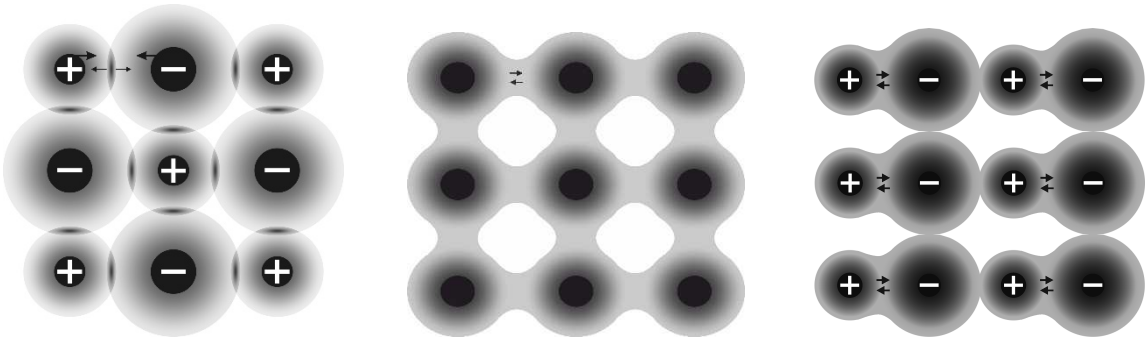

a *b* *c*

Fig. 3.11. Two-dimensional image of electronic charge distribution in: *a* – ionic crystal, where ions attraction is balanced by partial overlapping of electronic shells; *b* – covalent crystal, black diffused circles represent atomic residues surrounded by regions, where electronic density reaches significant values; *c* – polar crystal with mixed ionic-covalent bonds

Secondly, in some dielectric and semiconductors the covalent bonding exists as the main type of inter-atomic connection, Fig. 3.11*b*. Its nature is very close to the metallic bond, but in the covalent crystals the valence electrons are shared only between nearest neighboring atoms while in the metals their valence electrons are shared within crystal lattice (further, the cases will be described, when a covalent bond actually transforms into a metallic one). Covalent (or homeopolar) bonding is realized by a pair of valence electrons, which have opposite spin directions, at that, the reduction of total energy of crystal is achieved by the quantum effect of exchange interaction. As can be seen from Fig. 1*b*, the open structure (low coordination number) provides a significant distance between atoms and hence a high electron mobility: (10^4–10^5 $cm^2V^{-1}s^{-1}$ in the semiconductors, which is many orders of magnitude higher than their mobility in ionic crystals.

Thirdly, consider the mixed covalent-ionic bonding, shown in Fig. 3.11*c*, which creates the main properties of polar-sensitive crystals, including special effect on the conductivity. Under the influence of external factors, in some of these finely balanced structures, either the ionic bonding (lowering electronic conductivity) or the covalent bonding (promoting this conductivity) becomes predominate.

It should be noted, that polar state in crystals is ensured by the fundamental properties of one or the other ion, in particular, the peculiar electronic shells, accompanied by the different electronegativity of nearest ions. One-dimensionally directed polarity can promote electronic transport, while complex spatial distribution of polar bonds significantly slows down electrons movement, contributing to their transformation into slow polarons: the entanglement of electrons in the complexly distributed three-dimensional polar bonding occurs.

Fourth, in connection with the conductivity anomalies, the following feature should be noted. In the dielectrics, low concentration of the charge carriers and their low mobility, in its turn, makes it possible a long time existence of the electrostatic field, while in the conductors this field is screened by free charge carriers (in metals, for example, screening radius is approximately equals to inter-atomic distance). Thus, ionic polarization contributes to the emergence and existence in the dielectrics of a relatively stable state with low electronic conduction. However, this stability may be broken in dielectric by its heating or by high intensity irradiation, particularly, by the coherent optical (laser) irradiation.

At that, the charge carriers, being generated in very high concentration, shield the electrical field, so dielectric can be converted into a conductive medium. The stability of the non-conducting state in dielectrics may be compromised also by the strong electrical field, which accelerates freed electrons (or holes) up to the energy, at which they can no longer be "captured" by polarization of nano-size surroundings. These fast electrons cause the percussive ionization in a dielectric, as a result, the number of free electrons grows that ultimately gives rise to the electrical breakdown, and insulator transforms into conductor.

In fact, certain interdependence of polarization and conductivity always takes place. The point is that in any dielectrics the applied electrical field has an impact on the existing charged particles, which might be as bound so relatively free. However, in some, very rare cases, the internal polarity of dielectric or semiconductor leads to a huge influence on the process of charge transfer – both in weak and in strong electrical fields. Such unusual dependence of conductivity (resistivity) on temperature or electrical voltage, i.e., its unusual change by hundreds and thousands of times (without electrical breakdown) takes place in the non-

centrosymmetric (polar) crystals possessing the pyroelectric or piezoelectric structure. The top priority is to find out, firstly, what are features of internal polarity in different crystals, and, secondly, why strong impact of polarity on the conductivity is a rare exception.

The supposed reason of polar bonds existence in the non-centrosymmetric crystals (as well as their formation) is the structural compensation of ions electronic states features, which leads to the polar structure arising. The primary cause of internal polarity is the asymmetry in electronic density distribution along the inter-atomic bonds. In turn, this peculiarity is conditioned by the adjoining ions distinction in electronic shells singularities, which, in particular, manifests itself as the electronegativity.

The ion with increased electronegativity displaces the shared electrons towards itself, so its operating charge is more negative, while the ion with lower electronegativity acquires, respectively, the increased positive charge.

Together these ions create a polar bond with the inhomogeneous distribution of electron cloud density along the inter-ionic bond. So it might be concluded that the internal polarity, seen in the non centre symmetric crystals, arises due to the structural compensation of different structural features of electron shells of neighboring ions.

Polar crystals are characterized by finely balanced structure of their inter-atomic bonds, which makes these crystals highly sensitive to any external influence. It is claimed, that mixed ionic-covalent polar-sensitive bonds can affect the transfer of electrons in the applied electrical field.

At that, explanation of unusual jump-like change in the conductivity of some polar crystals reduces to the clarification principal physical cause: why the polar-sensitivity, leading to non-centrosymmetric structure, might have especially strongly influence on the electrical conductivity.

An evident reason for the lack of symmetry center in crystal is a special kind of atomic bonding – mixed ionic-covalent bonds. This kind of atomic bonding represents the intermediate case between the ionic and covalent bonds: the pure-ionic, as well as the pure-covalent crystals always demonstrate the central symmetric structure, and this means that in such crystals there is no intrinsic (hidden) polarity.

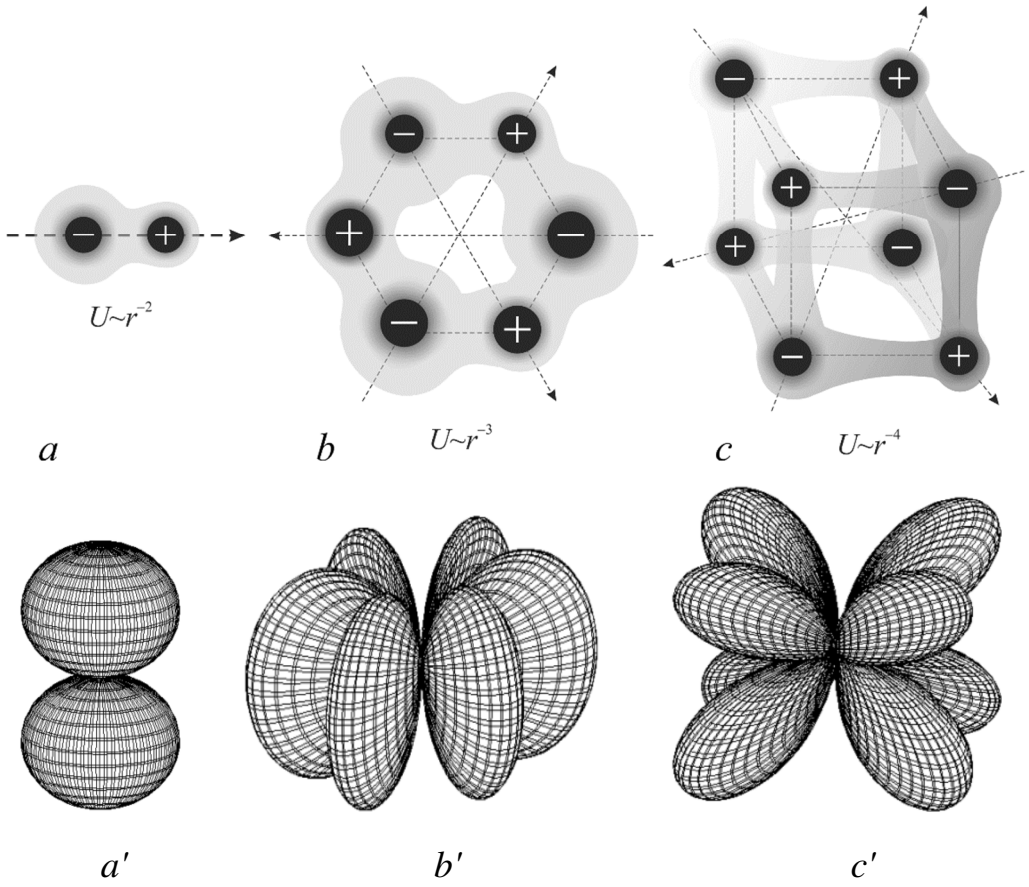

Fig. 3.12. Polar structures modeling: *a* – 1D dipole model; *d* – 2D polarity modeling; *c* – 3D polar construction; polar directions are shown by arrows, while the rate of energy decrease with distance $U(r)$ is shown by power functions; corresponding indicatrices of polar bonds intensity distribution are shown by *a′*, *b′* and *c′*

Figure 3.12 represents the simplified modeling of 1D, 2D and 3D non-centrosymmetric structures with spatial distribution of hybridized ionic-covalent (polar) bonds; their intensity is obtained using the value of longitudinal piezoelectric modules. One dimensional case, Fig. 2*a′,* corresponds to the ten pyroelectric classed of symmetry, and this modulus is the material vector (tensor of first rank): $d_i(\varphi) = d_{imax} \cdot \cos\varphi$, where φ is the angle between polar direction and slanting cut of a crystal, where piezoelectric effect is studied. The 2D model, Fig. 3.12*b′*, describes in polar coordinates the internal polarity distribution in piezoelectrics of quartz type, where the piezoelectric module is the second rank tensor: $d_{ij}(\beta,\varphi) = d_{max}\sin^3\theta \cdot \cos 3\varphi$, where β is the azimuth angle and φ is the in-plane angle. By the radius vector, directed from a center of shown figure, one can determine magnitude of polar-sensitivity response in any slanting cut of quartz-type crystals. The 3D model, Fig. 3.12*c′,* is adapted to the piezoelectrics-semiconductors of gallium arsenide type, where third-rank tensor is $d_{ijk} = M_{111}\sin\beta \cdot \sin 2\beta \cdot \cos 2\varphi$. It is appropriate to note that same octupole type distribution of polar bonds takes place in many polar-neutral crystals.

At that, shown polar models may coexists in a different combinations. In the discussed case, the most important is the influence of polar-sensitivity on crystal conductivity. The simple case of one-dimensional polar ordering does not create any special obstacles for electrons transport. However, if the internal polarity is distributed in a complex manner, than the charge carriers is obliged to lead the way through the alternating bipolar nano-size districts that dramatically decreases their mobility (just as the electron in antiferromagnetic with the big difficulties leads its way through the anti-parallel magnetized sub-lattices). On the contrary, if the internal polarity is quite ordered (or becomes ordered by the external field), than the charge carrier mobility should be much higher – just like a big conductivity is peculiar to the ferromagnetic with parallel ordered spins.

Below it will be shown, how the polar type bonding can be applied to explanations: firstly, the nature of resistivity critical temperature dependence, and, secondly, the reasons of stimulated by electrical field large jumps of conductivity in polar crystals, including field-controllable switching elements.

3.6 Temperature anomalies of conductivity in polar structures

In some cases, the polarity of a structure has strong effect on the temperature dependence of conductivity $\sigma(T)$, which is more convenient to trace from resistivity dependence $\rho(T) = 1/\sigma$. The temperature change of resistivity of some solid materials is widely used in electronics and instrumentation for temperature sensors; figure 3 demonstrates different types of the thermistors – electronic components based on resistance alteration $R(T)$.

As known, the temperature dependence of metals resistance (curve *1*) has been used for a long time, although this effect is rather weak; at that, the *positive* temperature coefficient is explained by the scattering of conduction electrons on lattice vibrations (phonons). Others thermistors find wider application, in which the *negative* temperature coefficient of resistivity is used (curve *2* in Fig. 1), so they are called the negistors [7]. Usually they are made of semiconductor oxides, in which their resistance decreases noticeably with temperature increase due to the increase of free electrons concentration in semiconductor when temperature rises. The physical mechanisms of these two types of thermistors are well understood. Another thing is a very sharp, almost critical temperature dependence of resistivity shown in Fig. 3.13 by curves *3* and *4*, which is the subject of further discussion.

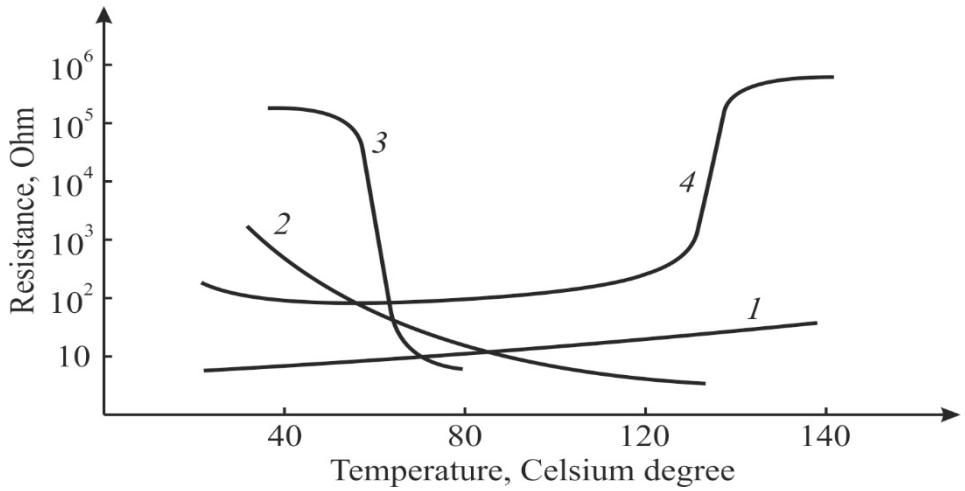

Fig. 3.13. Different thermistors characteristics: *1* – platinum wire thermistor; *2* – negistor based on transition-metals oxides; *3* – critistor based on vanadium dioxide; *4* – posistor utilizing doped barium titanate

As seen in Fig. 3, there are some materials, in which their resistivity in a certain temperature interval is much more sensitive to temperature variation, and it is important to note that all of them are the polar crystals. The critistors (curve *3* in Fig. 3) and the posistors (curve *4*) have large negative or positive temperature coefficients of resistance. This feature can be explained by the structural phase transitions accompanied by changing of crystal internal polarity which influences on the electronic charge transfer. However, in those shown in Fig. 3.13 cases (curves *3* and 4) we are not talking about the impact of strong fields and strong changes in temperature: these big changes in conductivity occur due to the internal changes in the structure of crystals. Indeed, the critistors are based on the vanadium dioxide (VO_2), which refers to the polar triclinic (piezoelectric) symmetry, while the posistors also use polar tetragonal barium titanate ($BaTiO_3$), which is a ferroelectric possessing pyroelectric structure.

3.1. ***Critistors*** in the weak electrical field sustainably keeps the low-conducting (nearly dielectric) state, but at a certain temperature they are fast transformed into the conductive matter [7]. This exceptional case corresponds to vanadium oxide crystals which have polar properties and is the basic component of polycrystalline critistors. In the vanadium dioxide, the change of external conditions (pressure, temperature, mechanical stress or electrical field) can lead to a huge increase of conductivity (up to 10^4–10^6 times). At that, large jump of conductivity (or resistivity), usually is accompanied by the change in crystal symmetry, associated with re-arrangement of electronic interaction between ions. This effect first and foremost is considered as the phase transition of insulator-to-metal type. At lower temperatures the VO_2 and V_2O_3 are wide-gap semiconductors (near

dielectrics), but when temperature increases they exhibit metallic-type behaviour: band gap of electronic spectrum in these crystals almost disappears. As a result, in the narrow temperature interval their conductivity changes in thousands times; at that, the critical temperature can be controlled by chemical composition (within a limited range).

It is natural to assume that this feature is due to the peculiarity of the inter-atomic bonds of vanadium oxides. As well known, the covalent bond, in which adjoining atoms are divided by a pair of valence electrons, on one hand, is rather close to metal bond, in which all valence electrons are generalized in the lattice of a metal. But, on other hand, the covalent bond is close to ionic bond as well, in which cation entirely delivers its valence electrons to anion, and together they constitute the ionic lattice of a dielectric. It would seem that exactly this feature of covalent bond could be used to explain discussed phase transition in the vanadium oxide. However, crystals with dielectric-metal type transition, having strong $R(T)$ dependence, are extremely rare case. The point is that a key role in this phenomenon belongs to the hybridized covalent-ionic bonds, which give rise to the polar-sensitivity and to non-centrosymmetric structure creation.

Besides critical dependency of conductivity on temperature, experiments confirm critical dependency of VO_2 conductivity on crystal compression. As compression force exceeds threshold value, vanadium dioxide converts into conductor, and dielectric phase is no longer observed. This serves as indirect confirmation of discussed phase transition mechanism in VO_2. Similarly, in ferroelectrics decrease of critical temperature under pressure is a characteristic of polar-sensitive coupling [6]. As crystal's atoms move closer under external pressure force, no space remains for hybridized ionic-covalent polar bonds mutual orientation. As a result, valence electrons get delocalized in form of electronic gas filling the lattice, just like metallic bonds. This happens as abrupt rise of conductivity in crystal, unlike blurred characteristic of critistor made from the ceramic vanadium oxide (Fig. 3.13, curve *3*), which is defined as polycrystalline structure of the ceramic, so by alloying additives used.

Summarizing, we can conclude that mechanism of temperature-induced phase transition in the vanadium dioxide looks like this: in the insulating state of a rather complex distribution of polar-sensitive bonds of 3D-orientations promotes extremely low mobility of polaron-type charge carries. The point is that vanadium dioxide in its lower-temperature (dielectric) state has several competing phases with dominating of monoclinic polar-sensitive structure. Exactly the instability of these phases with their variability and mutual transitions contributes to the formation

charge carriers with the bound (polaron) states. However, when temperature rises, growing energy results in a fast liberation of electrons, creating fast decrease of resistivity.

3.2. ***Posistors,*** in contrast to critistors, can stably retain highly conductive state over need temperature range, but at a certain temperature, by rapid increase of their resistivity, turn into the dielectric state. In the ordinary ferroelectrics, near their phase transition the change of electrical resistivity usually is small: ferroelectric transition, in most cases, does not significantly change general activation-type $R(T)$ decrease with growing temperature, Fig. 3.14*a*, dotted part of line. The band gap of electronic spectrum in the most of ferroelectrics is big, and, therefore, they usually can be considered as the dielectrics: both above and below their phase transition.

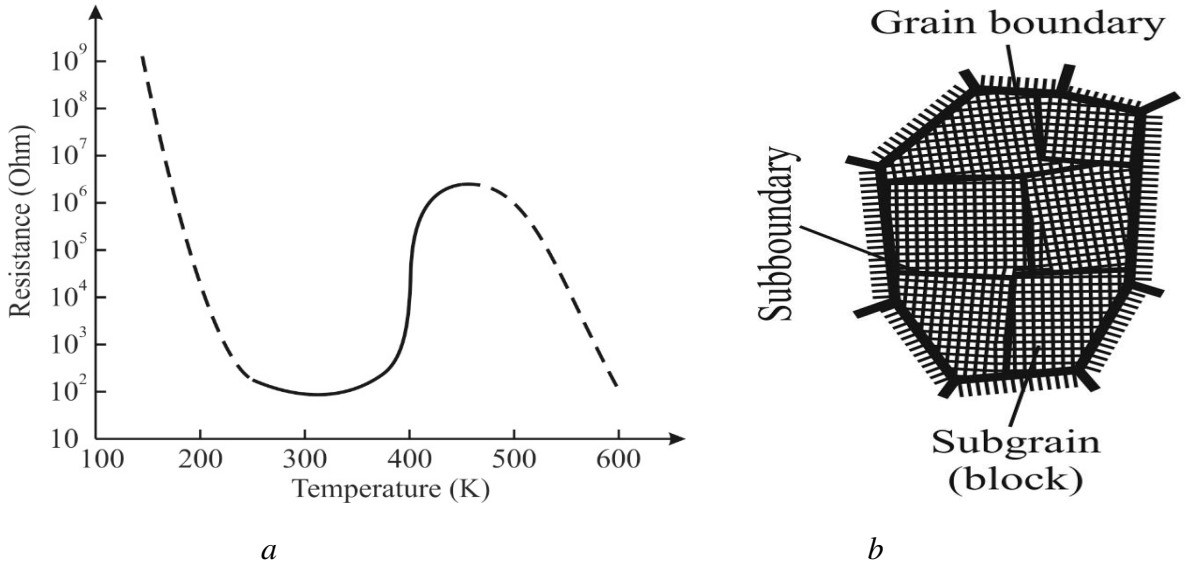

a *b*

Fig. 3.14. Resistance temperature dependence in dysprosium doped barium titanate (*a*) and scheme of crystallite (grain) with (mosaic) structure inside crystallite (*b*)

In some ferroelectrics, it is possible to reduce their resistance with a certain doping, Fig. 3.14*a*. On background of that reduced resistance, some titanate type ceramics rather than crystals demonstrate posistor effect as sharp increase of resistivity near the ferroelectric Curie point. In barium titanate ceramics this phenomenon is observed towards 400 K, where $BaTiO_3$ has its transition point, Fig. 3.14*a*. Low resistance is a specific feature of polar-sensitive phase, as with transition to non-polar phase the resistance stepwise increases as much as thousand times. This posistor effect is different from regular dielectrics' behaviour, where activation-type resistance reduces under heating well above Curie point.

The investigation of doped ferroelectrics' increased conductivity nature suggest that no polaron states formation occurs in the structure of tetragonal symmetry of 4*m* class with one-directed polar-sensitive bonds. However, charge

carriers form these polarons with large effective mass, when polar bonds disappear after $BaTiO_3$ transition into high-temperature non-polar *m*3*m* phase. Electrical resistance increases because of charge carriers binding, which is more likely to happen due to the disordering, peculiar to polycrystalline structure. As heating progresses beyond posistor usable range, thermal motion bonds charge carriers into polarons, and further (above t > 500 °C) the thermal dependency of resistivity resembles that one of semiconductors and dielectrics, Fig. 4*a*.

Discussed dependency of resistivity of doped polycrystalline ferroelectrics is largely defined by the grains boundaries properties. In the ordered (polar) phase grain boundaries only a little slow down the charge carriers movement, that is observed as a reduced resistivity below ferroelectric transition point. Conversely, in the non-polar phase, the electrons transform into the polarons of much smaller mobility, and this phenomenon is observed macroscopically as posistor effect. Polycrystalline grains (crystallites) is schematically depicted in Fig. 3.14*b*. Although their stoichiometric composition is close to that of crystalline ferroelectric, the structural defects of much larger density form the subgrains which have wider boundaries. However, in the of polar phase, a proximity effect in those irregularities define the lower resistivity

The temperature of a sharp increase of resistance in the posistors can be changed by applying various doped ferroelectric solid solutions. For example, in the composition $(Ba,Pb)TiO_3$, the resistance jump can be increased up to 600 K, while in the composition $(Ba,Sr)TiO_3$, the temperature jump of resistance can be reduced down to 300 K. Thus, the ceramic posistors can be designed for applications in a wide range of temperatures, being unusual ceramic elements with low "cold" electrical resistance and high "hot" resistance state.

This is used in the thermal control systems, in the devices that prevent thermal and current overload, in the engine-start systems, in the measurement technology, as well as in the automatic control systems. Posistors are also applied to protect against overvoltage and to avoid large current in short circuit: when posistor is would be connected in series with the load, the current in circuit will be limited to a safe level [7].

It is appropriate to note that in all shown in Fig. 3 temperature characteristics the magnitude of electrical fields and currents practically does not matter: in various electrical field the resistivity demonstrate practically linear properties. However, in some other cases, the polar-sensitivity of material stimulates the nonlinear properties in some oxide dielectrics-semiconductors.

3.7 Field controlled conductivity in some polar structures

The next is related to the effect of intrinsic polarity on the non-linear behaviour of resistivity used in the varistors and in field-controllable switching elements. Figure 3.15 demonstrates conditionally how the strong electrical field affects electrical resistance in different materials. Dielectrics usually can retain very high resistance up to very big field strengths (curve *1*), but there is a limit: the phenomenon of electrical breakdown due to the electronic avalanches, when the resistance of dielectric drops to zero (usually with complete destruction of material). Similarly, in the semiconductors (curve *2*), at much lower voltages, but also the irreversible breakdown occurs due to increase of charge carries avalanche in the strong electrical field [1]. The influence of internal polarity on the electrical strength in crystals was not considered.

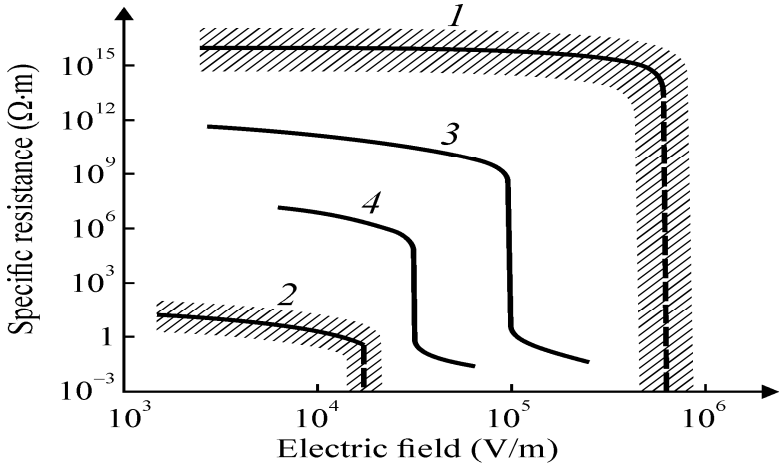

Fig. 3.15. Field dependence of resistance: *1* – typical dielectric; *2* – typical; semiconductor; *3* – zinc oxide varistor; *4* – silicon nitride varistor; the shading indicates a wide range of resistance in different materials

It's quite another matter, when in the strong electrical field the resistance can be reversibly changed in thousands times without any electrical breakdown. This phenomenon is due to a peculiar electro-physical process (curve *3* in Fig. 3.15) or might be ascribed to tunnel effect (curve *4* in Fig. 3.15). Unlike the irreversible effect of electrical breakdown, these $R(E)$ transfer from the nearly insulating state to the practically conducting state is fully reversible and repeatable any number of times, because the dielectric-semiconductor does not undergo to any destruction, as it happens in the case of usual electrical breakdown.

This phenomenon finds its technical application in voltage limiters (varistors), fabricated from ZnO based on the dielectric or semiconductor ceramics or from polycrystalline SiC. A steep drop of the impedance in strong electrical field occurs

reversibly, without destructive breakdown, and it happens without phase transition unlike VO_2 critistors. At that, million times conductivity changing is connected to materials polar properties. The transition of sphalerite (piezoelectric) structure to the wurtzite (pyroelectric) structure is a feature of non-centrosymmetric classes, and both considered varistor materials represent this type.

Varistors are characterized by the linear current-voltage dependence, i.e., $j \sim E$, both in the low and in increased levels of electrical field, Fig. 3.15*a*. At that, in lower electrical field, varistor has high electrical resistance, which is close to dielectric, while in strong electrical field its resistance decreases millions of times, and varistor becomes the typical semiconductor [1]. While this transformation, any electrical breakdown in the varistor does not occur, since the growth of electrical current in it is limited. It is important to note that increased current, passing through a varistor, remains stable while its characteristic *j(E)* is reversible. Therefore, physical phenomenon of stepped-grows of electrical current in thevaristor is essentially different from conventional electrical breakdown.

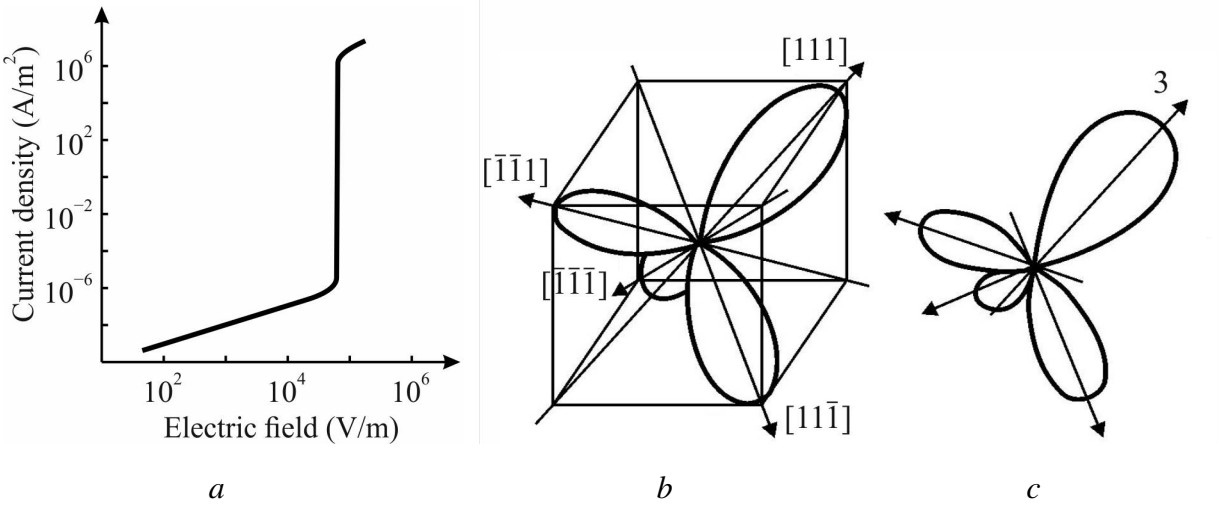

Fig. 3.16. Zink oxide non-linear property: *a* – current-voltage characteristic; *b, c* – polarity changing from polar-neutral sphalerite into polar wurtzite (only positive directions of polar axes are shown)

The features of carborundum varistors and zinc oxide varistors are similar, but the jump of resistance in the zinc oxide varistors is much bigger. At that, zinc oxide crystal has bigger electronic energy band gap (~ 3.4 eV) in comparison with carborundum (~ 2.5 eV). Advantages, associated with larger band gap, include the higher breakdown voltages and the ability to withstand to increased electrical fields, as well as the possibility of applications in higher-temperature and higher-power conditions.

The nonlinear conductivity of ZnO can be explained as follows. The crystal structure of a zinc oxide is stable in two main modifications: the hexagonal wurtzite and the cubic sphalerite. Both of these structures belong to non-centrally symmetrical classes of crystals. At that, the polar bonds in both cases form a complex spatial structure, but it has dominated structural features shown in Fig. 6*b*. One of the structures of ZnO is the polar-neutral sphalerite with the piezoelectric symmetry, while second structure has the pyroelectric symmetry of a wurtzite with one pronounced polar direction, Fig. 3.16*c*. Generally speaking, under the influence of external factors, zinc oxide easy changes its structure, for example, with increasing pressure, all polar properties of ZnO disappear, and it acquires the non-polar structure of a rock salt. Such a high sensitivity of the zinc oxide to external influences makes it possible to use it in various sensory devices.

Figures 6*b,c* demonstrates possible physical mechanism, explaining how the external electrical field, being applied to the zinc oxide in its insulating phase, induces the change in distribution of internal polarity, which, in its turn, has a strong impact on the electrical conductivity. Of eight possible [111]-type directions of the inner polarity (Fig. 6*b*), one directions obviously should be settled close to the direction of applied field, which strengthens the polarity in this direction (following axis *3*) at the expense of others axes, Fig. 6*c*, where for convenience only the positive directions of polar axes are shown.

It is important to note that the sphalerite structure of ZnO has almost dielectric properties, since in it the charge carriers are "entangled" in the competing three-dimensional internal polar structure: the electrons activated by thermal motion are converted into the low-mobility polarons with increased binding energy. However, the quasi-dielectric phase of sphalerite, when exposed to a significant electric field, transforms into a phase of one-dimensionally oriented polar wurtzite, in which polarons are released from their polar environment, and formed electrons can relatively freely move in the direction of applied field. The polarity of wurtzite, like the polarity of doped barium titanate in the posistors, contributes to increased electrical conductivity, while in the sphalerite the complex orientation of polar bonds deepens the potential barriers of the polaron state, reducing the mobility of charge carriers. In other words, the nonlinearity of the zinc oxide conductivity is explained by the electrically induced transition from the quasi-dielectric sphalerite structure to the electrically conductive wurtzite structure.

Varistors are widely applied to protect electrical circuits from sudden jumps of voltage: when voltage increases, the current flows through varistor but not others elements of a circuit.

Field-controllable switching elements use the liberation of bound charge carriers by the applied electrical field, that is, the transformation of polarons into mobile electrons. The electrical field forcibly transfers vanadium dioxide from its usual quasi-dielectric phase at 300 K to the electrically conductive phase (at a temperature much lower than temperature jump in conductivity, Fig. 3.15a). Unlike the quasi-dielectric phase, where vanadium oxide is optically transparent, its quasi-metallic phase is not transparent and reflects electromagnetic waves. Such electrically controlled reflection is extremely fast, and on this basis the electronic elements have been developed for controlled reflection of both infrared and optical waves.

The explanation for this phenomenon lies in the fact that in a complex polar-sensitive structure, there is a strong bonding of charge carriers with their nearest ions of crystal lattice. The very low mobility of the resulting polarons causes the resistivity of vanadium oxide, but the balance of polar structure existence can be easily disturbed, as follows from the natural temperature jump in conductivity. The spurt of breaking this delicate balance and transitioning to high conduction occurs like in a game of "destroying the house of cards" or as "domino effect". The released electrons shield the local fields that slow down their movement, which leads to an avalanche of already highly mobile charge carriers and increase in free charge carriers concentration. Unlike the polar dielectric phase, the highly conductive VO_2 phase is a non-polar rutile structure. There is also another motive for the transformation of a quasi-dielectric state into a quasi-metallic one: the first of them is characterized by the antiferromagnetic ordering. It should also be noted that the this ordering in quasi-dielectric phase contributes to lower mobility of electrons, can also have some effect on the electrical conductivity, while the quasi-metallic phase is the paramagnetic.

The technical application of the described phenomenon is facilitated by the fact that the dielectric⇔metal transition is fast and reversible: when the temperature drops or control voltage is turned off, VO_2 instantly returns to the quasi-dielectric phase. Due to the controlled transition of charge carriers from polaronic into to electronic state, the electrical resistivity and optical transparency change by several orders of magnitude. On the basis of vanadium dioxide, the high-speed optical shutters have been developed that are used in modulators, cameras and information storage devices. The elements of devices obtained on the basis of vanadium dioxide belong to the switching elements controlled by fields. Figure 7*a* shows the control of resistance by an electrical field while in Fig. 3.17*b* this control is performed by a magnetic field.

The physical basis for the use of vanadium oxides as switching elements is the displacement of its temperature phase transition in an electrical field. Vertical curves "$E \approx 0$" and "$E > 0$" in Fig. 7a separates the dielectric ("D") and metallic ("M") phases of vanadium oxide at different temperatures and fields. If $E \approx 0$, then this boundary passes at a temperature of about 60°C, and with a field $E > 0$ – at a temperature of 35°C. However, if electrical field is applied to VO_2 at a temperature of, for example, 50°C, then the resistance under the action of control field will decrease by hundreds of times, as shown in the graph by the vertical line $1 \rightarrow 2$ in Fig. 3.17*a*. For control at lower temperatures, stronger fields will be required.

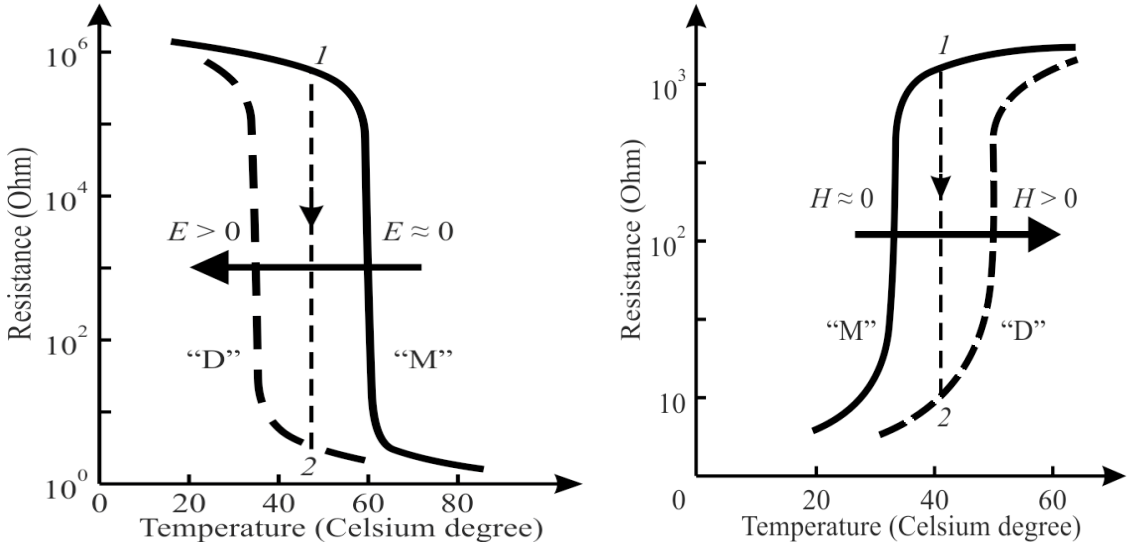

Fig. 3.17. Resistance control by external fields: *a* – electrical bias field manages *R*(*T*) value in VO_2; *b* – magnetic bias field manages *R*(*T*) value in $(La_{1-x},Ca_x)MnO_3$ (dotted line *1* → *2* shows large fall in resistance).

Magnetic field control of electrical resistance is shown in Fig. 3.17*b* on the example of manganites (compounds having a perovskite structure). These are the polar-sensitive crystals, but they also have the magnetic ordering in addition to electrical polarity. These compounds are notable for the colossal magneto-resistance effect observed in them [8].

For example, in the polar compound $(La_{1-x},Ca_x)MnO_3$, where Ca varies within $0 \le x \le 1$, the phase transitions occur with both magnetic and dielectric ordering. In this case, the magnetic ordering, associated with polar properties, is accompanied by electronic transfer through the intermediate oxygen ion: $Mn^{+3} \Leftrightarrow O^{-2} \Leftrightarrow Mn^{+4}$.

The ordered phase of $(La_{1-x},Ca_x)MnO_3$ at low temperatures is characterized by small resistance, dut at elevated temperatures this compound is wide-gap

semiconductor with high resistance. The controlling magnetic field stimulates magnetic ordering with low electrical resistance.

The magnetic method of resistivity control is implemented in the compound $(La_{1-x},Ca_x)MnO_3$ – similarly to the electrical control of resistivity in VO_2. The physical reason for this control can be considered as the field-induced parallel orientation of spins in the “M” phase, which is accompanied by a decrease in electrical resistance, Fig. 7*b*. As temperature rises, the increasing thermal motion disrupts the dual electronic exchange mechanism, so that the ferromagnetic "M" phase passes over into the disordered paramagnetic "D" phase.

The magnetic ordering in manganite can be forcibly restored by magnetic field applying in high-temperature “D” phase, the curve $H > 0$ in Fig. 7*b*. The corresponding drop in resistance by hundreds of times is shown by the dotted line $1 \rightarrow 2$. The magnetic field-induced insulator-conductor junction is otherwise called the "colossal magnetoresistance", which can be used in many electronic devices.

Thus, in the polar-sensitive material, both electrical and magnetic fields can shift the temperature of insulator-conductor phase transformation, which leads to the large changes in resistivity. In this case, the phase with reduced resistance can be both at elevated temperature and at lower temperature. A magnetic way of controlling resistivity is also possible by field-induced ordering of electron spins.

In addition to the above effects, it can be noted that nano-structured polar dielectrics, based on zinc oxide demonstrate a very strong sensitivity to the external influences seen in a large change of conductivity. Zinc oxide properties are shown in Fig. 3.15 which can serve as a physical model for the functioning based on ZnO sensors. The finely balanced polar-sensitive structure of zinc oxide always is ready for a strong change of its electrical properties under the external influence that is used in sensors for indication of various external influences.

This is explained by the fact that polar zinc oxide easily change its high conductive wurtzite (pyroelectric) structure into a low conductive sphalerite (piezoelectric) structure. Very thin films of zinc oxide (and, particularly, its nanostructures) are used as the components in solar elements, in the piezoelectric nano-generators, as well as in luminescent materials, light-emitting diodes, lasers, etc. [9]. The ZnO-nanostructures are very sensitive to temperature, illumination, humidity, and even to the composition of surrounding gas.

The poin is that such nanoparticles demonstrate the structures with quite developed surfaces and very tender forms, which despite its small size and unusual shape, retains the regularity of its structure inherent in bulk crystal.

Conclusions. When increase of electrical field frequency, there is a frequency dispersion of both the permittivity of dielectrics, which is due to the delay in the reaction of bound charges, and the conductivity of conductors, which is due to the inertia of free charge carriers.

Usually the dispersion are described separately: by the complex permittivity $\varepsilon^*(\omega) = \varepsilon'(\omega) - i\varepsilon''(\omega)$ and the complex conductivity $\sigma^*(\omega) = \sigma'(\omega) + i\sigma''(\omega)$ but formally these parameters can be used as equivalent.

This possibility has been explored using the relaxation and the resonance models with the examples of dielectrics, semiconductors and metals. It is shown that the "conductivity" arising instead of delayed polarization is not adequate to a classical understanding of this parameter and can only be considered only as the effective conductivity.

In the dielectrics and wide-gap semiconductors, the relaxation and resonant dispersion models (both leading to the appearance of effective conductivity) are considered separately.

But in conductors, frequency dispersion of conductivity are observed as the relaxation and resonance phenomena simultaneously. It resulting in the negative effective permittivity that is obviously not adequate to usual understanding of this parameter and should be considered as effective ones.

In some polar crystals, their electrical conductivity can change in thousands of times even with small change in temperature or under electrical or magnetic fields action. Appropriate materials are widely used as highly sensitive thermistors with positive or negative temperature coefficient, in the non-linear and field-controllable switching elements and in very susceptive sensors.

It is argued that main reason for such properties is a finely balanced ionic-covalent polar inter-atomic bonding, arising due to difference in the electronegativity of neighboring ions.

Complicated spatial distribution of internal polarity in the polar-neutral crystals explains the entanglement of charge carriers in the electrically alternating structure that contributes to formation of little mobile polarons and low electrical conductivity. In this case, the quasi-one-dimensional polar structure, which, in particular, can be induced by applied electrical field, has much lower resistance to the electrons transport as compared to complex multidimensional arrangement of polar bonds, which contribute to high electrical resistance by polarons formation.

The alteration in the polar structure under external factors influence can lead to a large change in conductivity that is used in electronics.

3.8 Summary Chapter 3

Conclusions

It is shown that the conductivity arising instead of delayed polarization is not adequate to a classical understanding of this parameter and can only be considered only as the effective conductivity. In dielectrics and wide-gap semiconductors, the relaxation and resonant dispersion models (both leading to the appearance of effective conductivity) are considered separately. But in conductors, frequency dispersion of conductivity are observed as the relaxation and resonance phenomena simultaneously. It resulting in the negative effective permittivity that is obviously not adequate to usual understanding of this parameter and should be considered as effective ones. In some polar crystals, their electrical conductivity can change in thousands of times even with small change in temperature or under electrical or magnetic fields action.

References

[1] Yu. M. Poplavko, *Electronic materials. Principles and applied science,* ELSEVIAR, 2019.
[2] R. E. Newnham, *Properties of materials: anisotropy, symmetry, structure*, Oxford University press, Oxford, 2004.
[3] L. Levinson, H.R. Philip, *Zinc oxide varistors*, American Ceramic Society Bulletin 65(4), 639. 1986.
[4] A. P. Ramirez, *Colossal magnetoresistance*. Journal of Phys: Condensed matter. 9 (39): 8171. 1997.
[5] Yoon-Bong Hahn, *Zinc oxide nanostructures and their applications*, Korean J. Chem. Eng., 28(9), 1797, 2011.
[6] A. Von Hippel, Dielectrics and waves, Jon Wiley, New York. 1954.
[7] C. Kittel. Introduction to solid state physics. John Willey & Sons. New York. 1975.
[8] A.K. Jonscher, Dielectric relaxation in solids. Chelsea Dielectrics Press, London, 1983.
[9] M. J. Weber, Handbook of Optical Materials. Boca Raton: CRC Press, 2003.

Questions

1. List the types of charge carriers, types of their generation and methods of charge transfer.

2. List the main particles involved in polarization and explain the mechanisms of polarization.

3. From what equation of electrodynamics follow the formal affinity of the manifestation of conductivity and polarization?

4. How it manifests itself and how it is mathematically described inertia of electrical polarization mechanisms?

5. How it manifests itself and how it is mathematically described Inertia of electrical conduction mechanisms?

6. Why can the polarity of the structure significantly affect the electrical conductivity?

7. Main anomalies of conductivity in polar structures in weak electrical field.

8. Anomalies of conductivity in polar structures in strong electrical field

9. Applications of field controlled conductivity.

CHAPTER 4. POLAR-SENSITIVE STRUCTURES OF NON-CENTRAL SYMMETRIC CRYSTALS

Contents

The concept of spontaneous polarization in the pyroelectrics is called into a question, since the always existing free electrical charges make it impossible for any equilibrium and time-stable polarized state. It is assumed that pyroelectricity in the polar crystals and piezoelectricity in the polar-neutral crystals are due to hybridized ionic-covalent polar-sensitive bonds which do not create any internal field, but are capable of generating the electrical response to the uniform non-electric effect (heat, pressure, etc.). This response is described by a three-dimensional electrical moment, decreasing with temperature and its components in the piezoelectrics is measured by method of partial limitation of thermal deformations. Ferroelectrics are distinguished by the fact that in electrical field they reorient their polar-sensitive bonds with a non-linear response, which gives impression of spontaneous polarization.

As is known, electrical polarization occurs in any dielectric in the external electric field, but only the polar (non-centrally symmetric) dielectrics can be polarized in a non-electric way [1]. To explain this phenomenon, the term "spontaneous polarization" is traditionally used [2] as the analogue of spontaneous magnetization, due to dielectric hysteresis discovery 100 years ago in the Rochelle salt (analogue of magnetic hysteresis). However, the similarity of these phenomena is purely external. The fact is that the magnetic charges, which would screen the spontaneous magnetization, do not exist in a nature, so that spontaneous magnetization can exist unchanged for any time. On the contrary, the ubiquitous electric charges must, sooner or later, screen the spontaneous polarization already at elementary level. Subsequently, the concept "spontaneous polarization" was applied to the polar pyroelectric crystals, in which it cannot be detected directly, not to

mention the polar-neutral crystals-piezoelectrics, in which the pyroelectric effect and volumetric pyroelectric effects can also be obtained only by the partial limiting of strain [3]. It is this method that was used in a given work for proposed concept experimental confirmation.

The fact is that for electrical measurements of polar structure parameters (voltage or current), it is necessary to obtain the vector type response from a scalar action, as for example in the case of uniformly heating pyroelectric. However, in the polar-neutral piezoelectric, such a response, which allows one to measure its polarity, is possible only if its thermal deformation is partially limited by rigidly fastening polar cut of this crystal on the non-deformable substrate. This method of thermo-piezo-polarization is used to obtain an artificial pyroelectric effect, and a similar method is also possible to obtain the volumetric piezoelectric effect in the polar-neutral crystals such as quartz.

Further it will be shown in more detail that the description of polar crystals properties by the presence in them spontaneous polarization encounters some difficulties. Therefore, it is assumed that in polar and polar-neutral crystals the peculiar arrangement of the interatomic bonds exists, which drive in them the electrical response onto non-electrical actions (some doubts about spontaneous polarization existence are also expressed earlier [4, 5]. It will be shown that the mixed covalent-ionic (polar-sensitive) bonds, which form the polar or polar-neutral crystal are a consequence of the structural compensation in dissimilarity of nearest ions electronic structure, giving opposite contribution to electronegativity. It is this feature, which cause in polar crystals many electrical, mechanical, thermal and optical properties, quite different from the ordinary dielectrics.

4.1 Polar crystals - pyroelectrics

Some of dielectrics behave in the absence of external electric field as if they are polarized. This peculiar internal electrical state in the dielectrics can be as *energetically advantageous* (being associated with particular crystal structure – presence of polar axis), so the *metastable* (which can be disturbed by external external influences). In the former case internally polarized electrical state is characterized by the *spontaneous polarization* (pyroelectricity) while in the second case is characterized by *residual polarization* (electrets).

Pyroelectric effect traditionally is considered as a property of spontaneously polarized crystal, but it is preferable to assume that structure of pyroelectric crystal is such that it demonstrates electrical response when its temperature changes.

Thermal energy in the pyroelectric can be converted directly into electrical energy due to electrically active intrinsic structure of such crystal. Therefore, pyroelectric as well as piezoelectric presents solid-state energy converter; however, piezoelectric is the electromechanical (or vice versa mechanoelectrical) power converter, while pyroelectric is the thermoelectric (or vice versa electrothermal) power converter.

In principal, energy transformation in solid dielectric is only possible, if the crystal (texture or polymer) is polarized. However, in the absence of external influences the existence of intrinsic polarization is not evident. The point is that intrinsic polarization at constant temperature should be completely compensated by the electrical charges, which are precipitated on the surface of polar dielectric or on its electrodes. So called spontaneous polarization manifests itself only when external conditions *change dynamically*. As it was noted in previous Section, it might be the *change of stress* that results in the piezoelectric polarization of polar dielectrics. The pyroelectric polarization in polar dielectric also occurs only *due to temperature changes*.

Temperature raising or lowering changes the intensity of particles thermal motion in polar dielectric, and, therefore, changes as the orientation of polar complex (molecules) so the distance between them, leading to a change of the spontaneous polarization. Consequently, on the surface of polar dielectric the uncompensated electrical charges appear. If pyroelectric element with electrodes is connected to amplifier, then the pyroelectric *current* flows through this device and next amplified. In the case of open-circuited crystal the pyroelectric *voltage* appears on a crystal. Over time, however, if temperature of pyroelectric remains invariable, pyroelectric current (or pyroelectric potential) decreases gradually to zero.

Pyroelectric effect has been described (but not understood) in the ancient sources, mentioned about 2000 years ago by Greek philosopher Pliny. This effect was observed in the semi-precious mineral tourmaline (with time, this crystal become called as "electrical" crystal). The term "pyro-" comes from the Greek word for "fire", because the effect is elicited itself during tourmaline heating in fire. When heating, the electric charges are generating, accompanied by cracking sound – electrical discharges. Moreover, heated tourmaline attracts light objects. Recent measurements have shown that in rather thin (about 1 mm) plate of tourmaline the electrical potential of about 1 kV is generated when temperature changes only on 10 degrees. However, it should be noted that tourmaline is still relatively weak pyroelectric.

As the *electrical* phenomenon, pyroelectric effect was qualified about 200 years ago by F. Aepinus. However, main aspects of symmetry and physical

mechanism of pyroelectric effect have been described only in early twentieth century by W. Voigt. As among minerals, so among artificially synthesized crystals pyroelectrics are relatively rare materials. Natural pyroelectric minerals is tourmaline: $NaMg[Al_3B_3{\cdot}Si_6(OOH)_{30}]$ with different impurities, while among synthetic pyroelectrics are lithium sulphate ($LiSO_4{\cdot}H_2O$), lithium niobate ($LiNbO_3$), potassium tartrate ($K_4C_8O_{12}{\cdot}H_2O$) and many others. Semiconductors of $A^{II}B^{VI}$ group (CdS, ZnO, etc.) by their symmetry also relate to pyroelectrics, but pyroelectric effect in them is small. Interestingly to note that among pyroelectric crystals there is sugar ($C_{12}H_{12}O_{11}$); that is why it is used in the homeopathic medicine.

All *ferroelectric* materials, potentially, are pyroelectrics, because they are spontaneously polarized. But in order to use ferroelectric as pyroelectric element it must have *single-domain* structure. Otherwise pyroelectric effect, occurring in many different-ways oriented ferroelectric domains, is mutually compensated. Mono-domainization of ferroelectrics (converting them in homogeneously polarised structure) can be realized in many ways, including temperature polarization: heating ferroelectric in the externally applied electrical field. Nowadays, to obtain single-domain ferroelectric-pyroelectric crystal several methods for crystals growing are developed that permits already in the process of crystal growth to get practically single-domain structure.

Pyroelectrics are applied in electronics as uniquely sensitive uncooled temperature sensors and as detectors of radiation. Compared with semiconductor temperature sensors, pyroelectric sensors have several advantages: they do not require cooling (can be used at room temperature) and show the wide spectrum range of sensitivity. Numerous technical applications stimulate rapid development of physics of pyroelectric. At present time, dozens of new pyroelectrics are synthesized and investigated, and many of them have already found technical application. Thus, it is supposed that pyroelectric effect is caused by the temperature change of spontaneous polarization in the *polar crystals*; however, similar effect can be artificially induced in any solid dielectric, if external electrical field would be applied to them. Without application of external electrical field, and in absence of mechanical influences the change of polarization with temperature is possible only in such crystals, where peculiar structure is traditionally described as spontaneous polarization.

Simplified model of pyroelectric effect. Pyroelectrics are closely connected to piezoelectrics. In all pyroelectrics also piezoelectric effects (direct and inverse) are observed, but only in the pyroelectric it is possible to observe very important for

practical applications *volumetric piezoelectric effect* that is the electrical response to hydrostatic pressure.

Pyroelectric effect can be explained by the simplest model of one-dimensional polar crystal, Fig. 4.1. This model of pyroelectricity comes to a simple molecule consisting of pair of ions separated by distance *a,* which is larger than distance *b* between the neighbouring polar unit cell. This asymmetry is explained by large difference in the electronegativity of positive and negative ions.

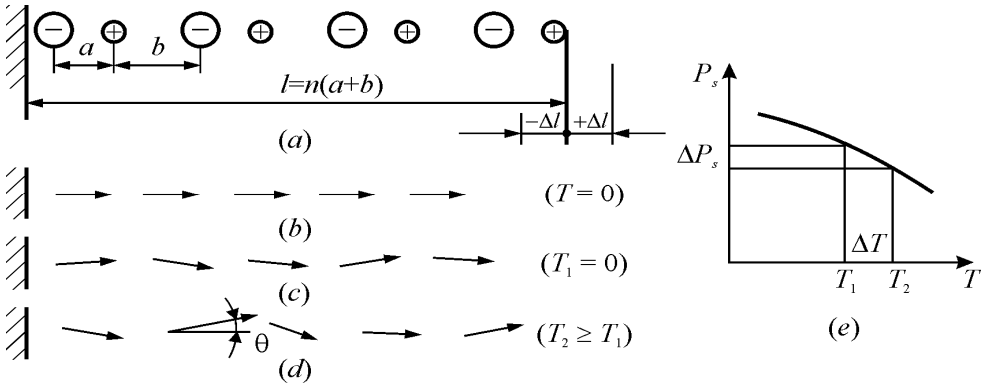

Fig. 4.1. One-dimensional model of pyroelectric crystal: *a* – polar file of two-ions molecules; *b* – dipole moments orientation without thermal motion ($T = 0$); *c* and *d* – different degrees of thermal disordering and thermal expansion of a dipoles chain; *e* – spontaneous polarization dependence on temperature

The hidden (or latent) internal polarity of pyroelectrics is no more than the *ability to provide electrical (vectorial) response to any non-electrical scalar impacts*, in a given case – when temperature changes. To describe this ability, it is assumed that polar crystal has intrinsic electrical moment P_S, which summarizes many elemental moments p_0; that is why each unit cell is marked in Fig. 4.1, *b, c, d* as simple dipoles. Possible example of such structure is spontaneously polarized (at low-temperatures) pyroelectric crystal HCl; wherein Fig. 4.1*a* is intended to remind the wide-gap semiconductor of CdS ($A^{II}B^{IV}$ type crystal) belonging to pyroelectrics of 6*mm* point symmetry class. In this one-dimensional model one can observe not only pyroelectric, but the piezoelectric effect as well, which contributes to the pyroelectric response. Indeed, mechanical stretching or compression of shown dipole chain results in the change in specific electrical moment: $P \sim \Delta l/l$. Thus, not only from general considerations, but also from simple model it follows that any pyroelectric should have piezoelectric properties (but opposite conclusion is not fair).

Thus, shown in Fig. 4.1*b* polar molecules are replaced by the arrows that present single dipole moments. In the idealized state (when absolute temperature $T = 0$) all dipoles are strictly oriented. As temperature increases, the thermal chaotic

motion, firstly, results in a partial disordering of dipoles, and, secondly, leads to thermal expansion of crystal. In mechanically *free crystal* both of these mechanisms give rise to spontaneous polarization P_S decrease with increasing temperature, Fig. 4.1, *e*. First mechanism (polar units disordering) is *always* found in any polar crystal (clamped or free) but second mechanism (crystal thermal expansion) is possible to observe in *mechanically free* crystal only.

Temperature rise changes P_S in the *linear* ("hard") pyroelectric, such as tourmaline or lithium sulfate crystals mostly due to their thermal expansion or compression. This type of pyroelectricity is produced by the *piezoelectric conversion of thermal strain* that is referred as *secondary* pyroelectric effect.

The temperature change of P_S of the *non-linear* ("soft") pyroelectrics (which include most of ferroelectrics) is caused mainly by *thermal disordering* of dipole structure. Dipoles orientation alteration results in the *primary* pyroelectric effect.

Due to fast decrease of spontaneous polarization with temperature rise in ferroelectrics near Curie point (abrupt change in dependency: dP_S/dT) exactly these materials are mostly used as the pyroelectric sensors. In the model, shown in Fig. 4.2, elementary electrical dipole moment change is $dp = p_0(1 - \cos\theta)$. Since angle θ is small, it can be considered as being proportional to intensity of thermal motion: $\theta \sim k_B T$. Therefore, the change in polarization is $\Delta P = \gamma^{(1)}\Delta T$, where $\gamma^{(1)}$ is *primary pyroelectric coefficient*.

For secondary pyrolectric effect proportionality in ΔP and ΔT changing is, firstly, the result of thermal expansion linear law: $\Delta l = \alpha\Delta T$, where Δl is linear deformation while α is thermal expansion coefficient. Secondary, the linear direct piezoelectric effect is described as $\Delta P = e\Delta l/l$, where e is piezoelectric strain constant. From these two formulas it is possible to obtain linear equation for secondary pyroelectric effect: $\Delta P = \gamma^{(2)}\Delta T$, where $\gamma^{(2)}$ is the *secondary pyroelectric coefficient*.

Consequently, taking into account the deposits from both mechanisms of pyroelectricity, it is possible to obtain for thermally induced polarization: $\Delta P = (\gamma^{(1)} + \gamma^{(2)})\Delta T$. As temperature T is the scalar value but polarization is vector value, pyroelectric coefficient γ is the vector. However, it is a peculiar ("*material" vector*) that differs fundamentally from the "force-type" vectors (such as vectors E, D, or P).

First rank material tensor describes a spatial distribution of pyroelectric response in a crystal; appropriate *indicatory surface* (indicatrix) is shown in Fig. 4.2, being represented by two spheres. They are located above and below of the symmetry plane *m,* and can be characterized by equation $\gamma(\varphi) = \gamma_{max}\cos\varphi$. It is evident

that spatial distribution of pyroelectric coefficient corresponds to spontaneous polarization orientation in polar crystal: $P = P_{max}\cos\theta$. The upper sphere is indicatory surface for upper orientation of P_S, while the bottom sphere means only a change in sign of γ_i, if spontaneous polarization has opposite direction.

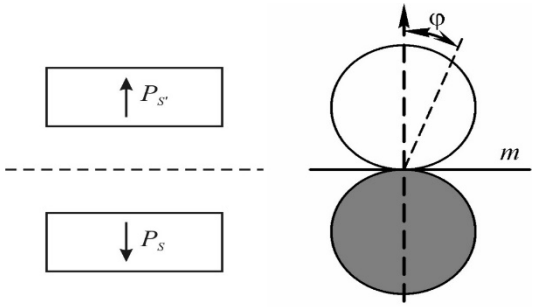

Fig. 4.2. Orientation of spontaneous polarization in crystal and correspondent guide surface (indicatrix) for pyroelectric coefficient; black area shows negative part of pyroelectric coefficient.

Material vector γ shows maxim in that direction of ordinate, which coincides with spontaneous polarization direction. So the γ_{max} might be measured in such cut of a crystal that is perpendicular to the polar axis. The angle φ between the ordinate and the vertical to slanting cut of crystal determines the magnitude of pyroelectric effect. By the radius vector drawn from the center of a figure (shown in Fig. 4.2) it is possible to determine pyroelectric effectiveness in any *slanting cut* of a crystal. It is obvious that perpendicularly to ordinate any pyroelectric effect is absent.

Pyroelectricity, as piezoelectricity, is determined by crystal symmetry. However, if in event that piezoelectric properties, the necessary condition is the *absence of centre of symmetry* in crystal, the pyroelectric effect is possible only in the crystals, which have a special element of symmetry – the *peculiar polar axis*. It is this axis that provides polar acentricity of a crystal, so that any pyroelectric should have piezoelectric properties as well (but not vice versa).

Of the 20 classes of piezoelectric crystals (described in previous section in Table. 9.3), only 10 classes are the pyroelectric ones; their designations are as follows: 1, 2, 3, 4, 6, *m*, 2*m*, 3*m*, 4*m* and 6*m*. As it was noted above, the number indicates the order of polar axis, while the letter *m* means the plane of symmetry, which passes through the polar axis [12].

Besides polar crystals, the polarized ferroelectric ceramics also have pyroelectric properties: in conditions of increased temperature and under the influence of externally applied electric field most of ferroelectric domains (spontaneously polarized micro-regions) become oriented. Thus, after cooling down to normal temperature and turning off the field, the pyroelectric *texture* occurs with

a group of polar symmetry $\infty \cdot m$ (∞ is the order of symmetry axis). Because of mechanical strength and high chemical resistance, the polarized ferroelectric ceramics, as well as polar crystals, are used in the pyrometry, although pyro-sensitivity in the ceramics is less than in ferroelectric crystals.

Similarly to electromechanical coupling coefficient K_{EM} in the piezoelectrics, analogues power conversion factor – the coefficient of *thermoelectric coupling* K_{TE} – might be introduced for pyroelectrics (it plays the role of efficiency). In the basic pyroelectric materials this ratio is seen in the range of 1 - 4%. Such relatively low efficiency of thermoelectric power conversion K_{TE} is due to physical nature of this phenomenon in crystals, which tend to be "electrically hard" relatively to external influences. To describe the efficiency of pyroelectric sensors that convert infrared radiation into electrical energy not only pyroelectric coefficient γ but several *quality parameters* are evaluated: γ/C_V, $\gamma/(C_V\varepsilon_0\varepsilon)$ and $\gamma/[C_V(\varepsilon_0\varepsilon \mathrm{tg}\delta)^{1/2}]$, where C_V is volumetric heat capacity. There are a number of options for pyroelectrics; these quality parameters define the *current sensitivity* ($S_J = \gamma/C_V$) and the *voltage sensitivity* $S_V = \gamma/(C_V\varepsilon_0\varepsilon)$.

The *fist* group of pyroelectrics are *non-linear* pyroelectrics-ferroelectrics: triglycine sulphate and isomorphic to it crystals (they are grown with special additives for the purpose to obtain single domain samples); lithium niobate and lithium tantalate (polarized by the current bias during crystal growth); thin films of potassium nitrate in the ferroelectric phase; lead titanate and lead zirconate-titanate polarized ceramics with different impurities. Pyroelectric properties of in ferroelectrics are due mostly to the *primary* pyroelectric effect. Near Curie point (T_C), when spontaneous polarization change with temperature is expressed very strongly, pyroelectric coefficient reaches maxim, so pyroelectric effect can be used with maximal efficiency.

The *second* important group of pyroelectrics is the *linear* pyroelectric crystals. In contrast to ferroelectrics (which are usually divided into domains with arbitrary direction of P_S), in the linear pyroelectrics P_S has same direction throughout a crystal. Furthermore, this direction can not be changed by external electrical field. The value of P_S in the linear pyroelectrics, varying with the temperature, never decreases to zero (as in ferroelectrics). These crystals may belong to pyroelectrics of CdS-type ($A^{II}B^{VI}$ crystals with wurtzitic structure), as well as lithium sulfate, lithium tetraborate, and others. It is important to note that in such pyroelectrics the contribution from *secondary* pyroelectric effect dominates, exceeding contribution of primary pyroelectric effect.

The *third* group of pyroelectric materials is the *polar polymers,* such as PVDF film. Since special processing, which consists in film stretching in 3 -.5 times with next temperature polarization (in field close to 1 MV/cm at 130 °C), polymeric film acquires pyroelectric properties. Despite the fact that pyroelectric coefficient of polymeric materials is lower than in single crystals and pyroelectric ceramics, technical application of pyro-polymers is very promising due to their excellent mechanical properties (thin and elastic films).

According to Curie principle, any linear effects in crystals must have the *opposite effect*. For example, opposite to the direct piezoelectric effect is the inverse piezoelectric effect. Similar, inverse to pyroelectric effect is the *electrocaloric* effect. This effect can be applied for electrically controlled reduction of temperature (e.g., to achieve better cooling). Thus, pyroelectric not only can convert thermal energy into electrical energy, but vice versa. Controlled by a voltage, the electrocaloric cooling (or heating) depends on the polarity of applied electrical field. The alternation voltage can generate extended temperature wave. In polar crystals electrocaloric effect influences on value of permittivity. When thermal equilibrium in studied sample is entirely established at the time of electrical field application (possible at very low frequency), the pyroelectric crystal completely absorbs applied to a crystal electrical energy and converts it into the thermal energy. This is the isothermal process of pyroelectric polarization that is characterised by *isothermal permittivity* ε^T. On the contrary, in case of rather fast changing of electrical field, the energy process is the adiabatic one (thermal equilibrium has no time to be set). It looks like a decrease in the capacitance of pyroelectric element. Therefore, at higher frequency, *adiabatic permittivity* $\varepsilon^S < \varepsilon^T$ can be already determined.

4.2 Polar crystals - ferroelectrics

Traditional and comfortable modelling of ferroelectric is the assumption of its *spontaneous polarization* P_S, direction of which can be switched by externally applied electrical field. Currently, there is opinion as to another nature of ferroelectricity: it might be assumed that structure of ferroelectric is able to demonstrate such nonlinear polar response to externally applied field, as if the *switching of polarization* occurs in it. Otherwise, it is customary to say that ferroelectrics are crystals with reversible spontaneous polarization.

As stated above, other than in ferroelectrics internal polarization is peculiar to the electrets and pyroelectrics. However, unlike residual polarization of electrets, so cold spontaneous polarization represents the *stable thermodynamic state* of polar

dielectrics. Indeed, residual polarization in electrets disappears during their heating or irradiation, while spontaneous polarization looks like a structural feature of polar crystal. Really, its value can be changed under external influences, but then completely restores when initial conditions return.

It should be recalled that pyroelectricity is one of possible manifestations of polar crystals peculiar structure. However, applied electrical field can not change the direction of spontaneous polarization in the *linear* pyroelectric, which persists up to the melting of a crystal. Being the *non-linear* pyroelectric ferroelectric not only switches its P_S in electrical field, but shows significant change in $P_S(T)$ dependence until P_S completely disappears well before the melting of crystal.

Thus, ferroelectrics are subclass of pyroelectrics, in which polarized state is not stable enough but it is quite labile. This polarized state can be changed by many external influences: electrical field, temperature and pressure.

An important feature of ferroelectrics that suggests them as the electrical analogue of ferromagnetics is their spontaneous division into a plurality of domains. Within each domain the spontaneous polarization P_S is same, but in various domains P_S has different orientation. The subdivision of ferroelectric structure into great number of domains is energetically advantageous, since the single-domain crystal would create in environment external electrical field (as in case of electrets). Obviously, energy of this field decreases with diminution of size of domains.

Externally applied electrical field causes, at first, junction of randomly oriented ferroelectric domains into one domain; next its polarization reaches saturation. As it can be seen in Fig. 4.3*a* after external field switching off polarization tends to maintain its constant direction. If polarity of externally applied field would be changed, polarization, without changing its absolute value, will change its direction abruptly.

For such "forced" change in the direction of P_S, that is, for ferroelectric polarization reversal, it is necessary to apply electrical field of a certain value, which is the *coercive field* E_C (see Fig. 4.3*a*). Sometimes the value of this field reaches very large values, and then the ferroelectric cannot be repolarized and behaves like the pyroelectric. However, during such "hard" ferroelectric heating, as it approaches the temperature of Curie point T_C, its coercive field E_C mush reduces, and, therefore, close to Curie point it becomes possible to observe hysteresis. The coercive field E_C as well as the P_S in ferroelectric becomes zero, if $T = T_C$. The pyroelectric, however, has no Curie point, and until electrical breakdown its internal polarisation does not change direction – such crystal rather can be destroyed than change the direction of polarization.

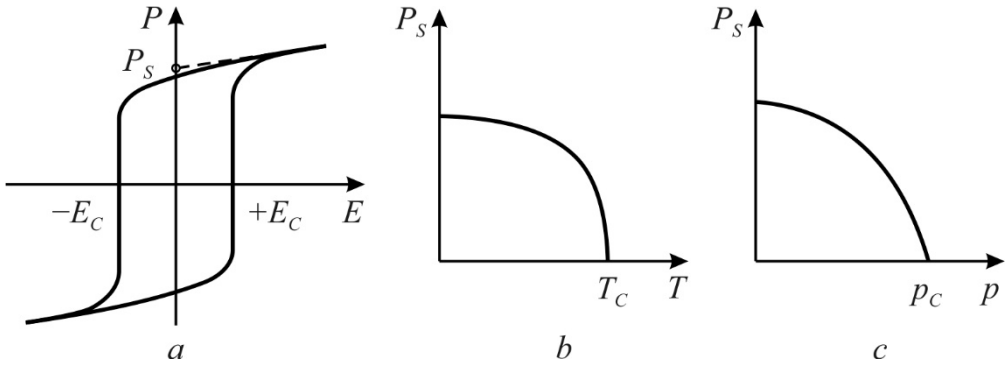

Fig. 4.3. Ferroelectric polarization dependence on electrical field (*a*) and spontaneous polarization dependence on temperature (*b*) and pressure (*c*).

It is therefore believed that availability of dielectric hysteresis is *necessary and sufficient property* of ferroelectric state. If temperature exceeds the critical value T_c then as hysteresis loop so ferroelectric state disappears. In same way on ferroelectric P_S affects increase of hydrostatic pressure, Fig. 4.3*c*. In contrast, linear pyroelectric does not change its polarized state under a pressure up to being destroyed. Summarizing, it might be concluded that ferroelectric is a special, nonlinear pyroelectric. Ferroelectrics are significantly different from linear pyroelectrics of tourmaline or lithium sulphate types.

In case of *active dielectrics applications*, first of all, ferroelectrics or close to them dielectrics have largest interest. In fact, exactly in ferroelectrics their "transforming functions" are most pronounced. For example, the greatest value of piezoelectric module is observed in Rochelle salt crystals and in the ferroelectric antimony sulfoiodide (SbSI). The highest values of pyroelectric coefficients are also seen in ferroelectric crystals (threeglycine-sulphate). Therefore, for thermal infrared receivers manufacture that use pyroelectric effect just the ferroelectrics (nonlinear pyroelectrics) are applied. The most applied piezoelectrics are also ferroelectrics, in particular, the ferroelectric ceramics of PZT-type ($Pb(Zr,Ti)O_3$). In optical detectors (that use photo-polarization effect) also some of ferroelectric crystals are applied, while for optical holograms recording ferroelectric crystals strontium-barium niobate and lithium niobate are employed.

Model conception of ferroelectricity. It is important to establish main cause of ferroelectricity appearance in the ionic crystal. It can be shown that great importance for ferroelectricity constitutes the anharmonicity in ions movement. This means a substantial non-linearity in the law of reciprocal displacement of neighboring ions in the crystal lattice. This peculiar property arises in some special structures.

For simplest analysis the one-dimensional chain of ions is investigated. The energy of linear chain of ions can be expanded in a row in power of dynamic displacement x:

$$U(x) = ½\, cx^2 + ¼\, bx^4 +$$

When considering polarization of ordinary ("linear") dielectric, sufficient approximation is to take into account only the first term of this expansion: $U(x) = ½\, cx^2$, where c is coefficient of elasticity. To determine the role of anharmonicity, it is enough to account the next (anharmonic) term $¼bx^4$ with coefficient of anharmonicity $b > 0$. The concerned lattice can be stable only with assumption that coefficient of anharmonicity is positive: $b > 0$. Exactly this guarantees the stability of given lattice in case of large fluctuations. As to the coefficient of elasticity, it might be as positive ($c > 0$) so negative ($c < 0$).

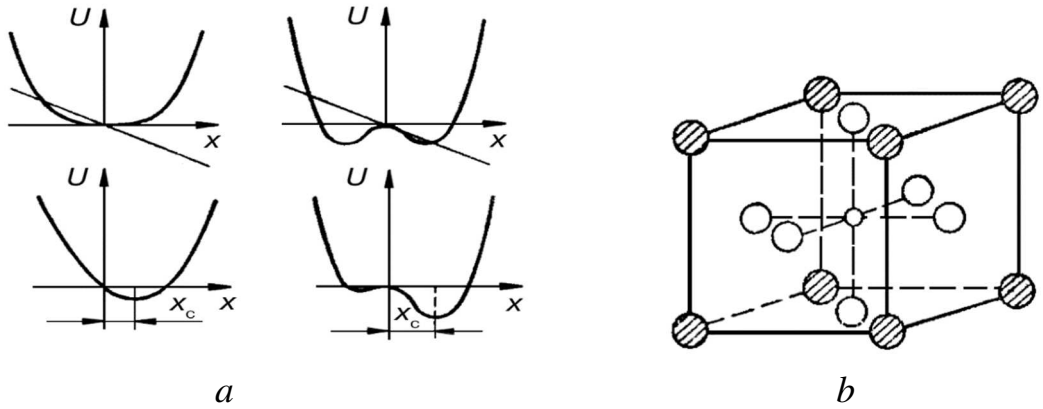

Fig. 4.5. Anharmonicity and ferroelectricity: energy U dependence on «ferro-active" ion deviation from equilibrium state in a lattice (a); Angarmonic crystal structure of perovskite ABO_3: "ferro-active" ions O = B is surrounded by octahedron of oxygen O, while crosshatched A ions are located between octahedra (b)

This equation corresponds to the fact that ferroelectric is found *above* Curie point (T_C), i.e., in the non-polar (paraelectric) phase that has the centrosymmetric structure. Below T_C this $1D$ crystal passes onto the non-centrosymmetric (ferroelectric) phase. In case of transition to spontaneously polarized state (below T_C), to expansion series (9.28) the energy of ion spontaneous displacement $F \cdot x$ should be added:

$$U(x) = ½\, cx^2 + ¼\, bx^4 - Fx,$$

where x is ion deviation from equilibrium state and F is internal (spontaneous) electrical field. Figure 4.5 shows functions $U(x)$ for both cases: when $c > 0$ (on the left) and when $c < 0$ (on the right). It is seen that below Curie point the spontaneous deformation x_S arises, at which energy $U(x)$ becomes minimal. Since polarized state

at $x = x_S$ now is the equilibrium state, a total force acting on system of charges in this state equals zero: $\partial U(x)/\partial x = 0$, that means

$$cx + bxc^3 - F = 0.$$

With spontaneous polarization the electrical field is associated, called the coercive field: $F_C = \beta P_S$, where β is the Lorentz factor. In case of one-dimensional model of ferroelectric represented by simple linear chain of ions polarization $P_S = np_S = nqx_S$, where n is ions concentration and q is ions charge. By substituting this data to above equation a cubic equation can be obtained

$$cx_S + bx_S^3 - nq^2\beta x_S = 0,$$

where term cx_S describes the "elasticity" while member bx_S^3 characterizes the anharmonicity. This equation has three roots:

$$x_1 = 0; \quad x_{2,3} = \pm [(nq^2\beta - c)/b]^{1/2}$$

As far as the only *spontaneously polarized phase* (with spontaneous deformation $x_S \neq 0$) is taken into consideration, the first solution $x_1 = 0$ of given equation is a side effect and will not be implemented here. The analysis of other two obtained solutions provides an opportunity to obtain to make following conclusions.

Firstly, the signs «±» means two equivalent possible directions of the spontaneous polarization, which corresponds to two equal in magnitude but opposite in direction ions displacements: $\pm x_S$. This corresponds to two opposite values of P_S. Indeed, spontaneous polarization of ferroelectric material in some parts of a crystal can be directed in one direction, but in others parts – in the opposite direction (these areas of P_S opposite direction are called domains).

Secondly, in crystals with very small anharmonicity (when $b \cong 0$) the spontaneous displacement of ions is impossible. Therefore, the anharmonicity of ionic displacements is one of *defining properties* of ferroelectric crystals.

Third, the above equation has real roots $x_{2,3}$ only at the conditions, when $nq^2\beta > c$ (because parameter $b > 0$). To clarify physical meaning of this important inequality (that is, essential conditions for spontaneous polarization arising), it is necessary to multiply the left and the right side of expression $nq^2\beta > c$ by deformation x:

$$nq^2\beta x > cx.$$

The right-hand side of equation corresponds to the elastic force that counteracts ferroelectric spontaneous displacement x_S. The nature of electronic shells interaction is such that seeks to *return* the non-polar state. Obviously, that left side of inequality (9.33), namely, the $nq^2\beta x$ has also the dimensions of force that is the *leading interaction* (i.e., leads to ferroelectricity). Therefore, spontaneous

polarization occurs in such crystals, where *the leading interaction exceeds the returning interaction*.

At the further analysis of above expression there is an opportunity to make the conclusion what should be atomic parameters that contribute to the emergence of ferroelectric state in the ionic crystals. First of all, it is the *high density* of a crystal (in this simple model it is represented by parameter n).

As a second factor the *big electric charge q* of shifting ions can be considered: q^2 in above inaquality. Third parameter is the *increased Lorentz factor* β. Comparing this qualitative results with experimental data, it is seen their correctness. Indeed, among large number of well-studied alkali halide crystals (such as NaCl) no ferroelectrics exist: ions in these crystals are single charged (Na^{+1} and Cl^{-1}), while Lorentz factor is small: $\beta = 1/3\varepsilon_0$ (ε_0 is permittivity of free space).

At the same time, in the barium titanate, for example, ($BaTiO_3$ is best-known ferroelectric) titanium ion (Ti^{+4}) has valence +4 (i.e., q^2 in Ti^{+4} in 16 times over q^2 of alkali halides). The Lorentz factor in barium titanate is also in five times higher than its usual value in the simple cubic ionic crystals due to peculiarities of perovskite structure (this term comes from mineral $CaTiO_3$ = perovskite).

In the perovskites that have general formula ABO_3 small size cation B^{+4} is surrounded by the octahedron formed of six oxygen ions O^{-2}. Any displacement of particular "ferro-active" ion B^{+4} makes great contribution to the dipole moment of unit cell in which spontaneous polarization occurs.

The significant shift of small size tetravalent cation in the octahedron is conditioned by the fact that surrounding very small ion B^{+4} large anions O^{-2} leave considerable space inside octahedron for ion B^{+4} easy displacement. This effect causes to appearance of spontaneous polarization in the perovskites.

Barium titanate is one of many *ferroelectrics with perovskite structure*. In Curie point of barium titanate its permittivity shows step increase and gradual decrease in the paraelectric phase. As temperature increases, spontaneous polarization first gradually declines and then abruptly falls to zero at phase transition. Heat capacity shows typical for phase transition maximum.

Another class of ferroelectrics that have phase transition of order-disorder type is quite different from barium titanate (mostly these are ferroelectrics with hydrogen bonds). First of all, Curie-Weiss parameter C in them is less by two orders of magnitude; secondly, their phase transition temperature T_C is very close to Curie-Weiss temperature θ. Phase transition in these crystals is well described by second-order transition theory (see Section 10.1).

Main experimental characteristics of ferroelectrics of order-disorder type ferroelectrics are shown in Fig. 4.6. Temperature dependence of dielectric constant, spontaneous polarization and specific heat corresponds to thermodynamic theory of phase transitions of the second type.

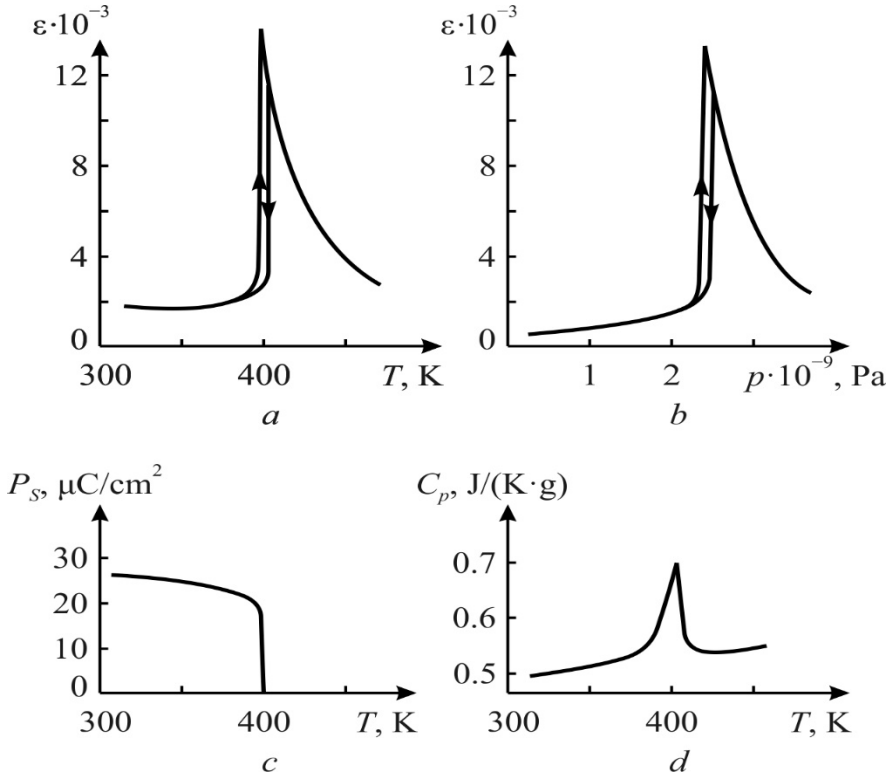

Fig. 4.6. Main characteristics of barium titanate: *a, b* – permittivity dependence on temperature and pressure; *c, d* – spontaneous polarization and specific heat dependences on temperature

Dynamic properties of these crystals differ from the properties of ferroelectrics with displacement-type transition. Special and interesting property of crystals with order-disorder transition is the isotopic effect – the displacement of Curie point in case of hydrogen replacement by deuterium.

This peculiarity demonstrates the importance of hydrogen bonds for majority of these types of ferroelectrics.

There are also ferroelectric crystals that do not contain oxygen. Mostly they are represented by the *chalcogenides*. These ferroelectrics have narrow band gap in their electronic spectrum, that is, such crystals belong to the ferroelectrics-semiconductors. Ferroelectrics properties are considerably dependent on their ***domain structure.*** The origin of multidomain structure in ferroelectric crystal below phase transition is energetically favourable. Single-domain crystal (Fig. 4.8*a*) creates an electrical field in the surrounding space (like electrets), to which spent

some energy W_1. As can be seen from Fig. 4.8*b,* the energy of external field in a two-domain crystal is smaller than in single-domain crystal.

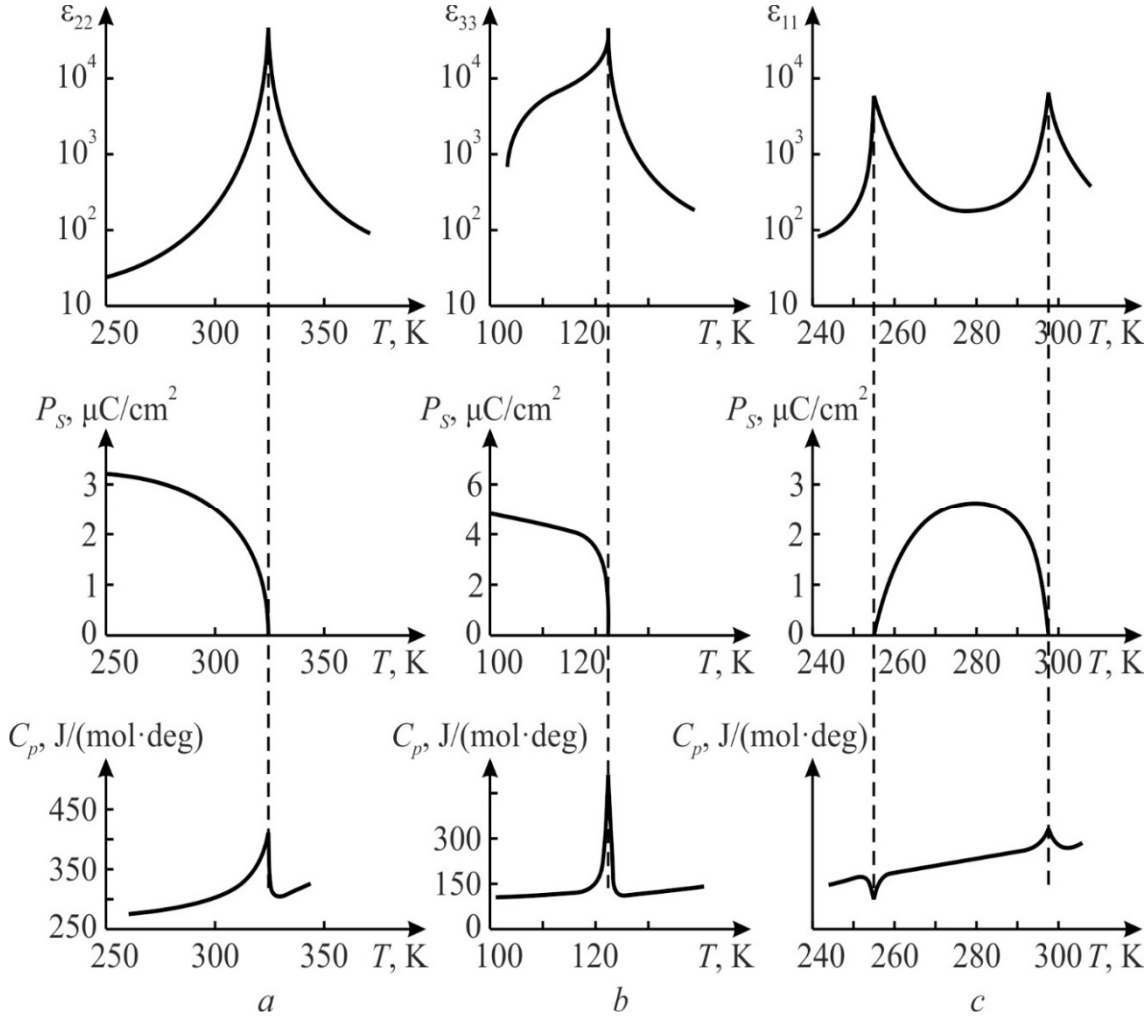

Fig. 4.7. Temperature dependence of relative dielectric constant, spontaneous polarization (μC/cm^2) and specific heat (J/(mol·deg) crystals, close to model of order-disorder phase transition: *a* – TGS = triglycinesulphate ($NH_2CH_2{\cdot}(COOH)_3H_2SO_4$); *b* – KDP = potassium dihydrogen phosphate (KH_2PO_4); *c* – Rochelle salt (RS) $KNaC_4H_4O_6{\cdot}4H_2O$

Thus, in case of many-domain structure the total energy of crystal must be reduced. This reduction in energy is limited by the growth of energy W_2, expended on the formation of domain walls that separate regions with different directions of P_S, Fig. 4.8*c*). The average size of domains (at which the sum $W_1 + W_2$ is minimal) depends on temperature, structural defects and electrical conductance of dielectric, as well as on environment properties. Multidomain structure in ferroelectrics is relatively stable; at that, the equilibrium state of ferroelectric domains usually corresponds to domain size from a few hundredths of millimetre to several millimetres.

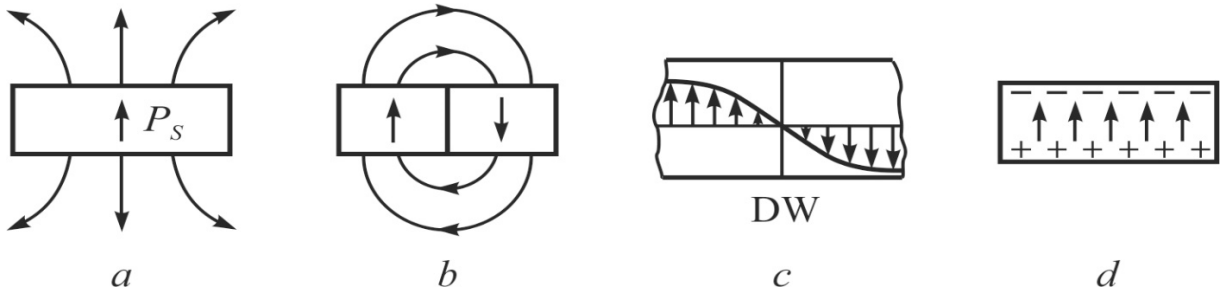

Fig. 4.8. Domain structure of ferroelectrics: *a* – single-domain crystal creates in surrounding area depolarizing electrical field; *b* – in two-domain crystal depolarizing field is reduced; *c* – domain wall structure in the vicinity of which P_S gradually changes its direction to opposite; *d* – comparison with pyroelectric, wherein field is shielded by charges on surface

Linear pyroelectrics that are characterized by the "hard" orientation of spontaneous polarization never split up into domains. However, they usually do not induce electrical field in the environment as their spontaneous polarization is shielded by electrical charges accumulated on surface (Fig. 4.8*d*). With change in ambient temperature the alteration in polarization has not enough time to be compensated by conductivity and a pyroelectric effect appears. Over time spontaneous polarization in crystal again remains compensated. The possibility of spontaneous splitting into the domains is caused by the changeableness of "soft" ferroelectric state in comparison with "hard" pyroelectric state. In this regard, sometimes ferroelectric is defined as *pyroelectric which divides into domains.*

However, in technical applications, sometimes just single-domain ferroelectric crystals should be used. This is need, for example, in the pyroelectric temperature sensors, particularly, in heat television tube (vidicon) that convert invisible infrared image of objects into optical image seen on a screen. Single-domain structure in ferroelectrics can be created by various methods: thermal electrical polarization, radiation exposure of crystals with applied electrical field or by the introducing specific impurities that impede as formation so movement of domain walls. Application of ferroelectric ceramics also needs to create polarised structure: inasmuch as ceramic sample would consist of a plurality of domains and crystallites, oriented in different directions, and piezoelectric effect will not occur. The polarized piezo-ceramics often are obtained as thermo-electrets – by heating and subsequent cooling in the strong direct electrical field. This method uses temperature dependence of coercive field E_C that is significantly reduced when temperature increases (in Curie point $E_C = 0$). In heated ceramics ferroelectric domains can be easily oriented by electrical field; later, when temperature decreases, most of domains remain in the polarized state. Thus, the piezoelectric ceramics is the *texture of oriented ferroelectric domains*. That is why, when operation with

polarized piezoelectric ceramics, their overheating should be avoided, because it may result in domains depolarization, and, consequently, in the loss of piezoelectric properties, since domains become disordered at high temperature.

Frequency and optical nonlinear properties of ferroelectrics can be also determined by the motion of domain walls under influence of electrical field. Low frequency non-linearity is characterized by the hysteresis. In its first cycle, the hysteresis loop (Fig. 4.7*a*) is due to forced orientation of domains; then they partially keep their polarisation until the field of opposite direction (E_C) makes domains switching. Reversal polarization in ferroelectrics specifies domain contribution to the dielectric constant: $\varepsilon_{dom} \sim dP/dE$. This contribution depends on electrical field; this non-linear dependence $\varepsilon(E)$ sometimes is applied in technique. However, at microwave frequencies switching of domains, as a rule, does not have time to occur. Therefore, the use of nonlinearity conditioned by domains motion is limited by the radio frequency range. Dielectric hysteresis loop characterizes two different states of polarization of ferroelectric crystal. This bistability is clearly manifested, if coercive field of ferroelectric is big enough. Exactly the bistable polarized state can be used in the memory devices of computers and in other devices of modern electronics. It should be noted that in the bulk ferroelectrics domains switching is possible only at relatively low frequencies (typically, less than 10^6 Hz). However, in the thin ferroelectric films (less than 1 micron) switching time can be reduced to 10^{-8} s.

4.3 Polar-neutral crystals - piezoelectrics

Piezoelectric effect was discovered by Pierre and Jacques Curie in 1880. First technical application of piezoelectrics becomes known in year 1920 when P. Lanzheven created ultrasonic transducer for transmitting and receiving signals in the water, which became the prototype of modern ultrasonic transducers used now for navigation in submarines as well as to detect shoals of fish and for other purposes. Somewhat later B. Cady developed piezoelectric filters for use in the telephony. The area of practical application of instruments and devices that use piezoelectric effect in their designs are constantly expanding. Some products, such as watches, cameras, mobile phones, televisions, computers, and piezo-lighters have become the objects of everyday life. Many electronic devices are not possible without piezoelectric elements. There are radiators and antennas of sonar, frequency stabilizers in computers, electronic devices for reference time, power line filters and delay lines in radio and telephone communications, sensors to measure acceleration, vibration,

acoustic emission non-destructive testing, piezo-transformers and piezo-motors, medical ultrasound imaging and medical instruments for various purposes, etc [8].

Piezoelectric materials include bulk ceramics, ceramic thin films, multilayer ceramics, single crystals, polymers and ceramics-polymer composites. In recent years many types of piezoelectric films have been developed and tested for different micro-systems and microelectronic components. Film and bulk piezoelectrics can be used also in microwave MEMS devices. New relaxor-ferroelectric ceramics and crystals exhibit extremely high efficiency of piezoelectric energy conversion, which is of interest, in particular, for medical imaging devices and for other applications, such as special drives for industrial non-destructive testing.

In dielectrics, while electrical field is applied, different electromechanical effects occur: the "free" crystal under the influence of field is deformed, while in the "clamped" crystal elastic stress arises. Physical cause of electro-mechanical effects are the *microscopic displacement of electrical charges* in the applied electrical field because electrical polarization is obviously accompanied by mechanical effect. The dependence of electrically induced mechanical strain on electrical field is determined by the symmetry of dielectric structure. In the dielectrics with centrosymmetric structure sign of their deformation in applied electrical field (compression or tension) is independent on field polarity. This effect is called *electrostriction*, which occurs in all dielectrics without exception. At that, in most dielectrics the mechanical stretching is observed in direction of applied field, however, usually this effect of electrostriction is very small.

In dielectrics with non-centrosymmetric structure a more pronounced effect is observed: the *piezoelectricity*. It is assumed that the reason for this effect is the *intrinsic electrical moment* existing due to structural peculiarities: it is internal interaction of electronic shells of ions or molecules that results in their shift. In the event of piezoelectric effect, if electrical polarity of externally applied electrical field is changed, the sign of electrically induced mechanical deformation reverses. Moreover, in the non-centrosymmetric dielectrics an opposite effect is observed: external mechanical stress causes electrical polarization. Thus, the piezoelectric is capable to convert mechanical energy into the electrical energy, or, conversely, to convert electrical energy into mechanical one. The first of these effects is the direct piezoelectric effect while the second is denoted as the inverse effect.

In case of direct piezoelectric effect under the influence of mechanical stress X (or caused by mechanical stresses elastic deformation of x) non- centrosymmetric dielectrics (piezoelectric) generates electrical polarization, Fig. 4.9, *b, c*. Since electrical conductivity of piezoelectric (which is usually good insulator) is very

small, its polarization expresses in a form of induced electrical charges that appear on the surface of deformed piezoelectric. The density of these charges is described by the polarization *P,* at that, direction of polarization vector is selected from the mark "–" to the mark "+", as it is shown in Fig. 4.9, *b, c*. Polarization is proportional to electrical induction *D*, Fig. 4.9, *g*.

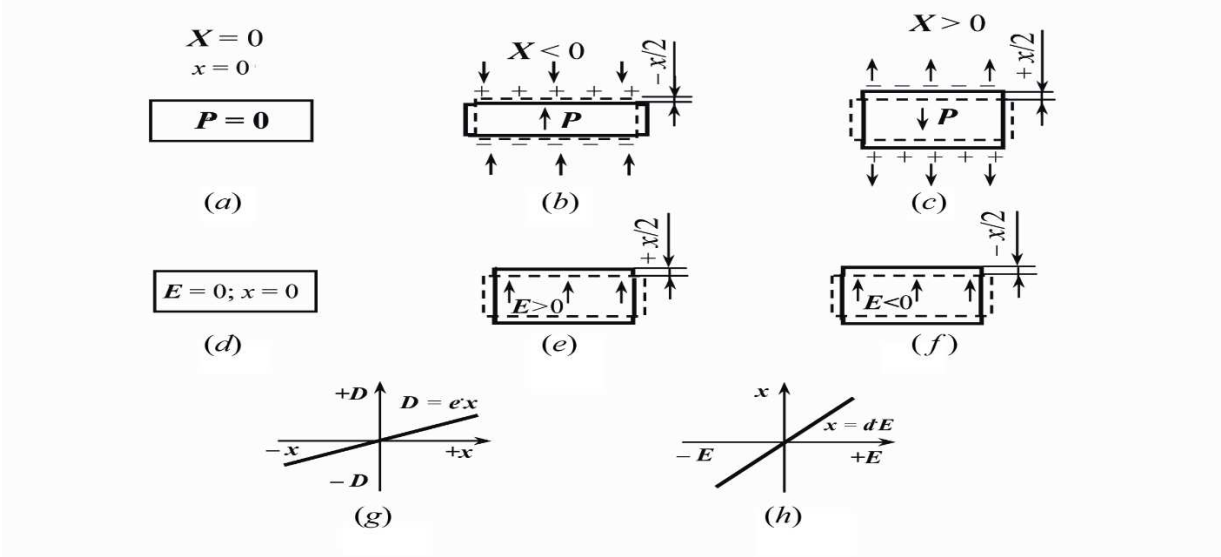

Fig. 4.9. Explanation of direct (*a, b, c, h*) and inverse (*d, g, h, e*) piezoelectric effects

If mechanical stress is not applied ($X = 0$), no free charges on the surface of piezoelectric exist, and, therefore, it is electrically neutral, Fig. 4.9*a*. Piezoelectric becomes polarized as a result of positive (stretching) deformation when $x > 0$ or negative (compression) deformation $x < 0$. While mechanical stress changes its sign of (such as compression is changing to stretching, Fig. 9.3, *b* and *c*), the sign of mechanically induced electrical polarization *P* supersedes. In case of direct piezoelectric effect polarization is directly proportional to strain:

$$P = ex,$$

where parameter *e* is the *piezoelectric strain constant*. Inverse piezoelectric effect occurs, when electrical field deforms the non- centrosymmetric crystal, Fig. 4.9, *i, f*. The sign of electrically induced strain varies with sign of electrical influence, Fig. 4.9, *h*. At that, deformation (strain) linearly varies with electrical field:

$$x = dE,$$

where *d* is *piezoelectric modulus*.

Most simplified explanation of direct piezoelectric effect in the α-quartz (SiO_2) is presented in Fig. 4.10. Generally accepted model of hexagonal quartz structure is the hexagon with positive silicon ions and negative oxygen ions that form a non-centrosymmetric structure. Some manners of hexagon deformation can produce electrical polarization. If deformation is absent, no polarization is observed,

Fig. 4.10*a*. The stretching of a model cell in the horizontal direction induces charges and electrical field, Fig. 4.10*b*; this is *direct longitudinal* piezoelectric effect. At that, the "–" charge dominates on the left side of a cell while the "+" charge appears on the right side of a cell. The upper and lower parts of concerned cell have no generated charges: they remain neutral (no transverse effect).

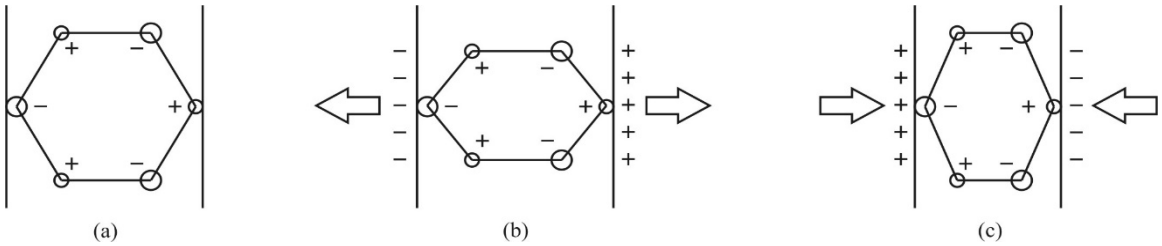

Fig. 4.10. Simplified model of piezoelectric effect in quartz

Similar result might be obtained by the compression of concerned cell in the vertical direction, Fig. 4.10*b*: at that in the vertical direction no longitudinal effect is seen as on upper so on lower parts of a cell. However, due to vertical compression, the *transverse* piezoelectric effect occurs, again on the left and on the right parts of a cell. The point is that horizontal direction of selected cell is the *polar direction*, while the vertical direction is non polar. Figure 9.4, *c* demonstrates that change in a sign of mechanical impact gives rise to the change in piezoelectric polarity, as it should be in case of *linear effects*.

Therefore, the simple model shown in Fig. 4.10 describes the longitudinal piezoelectric modulus, when electrical response has same direction as mechanical influence. In this case the highest value of piezoelectric modulus (d_{max}) is determined. In various directions of quartz crystal modulus d has another value, while piezoelectric response distribution might be rather complicated, Fig. 4.11. From Fig. 4.11 one can see that piezoelectric effect in quartz is absent in the vertical axis of a cell; in Fig. 4.11*a* it is denoted as axis *3* (this three-order axis is quartz is non-polar). Similarly, piezoelectric effect cannot be observed along other three *non-polar* axes that are indicated as *2, 2′* and *2″*).

The highest possible piezoelectric effect is seen along three *polar* axes *1, 1′* and *1″*. The cut of quartz crystal, made perpendicularly to this direction, is the *Curie cut.* Slanting to Curie cut planes shows decreased piezoelectric activity, and its distribution in a plane is described as $d = d_{max} \cdot \cos 3\varphi$, where φ is the plane angle. Spatial distribution of piezoelectric modulus in the polar coordinates is described as $d = d_{max} \cdot \sin^3\theta \cdot \cos 3\varphi$, where θ is azimuth angle. This spatial pattern, shown in Fig. 4.11*b,* looks like almond grains: six surfaces joined in a centre. In *Z*-direction, as

well as in three *Y*-directions piezoelectric effect in quartz does not occur. Through the radius vector directed from the centre of figure as certain angle the size of piezoelectric modulus can be determined in any cut of quartz. It is obvious, that highest possible effect occurs along any of three *X*-axes.

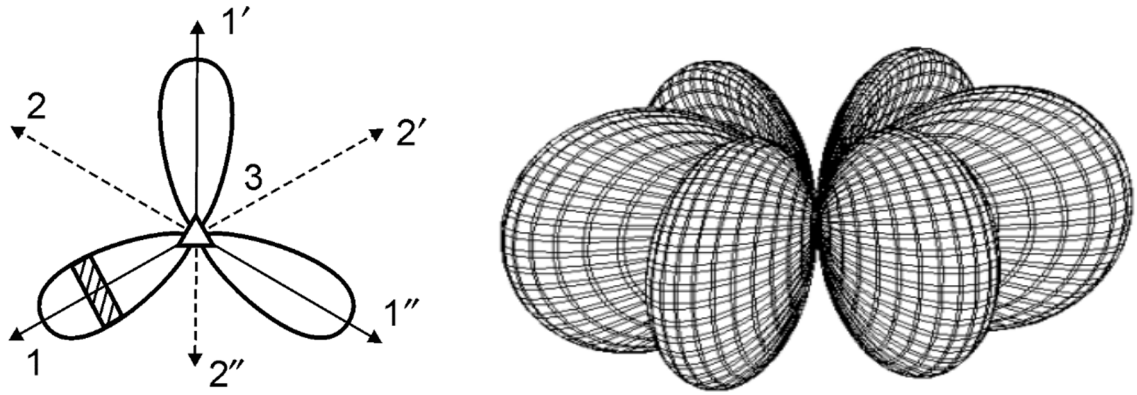

a *b*

Fig. 4.11. Longitudinal piezoelectric modulus of quartz: *a* – planar distribution, Curie cut is shown by strokes [7], *b* – spatial distribution of modulus (guide surface – indicatrix [11])

Typically, in solid state physics mechanical and electrical properties are studied as independent. However, in the piezoelectrics, due to their special structure, electrical and mechanical properties are mutually conditioned. At that, piezoelectricity and electrostriction are the electromechanical effects that are close to each other by their physical nature. The piezoelectric effect refers to special electromechanical properties of certain dielectrics that have polar structure (maximal effect is seen just in polar directions).

Electromechanical parameters of crystals include piezoelectric modules, electromechanical coupling coefficients and piezoelectric *Q*-factors (mechanical and electrical), which indicate energy loss in the piezoelectric transducers. Besides aforementioned parameters, in accordance with one or another technical application of piezoelectric materials, other "quality factors" are applied to compare different piezoelectric materials, in order to select them for certain practical applications.

Therefore, as already noted, internal polarity of non-centre symmetric crystals allows convert mechanical energy into electrical energy (direct piezoelectric effect) or, opposite, convert electrical energy into mechanical one (inverse piezoelectric effect). All these effects are described by different *linear relationships* in dependence on combination of various boundary conditions, under which polar crystals are used or studied.

4.4 Main features of polar crystals

The primary cause of the internal polarity in the non centre symmetric crystals is the asymmetry in electronic density distribution along the inter-atomic bonds. In turn, this feature is conditioned by the adjoining ions distinction in their features of electronic shells, which, in particular, manifests itself as the electronegativity.

The ion with increased electronegativity displaces the shared electrons towards itself, so its operating charge is more negative, while the ion with lower electronegativity acquires, respectively, the increased positive charge.

Together these ions create a polar bond with the inhomogeneous distribution of electron cloud density along the inter-ionic bond. So it might be concluded that the internal polarity, seen in the non centre symmetric crystals, arises due to the structural compensation of different structural features of electron shells of the neighboring ions [3].

For further discussion, it should be noted that the pyroelectrics and piezoelectrics demonstrate amazing proximity in the manifestation of completely different properties. At that, the nature of intrinsic polarity and all the more its existence in the polar-neutral piezoelectric in many respects looks as unclear.

It will suffice to mention that even the diamond (monatomic carbon crystal) occasionally could have a form of pyroelectric wurtzite with symmetry class 6*mm,* in addition to its principal form of *m*3*m* cubic diamond structure [1].

Among various piezoelectrics, some others monatomic crystals exist: the examples are Te and Se crystals, which belong to the piezoelectric structure of quartz-type (32 class of symmetry). In the mentioned examples of the monatomic crystals, undoubtedly, the only a dissymmetry of electronic atomic shells could be responsible for their intrinsic polarity.

The impressive example of pyroelectrics and piezoelectrics affinity is the polymorphism of $\bar{4}3m$ (piezoelectric) and 6*mm* (pyroelectric) structures seen in zinc sulphide crystal, Fig. 4.12. Interatomic interactions provide some relatively stable configuration of 4ZnS type, from which both the sphalerite and wurtzite structures could be built.

In the first case, the polar-neutral structure of the piezoelectric ZnS can be well defined by the 3D octupole (eightfold) electrical moment, and this simulation can be successfully represented by the four [111] type 3-rd order polar axes, which intersect at angle of 109.5° as shown in Fig. 1*a*. Such a neutral three-dimensional polar structure is electrically self-compensated, if crystal is free from mechanical stress.

The second fundamental structure of ZnS crystal is the pyroelectric wurtzite, which can also be described by the octupole arrangement of polar axes, but it additionally has the dipole (1D) polar component, Fig. 1*b*. Despite fundamental difference in the symmetry of two main forms of the zinc blende, the real structural difference is so small that these structures can alternate in one crystal.

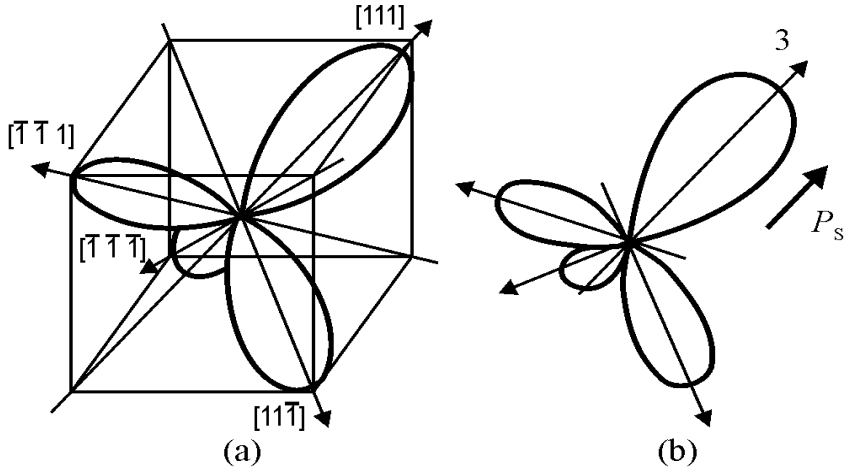

Fig. 4.12. Spatial distribution of positive part of piezoelectric responsibility in 3D polar crystal (only positive direction of [111] axes is shown): *a* – total compensation of polarity in polar-neutral crystal; *b* – appearance of additional dipole component that means polar (pyroelectric) polarization

With a good reason, it can be assumed that the ferroelectrics are a special case of pyroelectrics, having, in contrast to them, the reversibility of polar bonds direction. Thus, there is a lot of experimental evidences of similar manifestation in these polar crystals in their electrical, mechanical and thermal properties.

Therefore, below only the evidences of "hidden" polarity will be presented in the piezoelectric crystals, which are here considered to be the polar-neutral ones.

Firstly, during crystallization process, the density of polar crystals decreases in comparison to their melt: for example, growing GaAs polar crystal swims in its melt as ice in water. So it may be deduced that the fixation of polar bonds expands a material, at that, transforming its structure into the non-centre symmetric one.

Secondly, the chemical properties of polar crystals exhibit the unipolarity of their surface: for instance, the etching of quartz crystal occurs more rapidly on the "positive" end of polar *X*-axis, while the etching is more slow at the "negative" end of *X*-axis. So the etched patterns for quartz plates are very different for "+" and "–" surfaces [6].

In just the same way, in the cubic class polar GaAs crystal, one can see a considerable distinction in the chemical properties between two surfaces of [111]-

plate [3]. By the way, exactly the chemical unipolarity of polar crystal is widely used while ferroelectric domains study [7].

Thirdly, the polar crystals show unique thermal properties: their resistance to a heat transfer far exceeds ones of center symmetric crystals due to peculiarities of phonon dissipation process in the polar structure.

Moreover, in such crystals the thermal expansion coefficient acquires the negative value at low temperatures, instead of showing its classical dependence of $\alpha(T) \sim T^3$. The point is that the nature of inter-ionic attraction essentially changes at a small distance between ions. For the same reason, due to the negative thermal expansion, in some polar crystals their pyroelectric coefficient changes its sign at lower temperatures.

And it goes without saying that the electrical properties of polar and polar-neutral crystals differ significantly from usual dielectrics. In the polar and polar-neutral crystals, their fundamental very high frequency absorption $\varepsilon'' = \varepsilon' \cdot \tan\delta$ vastly superiors this absorption in the center symmetric crystals [8].

Moreover, at microwaves, the dielectric losses $\varepsilon''(\omega)$ of piezoelectrics show an additional maximum of the quasi-Debye type, due to interaction between optical and acoustical phonons. The above mentioned special features of polar crystals correlate with their acoustic phonon spectrum near the Brillouin zone boundary, where acoustic mode has anomaly, bending down at the very border of zone [8].

[***Note:*** parameter γ is pyroelectric coefficient; ζ is volumetric piezoelectric module; d is piezoelectric module; c is elastic stiffness; C is specific heat. For simplicity, this table does not include:
(1) *flexoelectricity,* possible in all dielectrics under non-homogeneous mechanical action;
(2) *actinoelectricity,* which occurs in the piezoelectrics under the grad$T$ action;
(3) *photopolarization* effect in the polar (non-centrosymmetric) dielectrics].

How much polar crystals in their electrical properties differ from non-polar ones can be judged from Table 4.1.

Main property of any dielectrics is their electrical polarization, i.e., the effect of separation of electrical charges, which remain bonded in spite of their shifting. As a result, the electrical moment appears (as product of charges magnitude by their displacement); the volumetric density of this moment is the polarization P. One peculiar feature of polar dielectrics is that electrical polarization in them can occur not only being induced by electrical field, but also by others reasons. A comparison of conventional (non-polar) dielectrics and two categories of polar dielectrics are

shown in Table 4.1. Essential distinction between active (functional) dielectrics and ordinary dielectrics is obvious.

Table 4.I

Electrical polarization *P* as a response on various actions

Actions	**Non-polar crystals**	**Polar-neutral piezoelectrics**	**Polar crystals - pyroelectrics**
Scalar action: Temperature **d***T* Pressure **d***p*	–	_ _	Pyroelectric effect: $\mathbf{d}P = \gamma \mathbf{d}T$ Volume piezoelectric effect: $\mathbf{d}P = \zeta \mathbf{d}T$
Vector action: Electrical field ***E***	$P = \varepsilon_0 \varepsilon E$	Electrically induced polarization $P = \varepsilon_0 \chi E + (e^2/c)E$	Electrically induced polarization $P = \varepsilon_0 \chi E + (e^2/c)E + (\gamma^2 T)E/(\varepsilon_0 C)$
Tensor action Mechanical stress ***X***	–	Direct piezoelectric effect $P = dX$	Direct piezoelectric effect $P = d'X$

In many applications of the polar dielectrics (as sensors, actuators, filters, transformers, motors, etc.), they are subjected to the external thermal, electrical, mechanical and other influences – scalar, vector, or tensor types.

Table 4.1 shows that conventional dielectric electrically reacts only on the electrical field action: $E \Rightarrow P$, while polar piezoelectrics and pyroelectrics, besides their $E \Rightarrow P$ peculiar response, are capable of electric response on other actions: the mechanical $X \Rightarrow P$ and the thermal $dT \Rightarrow dP$. At the same time, the piezoelectric responds to electrical action not only by ordinary polarization ($P = \varepsilon_0 \chi E$), but also produces the electromechanical response: $P' = (e^2/c)E$, while the pyroelectric, in addition, gives even more: the electrothermal response: $P'' = (\gamma^2 T)E/(\varepsilon_0 C)$.

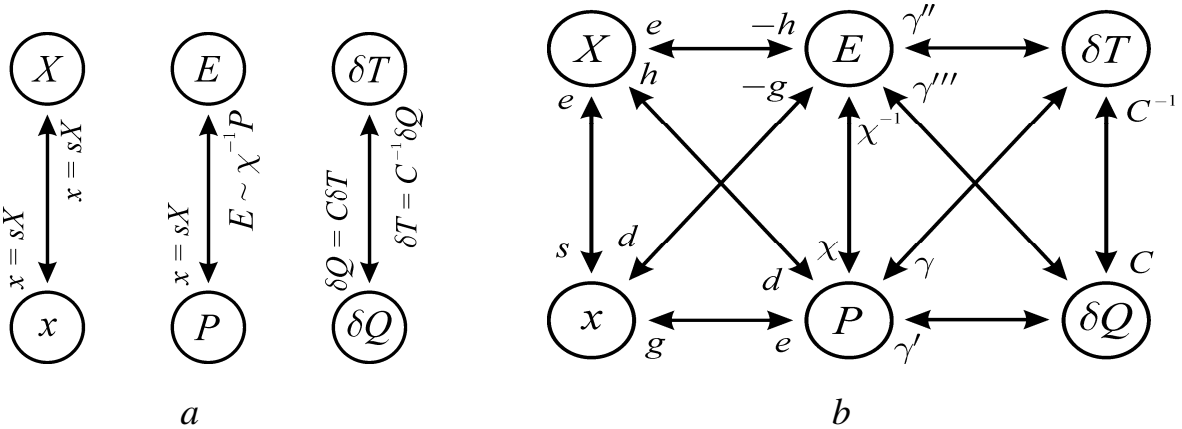

Fig. 4,13. Mechanic, electrical and thermal effects: *a* – in non-polar dielectric; *b* – in polar dielectric.

It might be that most striking features of polar dielectrics is, firstly, the mutual influence of the mechanical, electrical and thermal properties on each other and, secondly, the dependence of these properties from conditions, in which polar crystals are studied or applied. To demonstrate this interdependence, the basic mechanical, electrical and thermal linear effects in the non-polar and polar dielectrics are symbolically compared in Fig. 4.13. It is seen that in the ordinary dielectrics these properties are independent, but in the polar crystals all of them are connected by the quite complex interactions.

Figure 4.13*a* symbolically shows that in usual solid dielectrics their mechanical deformation x (strain) is proportional to applied mechanical stress $x = s \cdot X$, where s is the elastic compliance. Note that this linear relationship can also be written in the reverse direction: $X = c \cdot x$, i.e., the Hooke's law in which c is the elastic stiffness. Similarly, in any dielectric, the electrically induced polarization P is proportional to magnitude of applied electrical field: $P = \varepsilon_0 \chi \cdot E$, where χ is the dielectric susceptibility and ε_0 is the electrical constant in SI. If electrical polarization would be induced *non-electrically*, then another recording of this linear connection will be more convenient: $E = \varepsilon_0^{-1} \xi \cdot P$, where $\xi = \chi^{-1}$ is the dielectric impermeability. The thermal properties are described in Fig. 4.13*a* by proportionality of amount of heat δQ in crystal appeared due to ambient temperature change: $\delta Q = C \cdot \delta T$, where C is the specific heat.

In the polar crystals, their mechanical, electrical and thermal properties are *interdependent*, and the diagram of different properties interaction looks like two squares connecting by one side, Fig. 4.13*b*. This scheme shows how complicated might be description of the non-centrosymmetric (polar) crystals properties. The *piezoelectricity* is symbolically described by left the square in Fig. 4.13*b*. Two horizontal and two crossed-connecting lines with the arrows present eight linear piezoelectric effects that may be observed in the polar crystals at different conditions.

The number of piezoelectric effects equals eight, since this effect can be direct or converse (2), the crystal can be electrically open-circuited or short-circuited (2), as well as the crystal mechanically can be free or clamped (2), so that: $2 \times 2 \times 2 = 8$. These effects are described by four piezoelectric coefficients-modules (d, e, g, h); at that, simplified equations of the direct effects are: $P = d \cdot X$, $P = e \cdot x$, $E = -g \cdot x$, $E_j = -h \cdot X$ and for the converse effect equations are: $x = d \cdot E$, $X = e \cdot E$, $x = g \cdot P$, $X = h \cdot P$. However, all above mentioned four piezoelectric modules can be calculated through

each other and through known elastic constants, for example, in the simplified form: $d_{in} = \varepsilon_0\varepsilon \cdot g = e \cdot s = \varepsilon_0\varepsilon \cdot h \cdot s$, and so on. As can be seen, the description of electromechanical effects in polar crystals (even in the linear case) is not easy task.

In the polar-sensitive crystals, the description of electro-thermal effects is also not simple. The *pyroelectric* effect occurs when a disturbance factor is the thermal action on a crystal while the response has electric nature.

The *electrocaloric* effect is the converse effect: it arises, when the electrical field acts on the pyroelectric, while results is heating or *cooling* of polar crystal. Both these effects are symbolically presented in the right square in Fig. 4.13*b*.

Firstly, two horizontal lines and two crossed-connected lines with the arrows symbolically characterize four options in pyroelectric effect implementation: polar crystal can be electrically open-circuited or short-circuited; besides, pyroelectric effect can occur in two different thermal conditions: the adiabatic when $\delta Q = 0$ or the isothermal when $\delta T = 0$. So pyroelectric effect might be described by *four* equations: $P = \gamma \cdot \delta T$, $P_i = \gamma' \cdot \delta Q$, $E = \gamma'' \cdot \delta T$ and $E = \gamma''' \cdot \delta Q$, in which different pyroelectric coefficients correspond to various boundary conditions.

Secondly, four lines with arrows, shown in the right part of Fig. 2*b*, are used here for symbolical description of electrocaloric effect. As pyroelectric effect, this effect may be described by four different linear relationships (depending on thermal and electrical boundary conditions).

However, this effect under normal conditions (at temperature ~300 K) is as rather weak and not considered here in more detail. (However, recently large electrocaloric effect is discovered, arising when the antiferroelectric is switchrd electrically into the ferroelectric phase that can be considered as possible basis for electrocaloric refrigerator).

Important consequence of these relationships is the dependence of crystal fundamental parameters on thermal, electrical and mechanical processes, passing in the polar crystals at different boundary conditions.

For example, dielectric permittivity of free crystal ε^X (stress $X = 0$) and of clamped crystal ε^x (strain $x = 0$) can differ, at that $\varepsilon^X = \varepsilon^x + e^2/c$ (e is piezoelectric constant and c is the elastic stiffness), Fig. 4.14.

Similarly, the elastic compliance (s) of polar crystals depends on the electrical conditions: in open-circuited crystal the compliance (s^D) is less then it is in closed-circuited crystal (s^E). As seen in Fig. 4.14*a*, the strain $x^D = s^D X = (s^E - d^2/\varepsilon_0\varepsilon)X$, which is confirmed experimentally by example of barium titanate ($BaTiO_3$) in its ferroelectric phase. Above the phase transition this crystal has a centre-symmetrical

structure and, therefore, piezoelectric effect on compliance is absent: $s^E = s^D$, Fig. 4.14*b*.

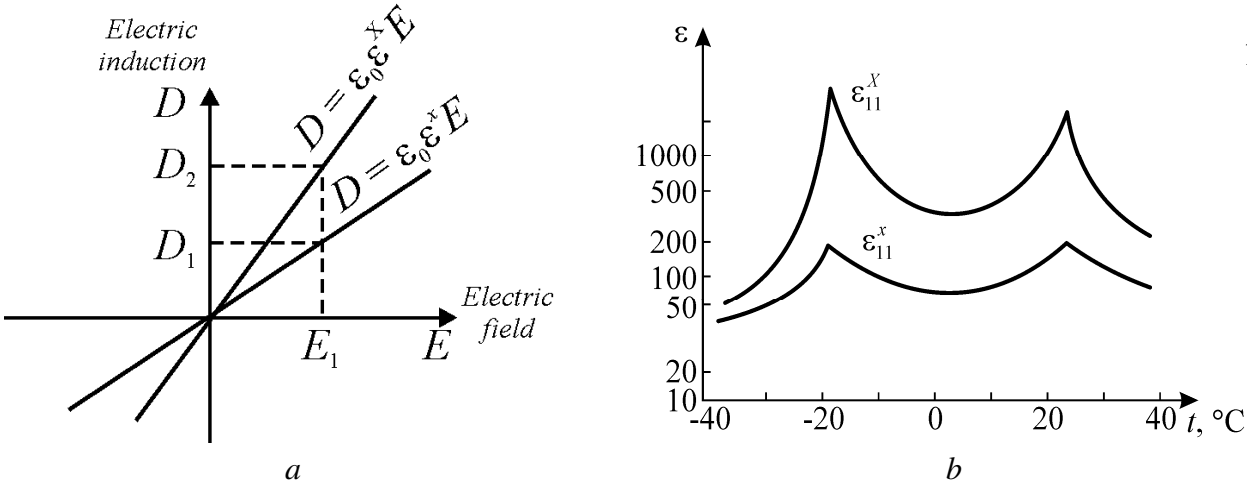

a *b*

Fig. 4.14. Effect of mechanical conditions: *a* – electrical induction *D* dependence on electrical field *E* for free ($X = 0$) and clamped ($x = 0$) piezoelectric; *b* – dielectric permittivity for free (at 10^3 Hz) and clamped (at 10^{10} Hz) Rochelle Salt crystal [3]

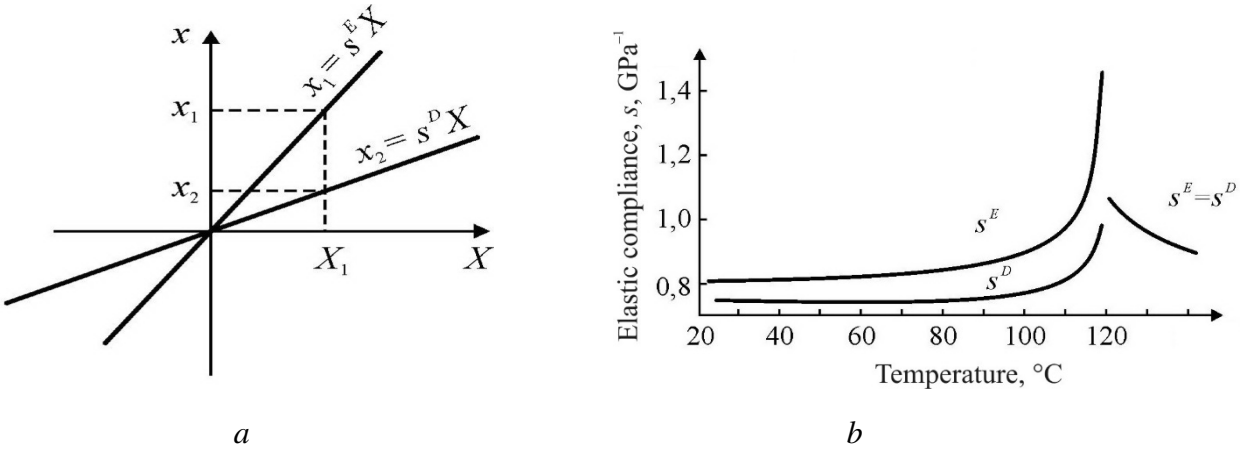

a *b*

Fig. 4.15. Effect of electrical conditions: *a* – elastic compliance in open-circuited (s^D) and in short-circuited (s^E) piezoelectric; *b* – barium titanate elastic compliance

Moreover, when Hooke's law is studied in polar crystal, its elastic stiffness depends on the isothermal (c^T) or adiabatic (c^S) conditions. Even most conservative parameter of a crystal – its heat capacity *C* at normal temperatures – turns out to be dependent on electrical and thermal boundary conditions, in which crystal is studied.

For example, in open-circuited polar crystal its specific heat C^E differs from specific heat C^D of close-circuited crystal. In the same manner, the difference is seen in specific heat of mechanically free (C^X) and mechanically clamped (C^x) polar crystals.

The above-discussed classification, does not exhaust all the possible effects, caused by intrinsic polarity of non-centrosymmetric crystals. These possibilities are shown by highlighted frame in Table 4.2.

Table 4.2.

Polar responses in dielectrics including partial limitations of strain

PIEZOELECTRICITY induced by stress	**COMBINED EFFECTS** at partial clamping	**PYROELECTRICITY** induced by heat
Conventional piezoelectric effect in 20 polar classes (”piezoelectric” classes)	Artificial pyroelectric effect in 10 “piezoelectric" classes	Conventional pyroelectric effect in 10 polar classes (”pyroelectric” classes)
Volumetric piezoelectric effect in 10 ”pyroelectric” classes of polar crystals	Artificial volumetric piezoelectric effect in 10 "piezoelectric" classes	Tertiary pyroelectric effect in 20 classes of polar crystals

The point is that some components of 4-th rank strain tensor can be artificially forbidden in the polar crystals by rigid fastening of their thin polar cut onto non-deformable substrate. As a result, the intrinsic polarity (usually spatially compensated both in the free and clamped piezoelectric crystal) in the partially clamped crystal demonstrates electrical response. This allows, firstly, to measure these components of compensated polarity, and secondly, to obtain both artificial pyroelectric effect and volumetric piezoelectric effect, which are impossible in mechanically free 10 polar-neutral classes of "true" piezoelectrics (non-pyroelectrics), such as, for example, in the quartz.

It is difficult to explain all this multitude of various effects by a simple idea of the spontaneous polarization, so the purpose of this work is to modify the concept of intrinsic polarization peculiar for the non-centre symmetric crystals.

The assumption of spontaneous polarization (P_S) existence in some dielectrics arose a hundred years ago by the analogy with spontaneous magnetization (B_S) of ferromagnetics, when the dielectric hysteresis loop $P(E)$ was discovered in the Rochelle salt crystal, similarly to magnetic hysteresis $B(H)$. The dielectric analogues of *ferro*magnetics began to be called *ferro*electrics, and the polarization, switched in them, was called spontaneous. In fact, however, similarity between ferromagnetism and ferroelectricity is only external and formal. The point is that there are no magnetic charges in a nature, so that magnetism is caused by the closed microscopic electrical currents, which can exist in the equilibrium state for arbitrarily long time (as well as spontaneous magnetization of ferromagnetic). At that, it is important to note that as magnetic field H so magnetic induction B are the axial vectors.

In contrast, both the electrical field E and polarization P are the polar vectors, generated by the existing in nature electrical charges. The electrical field E is gradient of electrical potential, which starts and ends on the electrical charges. The electrical polarization P is induced in dielectric by this field, and, in accordance with Lorentz relation ($E = \beta P$), the polarization should be accompanied by the electrical field E existing inside dielectric. If no external field is applied, the existence of spontaneous polarization (proposed for ferroelectrics on basis of hysteresis loop) is unreasonably transferred to all pyroelectrics, while ferroelectrics is only a subclass of pyroelectrics. Thus, the pyroelectric looks like an electrical analogue of the permanent magnet. However, in their equilibrium state and when absence of external influences, both the pyroelectric and ferroelectric are not surrounded by the external electrical field (as the permanent magnet is surrounded by the magnetic field).

In this regard, one should remember about the electrets, which are really generate the external electrical field (consistent with their internal field) for a considerable time. But there is a fundamental difference between the electrets and pyroelectrics: pyroelectrics are capable to generate the polarization under non-electrical action being in the equilibrium state, naturally acquired in them during crystal formation from liquid or gaseous phase, and disappearing only when crystal melts. At that, the pyroelectric effect can occur in the polar crystal an infinite number of times. On the contrary, the *residual* polarization of electrets is created artificially using special technology: as a result, their polarized state is thermodynamically non-equilibrium and temporary: when the electret is exposed to heat, the depolarization current is generated by it only once, and the electret ceases to be polarized.

It is known also, that to justify the existence of spontaneous polarization in the pyroelectric, the idea about electrical compensating charges was proposed, which can temporary screen P_S. Without involving this compensation mechanism, i.e., if the pyroelectric would be an ideal insulator (which does not create electrical field around itself), then a concept of spontaneous polarization becomes unacceptable (otherwise, the state with P_S should be non-equilibrium). For example, in the well-known pyroelectric lithium sulfate Li_2SO_4-H_2O at temperature 115 K (when conductivity is practically absent) one can see the change in a sign of pyroelectric effect and, hence, the change of polar bonds direction – at that, no evidences are as to surrounding field presents or changing.

Thus, in those pyroelectrics, in which their polarization is not electrically switchable, the P_S presence is only assumed. Peculiar electrical properties of such crystals can be manifested by pyroelectric effect or by volumetric piezoelectric effect, but any correspondent measurement does not allow to determine the value of

intrinsic polarization: only its change with temperature is seen. Therefore, exactly traditionally these responses can be interpreted as the "P_S change" but without measure the P_S value. It should be mentioned that in some theoretical works the doubt is expressed about the truth of PS concept [1, 2], since it is possible to measure only by dynamically arising polar response of pyroelectric or volumetric piezoelectric effects.

Discussing below models, based on the asymmetry in the electronic density distribution along the atomic bonds, is free from any assumption of internal electrical field existence (which would need to compensate the polarity by the free charges). Asymmetric polar-sensitive bond does not a result of any internal field present in a crystal, but it can provide the polar response onto non-electrical homogeneous external impact (thermal, mechanical or irradiation) that is impossible in the centre symmetric crystals. It should be noted, that this not regards to the heterogeneous mechanical impact: in such case, the electrical response occurs in any dielectric, which is the flexoelectricity [6]. By the same way, the heterogeneous temperature influence (characterized by the gradient of temperature) induces in any piezoelectric something like “pyroelectric effect”, the actinoelectricity [6].

4.5 Simplified models of polar bonds connection

Polarity modeling is based on the fact that electrical field can forcedly change the structure of atomic bonds in any crystal, converting dielectric into electrically asymmetric (polar) state by inducing in a dielectric the polar axis. In this case, the inter-atomic bonds willy-nilly acquire an asymmetry, so any dielectric demonstrates the electrically induced piezoelectric and pyroelectric properties. At that, magnitude of these induced effects is strongly dependent on the dielectric permittivity, so that in the relaxor ferroelectrics (having $\varepsilon > 10^4$) these artificially supported by bias field effects can surpass polar electrical effects seen in natural polar crystals [3].

An example of electrically induced piezoelectric effect appearance in the constant electrical bias field E_b on one wing of electrostriction curve is shown in Fig. 4.16*a*. Variable electrical field E' generates practically linear mechanical response: $x' \approx d' \cdot E'$ imitating piezoelectricity with electrically induced module $d' \approx 2Q\varepsilon_0^2\varepsilon^2 E_b$, where Q is the electrostriction parameter [3]. Similarly, in the presence of electrical bias field, the pyroelectric effect can be also induced in any crystal, that also finds some application in the modern thermal sensors, which can exceed in sensitivity of natural pyroelectric effect in the polar crystals.

Based on the above, one can suppose that usual piezoelectric effect also can be represented as the "linearized electrostriction". This assumption might be advanced according to conception that fundamental reason of crystal intrinsic polar-sensitivity is the asymmetry in the electronic density distribution along polar bonds between adjacent ions, which have different electronic structure (manifested in particular in electronegativity) that replaces externally applied field.

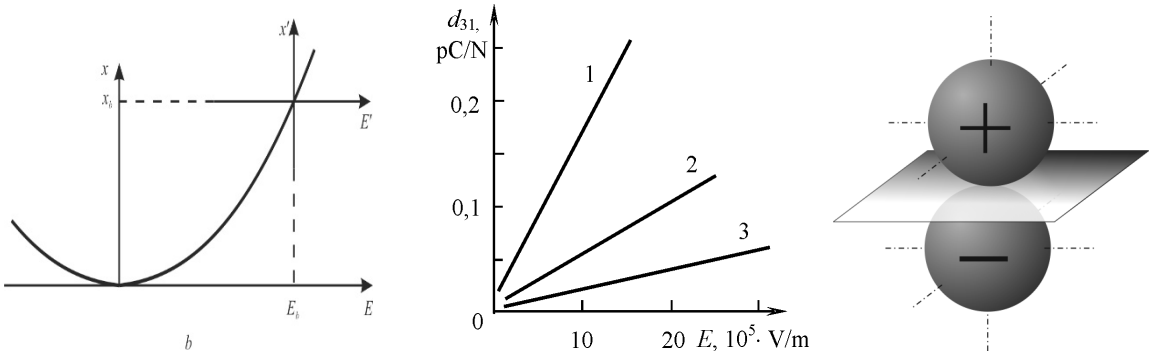

Fig. 4.16. Electrically induced polarity in dielectric: *a* – on parabolic electrostriction curve $x \sim E^2$ in bias field E_b a quasi-linear dependence $x'(E')$ imitates piezoelectric effect; *b* – induced piezoelectric effect in dielectrics $SrTiO_3$ with $\varepsilon = 300$ (*1*); $CaTiO_3$ with $\varepsilon = 150$(*2*); TiO_2 with $\varepsilon = 100$ (*3*); *c* –polar vector indicatrix describing induced piezoelectric or pyroelectric effects

In the extremely simplified form, three linear models of electronic density distribution (covalent, ionic and mixed bonding) are shown in Fig. 4.17, *left*, given as in a normal state so under electrical bias field influence. In the covalent crystal, the electrons are equally distributed around their atoms; at that, the electronic density between atoms is rather big. For further understanding of discussed model, it is important to specify that externally applied field deforms the electronic shells of atoms by the stretching them that leads to electrostriction $x = \Delta l/l \sim E^2$ with relatively free shits of the electronic density clots, Fig. 4.17*b*.

In the ionic crystal, the mutual attraction of cations and anions is compensated by repulsion of partially overlapping electronic shells and by essential deformation of the electronic shells of ions. In contrast to the covalent (atomic) crystals, in which magnetic attraction of spins dominates in the outer shells, in the ionic crystals the outer electronic shells are under the action of electrical field of dissimilar ions, Fig. 6c. In the bias electrical field, the cations and anions are forced to be displaced that gives such a deformation of electronic shells of ions, at which virtual formations of electron pairs become possible. In any case, being in the non-equilibrium polarized state under influence of bias field, both covalent and especially ionic crystals acquire the properties of polar crystals, namely, the ability to show ibduced piezoelectric, pyroelectric, linear electrooptical and others special effects.

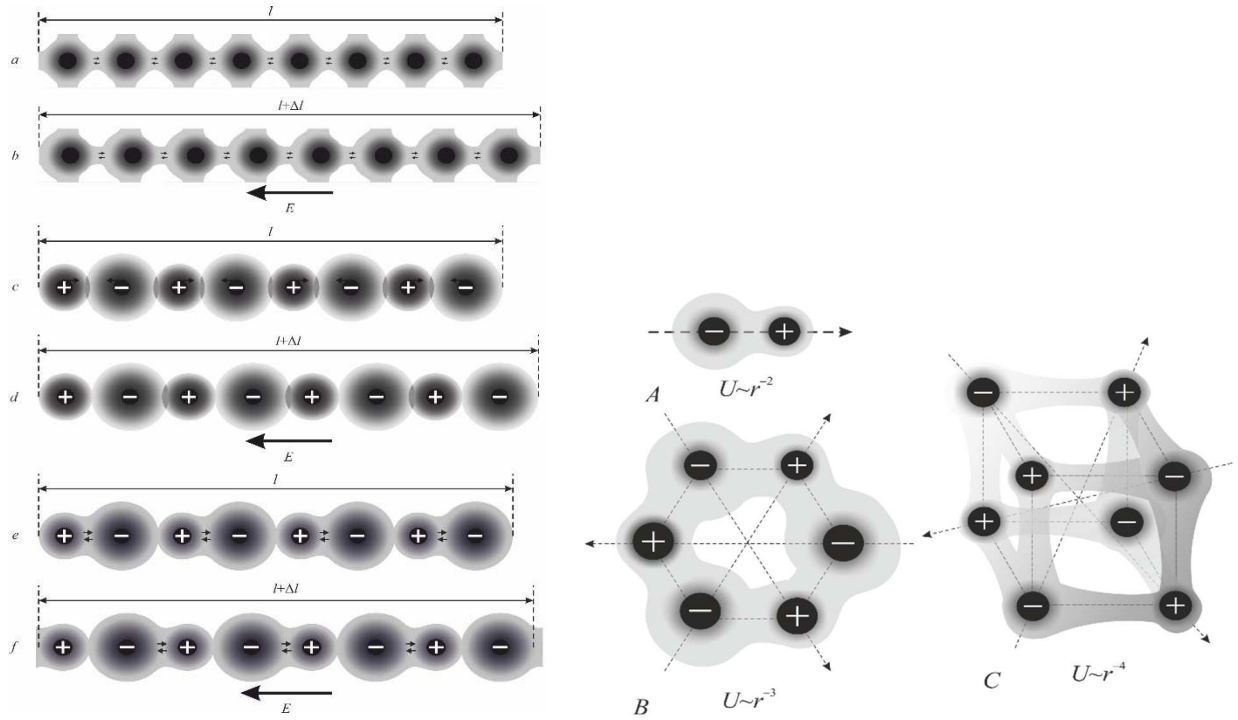

Fig. 4.17. Simple presentation of polar-sensitive structures: on left the covalent (*a*), ionic (*b*) and hybridized (*c*) bonds are shown; on the right: *A* – 1D dipole model; *B* – 2D polarity modeling; *C* – 3D polar construction; polar directions are shown by arrows, and specified rate of energy decrease with distance $U(r)$ are shown by power functions

The mixed covalent-ionic bonding, shown in Fig. 4.17*e*, is a distinctive feature of model under discussion creating main property of polar crystals such as piezoelectric and pyroelectric effects without external electrical field application. In this way, instead of external electrical field, which need to be connected to ionic or covalent crystals and forcing them to be in the polarized but non-equilibrium state (as shown in Fig. 1.10*b,d*), in the case of mixed covalent-ionic bonds in a crystal its polar-sensitive state is stable without any bias field application. Polar state is ensured by fundamental properties of given ions: their peculiar electronic shells accompanied, in particular, by different electronegativity. Thus, main point of model under discussion is that exactly the mixed covalent-ionic bonding, Fig. 4.17*e* guarantee the piezoelectric and pyroelectric properties without bias electrical field application to a crystal. In this way, instead of a bias field, which need to be applied to the simple ionic or covalent crystal and forcing it to be in polarized but non-equilibrium state (as shown in Fig. 4.17*b,d*), in the case of mixed covalent-ionic bonds, the polar-sensitive state of a crystal is stable without any external field.

In the polar crystal its state: “able to polarization by non-electrical way” is entirely equilibrium state at certain temperature (T_1) and pressure (p_1), and it is stored in absence of external influences as much as one wants. If any external acting on

polar crystal occurs (changing in temperature, mechanical stress, etc.), then a new stable state arises, already at T_2 and p_2. At that, the change in a state ($T_1 \rightarrow T_2$ or $p_1 \rightarrow p_1$) is accompanied by dynamic appearance of surface electrical charges (in other words, thermally or mechanically induced polarization arises), i.e., pyroelectric or piezoelectric effect becomes apparent.

The simplified model shown in Fig. 4.17*e* corresponds to the linear pyroelectric crystal, in which internal polar-sensitive bonds are “persistant”, but they can be deformed as by temperature change (giving pyroelectric effect) so by mechanical stress (giving piezoelectric effect).

Such intrinsic polar-sensitivity in the linear pyroelectric usually is conserved up to crystal melting. Under the action of external *electrical* field, in such pyroelectric only linear polarization (as in any dielectric) arises with the value of permittivity typical for ordinary ionic crystals.

However, in the case of ferroelectric (“non-linear” pyroelectric), which can be imagined by the *combined* Fig. 4.17*e* and Fig. 4.17*f*, its intrinsic polar-sensitive bonding is rather "gentle", i.e., not sufficiently stable and can change own orientation to the opposite in the applied electrical field, demonstrating the hysteresis loop and large dielectric permittivity.

Increase of temperature can violate the correlation between neighboring polar-sensitive bonds that leads to the phase transition into the non-polar phase at the Curie point. Similarly, the increase of hydrostatic pressure also destroys in ferroelectric its weakly-stable ordering of the polar-sensitive bonds that leads to the transition into disordered phase.

The polar-sensitive compound of ions is also based on the asymmetry in electronic density distribution between ions, and in the left side of Fig. 4.17 represents the one-dimensional (1D) model, which on the right side of this figure is extended to 2D and 3D non-centre symmetric distribution of the polar bonds.

Thus, the right side of Fig. 6 describes a simplified way of spatial orientation of asymmetric hybridized ionic-covalent bonds. One-, two- and three-dimensional arrangement of the polar bonds in a space can explain various properties of polar and polar neutral crystals. Proposed polar models may coexists in a different combination, for example in $LiNbO_3$ crystal the 1D and 3D polar models, as shown in Fig. 4.12*b*.

Presented models of the self-establishing of crystals polarity interprets the ability of polar crystal to generate electrical response onto dynamic uniform influences. If the external influence, after its emerging (or changing), next remains

constant, then changed polarization subsequently no manifests itself, since the new equilibrium state has already been established.

The dynamics of the polarization are regulating by the natural thermal motion; in this case, the temperature dependence of electrical response of polar-sensitive bonds can be described by the generalized law: $M_{ijk}(T) \sim (\theta - T)^n$, in which the components of electrical moment, which is the 3-rd rank tensor M_{ijk}, vanish at $T = \theta$, if the polar crystal does not melt earlier.

In the case of a spatial (3D) arrangement of polar bonds, the critical exponent is $n = 2$, but if the polar bonds are arranged in a plane (2D case), then $n = 1$ and M_{ij} is 2-nd rank tensor. For polar bonding of dipole type (1D), the M_i is 1-st rank tensor and index $n = 0.5$: note that it is the critical Landau index, traditionally used to describe $M_i(T)$ critical dependence, i.e., like $P_S(T)$ in the ferroelectrics.

As well known, the ferroelectrics in applied electrical field demonstrate the reorientation of their polar-sensitive bonds with a nonlinear response; sometime this was served as a basis for introducing spontaneous polarization concept.

Shown in Fig. 4.18, *a, b* two opposite positions of the polar bonds orientation are quite stable, that is confirmed by coercive field E_C measured along hyteresis loop investigation. This two-position steadiness is used in devices for long-term ferroelectric memories. The switching of two orientations of the polar-sensitive bonds occurs, if the applied field exceeds the coercive field, Fig. 4.18*c*.

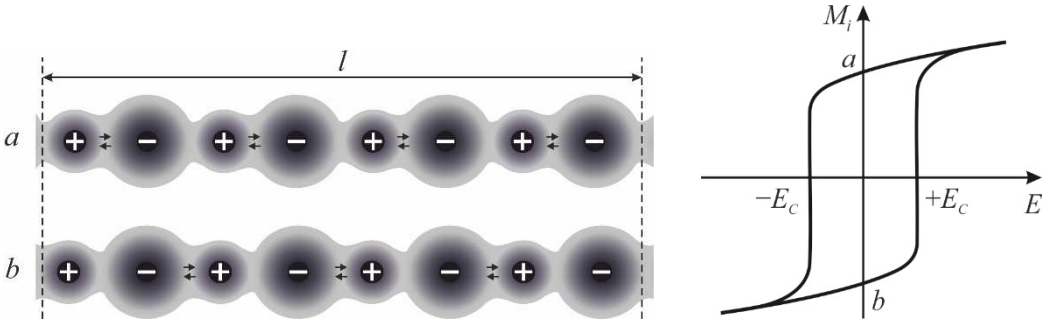

Fig. 4.18. Model description of two opposite orientations of polar bonds in ferroelectric; directions *a* and *b* are indicated on dielectric hysteresis loop

Above modeling makes it possible also to describe the peculiar features of antiferroelectrics, Fig. 4.19, which in the strong electrical field can be reversibly transformed into the polar state. The stability of the antipolar state is characterized by the magnitude of electrical switching field. A notable feature of the antiferroelectrics is a decrease in their volume during the phase transition to antipolar state (on the contrary, volume of ferroelectrics in their polar state increases). Thus, the applied electrical field, converting the antiferroelectic into the ferroelectric,

significantly changes the volume of a matter, which is used to obtain very large electromechanical and electrocaloric effects.

In general case, when phase transition is forced by external electrical field from the paraelectric phase to ferroelectric phase, the jump in volume leads to the change in temperature (this is clearly seen from relationship $PV = RT$: at constant P the change in V changes the T).

Usually this electrocaloric effect produces temperature change of 1-2 degrees, and this is not enough to be used in technology. However, electrically controlled volume jump when antiferroelectric⇔ferroelectric transition at least doubles this temperature jump. Such an electrocaloric effect in terms of technical application look as expedient [9].

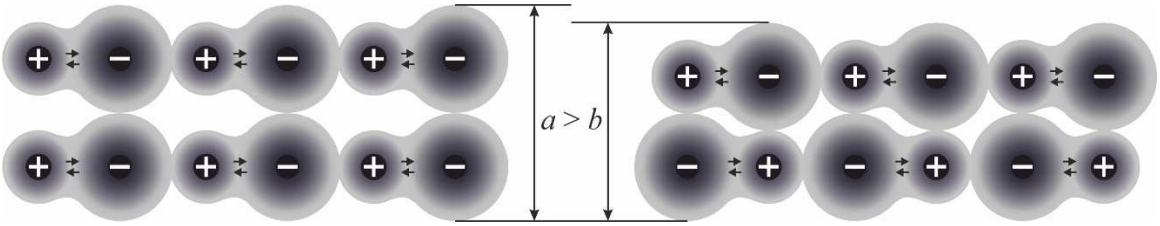

Fig. 4.19. Comparison of polar ordering (*a*) lattice with antipolar ordering (*b*): it is seen that $a > b$

The polar-sensitive arrangement of internal polarization explains also a number of other features seen in polar crystals:

- the structural proximity of piezoelectrics and pyroelectrics;
- the chemical anisotropy of polar crystals;
- the frequency dependence of polar crystals permittivity;
- the microwave absorption in polar dielectrics;
- the possibility of electric control of thermal and elastic properties;
- the heat capacity increase due to polar-sensitivity fluctuation;
- the negative thermal expansion coefficient at low temperatures;
- the reduced thermal conductivity due to polar-sensitive bonds;
- the effect of polar bonds on the electrical conductivity;
- the action of polar bonds on the dielectric losses in microwave dielectrics [8].

4.6 Experimental evidences of polar-sensitivity

The existence polar-sensitivity in non-centre symmetric crystals is confirmed by various experiments. Some of them were already mentioned above. Next, some

methods and results of experimental determining of compensated components of the polarity in case of 2D and 3D spatial arrangement will be shown.

1. In the case of well studied 1D oriented (dipole type) polar bonds, the pyroelectric effect is described by the pyroelectric coefficient γ_i, which is a material vector (tensor of first rank): $\gamma(\varphi) = dM_i/dT = \gamma_{imax} \cdot \cos\varphi$, where φ is angle between polar direction and slanting cut of crystal where pyroelectric effect is studied, Fig. 4.20*a*.

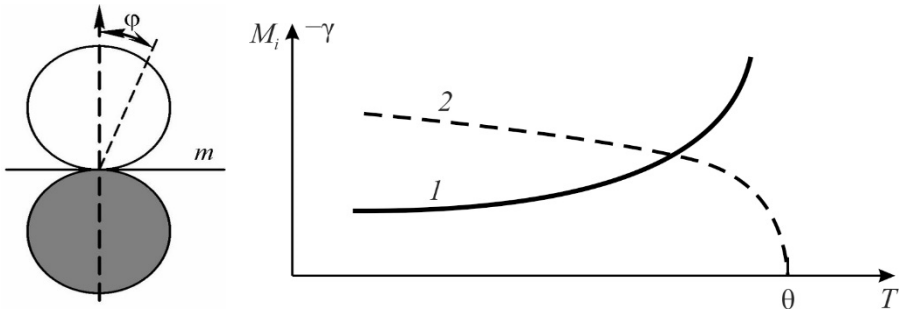

a *b*

Fig. 4.20. "Soft" pyroelectric characteristics in 1D polar structures: *a* – section of indicatory surface; *b* – pyroelectric coefficient (*1*) and internal polarity moment (*2*)

The indicatory surface in this case consists of two spheres located above and below symmetry plane *m*, while γ_i is maximal in both forward and reverse directions of internal polarity. In shown case, pyroelectric effect, seen in Fig. 4.20*b,* corresponds to typical ferroelectrics (which could be called as "soft" pyroelectrics), when the coefficient γ_i near Curie point first increases sharply and then breaks off at the Curie point $T = \theta$. In this case, the internal polarity M_i, shown by *curve 2* in Fig. 4.20*b*, can be measured independently using the hysteresis loop seen below phase transition. In this case, the so called primary pyroelectric effect dominates, at which the degree of polar bonds self-ordering competes with the intensity of chaotic thermal motion. At the Curie point, the dynamic equilibrium, which keeps polar bonds in agreed orientation, gradually suppresses by the thermal motion and disappears at $T = \theta$ along with the primary pyroelectric effect.

However, in the so-called "hard pyroelectrics", the more stable retention in polar bonds 1D orientation usualy persists until crystal melting, and cannot change its direction even in very strong electrical field. In a such pyroekectric, the secondary pyroelectric effect usually dominates, produced by the piezoelectric conversion of thermal strain. At that, the proportionality of electrical moment changing ΔM_i to the temperature increment ΔT is a result of thermal deformation Δl dependence on temperature: $\Delta l \sim \alpha \Delta T$, where α is the coefficient of thermal expansion. In turn, the mechanically induced electrical moment ΔM_i is a result of direct piezoelectric effect:

$\Delta M_i \sim e\Delta l/l$, where e is piezoelectric strain constant. Thus, the secondary pyroelectric effect can be described as: $\Delta M_i = \gamma^{(2)}\Delta T$, where $\gamma^{(2)} = e\alpha$ is the secondary pyroelectric coefficient, and $\gamma^{(2)}(T)$ dependence follows temperature dependence of $\alpha(T)$, which in the polar crystals at low temperatures is firstly a negative value but than changes to the law $\gamma^{(2)} \sim \alpha \sim T^3$.

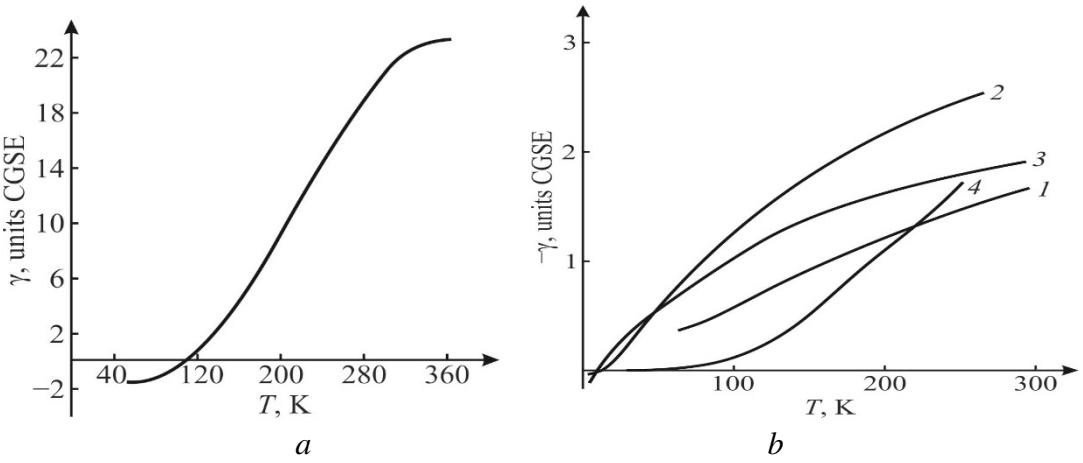

Fig. 4.21. "Hard" pyroelectrics charateristics: *a* – lithium sulfate crystal, Li_2SO_4-H_2O; *b* – tourmaline, $NaMg[Al_3B_3{\cdot}SiO_2(OOH)_{30}]$ (*1*), ZnO (*2*), CdS (*3*), BeO (*4*) [7]

The examples of $\gamma^{(2)}(T)$ dependences in the pyroelectric crystals are shown in Fig. 4.21 (note, that due to small permittivity and high stability, lithium sulfate has technical applications as thermal sensor). Note that from "spontaneous" polarization concept it is difficult to understand its negative value. The fact is that at low temperatures the pyroelectric coefficient decreases significantly down to the negative values (somewhat different $\gamma^{(2)}(T)$ dependence in BeO crystal is due to its large Debye temperature).

The energy of 1D dipole-to-dipole interaction decreases rather slowly with a distance (as r^{-2}, Fig. 4.17*a*). This has a significant effect on the polar-sensitive structure ordering, which becomes destroyed with temperature rise due to the chaotic thermal movement in crystal lattice. In shown cases, the ordering of 1D polar bonds looks relatively stable, since it is more resistant to the 3D thermal fluctuations. Therefore, many pyroelectrics (which are not ferroelectrics) can maintain their polar sensitivity until crystal melts. However, if the chaotic 3D type disordering yet can overcome the sustainability of self-ordered quasi-one-dimensional system (the case of ferroelectric, Fig. 9*b*), then its collapse occurs rather rapidly (critically), which leads to the phase transition into the disordered non-polar phase. Gradual disappearance of internal polarity moment M_i (first rank tensor) obeys the Landau law with a critical Landau index "0.5": $M_i \sim (\theta - T)^{0.5}$.

2. In addition to pyroelectric (polar crystals), the polar-neutral crystals (piezoeletrics) are also of great importance, which can be conditionally attributed to so-called "veritable" piezoelectrics (not pyroelectrics). In this case, a more complex distribution of polar sensitivity can be modeled by both planar (2D) and bulk (3D) arrangement of interatomic polar bonds, borrowed in Fig. 6,B,C from real crystals structures of quartz and sphalerite. Polar-neutral crystals electrical response onto external influences can be described by the tensors of second and third ranks. In contrast to 1D dipole-type structure, the 2D and 3D electrical moments, describing the arrangement of polar bonds in Fig. 6,B,C, are completely self-compensated. In these cases, any scalar action (i.e., hydrostatic pressure or uniform heating of a crystal) does not cause any vector-type response (electrical voltage or current) in such crystals, if they are mechanically fully free or fully clamped. Of course, the vector action in the form of electrical field applying immediately indicates that these crystals are polar ones, leading to the linear response in form of inverse piezoelectric effect (the non-polar crystal is only capable of the quadratic electrostriction effect).

In order to reveal the "hidden" polarity in a strain-free polar-neutral crystal without application of external electrical field, either vector or directed tensor actions are necessary. The external influences of a vector type might be temperature gradient (*grad T*), while the second rank tensor can act as directed mechanical stress. Both of them allow to get the electrical response from the polar-neutral crystal: these are the tertiary pyroelectric effect or the direct piezoelectric effect, see Table 2. However, these responses only indirectly can judge about the value of compensated polarity in the polar-neutral crystal. The fact is that, according to Curie principle, the symmetry of a response contains not only symmetry of crystal, but also symmetry of impact.

Nevertheless, there is a way (and it is used below) to measure the intrinsic polarity using the scalar influence: uniform change in temperature or pressure, providing in conditions when the compensation of a polarity is violated: the methods of partial limitation of thermal strain or piezoelectric strain. In the first case, the polar-neutral crystals show the artificial pyroelectric effect, observed for the first time in the quartz crystal plate stuck to a non-deformable substrate [3], and, in the second case, the volumetric piezoelectric effect in the polar cut of quartz crystal stuck on a rigid (steel) substrate. Thermodynamic calculations of thermo-mechanically induced pyroelectric effect, as well as the measurement technique of partial clamping method are described in detail in [10]. At that, in any piezoelectric the artificial pyroelectric effect can be obtained, which might have interest also for practical applications. Comparing the magnitude of mechanically induced

pyroelectric effect with the ordinary pyroelectric effect can be made by the example of polar lithium niobate crystal. In it, in addition to pyroelectric polar axis, there are also three polar-neutral axes like it is shown in Fig. 4.12*b*. The thin plates of $LiNbO_3$ crystal, being cut perpendicularly to these axes and next stuck onto silica glass substrate (n which $\alpha \approx 0$ to prevent any planar thermal deformation) makes it possible to get the artificial pyroelectric effect with the pyroelectric coefficient $\gamma^*_2 = 40\ \mu C \cdot m^{-2} \cdot K^{-1}$ that only a slightly inferior to usual pyroelectric coefficient of $LiNbO_3$ $\gamma_3 = 50\ \mu C \cdot m^{-2} \cdot K^{-1}$ [10].

The following shows how the thermo-mechanically induced pyroelectric effect is applied to study compensated polarity in 10 classes "veritable" piezoelectrics.

3. Quasi-two-dimensional (2D) system of self-compensated polar-neutral bonds is a characteristic of such piezoelectrics as quartz (SiO_2) and other crystals of the 32 symmetry: berlinite ($AlPO_4$), cinnabar (HgS) and tellurium (Te). In the polar coordinates, the distribution of internal polar-sensitivity in these crystals can be described as $M_{ij}(\beta,\varphi) = M_{max}\sin^3\theta\cos 3\varphi$, Fig. 4.22*a*, where β is the azimuth angle and φ is the in-plane angle. By the radius vector, directed from center of shown figure, one can determine the magnitude of polar-sensitivity response in any slanting cut of quartz-type crystals. In particular, the maxims of piezoelectric effect are seen along any one of three polar-neutral axes of *X*-type. At that, no piezoelectric effect is possible in the *Y* and *Z* axes directions.

Since these crystals have the α-β phase transition at temperature $T = \theta$, it is possible to calculate for them components of latent polarity response tensor $M_{ij}(T)$, which vanishes at phase transition, Fig. 4.22*b*. For this it is used excited in these crystals the artificial pyroelectric response to the homogeneous thermal effect under conditions of partial limitation of the thermal deformation [10]. In the case of 2D distribution of polar-neutral bonds, the energy of their interaction decreases with distance faster than for 1D dipole-to-dipole interaction: $U \sim r^{-3}$, Fig. 4.17*b*. Therefore, the 2D intrinsic polarity can be more easily destroyed by the 3D thermal fluctuations than 1D polarity: this follows from comparison of inclined straight line *1* in Fig. 4.22*b* with the falling dotted line *2* in Fig. 4.20*b*.

The component of electrical response moment: $M_{[100]} = \Delta M_1 = \int \gamma_1 dT$, calculated from the experimental data of $\gamma_1(T)$, decreases linearly with temperature rise: $\Delta M_1 \sim (\theta - T)$, that is, with a critical index of $n = 1$ (note that same dependence is observed early in the improper ferroelectrics [2], in which their polarity also relates to the piezoelectric effect). The artificial "pyroelectric" coefficient $\gamma_1(T)$,

obtained by the method of partially limiting thermal deformations, disappears at α-β phase transition (in quartz crystal θ = 850 K). Note that crystals of quartz symmetry remain the piezoelectrics up to the next β-γtransition when they become the non-polar ones.

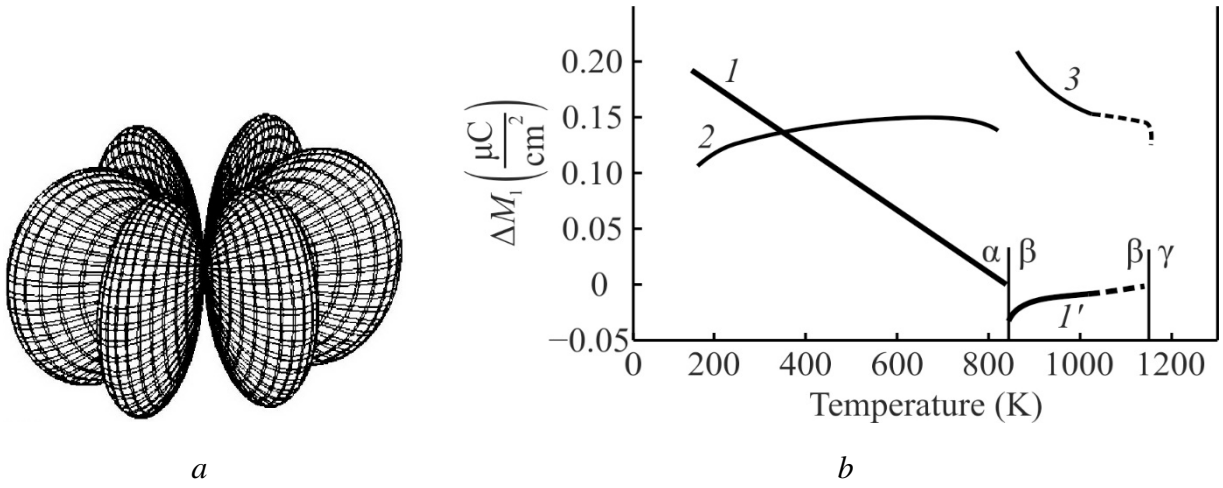

a *b*

Fig. 4.22. Internal polar-sensitivity in 2D structure (quartz): *a* – indicatory surface; *b* – temperature dependence: *1* – M_1 found in [100]-cut plate in α-quartz; *1′* – M_1 found in [110] rod in β-quartz; *2* – measured artificial pyroelectric coefficient in [100]-thin cut at partial limitation of strain, *3* – piezoelectric module d_{14}

4. Spatially distributed (3D) polar sensitivity occurs in many polar-neutral piezoelectric crystals. With temperature increase, in some crystals there phase transition to the non polar state can occur earlier than crystal melting. In this case, the components of the 3D response tensor can be measured by mentioned above method of partial limitation of thermal deformation. One of this case is shown below for the piezoelectric KDP = KH_2PO_4 studied in the paraelectric phase. At that, the third-rank tensor $M_{ijk} = M_{111}\sin\beta\cdot\sin2\beta\cdot\cos2\varphi$ is described by the indicatrix, shown in Fig. 4.23*a,* which corresponds to Fig. 6C. It is appropriate to note that same octupole type distribution of polar bonds takes place in many polar semiconductors, such as gallium arsenide.

Some properties of the KDP crystal in temperature range above ferroelectric phase transition are shown in Fig. 4.23*b*, where this crystal is the polar-neutral piezoelectric of 422 symmetry class. It is noteworthy that internal polar sensitivity decreases in this case very gradually and next vanishes: $M_{ijk} \sim (\theta - T)^2$, i.e., with the critical index n = 2. At that, crystals of the KDP type in paraelectric phase are characterized by the high-temperature phase transition, at which 422 polar symmetry class changes its symmetry to the non-polar one. Investigations are provided at the microwaves in a waveguide, because at lower frequencies large proton conductivity

of KDP crystal hinders any dielectric measurements. As shown in Fig. 4.23*b*, first it is seen smooth decrease of permittivity $\varepsilon_1(T)$, but then it falls down at temperature $\theta \approx 480$ K due to high-temperature phase transition. The presence of this transition we confirmed by measuring of thermal expansion coefficient, which has deep minimum at indicated temperature [11].

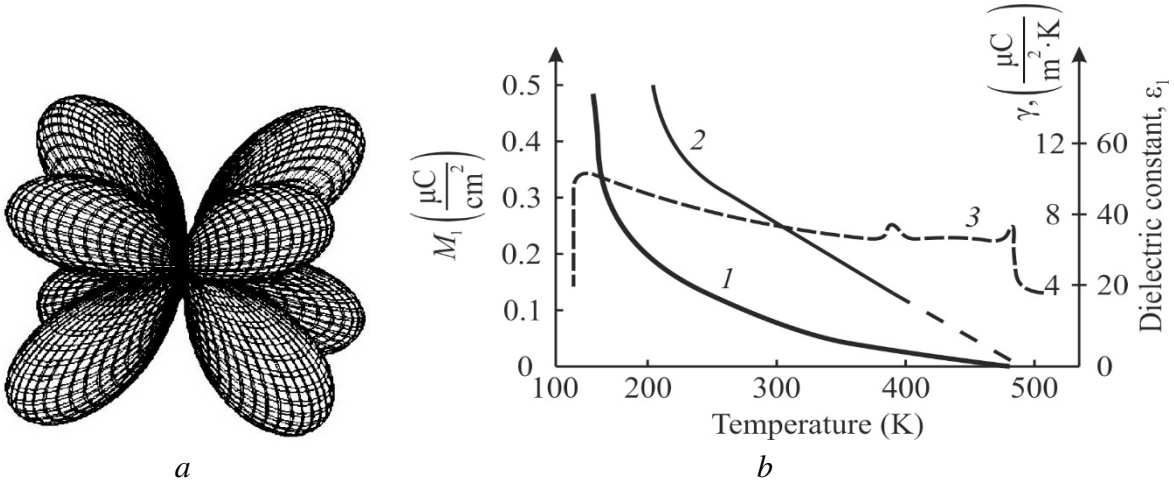

a *b*

Fig. 4.23. Intrinsic polarity in paraelectric phase of KDP crystal: *a* – indicatory surface; *b* – some characteristics of crystal: *1* – moment $|M| \sim (\theta - T)^2$; *2* – artificial pyroelectric coefficient γ; *3* – permittivity ε_1 measured at microwaves

Attention might be drawn to a very rapid destruction of the mutual influence of ordering polar bonds on each other in case of their three-dimensional arrangement. The energy of correlation between such polar bonds decreases with distance rather quickly ($U \sim r^{-4}$) that indicates a weakened stability of 3D-ordering in polar-neutral bonds, which is much easier to be destroyed by the same 3D-character of thermal fluctuations. The 2D model of the interaction of polar bonds is more stable to the thermal 3D chaotic motion, while the 1D model is the most stable, Fig. 4.24.

Thus, in order to confirm experimentally the proposed model of two- and three-dimensional arrangement of polar bonds in the polar-neutral piezoelectrics (non-pyroelectric) crystals, the thermo-mechanically induced pyroelectricity is investigated. In addition, this effect could also be of practical importance; therefore, some of results of our research on the artificial pyroelectric effect in the "veritable" piezoelectrics are given below.

5. A conception of the artificial pyroelectric effect (APE) is introduced as an effect induced by the homogeneous heating of non-central symmetric crystal in its polar cut, when the part of thermal strain is artificially restricted. The normal pyroelectric effect is defined as the change of internal polarization in the electrically ($E = 0$) and mechanically ($X = 0$) free crystal in case of uniform change in crystal

temperature. This pyroelectric effect consists of primary and secondary parts: $\gamma_i^{X,E} = \gamma_i^{(1)} + \gamma_i^{(2)}$. Contribution of primary effect is determined when study of completely clamped crystal which has no strain ($x_n = 0$), i.e., $\gamma^{(1)} = \gamma_i^x$ while the contribution of secondary effect corresponds to the difference of coefficients: $\gamma_i^{(2)} = \gamma_i^{X,E} - \gamma_i^x$.

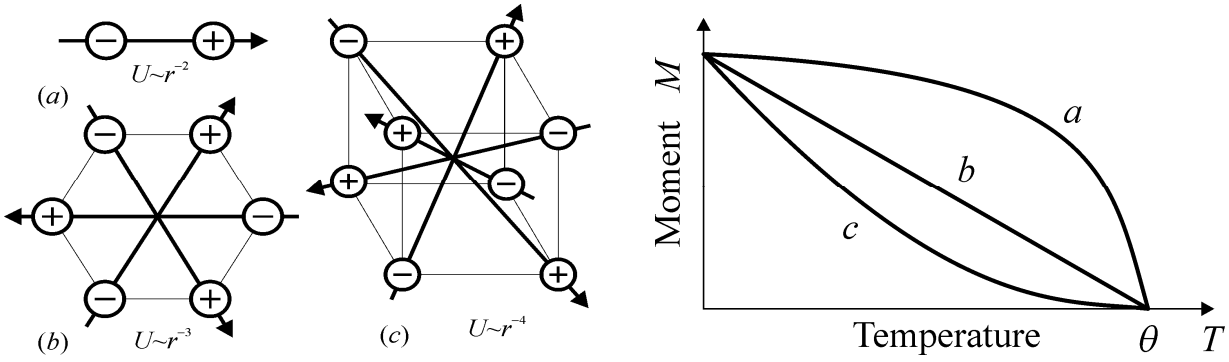

Fig. 4.24. Modeled 1D (*a*), 2D (*b*) and 3D (*c*) polarity and correspondent temperature dependence of generalized electrical moment components

In the piezoelectric materials, the thermoelectric response might be obtained either under inhomogeneous influence (temperature gradient over a sample) or in the case of inhomogeneous boundary conditions. In the first case, the polar response produced by temperature gradient in early studies called as actinoelectricity [6] but later it was identified as the tertiary pyroelectricity, see Table 2. Tertiary effect is defined as the temperature variation of the polarization induced by thermal stress:

$$dP_i = d_{im}{}^T c_{mn}{}^{X,E} \cdot (x_n - \alpha_n{}^{X,E} dT).$$

The second case, a boundary conditions heterogeneity, is precisely the subject of this study. When artificial pyroelectric effect implementation, the polar response is obtained under the *uniform* thermal excitation of a piezoelectric (when *grad T* = 0), but such conditions are created which excludes the part of possible thermal strains. In this case, the permissible thermal strain induces the piezoelectric polarization, and due to a partial clamping of crystal it is compensated. At that, the state of a crystal is same at all his points, but it is uniformly stressed. In the experiment, limitation of thermal strain can be implemented in different ways: by the artificial fixing of piezoelectric thin plate on a rigid substrate or by natural limitation of the radial strain of thin disk studying effect above the frequency of electromechanical resonance. Both of these methods were used in our APE studies [12,13]; the calculations and techniques presented below can be useful for the modern direction of controlling the polarity of thin ferroelectric films [14].

Thus, the artificial pyroelectric effect is defined as the induced by mechanical stress polarization in the electrically free, but mechanically partially clamped piezoelectric under the uniform thermal exposition. Partial clamping is provided by

the inhomogeneous boundary conditions, which anisotropically limit thermal part of strain of a non-central symmetric crystal, so it is homogeneously but anisotropically stressed. Artificial pyroelectric effect manifests itself maximally in the direction of any polar-neutral axes of a piezoelectric crystal.

This axis, under the influence of stress, is transformed into a peculiar polar axis in accordance with Curie principle. Correspondent equations are found that allows to determine the APE-coefficient (that is similar to the pyroelectric coefficient) for various classes of non-central symmetric crystals using components of piezoelectric tensor, elastic compliance and thermal expansion coefficient [10]. Effective pyroelectric coefficient, which characterizes APE, depends on the elastic and thermal properties of a crystal, as well as on the experimental method of thermal deformations limiting:

$$\gamma^*_{APE} = \gamma_k^{Xk,E} = d_{km}{}^T \lambda^*_m,$$

where λ^*_m is thermo-elastic coefficient of the partially clamped crystal. Index at the APE coefficient ($\gamma_k^{Xk,E}$) indicates that only a part of elastic stress tensor components X_k are zero. The partial clamping turns the piezoelectric into the artificial pyroelectric with coefficient $\gamma^*_{APE} = 10^{-6}–10^{-4}$ C·m^{-2}·K^{-1}, which magnitude is comparable to $\gamma_i^{X,E}$ of usual pyroelectrics.

The artificially obtained pyroelectric effect is highly desirable to compare with others long-studied thermo-polarization effects. It may seem that APE would be classified as the "secondary" pyroelectric effect in view of similarity in the calculation methods. However, this definition is incorrect, as secondary pyroelectric effect is manifested in the mechanically free crystals, while the artificial pyroelectric effect is observed in the partially clamped crystals only. Besides, it is need to compare the APE with the tertiary pyroelectric effect: both of them originate from the thermal stresses in piezoelectrics. However, in the case of tertiary pyroelectric effect, these stresses are caused by the spatial heterogeneity in crystal temperature (crystal is exposed to *grad T*). At the same time, the APE looks like conventional pyroelectric effect that occurs during the uniform heating or cooling of a crystal. But it appears under the restriction of certain strains of crystal, i.e., it arises as a result of the inhomogeneous boundary conditions. In all cases, induced in the piezoelectrics APE can be regarded as a consequence of the superposition of crystal symmetry and impact symmetry. The most accurate (but not brief) definition of the APE physical effect would be "pyroelectricity in the partially clamped piezoelectrics", but using here term “artificial pyroelectric effect” also quite clearly indicates the physical mechanism of a phenomenon under discussion.

Detailed theory of APC in the form of three adjoint equations and the examples of calculations made for important piezoelectrics are given in [10]. As a simplest case, consider the symmetry class 32, to which belong the well-studied piezoelectric quartz. Its artificial pyroelectric coefficient is determined by the formula:

$$\gamma_{1\,APE} = d_{11}(\alpha_1 s_{33} - \alpha_3 s_{13})(s_{11}s_{33} - s_{13}^2)^{-1}.$$

In the *X*-cut of quartz (SiO_2) at temperature of 300 K the γ_{1APE} = 2.5 $\mu C \cdot m^{-2} \cdot K^{-1}$. For others 32 symmetry crystals is obtained: for berlinite crystal ($AlPO_4$) γ_{1APE} = 5.7 $\mu C \cdot m^{-2} \cdot K^{-1}$, for calomel ($Hg_2Cl_2$) $\gamma_{1\,APE}$ = 8.7 $\mu C \cdot m^{-2} \cdot K^{-1}$ and for tellurium (Te) γ_{1APE} = 10 $\mu C \cdot m^{-2} \cdot K^{-1}$. The spatial distribution of γ_{1APE} for crystals of 32 symmetry class is shown in Fig. ... from which it follows that along the axes *Y* and *Z* there is no artificial effect.

Similarly, when researching KDP crystal, Fig. ///, for internal polarity investigation a standard crystallographic orientation should be changed by turning the axes *1* and *2* around the axis *3* at the angle of $\pi/4$. In this case, piezoelectric sample is prepared as a long rectangular rod extending along one of new axes (*1′* or *2′*) with the electrodes deposited on sample surface perpendicular to axis *3′ = 3*.

The prohibition of this rod longitudinal deformation allows obtain artificial the pyroelectric response with coefficient $\gamma^*_3 = 2\, d_{36}\alpha_1(2s_{11} + 2s_{12} + s_{66})^{-1}$. In the paraelectric phase polar-neutral of KDP crystal of 422 symmetry group shows the artificial pyroelectric coefficient γ^*_3 = 6 $\mu C/m^2K$. The spatial distribution of γ^*_3 for crystals of 422 symmetry class is shown in Fig. 4.23. However, for practical applications of the APE, the most promising are the semi-insulated semiconductors of 43m symmetry: sphalerite structure of polar-neutral symmetry (GaAs, GaAl, GaN, AlN and their solid solutions).

These crystals are simultaneously the thermoelectric and piezoelectric converters, and have very high electron mobility. In the specially oriented thin layers, using the restriction of some thermal deformations, APE coefficient is $\gamma_{111} = 2\sqrt{3}\, d_{14}\alpha / (4s_{11}^{E,T} + 8s_{12}^{E,T} + s_{44}^{E,T})$. In GaAs the γ_{111} = 1.5 $\mu C \cdot m^{-2} \cdot K^{-1}$ but in GaN it is much bigger (note that first known pyroelectric tourmaline has pyroelectric coefficient of 4 $\mu C \cdot m^{-2} \cdot K^{-1}$).

In gallium arsenide artificial pyroelectric effect in the directions of basic axes [100], [010] and [001] is impossible. The maximum of APE in all $A^{III}B^{V}$ crystals corresponds to [111]-type cut while its spatial distribution reminds the piezoelectric module indicatrix shown in Fig. 4.23. The results of the experimental studies and calculations of the APE for all polar-neutral classes of crystals are given in Table 4.3.

Table 4.3.

Artificial pyroelectric effect for 10 classes of actual piezoelectric crystals

Symmetry classes, axes orientation (x,y,z)	**Sample and its orientation as to basic axes**	**Calculation expressions for APE coefficient $\gamma_{n\,APE}$**	**Piezoelectric, γ_{nAPE} [$\mu C/m^2 \cdot K$)] found at 300 K**
32 (for basic coordinate system)	Rectangular rod with length l along y and thickness along x Disk with normal d directed along x	$\gamma_1 = \dfrac{d_{11}^T \cdot \alpha_1^E}{s_{11}^{E,T}}$ $\gamma_1 = \dfrac{d_{11}^T (\alpha_1^E s_{33}^{E,T} - \alpha_3^E s_{13}^{E,T})}{s_{11}^{E,T} \cdot s^{E,T}_{33} - (s_{13}^{E,T})^2}$	SiO_2, $\gamma_1 = 2.6$ SiO_2, $\gamma_1 = 2.7$
$\bar{4}2m$ (axes x and y are rotated around axis z at the angle of 45°)	Rectangular rod with length l and normal d directed along axis z *а*) l is directed on x, *б*) l is directed on y.	$\gamma_3 = \dfrac{\pm\ 2d_{36}^T \cdot \alpha_1^E}{2 \cdot s_{11}^{E,T} + 2 \cdot s_{12}^{E,T} + s_{66}^{E,T}}$	KDP, *а*) $\gamma_3 = -6$ *б*) $\gamma_3 = +6$ ADP, *а*) $\gamma_3 = -17$ *б*) $\gamma_3 = +17$
$\bar{4}3m$ and 23 (axis z is directed on the third fold axis)	Dist, d directed along z	$\gamma_3 = \dfrac{-2\sqrt{3} \cdot d_{14}^T \cdot \alpha^E}{4 \cdot s_{11}^{E,T} + 8 \cdot s_{12}^{E,T} + s_{44}^{E,T}}$	Tl_3TaSe_4, $\gamma_3 = -23{,}5$; $Bi_{12}GeO_{20}$, $\gamma_3 = -20$
222 (axes x and y are turned around axis z at the angle of 45°)	Rectangular rod with normal d directed along axis z and length l directed *а*) l along axis x, *б*) l along axis y	$\gamma_3 = \dfrac{\pm\, d_{36}^T (\alpha_1^E + \alpha_2^E)}{s_{11}^{E,T} + s_{22}^{E,T} + 2 \cdot s_{12}^{E,T} + s_{66}^{E,T}}$ *а*) corresponds to sign «+» *б*) corresponds to sign «–»	
622 and 422 (axes y and z are turned around axis x at the angle of 45°)	Rectangular rod with normal d directed along axis x and length l directed *а*) l along axis y, *б*) l along axis z	$\gamma_3 = \dfrac{\pm\, d_{14}^T (\alpha_1^E + \alpha_3^E)}{s_{11}^{E,T} + s_{33}^{E,T} + s_{44}^{E,T} + 2 \cdot s_{13}^{E,T}}$ *а*) corresponds to sign «+» *б*) corresponds to sign «–»	
$\bar{4}$ (standard)	Rectangular rod with normal d directed along axis z and length l directed *а*) l along axis x, *б*) l along axis y	*а*) $\gamma_1 = \dfrac{-d_{31}^T \cdot \alpha_1^E}{s_{11}^{E,T}} = R$ *б*) $\gamma_1 = -R$	
$\bar{6}m2$ and $\bar{6}$ (standard)	Disk, normal d is oriented along axis y	$\gamma_1 = \dfrac{d_{22}^T (\alpha_1^E s_{33}^{E,T} - \alpha_3^E s_{13}^{E,T})}{s_{11}^{E,T} \cdot s_{33}^{E,T} - (s_{13}^{E,T})^2}$	

Described effect, in addition to the physical nature of internal polarity investigation, opens up a possibility of using polar semiconductors in the single-crystal pyroelectric and piezoelectric sensors, obtained by the integrated technology.

4.7 Summary Chapter 4

Conclusions

To explain the unique properties of polar crystals, it is not necessary use the hypothesis of spontaneous polarization, which would have to be accompanied by some kind of "internal" electrical field, t/he existence of which is difficult to explain for thermodynamically equilibrium state of a crystal under conditions of inevitable presence of free charge carriers in it.

The supposed reason of polar bonds existence in non-centrosymmetric crystal structures (as well as their formation) is the structural compensation of electronic states features of the ions making up polar structure, in particular, the difference in their electronegativity. Polar crystals are characterized by finely balanced structure of their interatomic bonds, which makes these crystals highly sensitive to external influences.

The mixed ionic-covalent polar-sensitive bonds is a main reason to generate electrical response of polar crystal onto non-electrical influences (thermal, mechanical, optical, etc.). That is why, exactly the uniform change in temperature is used here to determine experimentally the magnitude of own polarity; at that, in case of polar-neutral (piezoelectric) crystals, the method of partial limitation of thermal strain in the polar cut of crystal is applied.

The response on such scalar impact can be described by the generalized electrical moment, critically changing with temperature: $M_{ijk}(T) \sim (\theta - T)^n$. In the case of 3D arrangement of polar bonds, critical parameter is $n = 2$; for 2D their arrangement $n = 1$, and in the 1D case (ferroelectrics) $n = 0.5$: this is critical Landau index.

Thus, the distinction between the pyroelectrics and piezoelectrics is not fundamental, and it consists in a different spatial distribution of their polar bonds. In the ferroelectrics, the polar-sensitive bonds are capable of changing their orientation with a nonlinear response to electrical field (hysteresis). The thermo-piezoelectric effect used in research can have technical applications in sensors.

References

[1] C. Kittel, *Introduction to solid state physics*, 5-th ed. New York: John Willey, 1976.
[2] M.E. Lines and A.M. Glass, *Principles and Applications of Ferroelectrics and Related*

Materials, Clarendon Press, Oxford, 2009.
[3] Yu. M. Poplavko, *Electronic mfterials. Princeples and applied science*, ELSEVIAR, 2019.
[4] R.D. King-Smits, D. Vanderbilt, *Theory of polarization of crystalline solids,* Phys. Rev. B 47, 1651, 1993.
[5] R. Resta, *Manifestation of Berry phase in molecules and condensed matter*, J. Phys. Condensed Matter, 12, R107, 2000.
[6] W.O. Cady, *Piezoelectricity*, Amazon com, New York, 1946.
[7] I.S. Jeludev, *Basics of ferroelectricity*, (in Russian) Atomizdat, Moscow, 1973.
[8] Yu.M. Poplavko. *Dielectric spectroscopy of electronic materials. Applied physics of dielectrics*. ELSEVIAR, 2021.
[9] Fansping Zhuo, Qiang Li, Huimin Qiao et. al. *Field-induced phase transitions and enhanced double negative electrocaloric effects in (Pb,La)(Zr,Sn,Ti)O_3 antiferroelectric single crystal.* Appl. Phys. Lett., 2018, 112, 133901.
[10] Yu.M. Poplavko, L.P. Pereverzeva, I.P. Raevskiy, *Physics of active dielectrics* (in Russian), South Federal University of Russia, Postov-na-Donu, 2009.
[11] L.P. Pereverzeva, I.Z. Pogosskaya, Yu.M. Poplavko, I.S. Res, *Dielectric anomalies in crystals KH_2PO_4, KD_2PO_4, RbH_2P0_4 at high temperatures*, Phys. Tverdogo Tela, 1973, Vol.15, N^o 4, p. 1250.
[12] Yu.M. Poplavko, L.P. Pereverzeva, N.I. Cho, Y.S. You. Feasibility of microelectronic quarz temperature ans pressure sensors. Jpn. J. Appl. Phys., Vo7.37,1998, p.4041.
[13] Yu.M. Poplavko, L.P. Pereverzeva, *Polar properties of non-isotropically clamped piezoelectrics* (in Russian) Ukrainskii Physichaskii Jurnal, 1993, Vol 38 p. 1383.
[14] D.G. Schlom, L.-Q. Chen, Ch. Eom, K.M. Rabe, S.K. Streifer, and J.M. Triscone, *Strain tuning of ferroelectric thin films*, Annu. Rev. Mater. Res., vol. 37, pp. 589-626, 2007.

Questions

1. What are the classical explanation of pyroelectricity mechanisms?
2. What are the classical explanation of piezoelectricity mechanisms?
3. What are the classical explanation of ferroelectricity mechanisms?
4. List main features of polar crystals.
5. What is new proposed explanation of polar crystals properties?
6. List an explain three simplified models of polar bonds connection.
7. List experimental evidences of polar-sensitivity.

CHAPTER 5. HIGH-PERMITTIVITY MICROWAVE DIELECTRICS

Contents

In the *high-permittivity* low loss dielectrics, usable in the microwave range, as a basic component providing high permittivity the "hard" paraelectrics should be applied which resist the manifestation of polarity (like rutile or perovskite). They are distinguished by under-damped soft transverse optical mode of crystal lattice vibrations. To obtain *low microwave losses*, it is necessary to provide in a composition the single-phase structure without any polar inclusions, which are the main cause of microwave absorption. The *stability* in thermal characteristics is ensured by the selection of solid solution components, in which the negative and positive temperature coefficients of permittivity are compensated, and by the of paramagnetic lanthanide ions embedding that suppresses Curie-Weiss law of hard paraelectrics. *Functional* microwaves dielectrics, as a rule, use dielectrics with electrically controlled permittivity like (Br,Sr)TiO_3 thin films tuned by electrical field. Another promising solutions are the controlled by piezoelectric dielectric-air gap composites with small insertion losses.

Before considering the latest developments regarding functional microwave dielectrics, it is advisable to dwell on the traditional concepts of these materials filed in the first two paragraphs.

5.1. Microwave dielectrics classification

Since the electromagnetic waves can propagate only in the dielectrics, from the very beginning of microwave technology development much attention has been paid to the dielectric materials study at microwaves. As a rule, in earlier microwave systems,

for signal propagation the metallic waveguides filled with *air* ($\varepsilon \approx 1$) were used. Later the *dielectric waveguides* with value of $\varepsilon = 2–10$ started to apply, in which the electromagnetic field is concentrated mainly inside a dielectric; but they found limited application due to the radiation of a part of microwave energy. Nevertheless, the dielectric waveguides are still applied in the millimeter and sub-millimeter wavelength range, where metallic waveguides already have unacceptable losses.

Usually for microwave applications it is necessary to have a "good radio transparent" materials with very low loss of energy, and, as a rule, with low dielectric constant. These are, for example, good-transparent microwave composites of the "ceramics-air" type (ceramic foam) with permittivity ε = 1.2–2, as well as the composites of "polymer-air" type with ε = 1.05–1.3. At that, in most cases (in military and space technologies) the microwave-transparent materials should have bigger permittivity (ε = 5–10) but obviously will have low dielectric losses and with high mechanical strength.

Dielectric materials are widely applied also for many microwave elements manufacture such as the microstrip lines, electrical capacitors, dielectric antennas, dielectric resonators, phase shifters, etc. Very different dielectrics (ceramics, glass ceramics, crystals, polymers and composites) are applied in microwave technology but usually their permittivity is within ε = 4–20 (but that is not enough for resonant and controlled devices). In the most of listed above technical applications, first of all, the *low losses* and the *high temperature stability* of properties (the ε constancy with temperature changes) are need. Thus, typical requirements of microwave technology to the dielectrics consist in *combining* in one material the increased permittivity (ε = 20–200), high thermal stability ($TC\varepsilon$ < 10 ppm·K^{-1}) and low microwave losses ($\tan\delta < 10^{-3}$); however such combination, at a first glance, looks as physically contradictory.

Current and future fields of microwave *high permittivity* dielectrics applications are listed in Fig. 5.1.

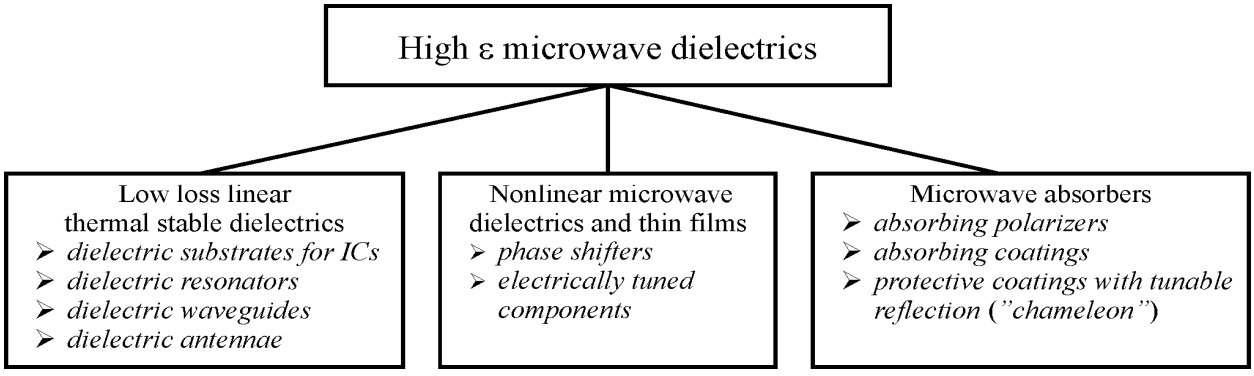

Fig. 5.1. Areas of application of microwave dielectrics with high value of permittivity

Linear thermostable dielectrics are main class of currently used microwave dielectrics with increased value of ε_{mw}. They are used mainly as miniature capacitors, dielectric resonators and substrates of the microwave circuits (reducing their planar dimensions in ε times). The selection of such microwave dielectrics is determined by the frequency range of their use: for the metric and decimetric waves devices the microwave dielectrics with value of $\varepsilon = 200–100$ are need, while in the centimetre and millimetre waves devices dielectrics with $\varepsilon = 40–20$ are more actual. Generally, the external heat setting for microwave devices is undesirable; that is why the parameters of microwave dielectrics should be stable in need temperature interval, usually these dielectrics must have small temperature coefficient of permittivity: $TC\varepsilon = \varepsilon^{-1}d\varepsilon/dT < 10^{-5}\ K^{-1}$.

Nonlinear microwave dielectrics, with electrically controlled permittivity: $\varepsilon(E)$ are intensively studied in many laboratories around the world, and now they are in the beginning of applications in the microwave engineering. In this case, it is impossible to guarantee high thermal stability and low microwave losses, nevertheless, nonlinear paraelectric film may be used in microwave phase shifters providing high operation speed.

Absorbent materials ("absorbers") are also subject of modern research. For them it is a necessary to have large dielectric losses even in the thin layers (or in the powders) in order to provide almost complete attenuation of microwave signals. One possible application is the millimetre and sub-millimetre waves polarizers, in which the strong anisotropy of microwave absorbance in one-axis ferroelectrics might be used.

The fact is that in the crystals and polycrystals the low absorption of energy at frequencies of 1–1000 GHz is peculiar exclusively to the dielectrics possessing *low-inertial* polarization mechanisms. This means that the only optical (electronic) and infrared (phonons) polarization mechanisms are acceptable in these dielectrics, however, in the most cases these mechanisms can not provide sufficiently high permittivity (need is $\varepsilon = 20–200$). At that, others mechanisms of polarization either do not make need contribution to permittivity in the microwave range or lead to the dispersion of permittivity, which is the main cause of significant dielectric losses.

Moreover, with the *rare exceptions*, as optical so infrared polarizations cannot provide large enough value of dielectric permittivity in *conjunction* with low dielectric losses and high thermal stability. At that, usual methods of technological control of electrical properties of solids (impurities introduction, regulation of defects concentration, etc.) is unsuitable in the case of *microwave* dielectrics, since they lead to the increase of losses. Fortunately, influence of electrical conductivity

on the energy losses in the microwave range can usually be neglected: even semiconductors (such as silicon and gallium arsenide, if they are not specially doped) can be applied in microwave microelectronics as low loss insulating substrates. The main mechanism of losses in ceramic microwave materials are their structural *defects* and, especially, the presence of *polar phases* in the structure. At the present moment, there are many models that describe different properties of high frequency dielectric materials.

Dielectric materials are used as structural elements of integrated circuits, such as undercurrent dielectric layer in transistors, storage capacitors, inter-element insulation, protective coatings, substrate, and for the manufacture of microwave components such as microstrip lines, electric capacitors, capacitors, dielectric modulators, detectors, etc. The manufacture of dielectric resonators is the most common use of dielectrics. Currently, a large number of resonant microwave devices have been developed, Fig. 5.2.

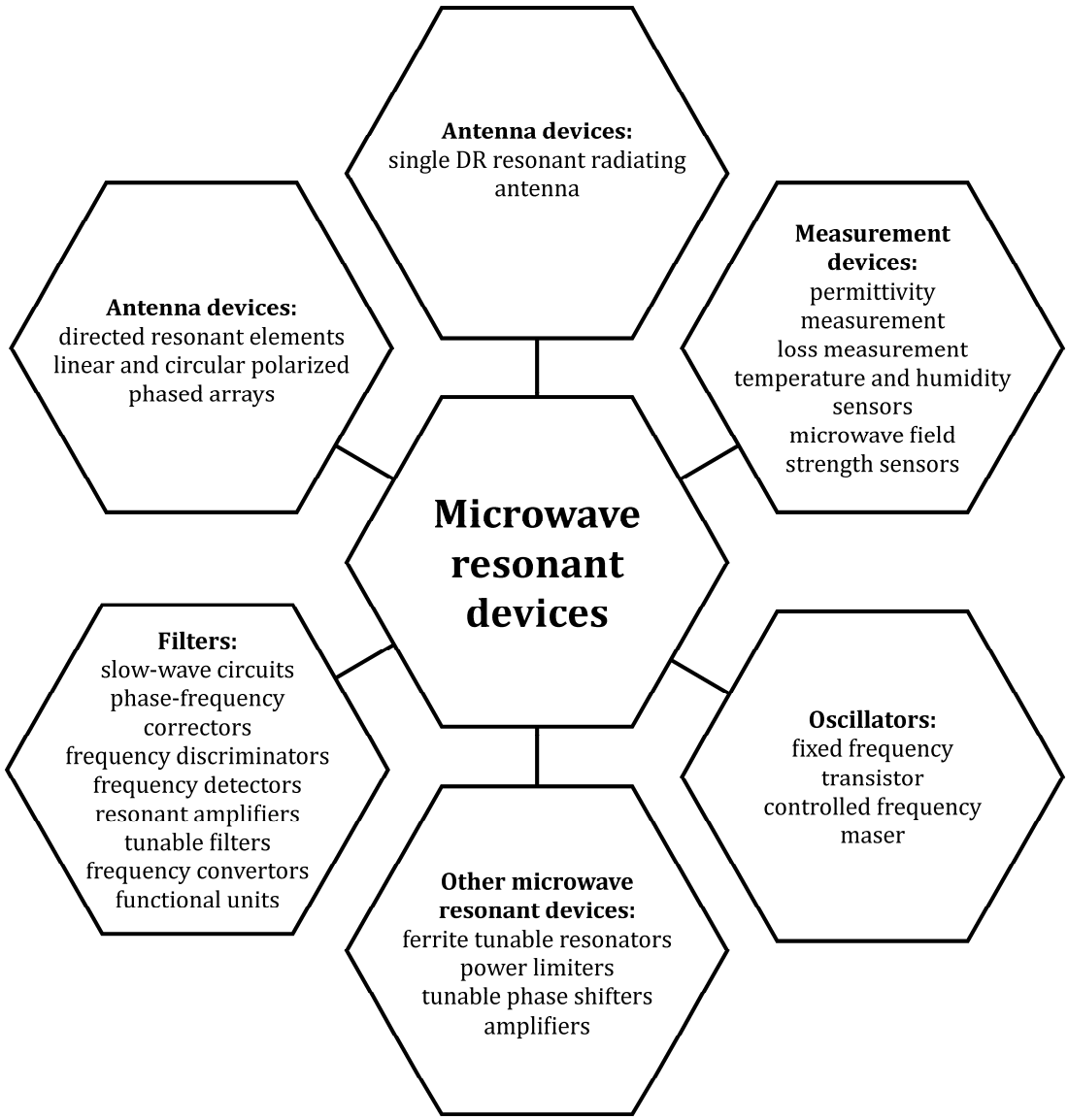

Fig. 5.2. Application of resonant microwave devices.

In connection with this, three approvals relating to the improvement of microwave dielectrics properties can be justified. First, high permittivity at microwaves can be obtained only in the crystals and polycrystals with *low frequency* transverse optical lattice mode in the paraelectric-like materials. Second, small dielectric losses can be reached only in the *monophase composition* based on the "hard-type" paraelectric material, which negates structural internal polarity. Third, to achieve thermal stability in dielectrics with high permittivity ($\varepsilon_{mw} \approx 80–160$) the phenomenon of basic material "paraelectricity" can be suppressed by the paramagnetic components. Below, for the most part, the thermal stable dielectrics are discussed.

5.2 Polarization mechanisms in microwaves dielectrics

Polarization is main property which determines peculiarity of dielectric as a kind of material and may occur both under applied electrical field and other external influences (change of pressure, temperature or irradiation). In this section, only the polarization which occurs in externally applied electrical field is considered. In a dielectric, electrical field induces only the of associated charges (creating the charge separation = polarization) and the *movement* of free charges (causing the charge transferee = conductivity); both of these phenomena arise simultaneously. At the same time, the charge *separation* (polarization) results in the bias current which anticipates in phase by $\pi/2$ the applied sinusoidal electrical voltage, and this current exists all time as long as electrical field is applied (this is rightly both for alternating and direct voltage). In the event, when the voltage is switched, the bias current exists only at that time, when the electrical field is changing, and this current is absent in case of permanent voltage. Continuing to discuss the differences of these two phenomena, it should be noted that conductivity relates to the *transport phenomena*, while polarization (with rare exceptions) is the *reversible property*. Moreover, the internal structure of dielectrics is unfavourable for moving of free charge carriers, so their number is *negligible*; on the contrary, *all particles* of dielectric anyway participate in the polarization.

Microscopic polarization mechanisms have already been considered, but mainly from point of view of their *internal polarity*. At that, several mechanisms of elastic, thermal and space-charged polarizations are described, in which the locally bound electrons, ions or dipoles shift in the electrical field. For microwave dielectrics, the most important aspect of these mechanisms is their *inertia*. At that, traditionally, different polarization mechanisms are considered as being

"independent", and this consideration is basically justified. Classification of dielectric contributions of various mechanisms to permittivity is given in Fig. 5.3.

The *quasi-elastic* (deformation type) induced polarization is the least-inertial polarization; being only slightly affected by temperature movement; so dielectrics with this polarization are good materials to use in microwaves engineering. Electronic quasi-elastic polarization (deformation of electronic shells of atoms, molecules or ions in electrical field), which determines permittivity ε_e, is a common mechanism for *all dielectrics*. thei onic quasi-elastic polarization is a characteristic property of such dielectrics and semiconductors, in which the ionic type of bonding in a crystal lattice is clearly pronounced; the ionic polarization mechanism is characterized by permittivity ε_i. The quasi-elastic dipole polarization with ε_d is observed in very rare case: when external electrical field induces orientation of closely constrained dipoles.

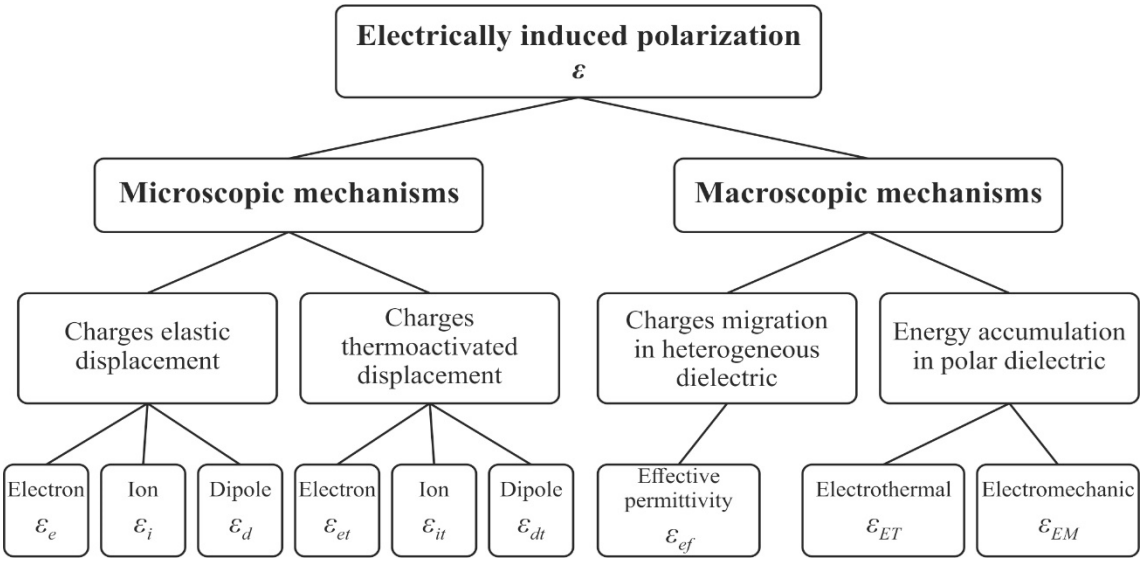

Fig. 5.3. Dielectric permittivity due to basic mechanisms of electrical polarization

As already discussed, only these polarization mechanisms can be fully installed at microwaves, and only they call forth microwave permittivity $\varepsilon_{mw} = \varepsilon_e + \varepsilon_i$, Fig. 5.3. However, the lower-frequency polarization mechanisms also indirectly affect the properties of microwave dielectrics, increasing their *dielectric losses.* The fact is that those microscopic movements of associated electrical charges of dielectric, which do not have time to be installed during quarter of oscillation period of applied field cannot accumulate energy during this time for reversible polarization process. However, they continue to move in-phase with electrical field like "free" particles that leads to irreversible phenomenon of conductivity, i.e., they convert part of electrical energy they receive into a heat – i.e., in the losses.

Thermally supported electrically induced polarization (relaxation) in solid dielectrics stipulate for dielectric contribution shown in Fig. 5.3 as ε_{rel}, and is designated as ε_{tl}, ε_{it} and ε_{dt}. This polarization, mainly caused by the structural defects, is essential, if the electrons, dipoles or ions are weakly bounded in structure of dielectric. Remaining localized in nano-scale areas, these charged particles or dipoles under the influence of thermal motion make thermally activated jumps, moving at distance of atomic dimensions order. Electrical field influences on the direction of these thermal hopping, which become asymmetrical and have sufficient time to generate electrical moment if frequency is not high. The inertia of thermally activated polarization is much bigger in comparison with quasi-elastic polarization, so that at sufficiently high frequencies this movement of charged particles no longer contributes polarization but for that increases electrical conductivity and losses.

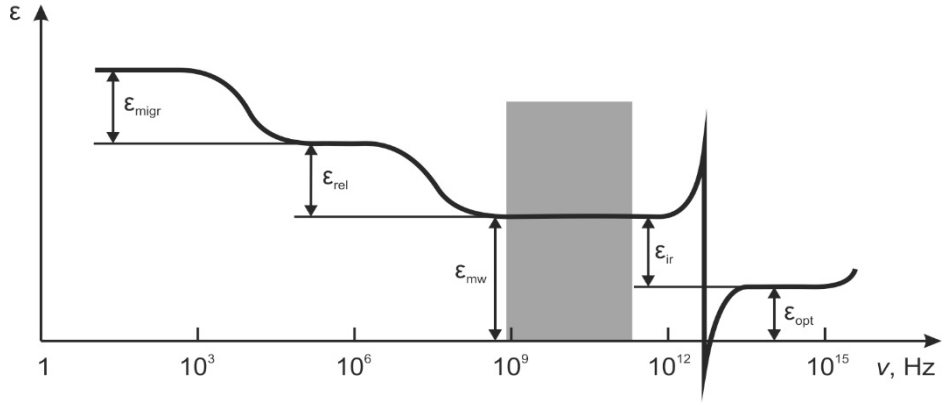

Fig. 5.4. Generalized frequency dependence of permittivity of no-polar dielectrics with shown dielectric investments from different polarization mechanisms; microwave frequency range is darkened; in order to simplify this figure, additional contributions to permittivity from ε_{EC} and ε_{EM} peculiar to *polar* dielectrics are not shown

Electrically induced *space-charge polarization* (saying otherwise the *migration* polarization), which dielectric contribution is shown in Fig. 5.3 as ε_{migr} and designated in Fig. 13.4 as ε_{ef}, is another additional mechanism of polarization, which is observed in some solids and composite materials with pronounced heterogeneous structure. The cause of this polarization is presence of layers or regions with different conductivity (for example, electro-conductive inclusions in dielectric). Conditioned by space-charge polarization is lowest-frequency (highest inertia) mechanism, which can have some effect on microwaves *absorbing composites* properties.

Thus, only some of listed polarization mechanisms are responsible for ε_{mw} at microwaves, Fig. 5.4. Firstly, this is the *electronic* elastic polarization, which exists in any material being the only mechanism which can response even to optical

frequencies; that is why correspondent permittivity is denoted as $\varepsilon_e = \varepsilon_{opt}$. Secondly, it is the *ionic* elastic-displacement polarization, which is too slow in visible optical range but has its own resonance at far infrared range (that is fast sufficiently for microwaves); so ionic contribution to permittivity is $\varepsilon_i = \varepsilon_{IR}$. Sum of these polarization mechanisms determines microwave permittivity ε_{mw}.

As shown in Fig. 5.4, others mechanisms of polarization usually are too slow: the migration polarization with permittivity ε_{migr} is late already above frequency of 1 kHz, while relaxation polarization (ε_{rel}) cannot give any contribution to permittivity above frequency of 100 MHz (nevertheless, there are some polar-sensitive dielectrics – ferroelectrics of the order-disorder type – in which the fundamental polarization occurs exactly in the microwave range, but these feature is not shown in Fig. 5.3.

5.3 Primary requirements to functional microwave dielectrics

Microwave electronics widely use various dielectric components, but in this paper we consider only dielectrics with high permittivity ($\varepsilon \sim 20–200$) providing small dimensions of devices. Such materials (usually ceramics) are used in the resonant devices (dielectric resonators, antennas, etc.) that is why they should have low losses ($\tan\delta < 10^{-3}$) and increased thermal stability ($TC\varepsilon = \varepsilon^{-1}d\varepsilon/dT < 10^{-5}\ K^{-1}$).

Getting in a combination of such parameters in one material is difficult task, and many works are devoted to the successful solution of which, summarized in books [1, 2], where empirical developments are mainly described. The given work, devoted to clarification of physical mechanisms, which ensure increased thermal stability of high-Q microwave dielectrics possessing high permittivity could be useful for further developments.

Main properties of functional dielectrics are the controlling field ($E_b < 10$ kV/cm), tunability ($n = \varepsilon/\varepsilon_b \sim 2$) and losses ($\tan\delta < 10^{-1}$) [3]. Another way to create dilelectric-based tunable microwave devices is the electromechanically tunable macro-composites, consist of a dielectric coupled with controlled air-gap, which makes it possible to realize microwave phase shifters, tunable resonators, antennas and filters, practically without insertion losses [4].

Firstly, on basis of thermodynamics a connection is established between the temperature dependence of permittivity and the processes of structural elements ordering in the dielectrics under the action of electrical field. This can serve as a

basis for understanding and predicting those mechanisms of electrical polarization, which can determine one or another temperature dependence of permittivity.

Secondly, the possibility of high permittivity, low dielectric losses with their thermal stability at microwaves is substantiated. It is argued that increased permittivity can only be obtained in the structures close to peculiar paraelectrics (such as rutile and perovskite), which are characterized by the high polarizability of weakly coupled electronic shells in ther oxygen octahedra. In them high permittivity is due to the low frequency of transverse optical mode of lattice vibrations, which, unlike ferroelectrics, are not over-damped and therefore does not lead to the large losses.

Thirdly, the reason for high quality thermal stable dielectrics with $\varepsilon = 30 \pm 10$, which are most commonly used in the centimeter wavelength range, has been studied. In their strongly polarizable structural, for example, based on the oxygen octahedra, a different sign of temperature coefficient of permittivity can be observed: the positive $TC\varepsilon > 0$ in antiferroelectrics and the negative $TC\varepsilon < 0$ in paraelectrics. Therefore, in their solid solution, with a certain ratio of components, one can obtain $TC\varepsilon \approx 0$; in this case, both paraelectrics and antiferroelectrics are not prone to the formation of a polar phase, which is the main source of microwave losses.

Fourthy, it has been established that microwave dielectrics with $\varepsilon = 120 \pm 40$, used in the decimeter and meter wavelength ranges, become thermal stable, when the Curie-Weiss dependence $\varepsilon(T)$ of "hard" paraelectrics (which cannot be ferroelectrics) is suppressed by the paramagnetism of rare earth ions introduced in composition. It is also argued that the main reason for microwave absorption in high-permeability dielectrics is polar phase presence; therefore, they should not contain polar inclusions.

Fifthly**,** the physical principles of operation of two types of functional microwave dielectric components are considered. Considered first are the paraelectric films, which give important opportunity of a rapid control of permittivity, which provides the phase shift of transmitted signal or restructuring of the resonant device. Correspondent "soft" paraelectrics, inevitably containing some polar phase, are applied above the temperature of ferroelectric phase transition, so losses in them are not great while the controlling electrical field can change permittivity by several times due to the increase of optical oscillations frequency of lattice. At that, a compromise may be found how to combine sufficient tunability with a minimal dielectric losses that is successfully implemented in the thin paraelectric films. Considered next is for dilelectric-based tunable microwave

functional devices: the application of macro-composites, consist of microwave dielectric coupled with air-gap which thichness is controled by the piezoelectric. This solution makes it possible to realize microwave phase shifters, tunable antennas and filters without insertion losses.

5.4 Main properties of functional microwave dielectrics

For high-permittivity microwave dielectrics, it is important to substantiate three main parameters: the nature of high permittivity, the ways to reduce losses, and the nature of permittivity thermal stability.

Increased permittivity in dielectrics, intended for use in microwave range, may be of interest only in the combination with their low losses. This combination of properties can be provided by the polarization of some crystals with a mixed ionic-covalent bonds and having a structure that promotes the formation of highly polarizable electronic shells, which at that does not lead to the formation of weakened polar bonds. The fact is that in purely-covalent crystals, the displacement of electrons leads to a small permittivity: $\varepsilon_{mw} = \varepsilon_{el} < 7$ at $TC\varepsilon < 0$. In purely ionic crystals, the displacement of sublattices usually leads to $TC\varepsilon > 0$, but also with low permittivity: $\varepsilon_{mw} = \varepsilon_{ion} < 12$, which is insufficient for many important microwave applications.

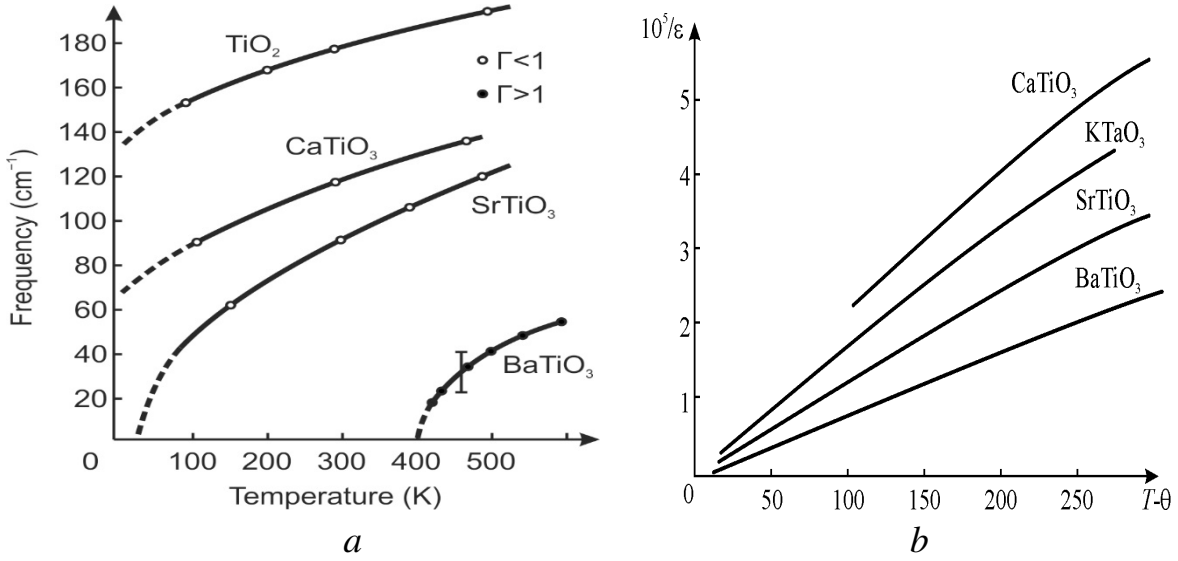

Fig. 5.5. Paraelectrics soft mode frequency ν_{TO} and damping factor Γ temperature dependence (*a*) and Curie-Weiss law fulfillment in paraelectrics (*b*) [3,4].

Only the crystals and polycrystals with a mixed ion-covalent bond make it possible to obtain ε_{mw} = 20–200 and $TC\varepsilon \approx 0$, since they have a structure that

provides high polarizability of easily deformable by the field electronic shells. In the ionic crystals, the lower the frequency of transverse optical vibrations ν_{TO} of the ionic crystal lattice, the higher the permitivity that follows from the Liddane-Sachs-Teller relation: : $\varepsilon_{mw} = \varepsilon_{el}\,(\nu_{LO}^2/\nu_{TO}^2)$. Low ν_{TO} frequency have ferroelectrics, antiferroelectrics, and paraelectrics, but as a rule the ferroelectrics have large microwave losses while the antiferroelectrics have insufficient permittivity. That is why, exactly the paraelectrics of the oxygen-octahedral type with a low-frequency optical mode ν_{TO} can be used as the basic composition for microwave applications, Fig. 5.5.

In the paraelectrics, temperature dependence of permittivity are characterized by Curie-Weiss law: $\varepsilon(T) \sim C/(T-\theta)$, where C is the constant and θ is the Curie-Weiss temperature. At that, the "soft" paraelectrics (such as $SrTiO_3$ or $KTaO_3$) have positive $\theta > 0$ K and in them the frequency ν_{TO} critically decreases in the center of Brillouin zone. Very strong anharmonicity of soft vibration mode affects the losses, Fig. 1*a* where $\Gamma \approx 1$, and therefore on microwaves in "soft" paraelectrics $\tan\delta \sim 10^{-1}$–10^{-2}. This hinders their use as a component of need composition with low losses, since in the compositions a polar phase will inevitably arise, leading to significant microwave losses. Moreover, these paraelectrics under the external influences can easily pass into polar (ferroelectric) phase, which is main source of unwanted microwave losses.

Unlike them, the "hard" paraelectrics (like $CaTiO_3$ and TiO_2) are described by negative Curie-Weiss temperature ($\theta < 0$ K by analogy with antiferromagnets), so in them Curie-Wess law $\varepsilon(T) \sim C/(T+\theta)$. Like antiferromagnets and antiferroelectrics, the "hard" paraelectrics are characterized by a very stable antipolar structural motivation, which prevents the interaction of optical and acoustic phonons near the center of Brillouin zone. This leads to the suppression of polar motifs in their structures, and, consequently, to much lower dielectric losses: $\tan\delta \sim 10^{-3}$–10^{-4}, This materials can serve as structural basis for microwave dielectrics compositions, possessing increased permittivity and low losses, with the expectation that their increased temperature dependence of permittivity would be technologically suppressed. Thus, in high-permittivity paraelectrics, the sing of Curie-Weiss temperature θ has a noticable effect on the microwave dielectric losses.

Dielectric losses in the microwave polycrystalline dielectric with increased permittivity are due to two main mechanisms: the presence of polar phases in some components of composition and the anharmonicity of crystal lattice vibrations. In addition, losses can be increased by the structural defects generating conductivity

and electrical relaxation; but these losses depend on technology improvement. Experimental and theoretical investigations show that dominating mechanism of losses in the high-permittivity dielectrics arises from the polar phase existence. In the case of polar-sensitive bonds between atoms, the inter-atomic potential manifests a pronounced anharmonicity that is main microscopic channel to transfer electrical energy into a heat (dielectric losses). The point is that anharmonic potential between ions results in a coupling between optical phonons (excited by electrical field) and acoustical phonons (which represents "heat reservoir" in a crystal). With increasing temperature, and, consequently, with the increase in amplitude of vibration of ions, the manifestation of anharmonicity becomes more noticeable and dielectric losses increase.

The high-quality microwave dielectrics with permittivity $\varepsilon = 30 \pm 10$ are used mainly in the centimeter wavelength range and meet the requirements $\tan\delta < 10^{-4}$. In them, the mixed covalent-ionic inter-atomic bonds is necessary to obtain increased permittivity, so anharmonism of lattice vibrations is increased. These losses linearly increase with frequency rise and can be dominant. In the microwave dielectrics of meter and decimeter ranges with a permittivity $\varepsilon = 120 \pm 40$, the main loss mechanism is due to polar phase, which presence in a structure must be minimized. When choosing a "hard" paraelectric as the base material, and by technological achievement of a single-phase structure, it is possible to obtain $\tan\delta < 10^{-3}$.

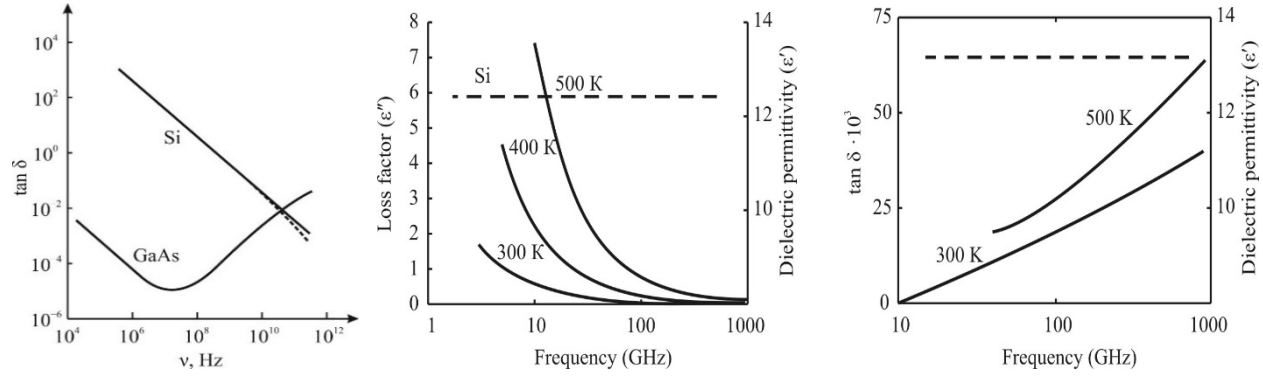

a b c

Fig. 5.6. Loss tangent frequency dependence: *a* – Si and GaAs comparison in wide frequency range of 10^4–$7 \cdot 10^{11}$ Hz at 300 K; *b* – Si in microwaves at different temperatures; *c* – impact of quasi-Debye mechanism in GaAs (dashed line is permittivity)

In its purest form, the effect of intrinsic polarity on the microwave losses can be traced by the comparing of nonpolar Si crystal with polar GaAs crystal, Fig. 5.6. The losses, conditioned by the conductivity, are described by the $\tan\delta$ decrease with

frequency rise, while the losses from polar phase are promoted by coupling of optical and acoustic phonons that increases with frequency (this mechanism is called the quasi-Debye losses). Such losses are especially big (and cannot be avoided) in the "soft" paraelectrics, which nevertheless are used in the functional microwave devices using electrical control of permittivity [5].

Thus, it is the polar nanoscale inclusions, which are the main reason of microwave absorption. That is why, in the technology of microwave ceramic, any appearance of polar phase should be avoided. Moreover, in the microwave dielectrics a part of dielectric losses are associated with possible structural mismatch, especially in the case, when at the same time the unwanted polar inclusion in the structure appears. It's obvious that any boundaries (interfaces) between the grains of ceramics have a disordered structure, and the "tail" from their frequency relaxation may reach the microwave range. Nevertheless, when microwave dielectrics are used in practice in the temperature interval of 200–400 K, sometimes, the extremely low-energy processes of electronic relaxation can increase the thermal stability, so one has to put up with their small contribution to losses. In any case, with the object of lower losses, when microwave dielectrics elaboration or application one needs to avoid or to suppress the polar (non-centre symmetric) components in the composition of a dielectric, since dielectric losses in them are big because of strong coupling of optical and acoustic phonons.

Thermal stability is an essential property of microwave dielectrics, especially those ones using in the resonant microwave devices. By thermodynamics, it is possible to draw a very general conclusions about the physical nature of this or that temperature dependence of permittivity [3].

In the case of a temperature-independent permittivity: $\varepsilon(T) = Const$, for the polarization process, the internal energy U, entropy S, and free energy F can be expressed in terms of the permittivity and the electrical field strength:

$$U = U_0(T) + \frac{1}{2}\varepsilon\varepsilon_0 E^2,$$
$$S = S_0(T),$$
$$F = F_0(T) + \frac{1}{2}\varepsilon\varepsilon_0 E^2.$$

This means that if in a dielectric its permittivity is independent on temperature, the entropy S during polarisation process does not change, while the change of the internal energy U equals to the change of free energy F.

If the dielectric is not thermal stable, i.e., in the case of $\varepsilon = \varepsilon(T)$, quite different result is seen:

$$U = U_0(T) + \frac{1}{2}\varepsilon_0 \frac{\partial \varepsilon}{\partial T} E^2;$$

$$S = S_0(T) + \frac{1}{2}\varepsilon_0 \left[\varepsilon + T \frac{\partial \varepsilon}{\partial T} E^2 \right];$$

$$F = F_0(T) + \frac{1}{2}\varepsilon_0 \varepsilon E^2.$$

This means that, when such dielectric is polarizing, the variation of its free energy is the same as in previous case. However, the temperature-varying permittivity leads to the change in the entropy. In means, that if the temperature coefficient of permittivity is positive (TCε > 0, i.e., permittivity increases with dielectric heating), then the change in entropy in the process of polarization is also positive: ΔS > 0. Correspondingly, if the TCε < 0 the ΔS < 0.

Obtained result of a general phenomenological analysis is a rule common to all dielectrics: the positive temperature coefficient of permittivity (TCε > 0) corresponds to the case when electrical polarization lowers the degree of molecular ordering in the structure as the entropy increases.

If, on the other hand, TCε < 0, then the entropy of dielectrics in the external electrical field decreases, that is, their polarization corresponds to the higher degree of structural ordering.

Figure 5.3 confirms the regularity established above: in the dielectrics with pronounced relaxation polarization, a temperature maximum of permittivity usually occurs (the ferroelectrics have same property). Below the ε(T) maximum during temperature increase, the connection between the charged particles, participating in the polarization, is weakened due to their chaotic thermal motion.

The disordering of particles, i.e., the increase in entropy (ΔS > 0) facilitates the displacement of these particles in applied electrical field increasing the polarization, therefore, TCε > 0.

However, above the temperature maximum of permittivity, the electrical field partially suppresses thermal motion of charged particles, and therefore increases their ordering (ΔS < 0), corresponding to decrease of permittivity with temperature rise: TCε < 0 (Fig. 5.7.).

In the thermodynamic analysis, it is possible to consider, together with permittivity temperature change, the dielectric non-linearity ε(T,E), Fig. 5.3b. In the bias electrical field, the ε(T) maximum shifts towards lower temperatures and, accordingly, ΔS changes, in accordance with described mechanism: below ε(T) maximum the permittivity increases in the bias field, and above this maximum the permittivity in bias field decreases.

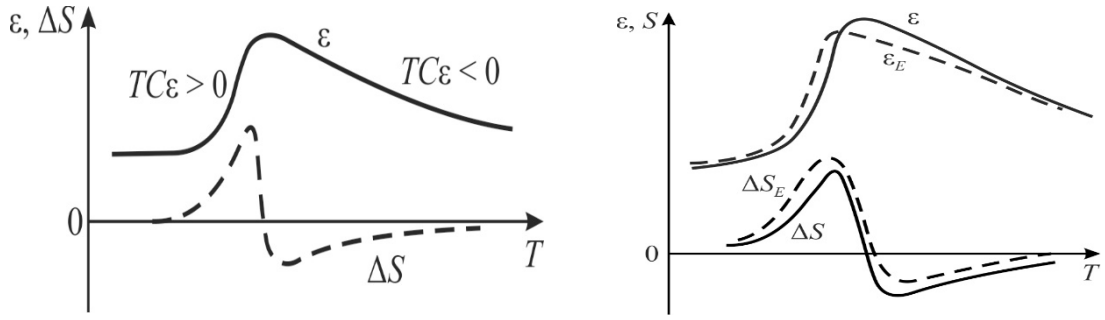

a b

Fig. 5.7. Temperature dependence of ε and entropy ΔS in dielectrics with thermally activated polarization: a – in weak electrical field, b – strong electrical bias field influence on ε and ΔS.

It is expedient to consider the above considerations on the examples of microwave dielectrics with increased permittivity. First, we can dwell on the ordered structures: on those ferroelectrics and antiferroelectrics, the parameters of which allow their application in the microwave range. In them, the structural ordering determines their parameter TCε > 0, since heating increases the disorder in their regular structure. Indeed, at frequency of 10 GHz, the ferroelectric $LiNbO_3$ has TCε = $+2\cdot10^{-4}$ K^{-1} (at $\varepsilon_{mw} \approx 50$ and $\tan\delta_{mw} < 10^{-3}$); while the antiferroelectric $NaNbO_3$ has TCε = $+10^{-3}$ K^{-1} (at $\varepsilon_{mw} \approx 200$ and $\tan\delta_{mw} = 2\cdot10^{-3}$). Both of these examples fully correspond to the thermodynamic prediction presented above: an ordered structure leads to a positive value of TCε, since the increase in temperature leads to the disordering and increase in entropy.

On the contrary, the paraelectrics have a disordered structure and, therefore, they must be characterized by the parameter TCε < 0, since the polarizing electrical field reduces their structural disordering. For example, the "soft" paraelectric $SrTiO_3$ has TCε = $-3\cdot10^{-3}$ K^{-1} (at $\varepsilon_{mw} \approx 300$ and $\tan\delta_{mw} = 3\cdot10^{-3}$) while the "hard" paraelectric $CaTiO_3$, described by TCε = $-1.6\cdot10^{-3}$ K^{-1} (at $\varepsilon_{mw} \approx 150$ and $\tan\delta_{mw} = 8\cdot10^{-3}$). Such a large temperature instability of permittivity hinders their application. Thus, the above examples confirm the general conclusions of thermodynamics, which should be taken into account when developing microwave dielectric compositions.

The nature of thermally stable permittivity in the polycrystalline microwave dielectrics can be different. In the centimeter waverange, the high-quality dielectrics with $\varepsilon \approx 30 \pm 10$ are mostly applied; their compositions is characterized by antipolar structure (close to the antiferroelectrics) with a weak tendency to have TCε > 0, which is compensated by the paraelectric component possessing TCε < 0. *The*

microwave dielectrics of the decimeter waverange with $\varepsilon \approx 120 \pm 40$ are based usually on the "hard" paraelectrics, thermal instability of which is suppressed by the paramagnetism of the rare-earth components and by the low-barrier electronic relaxation.

Permittivity electrical control**.** There are two significantly different ways to control dielectric permittivity with the aim of use microwave dielectrics in different functional devices.

First method lies in the direct electrical control by the permittivity of paraelectric film: this way allows to get high speed devices management but it is difficult to avoid noticeable losses in them.

Second technique is the electromechanically control by composite, consisting from low loss dielectric connected in series with air gap, which width is controlled by the piezoelectric.

Direct electrical control by permittivity on microwaves is appropriate only for the paraelectric phase of ferroelectrics, i.e., above the Curie point θ, where spontaneous polarization disappear, Fig. 5.8*a*, and there are no domains, which are the main source of dielectric losses.

Temperature dependence of permittivity of paraelectric is described by the Curie-Weiss law $\varepsilon = \dfrac{C}{(T-\theta)}$, Fig. 5.8*b,* while its dependence on applied electrical field shows the non-linearity, Fig. 5.8*c*.

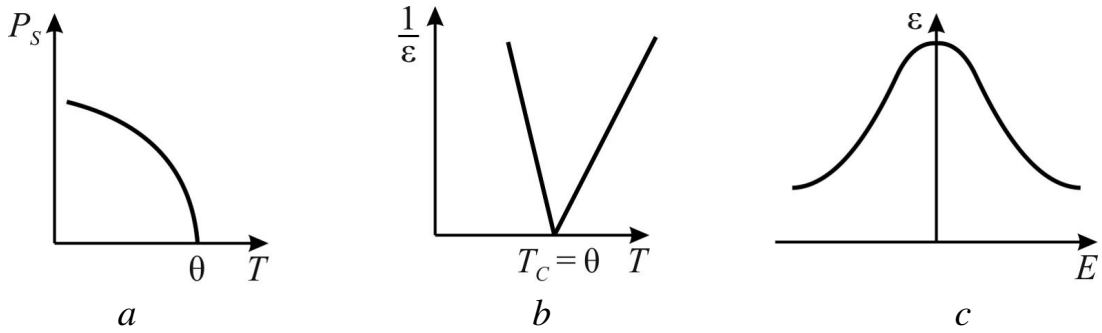

Fig. 5.8. *Temperature dependencies of spontaneous polarization* P_S *(*a*) and permittivity (*b*); as well as dielectric nonlinearity* ε*(*E*) in non-polar phase (*c*)*

General formula, that takes into account both ε-non-linearity and ε-temperature dependence is

$$\varepsilon(T, E) = \frac{C}{(T-\theta)}\left[1 + 3\beta\varepsilon_0^3 E^2 \frac{C^3}{(T-\theta)^3}\right]^{-\frac{1}{3}}$$

It is seen that in the paraelectric phase dielectric nonlinearity the higher the closer temperature to the phase transition point. The controlling field, at which the ε-tunability reach maximum, is $E_m = b[(T - \theta)/C]^{3/2}$. The values of a and b are the parameters of used material.

Electromechanical control by effective permittivity using tuneable dielectric composites with a controllable air slit. One way to achieve controllability of dielectric characteristics is the mechanical reconfiguration of microwave devices. In this case, the alteration of microwave devices parameters can be attained by the displacement of dielectric parts of devices.

Figure 5 shows the change in effective permittivity ε_{ef} in a rectangular waveguide partially filled by dielectric; with an increase in the thickness of the air gap Δ, the value of ε_{ef} decreases significantly, as does the value of dielectric lossesε $\tan\delta_{ef}$.

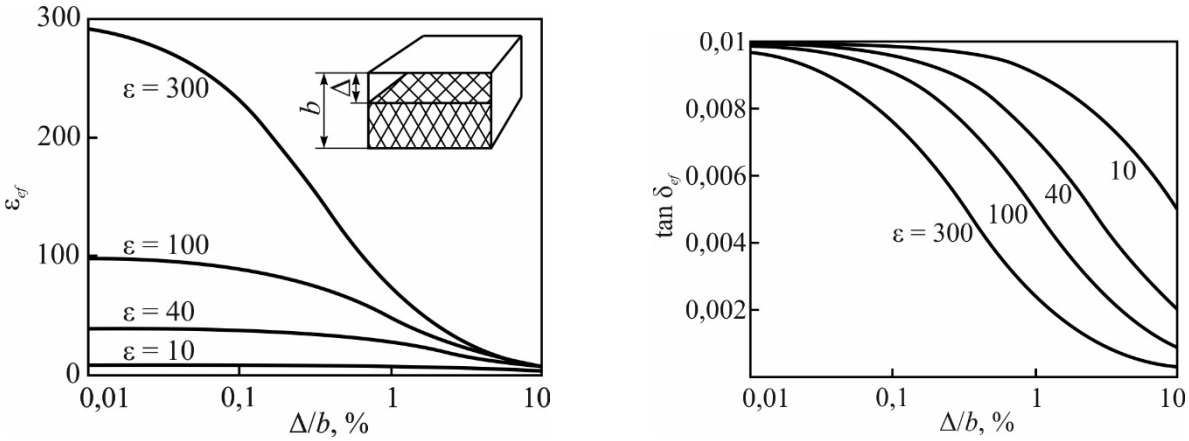

a *b*

Fig. 5.9. Effect of horizontal air gap between specimens in waveguide: *a* – effective permittivity, *b* – effective loss tangent

Electromechanical tuning is very promising to produce low insertion loss combined with good controllability of microwave subsystems. In case of electrical control by ferroelectric permittivity, the microwaves interact with the polar material, which is a part of microwave line; that is why transmitted energy is partially absorbed in the material. On the contrary, the mechanical system of controlling is located out of microwave propagation route, so it does not contribute to the microwave losses. Moreover, it will be shown that dielectric losses even have a trend to reduce in such devices. Mechanical control is valid at any frequency range, including millimetre waves range.

5.5 High quality thermal stable microwave dielectrics

Microwave dielectrics, which are mainly used in the resonant microwave devices of centimeter waverange, are characterized by a permittivity with $\varepsilon \approx 20$–40, which is the result of numerous scientific and technical developments summarized in books [1, 2]. The permittivity of these materials, although being not very high, Table 1, yet is quite sufficient for the excitation of dielectric resonances [3, 4]; at that, their losses is very small, providing the necessary Q-factor in resonant devices. As a rule, these polycrystalline materials have the oxygen-octahedral structure, representing multi-component compositions with a single-phase structure (multiphases increases dielectric losses). As main characteristic of these dielectrics, considered to be the quality factor $k = \nu/\tan\delta$, where ν is the frequency in gigahertz, Table 1, which takes into account the fact that $\tan\delta$ increases linearly with frequency rise. A successful combination of increased permittivity, low losses and thermal stability in these materials requires a more in-depth study of their physical nature in order to further progress in such developments.

Table 5.1.

Microwave permittivity ε_{mw} and quality factor k of some microwave dielectrics [1–4]

Ceramics	ε_{mw}	$k \cdot 1000$	Ceramics	ε_{mw}	$k \cdot 1000$
$(Mg,Ca)TiO_3$	20	50	$BaO_4 \cdot TiO_2$	37	30
$Ba(Sn,Mg,Ta)O_3$	40	200	$BaO_{4,5} \cdot TiO_2$	40	40
$Ba(Zr, Zn,Ta)O_3$	30	150	$CaTiO_3 \cdot LaAlO_3$	40	50
$(Zr, Sn)O_2 \cdot TiO_2$	38	50	$BaO \cdot Ln_2O_3 \cdot TiO_2$	80–120	3–7

[***Note.*** Ln – La, Gd, Nd, Sm, Eu]

The problem successfully solved in the development of these materials lies precisely in the single-phase structure achievement, which is possible to obtain if the components are close enough in their structure. (In principle, in multiphase mixtures it is possible to obtain need combination of components for one or another effective permittivity value, but inevitable phase boundaries are the source of microwave losses). In one of the given in Table 1 compositions, namely, the $CaTiO_3 \cdot LaAlO_3$, the single phase solid solution of the "hard" paraelectric $CaTiO_3$ (where $TC\varepsilon < 0$) and the antipolar material $LaAlO_3$ (close to antiferroelectrics) with $TC\varepsilon > 0$ is used.

It is obvious that when selecting their concentration, it is possible to get TCε ≈ 0.

Other methods of single-phase thermally stable microwave dielectrics obtaining are also being used, for example, by influencing on the mutual orientation of highly polarizable oxygen octahedra of "hard" paraelectrics. The reason for large permittivity in these paraelectrics is the high polarizability of electronic shells of oxygen ions forming the octahedron, while the location of central ions inside the octahedrons (visible in X-rays) can serve as the indicator of this interaction. The oxygen-octahedral structure almost always leads to a strong temperature dependence of the permittivity, but in some cases even leads to ferroelectricity. Fortunately, the degree of interaction of electronic shells between oxygen octahedra can be influenced by the placement of foreign ions with different configuration of electronic shells; and this is used in the development of microwave dielectrics. Single-phase structure of $BaTi_4O_9$ (barium tetratitanate) can serve as example of influence on oxygen electronic shells interaction in the octahedra, Fig. 5.10.

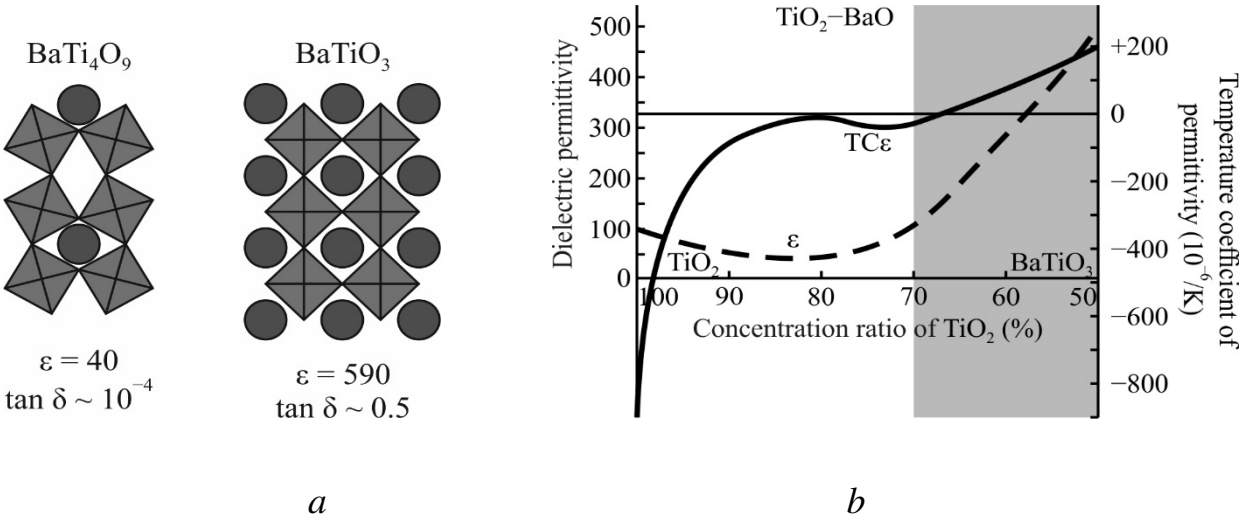

a *b*

Fig. 5.10. Oxides system of TiO_2–BaO peculiarities: *a* – two simplified structures; *b* – change of permittivity ε and $TC\varepsilon$ with TiO_2 content; shaded area corresponds to mixtures with big microwave losses

This thermal stable composition has increased permittivity and low microwave losses. Note that in the solid solution BaO-TiO_2 the temperature coefficient of permittivity changes significantly with the change in the components content. The fact is that the large Ba^{2+} ion with its unfilled 4f-shell is located between the oxygen octahedra of rutile effectively affecting the interaction of oxygen electronic shells. Simplified arrangements of Ba^{2+} ions between the octahedra in two compositions are shown in Fig. 5.10a. It is interesting to note that at a certain mutual arrangement of the octahedra a ferroelectricity can occur.

In the barium tetratitanate, the 4f/5d-hybrid orbitals of Ba^{2+} ions are localized

between the TiO_6 octahedra, preventing their usual interaction, so that only 20% of barium oxide reduces the permittivity of rutile by a factor of three. The point is that the electronic shells of O^{2-} ions, when interacting with the shells of Ba^{2+} ions, can lead to paramagnetic phenomena in the normally unfilled 4f shells of barium ions, so paramagnetism manifestation can suppress paraelectric's temperature dependence of permittivity that will be shown below. In any case, the main reason for decrease of large negative value rutile's TCε is a weakening in the interaction between electronic shells of the oxygen in octahedra. When their regularity changes, the agreement in mutual displacements of central Ti^{4+} ions is disturbed, and in $BaO:4TiO_2$ composition, the value of TCε becomes practically zero.

At the same time, the new regularity in the arrangement of octahedra (in comparison with rutile) does not prevent the formation of a single-phase structure, and, therefore, the microwave losses of barium tetratitanate are small. But with a subsequent increase of barium oxide, the TCε concentration dependence, crossing the zero value, goes to positive TCε, however, all subsequent compositions from $BaO\text{-}TiO_2$ system are already multiphase and have increased dielectric losses. Note that in this system at the 50% BaO concentration the $BaTiO_3$ ferroelectric is formed, its ordered structure upon polarization leads to a positive change in entropy $\Delta S > 0$ and naturally to a positive $TC\varepsilon > 0$. At that, such a structure promotes correlated displacement of central ions in octahedra with the appearance of internal polarity, which is accompanied by a very large microwave losses.

5.6 Large permittivity thermal stable microwave dielectrics

The thermally stable microwave ceramics required for use in the meter and decimeter wavelength ranges must have a large permittivity $\varepsilon \approx 80–160$, although it does not achieve big quality parameter, Table 1. The mechanism of thermal stability in these compositions is different than that described in the previous section: the main role play the oxides of paramagnetic atoms combined with a perovskite-like structure. Table 5.2 shows the permittivity and its temperature coefficient for special selected simple solid solution $Ln_{2.3-x}M_{3x}TiO_3$, where Ln is one of the rare earth elements of cerium series, and M indicates monovalent alkali metal ions need to compensate for trivalent ions of lanthanide. In all these compositions, from Ce to Gd, as the paramagnetism increases, TCε decreases strongly so the paraelectric Curie-Weiss law in the rutile becomes suppressed. This process develops so strongly that TCε changes its sign already at the Hb-Sm boundary. In this case, a very

important factor is the fact that the permittivity of all composition remains very high, and does not drop by a factor of three, as in the case of barium tetratitanate.

Table 5.2. Permittivity ε and $TC\varepsilon$ in lanthanoids

Parameter	***Lanthanoid***								
	^{0}La	^{1}Ce	^{2}Pr	^{3}Nd	^{5}Sm	^{6}Eu	^{7}Gd	TiO_2	$CaTiO_3$
ε_{mw}	110	90	85	83	80	75	65	100	150
TCε,*10^{-6}K^{-1}*	– 700	– 400	– 250	– 80	+ 60	+ 100	+ 160	– 900	– 1600

[***Note.*** Filling of 4*f*-shell is shown by index; TiO_2 and $CaTiO_3$ parameters are given for comparison].

With such results, the getting close to zero $TC\varepsilon$ seems to be a matter of common technique: in the solid solution one component should be characterized by the positive and the other negative temperature coefficient. Then it is not difficult to choose the required ratio of the concentrations of components, which makes it possible to achieve $TC\varepsilon \approx 0$. It follows from Table 2 that in the case of Ln = La, Ce, Pr, Nd, the composition $Ln_{2.3-x}M_{3x}TiO_3$ is characterized by $TC\varepsilon < 0$, but in the case of Ln = Sm, Eu , Eu, Gd, permittivity temperature coefficient is positive $TC\varepsilon > 0$. That is why, the (Nd-Sm) $M_{3x}TiO_3$ solid solution has compensated value $TC\varepsilon \rightarrow 0$ with almost the same ratio of components, while having significant permittivity $\varepsilon_{mw} \approx 80$.

Temperature dependences of permittivity and losses $\tan\delta$ in the solid solutions mentioned above, Fig. 5.7, indicate the anomalies in $\varepsilon(T)$, which are accompanied by the maxima of $\tan\delta(T)$, which is the usual characteristic of relaxation polarization. Taking into account low temperatures of these anomalies, we can conclude that the low-barrier electronic relaxation takes place in this case. At the same time, the maxima $\varepsilon(T)$ and $\tan\delta(T)$ decrease along the La-Pr-Nd line (but disappear for Sm), and shift to lower temperatures. On the contrary, with increasing frequency, the dielectric loss maxima shift towards higher frequencies. Owing to low activation energy, maxima of relaxation losses are also visible at sufficiently high temperatures, but at very high frequencies of 100–200 GHz.

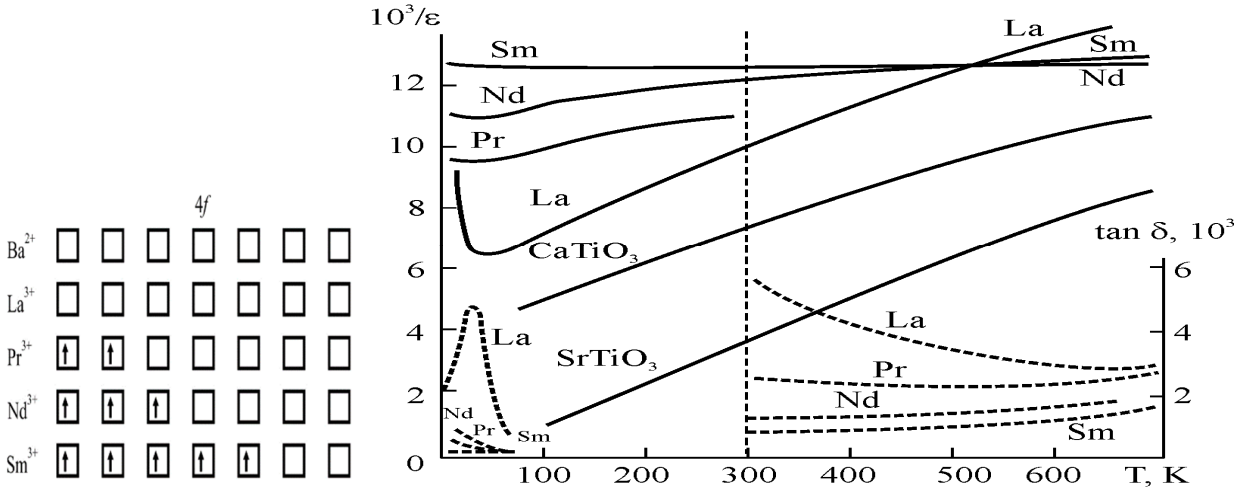

a *b*

Fig. 5.11. Temperature dependence of permittivity in based onTiO_2-Ln_2O_3 compositions: *a* – electronic spins filling in 4*f*-shells of REE; *b* – 1/*ε* (solid curves) and tanδ (dashed curves) for composition with Ln = La, Pr, Nd, Sm and in pure TiO_2, $CaTiO_3$ and $SrTiO_3$; below 300 K measurements at 1 MHz, above 300 K frequency is 10 GHz

In practice, more technological compositions are used $BaLn_2Ti_4O_{12}$ (BLTs) given the fact that Ba also belongs to 4*f* metals, although with the unfilled 4*f*-shell. This is also a microwave material close to the paraelectrics but containing rare earth oxides and BaO as components. These polycrystalline dielectrics differ significantly from other microwave ceramics: the permittivity in BLTs is several times higher than in other types of such materials. As was shown earlier with an example of rutile, there are certain possibilities to influence properties of this material by the distributing various ions between oxygen octahedra. In other words, BLTs dielectric properties can be controlled by the degree of interaction of electronic shells with their mutual displacement, using the introduction of various ions into a structure, like in Fig. 5.11*a*. The electronic configuration of the trivalent lanthanum ion is $5s^25f^6$ resembles the Ba^{2+} ion, but the size of the La^{3+} ion is much smaller than that of the Ba^{2+} ion. It should also be noted that both of them are diamagnets, since the La^{3+} ion (like the Ba^{2+} ion) has empty 4*f* shell. Nevertheless, when BaO is combined with rutile, the permittivity decreases by a factor of 3, while in the TiO_2–La_2O_3 compositions, their microwave permittivity remains almost same as that of rutile, i.e., of about 100, and $TC\varepsilon$ practically no changes, Table 2. Only when in 4*f* shells of rare earth elements the uncompensated spins appear and gradually increase their number, the important parameter $TC\varepsilon$ begins rapidly approach zero, i.e., the paramagnetism, as it were suppresses paraelectricity.

To explain a successful combination of large microwave permittivity and its

thermal stability in the BLTs, the following physical reasons can be proposed: firstly, the paramagnetism of rare-earth ions included in the composition, and, secondly, the low-temperature relaxation of weakly bound electrons, which smoothes the permittivity temperature dependence.

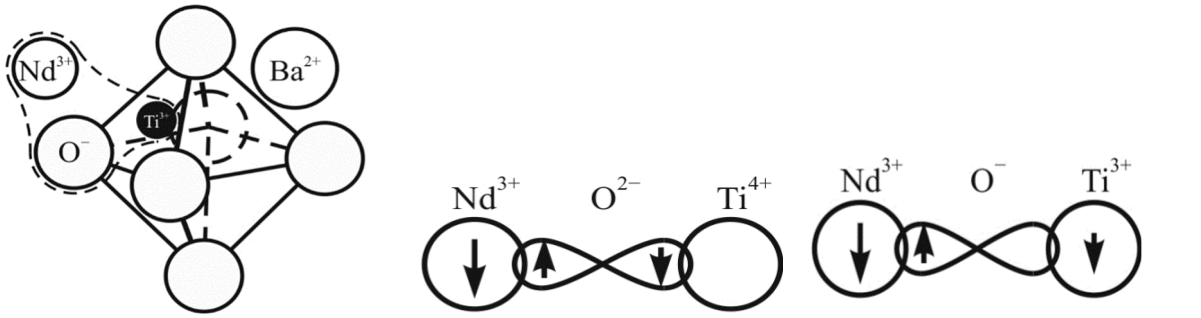

a *b* *c*

Fig. 5.12. Electronic spins interaction composition Ba^{2+}–Nd^{3+}–O^{2-}–Ti^{4+}: *a* – elementary cell, *b* – ground state; *c* – excited state

In the first case, the paramagnetic lanthanide ions, through the oxygen ions, can enter into the indirect exchange interaction with tetravalent titanium ions located in the center of octahedra, which largely determines the polarization of BLT structure. The magnetic moments of spins in the shells of 4*f* elements through diamagnetic oxygen ions perturb electronic shells: O^{-2}–$Ti^{+4} \Leftrightarrow O^{-}$–$Ti^{+3}$. According to thermodynamic analysis, such binding of electronic shells (destroying by thermal motion) increases the polarization entropy and makes need positive contribution to *TCε.* By this way, in the compositions of BLT type, paramagnesism of lanthanides significantly affects the BLTs thermal stability, Fig. 5.12 and Table 2. The increase in the magnetic moment from 1 to 7 Bohr magnetons in the cerium series of lanthanoids, possessing electronic configuration $4f^{(1\ldots7)}5s^25p^6$, consistently brings *TCε* value closer to zero and even leads to change in its sign.

Secondly, it is necessary to note the other possible mechanism that makes it possible to reduce *TCε*-parameter in BLTs compositions. Low-temperature studies of rutile-lanthonoid compositions in a wide frequency range [5] indicate a significant manifestation of the electronic relaxation due to movement of electrons belonging to 4*f*/5*d* hybrid bonds. They can suppress the temperature dependence of soft lattice mode responsible for temperature instability of perovskite paraelectrics. It is noteworthy that the configuration of $4f^05s^2$ shell for La^{3+} and Ba^{2+} ions is similar, and both of them are the diamagnetics, since in the still existing energy level 4*f* electrons are missing. It can be assumed, however, that a virtual appearance of electrons in the 4*f* level, accompanied by paramagnetic fluctuations in the strongly polarizable lattice, is quite possible. It is important to note that the radius of La^{3+}

ion (~ 0.1 nm) is much smaller than radius of the Ba^{2+} ion (~ 0.16 nm), so that the La_2O_3 component practically does not change the properties of a rutile (TiO_2), as can be seen from Fig. 5.12*b* and Table 2 (in contrast to the BaO component, which leads to the strongest effects shown earlier in Fig. 5.12*b*). The confirmation of the above assumption is Fig. 5.13*a* which shows the characteristics of La-BLT.

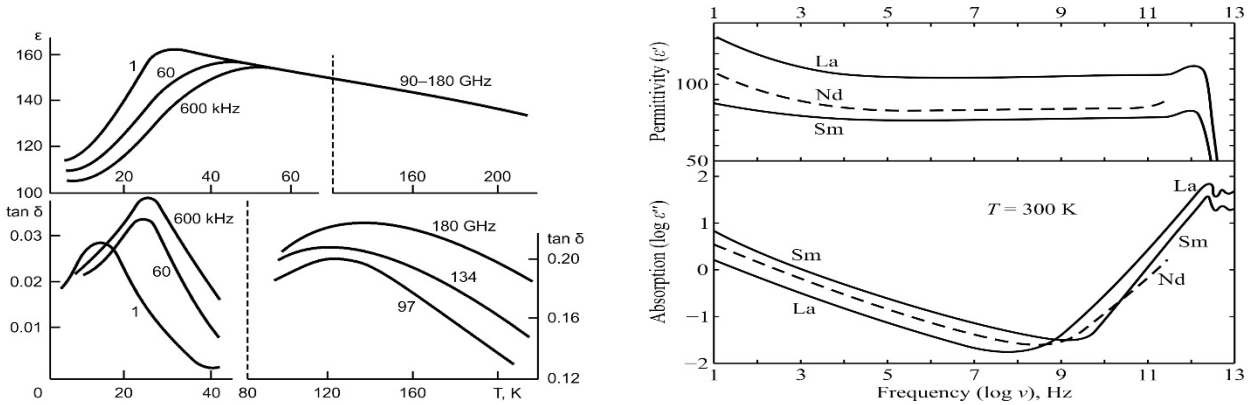

a *b*

Fig. 5.13. Electronic relaxation in BLT-type compositions: *a* – La-composition in frequency-temperature intervals; *b* – dielectric spectra of some BLTs at temperature ~ 300 K

Above temperatures 50–100 K, the properties of the La-composition are very close to those of TiO_2 in terms of both permittivity and $TC\varepsilon$, Table 2. This means that La^{+3} practically does not change the paraelectric properties of TiO_2 at normal temperatures. But at lower temperatures in the La^{+3}-composition, in contrast to rutile, permittivity decreases, which on average reduces the $TC\varepsilon$ of rutile. This relaxation leads not only to the maximum $\varepsilon(T)$ but also to the maximum $\tan\delta(T)$ with a shift higher temperatures as the frequency increases (characteristic of relaxation processes). It is important to note that the continuation of this relaxation process is also noticeable in the microwave range. In various BLTs, the traces of this relaxation are also visible at microwaves: the frequency dependence $\tan\delta$ shows minimum near 8–10 GHz, Fig. 5.13*b*, since decreasing with frequency relaxation losses are overlapped by the increase in fundamental lattice losses.

Dielectric losses in the structures of the BLT type can be caused by a structural mismatchб due to which the nanoscale islands of undesirable polar phase can appear. In addition, the grain boundaries of polycrystalline material always have disordered structure, the dielectric relaxation of which can extend to the microwave range. [6]. Thus, the larger permittivity of microwave dielectrics is due to the use of paraelectric octahedron structures, in which the ionic-covalent bonding leads to a soft mode of lattice vibrations. Both low-energy electronic polarization and paramagnetic

components of compositions affect the interaction of electronuc shells of oxygen octahedra, contributing to the smoothing of the temperature dependence of permittivity.

5.7 Electrically tunable microwave dielectrics

The field dependence of dielectric permittivity is known as *dielectric non-linearity*: $N_\varepsilon = \varepsilon^{-1} d\varepsilon/dE$, and this parameter increases in a cubic power with the ε-value: $N_\varepsilon \sim \varepsilon^3$. So it is obvious that the influence of electrical bias field is most pronounced near the ferroelectric phase transition, where $\varepsilon(T)$ has maximum at Curie temperature $T_C \approx \theta$. In the vicinity of its maximum, the permittivity can be strongly controlled by the electrical bias field E_b, and it is precisely this that is used for microwave signal phase controlling: $\varepsilon(E_b) = [C/(T - \theta)](1 + aE_b^2)^{-1/3}$. The bias field, at which tunability has maximum, is given by relation $E_m = b[(T - \theta)/C]^{3/2}$. The values of a and b are parameters of used material.

The permittivity in the paraelectric film is much lower than in the bulk material; obviously, this effect is accompanied by the decrease of film tunability. However, the smaller permittivity is quite desirable for microwave applications in order to increase the impedance condition of tunable part with transmission line. Thus, the elaboration of phase shifter needs to use a compromise between the value of permittivity and its tunability in the chosen paraelectric layer. Additional compromise needs between the film tunability and microwave loss. Mode of functioning for coplanar line phase shifter is explained in Fig. 5.14. The main principle of phase shifter operation is the control over the propagation constant in the tunable part of microwave line.

Paraelectric phase shifter. At lower frequencies, the ferroelectrics are well known tuneable dielectric materials: the permittivity of these materials can be changed under applied electrical bias field; in microwaves, the ability to control by permittivity in the waveguides is also possible but only with the use of paraelectrics above ferroelectric phase transition (below it ferroelectric components show large losses). Controllable permittivity leads to the alteration of microwave components characteristics such as the propagation constants, resonant frequency, antenna beam direction, etc. Recently the processing of paraelectric thin film becomes perfect enough, so the tunable microwave device based on them are competitive with the microwave ferrites (with μ-controlling) and PIN diode (with σ-controlling). At that, advantages of paraelectric (with ε-controlling) are greater speed, increased power,

good matching with MMIC technology. Processing of paraelectric thin films becomes perfect enough; as a result, tunable microwave device based on them film is competitive with the microwave ferrite and PIN diode. To compare with microwave ferrite devices (μ-controlling) and semiconductors (σ-controlling), the advantages of paraelectric (ε-controlling) are: essentially bigger rapidity, increased microwave power, good matching with semiconductor-based MMIC technology and possibility to use paraelectric device at much higher frequencies.

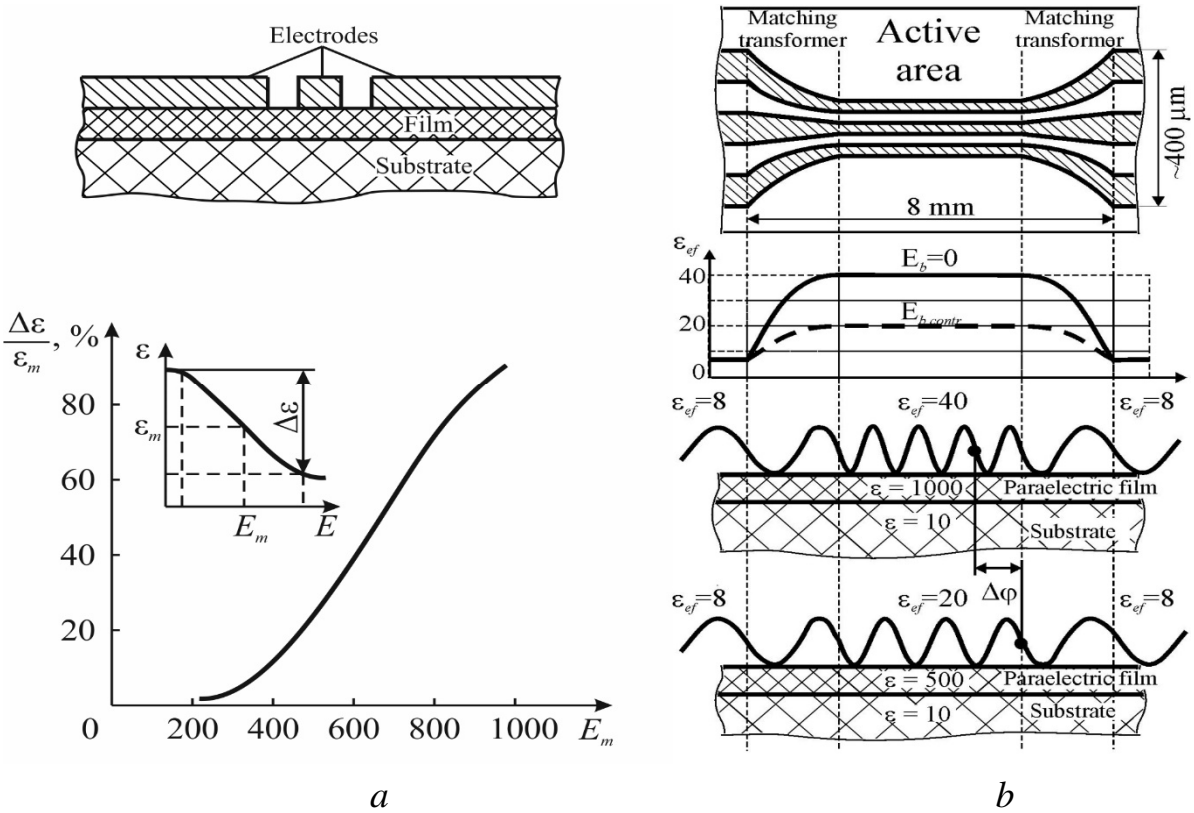

a *b*

Fig. 5.14. Coplanar line phase shifter: *a* – cross profile of controllable coplanar line (upstairs) and permittivity handling by electrical field (down), *b* – phase shifter operation

One of many possible applications is the phase shifters, based on integrated paraelectric film, which have advantages in high operation speed, low cost and size, and the possibility to use microwave integrated circuits (MMIC). The optimal design of phase shifters requires simulation; at that, for paraelectric films microwave application the coplanar line is chosen as a rational design. The point is that central electrode of this line is very convenient to apply the controlling voltage.

Permittivity control at microwaves by bias electrical field (E_b) is presented in Fig. 5.14*a*. As shown in the lower (left) insertion, permittivity decreases with controlling electrical field while the middle field E_m corresponds to themiddle value of permittivity: $\varepsilon_m = (\varepsilon_{E=0} + \varepsilon_{Em})/2$. Permittivity changing $\Delta\varepsilon = \varepsilon_{E=0} - \varepsilon_{Em}$ depends on ε-value. Its relative change is $\Delta\varepsilon/\varepsilon_m$ can provide a controllable phase shift runs

up to 2π. Field dependence of permittivity is the dielectric non-linearity: $N_\varepsilon = \varepsilon^{-1}\mathrm{d}\varepsilon/\mathrm{d}E$, and this parameter increases in a cubic power with ε-value: $N_\varepsilon \sim \varepsilon^3$. So it is obvious that the electrical field influence is most pronounced near the ferroelectric phase transition, where ε has a maximum at Curie temperature $T_C \approx \theta$. In the vicinity of temperature maximum, permittivity can be strongly controlled by electrical bias field E_b, and this that is used for microwave devices controlling. In contrast to ferroelectric, the paraelectric material has no domains, and no microwave dielectric dispersion.

As a result, microwave losses of paraelectrics are not large. The large permittivity is due to the low frequency of the transverse optical mode ω_{TO}, and its decreases in the controlling field due to increase in the rigidity of inter-ionic bonds. This rigidity is further increased in the paraelectric film deposited on hard substrate (usually this MgO with high speed of sound and large thermal conductivity). In this case, the temperature dependence of the permittivity and the dielectric losses of a paraelectric film decrease many times over. Because of ε-value in the paraelectric film is much lower than in bulk material, this is obviously accompanied by the decrease of ε-tuneability. However, smaller ε is quite desirable for microwave applications to increase the impedance of tunable part of transmission line. Thus, the elaboration of phase shifter needs to use a compromise between ε-magnitude and ε-tuneability in paraelectric layer; additional compromise needs between film tuneability and microwave loss.

The design of paraelectric a phase shifter requires simulation. As shown in Fig. 5.14*c* phase shifter consists of five important components: paraelectric thin film, dielectric substrate, electrodes and interfaces film/electrode and film/substrate. To obtain desirable microwave performances (phase shift $\Delta\varphi$, insertion loss I_L, impedance Z_0, etc.) the design of such phase shifter can be elaborated exceptionally with use of simulation. Exclusively by the optimization, required active and passive dielectric layers as well as metallic guides collocations might be obtained. The coplanar line is formed by electrodes deposited on film-on-substrate surface, Fig. 5.10c. Electrodes collocation has strong influence onto line impedance Z_0 and effective permittivity ε_{ef}. Simulations show that, for practical purposes, there is no considerable difference in values of Z_0 and ε_{ef} for buried electrodes and electrodes deposited onto film. In our experiments, gold electrodes were deposited as chemically inert and high conductivity material [8-10].

Mode of functioning for coplanar line phase shifter can be explained in such way. The main principle of phase shifter operation is a control over propagation

constant in the microwave line. Toward this end, MMIC substrate with ε_S ~ 10 (silicon, gallium arsenide, magnesium oxide, etc.) is covered by thin paraelectric film and next by electrodes that actually form the coplanar line. Film permittivity is changed within the limits of ε = 1000–500 by bias E_b voltage. As a result, the effective permittivity of this composite (film + substrate + air) is controlled in the range of ε_{ef} = 40–20. Coplanar design evidently shows advantage of composite structure: pure paraelectric with its middle ε ~ 700 reflects practically 100% microwave signal while created composite has middle ε ~ 30 which is possible to match with passive part of coplanar line. The controlling change of electrical length of line going on in its active area. It varies proportional to $(\varepsilon_{ef})^{1/2}$, that produces the required phase change $\Delta\varphi$. If E_b = 0, the active aria of phase shifter has electrical length equal to four waves, under the bias field it decreases to three waves that generates 2π phase shift. The matching parts are used to join low-impedance active area with other coplanar line, Fig. 8c, and this is quite necessary parts of device. While investigations with network analyzer, a broadband matching of 5–10 Ohms phase shifter active area with 50-Ohms line should be applied. The novelty of this broadband matching transformer is that it uses same film in which ε_{ef} is controlled by same bias voltage. This results in the self-acting trimming, correspondingly to actual phase shift. At that, applied matching transformers are quite long (being broadband) and they represents exponent taper transformer [11, 12].

Tuneable dielectric composites with a controllable air slit permits external control of dielectric-based devices using their electromechanical reconfiguration by displacement of some dielectric parts: for instance, to realize phase shifters with microstrip lines or coplanar lines. Mode of functioning of such devices is similar to the paraelectric phase shifter, but instead of control by the large permittivity by strong voltage, a much lower effective permittivity is governing by the low voltage. At that, such artificially tunable microwave air-layered composite has low insertion loss up to millimeter waves inclusively. In others such devices, microwaves directly interact with the "active" material (ferrite, semiconductor, or ferroelectric) which are the interior parts of devices, so microwave energy is inevitably partially absorbed by these materials. However, the electromechanical contrivances use for frequency tuning the fixtures located outside of microwave path, so they do not lead to the microwave losses of tunable device. Rather fast (10^{-5} s) and miniature piezoelectric actuators are elaborated and tested for dielectric composites tuning. Modern piezo-actuators made of electrostrictive materials show no hysteresis and work with a relatively small displacement (usually less than 100μm) but with a high accuracy

(about 0.01 μm). To make use of advanced actuators at microwaves, a new designs for many tunable microwave dielectric components is elaborated. The key idea is to provide a strong perturbation in the electromagnetic field in the region influenced directly by mechanical control. For that, tunable discontinuity (air gap) is created perpendicularly to the pathway of electrical field lines. Tunable air gap is placed between dielectric plates or between dielectric plate and electrode; in addition, to decrease the air gap thickness required for tuning, the microwave dielectrics with higher permittivity should be utilized.

As an illustrative example, here is first given the tunable dielectric resonator (DR) made from low loss microwave ceramics ($\tan\delta \sim 10^{-4}$) possessing high and thermal stable permittivity. Such controllable macro-composites of "dielectric – air slit" type might be used in the frequency-agile microwave device like filters. At that, the location of the controlled air gap is of great importance. Figure 9 shows two cylindrical DRs with the $H_{01\delta}$ mode separated by the air gap Δ constituting the binary DR. On Fig. 5.15*a*, the slot is located along the lines of electrical field inside of resonator, while in Fig. 9*b*, it intersects them, which leads to more efficient control of the resonator frequency, Fig. 5.15c, where slot DR creates a noticeable perturbation of electromagnetic field, and, as a result, it significantly shifts resonant frequency.

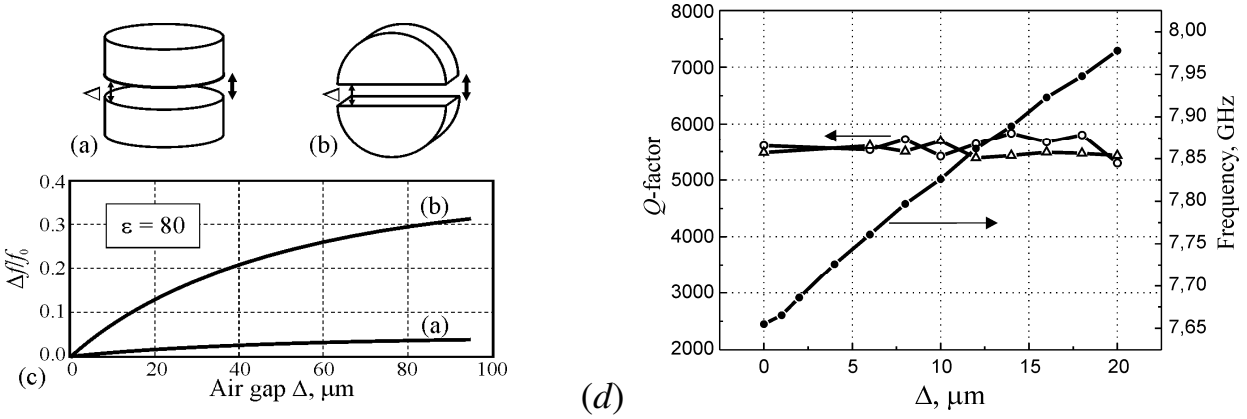

Fig. 5.15. Binary dielectric resonators mechanical tuning at 10 GHz: *a* – parallel location of gap; *b* –perpendicular location of gap; *c* – tunability comparison, *d* – resonant frequency f_0 and *Q*-factor dependence of slot dielectric resonator gap thickness

Slot DR testing is shown in Fig. 5.15*d*; it is remarkable that no change in quality factor *Q* is observed during air gap alteration. The resonant frequency of the basic mode changes up to tens percent while the displacement of slot DR parts is no more than tens of micrometer (depending on the permittivity of DR material). This range of displacement is achievable for modern piezo-actuators and MEMS. Second

example of the tuneable composite is integrated with stripline band-transmitting filter, which diagram and design are shown in Fig. 5.15.

Used technique of tuning is capable to transform any microstrip filter into a frequency agile device. With this purpose, the substrate located under the microstrip filter is converted into "tunable dielectric". Namely, the part of ground electrode (just under the filter) is removed being substituted by the closely adjoining to substrate metallic membrane moving by piezoelectric actuator. The thickness of the narrow air gap (Δ) is piezo-electrically controlled: the scope of air slit is changed. In given experiment, effective permittivity of layered dielectric "alumina – air" decreases from $\varepsilon_{ef} \approx 7$ till $\varepsilon_{ef} \approx 3$, while the air gap changes from $\Delta \sim 10$ μm till $\Delta \sim 100$ μm under controlling voltage of about 300 V.

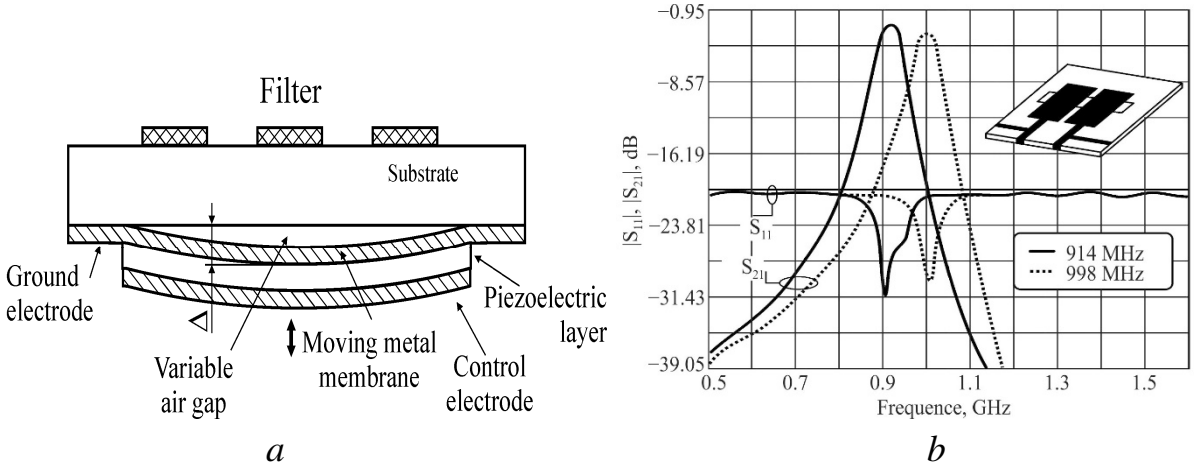

Fig. 5.15. Principle of effective permittivity tuning by moveable substrate: *a* – side view of piezo-moving ground electrode under substrate, *b* – two-resonator tunable filter` design

Tunable dielectric-air structures were studied as in the rectangular waveguide, so in microstrip and coplanar designs. This way of controlling allows to increase device's controllability while maintain low loss. Simulations were verified and proven by the experiment. With scaling down and move to higher frequencies, required displacements could be reduced to tens micrometers, thus allowing a utilization of small and fast piezo-actuators or MEMS.

Dielectric-air composite phase shifter with microstrip line looks convenient for use in modern microwave systems [3,14]. Microstrip lines interconnect oscillators, amplifiers, antennas, and so on. Sections of transmission lines also used as coupling element for resonators. Usually, characteristics of transmission line are defined at design time and remain constant in fabricated device. However, transmission lines can get some tuneability. For example, movement of dielectric body *above* the microstrip or coplanar line surface results in propagation constant change. It is possible to show that the most efficient control can be achieved, if one

of the conductors is detached from substrate's surface. By this way, a controllable air-dielectric composite is created. Because the tuneable discontinuity crosses electrical field strength lines, it results in high sensitivity.

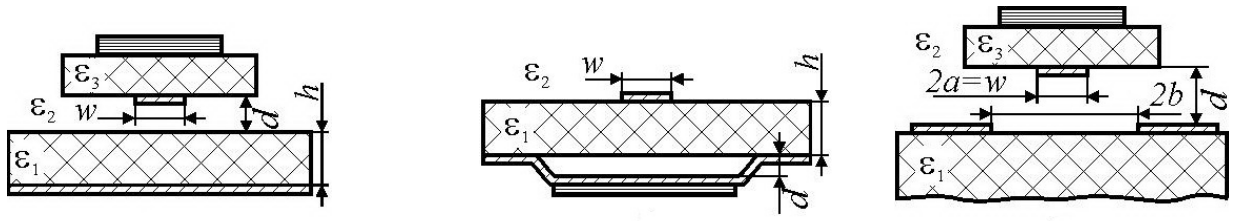

a *b* *c*

Fig. 5.16. Profiles of electromechanically controllable microstrip lines (*a, b*) and coplanar line (*c*); piezoelectric element is shown by horizontal touch lines

Principal designs of piezo-driven phase shifters based on the microstrip and coplanar lines are shown in , Fig. 5.16. Experiments and calculations show that their phase shifting is strongly dependent on the design architecture. It should be noted that designs, shown in Fig. 5.16, *a* and *c,* need some additional trouble in allocation of piezoelectric actuator. This problem is much easier in the case of the air slit opened *in the bottom* (ground) electrode which is partially substituted by the piezoelectric plate, Fig. 5.16*b*. In all cases, dielectric discontinuity is created in the plane perpendicular to electrical field of the microstrip (or coplanar) line. As seen, the tuneability of mictrostrip line with *detached upper electrode* is higher than for design presented in Fig. 5.16. It is obvious that designs shown in Fig. 5.16*c* shows higher effect because dielectric discontinuity is created in the plane perpendicular to the electrical field of microstrip line. It is necessary to note that tuneability of mictrostrip line with disconnected bottom electrode stays between two discussed designs but closer to design with detached upper electrode.

Situation becomes different as substrate permittivity is varied. As substrate's permittivity increases, the lesser is influence of the moving body. In contrast, with detached electrode the effect of electromagnetic field redistribution becomes stronger. The absolute values of the latter design exceed their counterparts in times. Presented analysis allows the conclusion that, generally, the low-impedance lines tend to exhibit higher controllability. This can be achieved not only by utilizing high-permittivity materials, but with a proper layout as well. Redistribution of electromagnetic energy to air-filled domains changes also the losses in the system. Because the air is almost lossless medium, the portion of energy confined in air filled domains experience practically no dielectric loss. Consequently more energy reaches output terminal, resulting in lower effective loss.

5.8 Summary Chapter 5

Conclusions

The general thermodynamic problem is considered regarding the mechanisms leading to the positive or negative value of temperature coefficient of permittivity. It is shown also that dielectric losses in the microwave dielectrics are due to the polar phase presence as in base material so in grain boundaries of ceramics. To improve properties of microwave high-permittivity dielectrics, three points are stated. First, high permittivity at microwaves can be obtained only in the crystals, possessing low frequency transverse optical lattice mode; as a rule, in the paraelectric-like materials. Second, small dielectric losses can be achived only in the monophase compositions based on "hard" paraelectric materials, in structure of which any internal polarity is absent for natural reasons. Third, thermal non-stability of the basic materials (oxigen-octahedral structures) can be suppressed by the imbedded between octahedrons foreign ions, including the paramagnetic components.

References

[1] M. T. Sebastian, *Dielectric materials for wireless communication*, ELSEVIER, 2008.

[2] M.T. Sebastian, R. Ubic, H. Jantunen, *Microwave materials and applications*, Wiley, 2017

[3] Yu.M. Poplavko, *Physics of dielectrics* (in Russian), Ed. Vischa shoola, Ukraine, Kiev. 1980.

[4]Yu. M. Poplavko, *Nature of dielectrics thermal stability in microwave range* (*in Russian*). Izvestia Akad. Nauk, Seria Physicheskay, 1996, 60, 10, pp. 167–172.

[5] Yu. M. Poplavko. *Dielectric spectroscopy of electronic materials*. *Applied physics of dielectrics*. ELSEVIAR, 2021.

[6] Yu. M. Poplavko, Yu. V. Didenko, *Polarization mechanisms in thermal stable microwave BLT ceramics*, Electronics and Electronics and Communications, 2015, 20, 1, pp. 18–22.

[7] Yu. M. Poplavko, *Nature of dielectrics thermal stability in microwave range* (*in Russian*). Izvestia Akad. Nauk, Seria Physicheskay, 1996, 60, 10, pp. 167–172.

[8] Yu.M. Poplavko, V.A. Kazmirenko. *Ferroelectric thin film microwave examination*. Ferroelectrics. 2003. Vol. 286. pp. 353–356.

[9] Yu.M. Poplavko, V.A. Kazmirenko, Yu. V. Prokopenko. *Measurement of bulk and film ferroelectric materials properties at microwaves* Microwaves, Radar and Wireless Communications, 2002. MIKON-2002. 14th Intern. Conference, Vol. 2, 2002, pp. 397–400.

[10] Yu.M. Poplavko,V.A. Kazmirernko, M. Kim, S. Baik, *Electrode-less technique of ferroelectric film study at microwaves,* 10th Europ. Meet. on Ferroelectricity. 2003, Cambridge UK, p. 178.

[11] Yu.M. Poplavko,V.A. Kazmirernko, M. Kim, S. Baik, *Contemporary waveguide technique of ferroelectric materials study by vector network analyzer*. Intern. Microwave Symposium, June 13, 2003, Philadelphia, ARF-61-14, P. 437–440.

[12] Yu.M. Poplavko, B. Kim, V. Kazmirenko, Y. Prokopenko, Non-resonant electrode less method for measurement the microwave complex permittivity of ferroelectric films, Measurement Science and Technology, Vol. 16, 2005, pp. 1792-1797,

[13] E. Furman, M, Lanagan, I. Golubeva, Yu. Poplavko. Piezo-controlled microwave frequency agile dielectric devices, IEEE International Frequency Control Symposium and Exposition, Montréal, Canada, Aug. 2004, P.266 – 271.

[14] Yu.V. Prokopenko, Yu.M. Poplavko, N. Ruda, Dielectric-Air structure as component of electromechanically controlled microwave devices, Int. Conf. Mathematical Methods in Electromagnetic Theory, 2010, Kiev, pp. 71-75.

Questions

1. List main classes of microwave dielectrics in connection with their applications.
2. What main polarization mechanisms provides microwaves dielectrics properties.
3. What means functional microwave dielectrics?
4. What properties of functional dielectrics are used in microwaves?
5. What are the reasons of high temperature stability in microwave dielectrics?
6. What are the reasons of large permittivity in thermal stable microwave dielectrics?
7. List main applications of electrically tunable microwave dielectrics.

CHAPTER 6. MICROWAVE ABSORPTION IN SHIELDING COATINGS

Contents

When analyzing the effectiveness of composites, which absorb microwave radiation, it is necessary to highlight the basic principles that describe the absorption of electromagnetic waves in solids, which is used in these composites. In these Chapter, the optimal electromagnetic parameters are analyzed need for the absorbing and shielding microwave composites. Main mechanisms are being discussed how electromagnetic wave loses its energy due to its interaction with absorber's molecular and electronic structure, which is different in the bulk and low-dimensional material. Different reasons of microwave absorption and its reflection in the metals, semiconductors, dielectrics and magnets are considered, taking into account the size effects, since these materials are included in composite in a crushed form. It is shown that absorption capacity of conductive and magnetic fillers decreases with increasing frequency, while fillers made of the high-loss dielectric increase their absorbance with frequency rise.

6.1 The need to create microwave absorbers

The interest in the radio-absorbing materials, especially for microwave technologies, is constantly growing: they have application not only in the military systems but also for civilian using (electromagnetic interference reduction between components and circuits, backward radiation reduction of microstrip radiators etc). In addition to the technological interests, the problem of microwave absorbers is important for biology and medicine, because in connection with fast expansion of telecommunication frequencies the public is concerned about possible influence of high-frequency electromagnetic field on human health.

Microwave absorbing materials are represented by different types of composites, which combine large microwave losses and small reflection of microwaves. These composites are used as low-reflection covering for metal and as elastic shielding materials. As a rule, the absorbing composite consist of polymer or rubber *matrix,* which contains different powder-like *fillers* – conductive, magnetic or high-loss dielectric powder. In most of composites, the mechanisms of microwave absorption are based either on losses which are generating by the *electrical conductivity* ($\varepsilon'' \sim \sigma$) or the losses given by the *ferromagnetic resonance* (μ''). It should be noted that the degree of absorption in both these mechanisms linearly *reduces* with increasing frequency, since the influence of the *active* conduction current in relation to the *reactive* current decreases in proportion to frequency: $\varepsilon''(\omega) = \sigma/(\varepsilon_0\omega)$. By the same way, at frequencies higher than ferromagnetic resonance the magnetic losses also *decrease*: $\mu''(\omega) \sim 1/\omega$. Therefore, when approaching to millimetre waves, other filler for composites might become relevant, in which, on the contrary, the absorption *rises* with frequency growing due to use as a filler to polymer the *polar dielectrics,* in which microwave absorbance grows with frequency increase. Composite absorbers, using conductors, ferrites or high-loss dielectric fillers in the combination with polymer or rubber matrix offer control of their properties, because they can be optimized only via the changes in both inclusions and host matrix. Absorbent properties of microwave composites can be tailored to a given application through the change of their composition and the volume fraction of a filler. It is important to note that broadband dielectric spectroscopy makes it possible to evaluate *in advance* the possibilities of using various fillers for composite materials.

In connection with a widespread use of microwaves in the telecommunications, industries and military equipment, the issues, related to the absorption of high-frequency electromagnetic (EM) radiation in different materials, is gaining a special urgency. High frequency electromagnetic pollution in the environment needs strong attenuation of the unwanted noise as for protection of electronic devices interference so for human health. Effective defense from the electromagnetic chaos can be realized by the layers of flexible absorbing microwave composite based on the polymers filled with conductive, magnetic or dielectric powder absorbers. The protection from the electromagnetic interference (EMI) requires materials capable of high absorbing microwave radiation with a minimal reflection. As known, the most effective EMI absorbers are the composite materials [1–3] consisting in turn of various dielectrics, ferrites, semiconductors and metals, which are the most effective absorbers in the form of micro- and nano-particles. For

this reason, the elucidation of fundamental microwaves absorption mechanisms in various components of EMI composites seems to be relevant.

The conducted studies of absorbing composites are as follows:

- Absorbing microwave composites should have low front-face reflection by the matching of impedance between air and absorber, in combination with large microwave losses in order to absorb electromagnetic waves due to material conductance, magnetic or dielectric losses; moreover, such composite might be applied in whenever possible widest frequency range. They are of interest in a wide range of applications: span radar absorbents, electromagnetic protection materials from natural phenomena (lightning), electromagnetic pulse protection, electromagnetic compatibility of electronic devices and protection from high-intensity radiated field.

- It's obvious that for the effective protection against electromagnetic radiation the metals can be used, but their disadvantage is high reflection of microwaves, big weight, corrosion, etc. An alternative may be the composite with filler made of carboneous materials (carbon black, graphite, nanotubes, etc.), but they are the *diamagnets* with permeability $\mu \approx 1$. Nevertheless, exactly the *increased* μ is an imperative for impedance matching between composite and free space. This would be achieved, when the permeability will close to the permittivity which in usual material is ε = 2-10. That is why, the effective absorber of microwaves should have the *increased* μ that is possible only by the ferromagnetic filler use.

- Shielding microwave composite absorbers, which use carbonaceous, metallic, ferrite or large-loss dielectric fillers in the combination with polymer or rubber matrix, should offer *good flexibility* need for design and properties control, because they can be optimized via changes in both inclusions and matrix. Absorbent properties of such composites can be tailored to the given application through the changes in their composition and in volume fraction of filler particles; dielectric spectroscopy is a useful tool for clarifying these circumstances when developing composites.

- Significant advantage of polymeric or rubber based composites is that, depending on filler particles incorporation-mixing process and by the adjustment of the nature and geometry of filler particles, they offer multiple degrees of freedom to tune particles aggregation state. There are many electromagnetic parameters that need to be studied for filler embedded to polymeric matrix, such as the type of inter-particle interactions, the long-range dipole-dipole interactions, the clustering, and the matrix-particle interactions, the multi-contact chain adsorption at surface of filler.

• The mechanisms of microwave absorption in most composites are based either on the losses produced by the electrical *conductivity* $\varepsilon'' \sim \sigma$ or on the losses given by the ferromagnetic *resonance* μ''. Note that the measure of absorption of both these mechanisms linearly *reduces* with increasing frequency, since the relevance of *active* conduction current in relation to reactive current decreases in proportion to frequency: $\varepsilon''(\omega) = \sigma/(\varepsilon_0\omega)$. By the same way, at the frequencies exceeding ferromagnetic resonance the magnetic losses also decrease with frequency growing: $\mu''(\omega) \sim 1/\omega$.

• When approaching millimetre waves, others composites might become relevant, in which the absorption occurs due to *polar dielectrics* imbedding in their composition, in which microwave absorbance, on the contrary, *rises* with frequency growing. The point is that in the polar dielectrics the optical-acoustic interaction is strongly pronounced, which allows translate energy obtained by microwave electrical excitation into acoustic oscillations, which in materials are the "thermal reservoir". The favourable factor is that effectiveness of such interaction at microwaves *increases* with frequency growing.

• Important feature of microwave composites is that the variations of metallic or ferrite particles content allow tune independently the real and imaginary parts of effective permittivity of a composite in order to match the requirement for absorption at given frequency range. One of significant advantage of polymeric or rubber composites is that, depending on filler particles and incorporation-mixing process, as well as by the adjustment of nature and geometry of filler particles, they offer some degrees of freedom in particles aggregation state and their investment to overall effective permittivity.

• In the composites with metal or carbon type fillers, the phenomenon of *percolation* is of great importance for conductivity, according to which charge transfer occurs along the percolation channels formed by the chains of conductive particles in contact with each other. In particular, when using nanotubes as a filler, due to the sharply *isometric nature* of nanoparticles even small change in their concentration is sufficient to transform the composite from dielectrics to conductors.

• High absorbing at microwaves dielectrics might increase the capabilities of shielding composites intended for millimeter waves. The basic mechanisms of microwave absorption in such dielectrics are the dipole-type relaxation near the ferroelectric phase transitions and the soft mode resonance in crystal lattice of displacement type ferroelectrics. The analysis of different fillers made of various ferroelectrics shows that the most promising are the relaxor ferroelectrics.

• Polymeric composites filled with functional electronic materials, combine electrical properties of solid filler with mechanical flexibility, chemical stability and high ability of processing peculiar to the polymers. To achieve desired properties, it is necessary to ensure connectivity between phases in 0–3 type composite by the selection of right materials (processed in special way), and reliable connection between phases. An important role in the composite properties is played by the particle size of a filler, the interfacial properties, and the level of percolation.

6.2 Interaction of EM waves with solids

The principles of this interaction are shown symbolically in Fig. 6.1, where a spatial dispersion of plane EM waves, propagating in the positive direction of abscissa axis, is compared for the vacuum, two types of dielectrics, typical semiconductors, ferrites and metals including in their finely dispersed form. When falling normally onto a solid, EM wave can be partially or nearly completely reflected, as well as it can penetrate into a material next being absorbed. The areas of fundamental absorption in Fig. 1 are shaded: just from them the large reflection occurs.

It is obvious that there is no reflection or absorption of EM wave in the vacuum where $\omega = ck$, Fig. 6.1a, but the reflection, in one or another manifestations, should be obviously present in any substance ina particular frequency range. In this case, exactly the phenomenon of dispersion is important, because it is accompanied both by reflection and absorption of EM energy, which is just subject of this work.

The simplest case of a dispersion is observed in the dielectrics possessing only electronic (optical) polarization, Fig. 6.1b. It is appropriate to clarify that $\omega(k)$ dispersion explains the permittivity dependence on frequency of electromagnetic field: $\varepsilon(\omega)$. The term dispersion is borrowed from optics, where dispersion is the frequency dependence of refractive index, i.e., $n = n(\omega)$. Note that in solid state physics, the dispersion means also the dependence of quasi-particle energy ($W = \hbar k$) on its quasi-momentum ($p = \hbar k$). These definitions are fully consistent with each other: in optical and infrared regions of spectrum, such $W(p)$ dependence is reduced to description of wave dispersion, described by $\omega(k)$, which expresses the frequency dependence of EM wave phase velocity, which eventually corresponds to the dependence $\varepsilon(\omega)$, i.e., frequency dependence of permittivity. The dispersion of electronic polarization is accompanied by one region of reflection and absorption in the optical ultraviolet range, Fig. 1b. Such characteristics are peculiar for many polymeric materials on the basis of which microwave absorbing devices are formed.

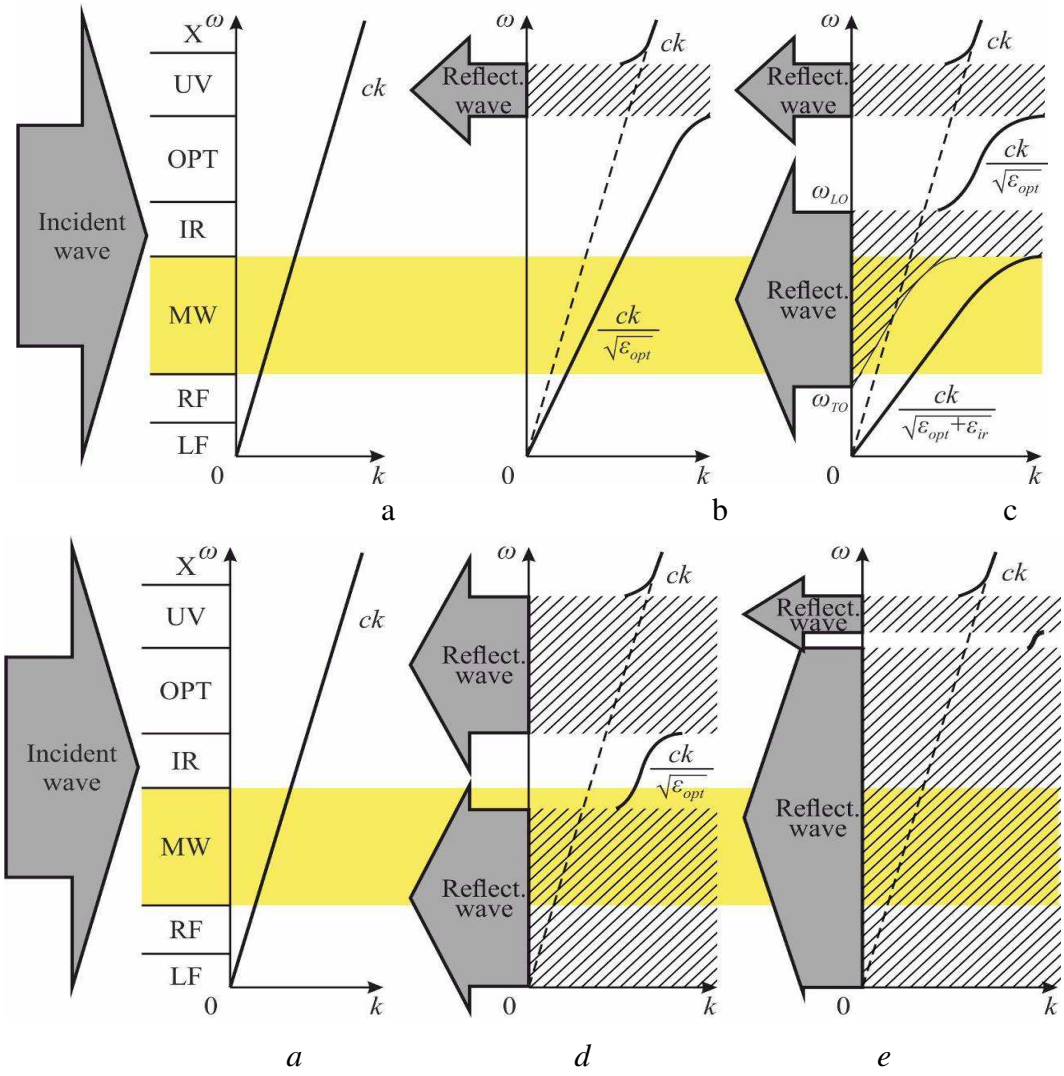

Fig. 6.1. Comparison of electromagnetic waves dispersion in wide frequency range: in vacuum (*a*), in dielectric with electronic (optical) polarization (*b*), in dielectric with ionic (infrared) polarization (*c*), in typical semiconductor (*d*) and in metal (*e*); the designations: LF – low frequency, RF – radio frequency, MW – microwaves range, IR – infrared range, OPT – optical range, UV – ultraviolet range, X – *X*-rays range, c – light speed in vacuum, k – wave number, ε – relative permittivity (the yellow color indicates microwave range, area of transparency is shown in white while high absorption areas are shaded)

Figure 1c describes two areas of reflection and absorption in the dielectrics characterized by ionic polarization; in both regions of dispersion (far infrared and ultraviolet), the EM wave significantly changes the velocity of its propagation. In general, a similar but more complex characteristic is the dispersion in semiconductors, Fig. 1d, where at lower frequencies the absorption and reflections of EM waves are affected by the electrical conductivity. In metals, Fig. 1d, the electronic electrical conductivity completely determines the high reflection of EM waves in the entire frequency range, but with exception of the ultraviolet region, where the movement of electrons is retarded by their inertia, and optical properties

are determined by the electronic shells of cations. In connection with metals use in the microwave absorbing composites, one has to consider the properties of finely dispersed (including nano-scale) metals, electrical properties of which change drastically.

It is obvious, that EM wave reflects from any substance (but from each in its own frequency range), with the exception of X-rays, which frequency is so large that electronic shells of atoms cannot be excited, providing the reflection and absorption of EM waves. However, in a certain frequency range. nearly zero reflection from material is yet possible: in the case of a material, in which permittivity equals to permeability (however, for any natural material this case is unknown).

6.3 Microwaves absorption general description

To analyze the effectiveness of microwave absorbent and protective coverings, first of all, it is necessary to outline briefly the fundamental principles of EM wave propagation in the absorbing medium. EM wave passing through a material can be described by some averaged (effective) parameters, determined in turn by the atomic and electronic structure of absorber. In the macroscopic description of this process, two effective material's parameters are used: the complex dielectric permittivity $\varepsilon^* = \varepsilon' - i\varepsilon''$ and the complex magnetic permeability $\mu^* = \mu' - i\mu''$.

The real parts of the permittivity and permeability (ε' and μ') characterize the EM wave propagation, while the imaginary parts (ε'' and μ'') describe the absorption of electromagnetic energy by a medium. At that, in the non-magnetic materials, the dissipation of energy is a result of dielectric relaxation and some conduction mechanisms; in other words, through the damping forces acting on the polarized atoms and molecules, and through the finite conductivity of material. In the magnetic materials, the cause of microwave absorption is the ferromagnetic resonance, at which the energy of spin waves, excited by magnetic field, partially transforms to the acoustic vibrations of crystal lattice through a spin-lattice interaction.

The following is an electromagnetic description of the absorbing medium itself as well as its reflection and absorption in the main experimental situations.

Absorbent material characterization. When describe the EM characteristics of absorbent material, consider the complex permittivity ε^* and complex permeability μ^* as known parameters. They are the ones who determine the complex propagation constant of EM wave in the absorbing material, i.e., $\gamma = \alpha + i\beta =$

$i\omega(\varepsilon^*\mu^*)^{1/2}/c$, The complex impedance of a material is $Z = Z_0(\mu^*/\varepsilon^*)^{1/2}$, where α is the attenuation coefficient, β is the phase constant related to wavelength as $\lambda = 2\pi/\beta$, $c = (\varepsilon_0\mu_0)^{-1/2}$ is the speed of light in a free space, at that $Z_0 = 377$ Ohm is the free space impedance (in the non-magnetic media, an expression for Z is more simple: $Z = Z_0(\varepsilon' - i\varepsilon'')^{-1/2}$).

From above relations, the attenuation and the phase constant can be determined:

$$\alpha = \mathrm{Re}(\gamma) = \frac{\omega}{c\sqrt{2}}\sqrt{\varepsilon''\mu'' - \varepsilon'\mu' + \sqrt{\left(\varepsilon'^2 + \varepsilon''^2\right)\left(\mu'^2 + \mu''^2\right)}}$$

$$\beta = \mathrm{Im}(\gamma) = \frac{\omega}{c\sqrt{2}}\sqrt{\left(\varepsilon'\mu' - \varepsilon''\mu''\right)\left(1 + \sqrt{1 + \frac{\left(\varepsilon'\mu'' + \varepsilon''\mu'\right)^2}{\left(\varepsilon'\mu' - \varepsilon''\mu''\right)^2}}\right)}, \quad (1)$$

where known parameters are the ε', ε'', μ' and μ''. Thus, for complete characterization of any medium, in which a transverse EM wave propagates, the knowledge of four listed above parameters is sufficient, and they can be obtained by the impedance spectroscopy.

At that, in a lossless environment (ε'' = μ'' = 0), the vectors of electrical and magnetic fields are changing with time in phase. However in the medium with losses, the electrical field vector can lag behind the magnetic field vector or move ahead – depending on the predominance of electrical or magnetic losses. In the ideal case of electrical and magnetic losses equality, the change in time of electrical and magnetic fields vectors going on in phase (as in case of losses absence), and it is such ratio that is difficult but desirable to achieve for non-reflecting absorbing covering.

In the non-magnetic absorbing media in which $\mu' = 1$ and $\mu'' = 0$ the expression (1) simplifies: $\gamma = \alpha + i\beta = i\omega(\varepsilon^*)^{1/2}c^{-1}$. In this case, the attenuation of absorbing material and the EM wave phase can be determined as

$$\alpha = \frac{2\pi}{\lambda_0}\sqrt{\frac{\varepsilon'}{2}\left(\sqrt{\tan^2\delta + 1} - 1\right)}, \quad \beta = \frac{2\pi}{\lambda_0}\sqrt{\frac{\varepsilon'}{2}\left(\sqrt{\tan^2\delta + 1} + 1\right)}, \quad (2)$$

where $\tan\delta = \varepsilon''/\varepsilon'$. *The expression for microwave wavelength in the absorbing media is the inverse of phase constant; in the* non-magnetic *material it is:* $\lambda = 2\pi/\beta$.

It should be noted that with respect to electromagnetic absorption the losses due to electrical conductivity and the losses caused by the delay of polarization are indistinguishable. In any case, specific absorption of EM wave in non-ferromagnetic material is characterized by the attenuation coefficient measured in decibels divided by centimeter (in case of wavelength is expressed in centimeters):

$$20\lg\left(\frac{E(0)}{E(x)}\right)=8.686\alpha=\frac{8.686\cdot 2\pi}{\lambda_0}\sqrt{\left(\frac{1}{2}\varepsilon'\left(\sqrt{\left(1+\tan^2\delta\right)}-1\right)\right)}\frac{\text{dB}}{\text{cm}}= \\ =\frac{54.54}{\lambda_0}\sqrt{\left(\frac{1}{2}\varepsilon'\left(\sqrt{\left(1+\tan^2\delta\right)}-1\right)\right)}\frac{\text{dB}}{\text{cm}} \quad (3)$$

This formula can be used to estimate the attenuation of both kind of material: as for the fillers so for the matrix of composite. It should be emphasized that above solution refers only to thr absorbing material itself, but in no way to the air–absorber system shown below in Fig. 2.

Simple EM analysis of microwave absorbing layer is considered for the case of normal incidence of EM wave; firstly, its reflection from a semi-infinite absorbent media, which concept is depicted in Fig. 2a, and, secondly, EM wave transmitting through the absorbing layer, Fig. 2b. At that, the three environments are denoted as follows: **1** – the air (or vacuum) with the impedance $Z_1 = Z_0$, **2** – the absorbing medium with the complex impedance Z_2, and **3** – the protected medium with the complex impedance Z_3.

The general formula for input impedance Z_{in} for shown systems can be obtained from the long transmission lines theory [4]:

$$Z_{in}=Z_2\frac{Z_3\cosh(\gamma d)+Z_2\sinh(\gamma d)}{Z_2\cosh(\gamma d)+Z_3\sinh(\gamma d)}, \quad (4)$$

where γ is the propagation constant and d is the thickness of studied media. This expression allows electromagnetic analysis for different cases, but all creating by using the single absorbing homogeneous layer.

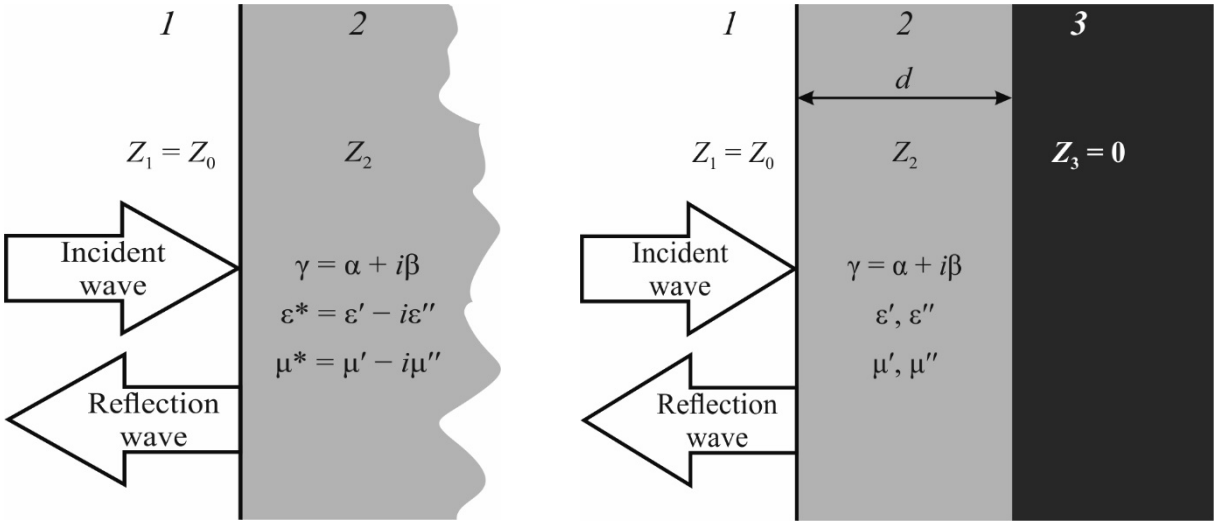

Fig. 6.2. Electromagnetic wave interaction with: *a* – semi-infinite absorbent material ***2***, *b* – in case when the ideal metal ***3*** (Z_3 =0) shorts absorbent layer

First case is often used when materials measurements; it is very convenient in the case if studied sample has rather big absorbance: $Z_{in} = Z_0(\mu^*/\varepsilon^*)^{1/2}$, where $Z_0 =$ 377 Ohm. For the non-magnetic media (characterizing by both dielectric polarization and conductivity) this expression is simplified: $Z_2 = Z_0\,(\varepsilon' - i\varepsilon'')^{-1/2}$, where the real part of permittivity (ε') is determined only by the dielectric polarization, while the imaginary part (ε'') includes not only the losses caused by polarization delay ($\varepsilon'\cdot\tan\delta$) but also by conductivity losses: $\sigma'/\varepsilon_0\omega$, where ε_0 is the electrical constant and ω is the circular frequency. The complex reflection coefficient ρ as in the absolute form so in the usual in microwaves logarithmic version are:

$$\rho = \frac{\sqrt{\mu^*} - \sqrt{\varepsilon^*}}{\sqrt{\mu^*} + \sqrt{\varepsilon^*}}, \qquad R = 20\lg\left(\left|\frac{\sqrt{\mu^*} - \sqrt{\varepsilon^*}}{\sqrt{\mu^*} + \sqrt{\varepsilon^*}}\right|\right). \quad (5)$$

It is seen that in the case of $\mu^* = \varepsilon^*$ there will be no reflection from absorber, but such a case in the condensed matter looks like impossible, since in the vast majority of materials $\mu \approx 1$ while $\varepsilon > 2$. In the process of measurements, the material under study (composite, polymer, fillers in bulk form, etc.) should be located in the waveguide, in the coaxial, strip or other measuring path, and the complex reflection coefficient is measured. The data obtained give grounds for calculating the active and imaginary parts of permittivity. However, when measuring magnetic materials, this method should be supplemented by the measuring of complex transmission coefficient of a sufficiently thin layer of material under study.

Non-reflective microwave coating reresents the second case, shown in Fig. 2*b*, also can be applied in the measuring technology, but its main interest is to decrease the reflection from metallic surface. In case of metal, $Z_3 = 0$ and for basic (elementary) calculations the expression (4) converts into a formula: $Z_{in} = Z_0(\mu^*/\varepsilon^*)^{1/2}\tanh(\gamma d)$.

In the non-ferromagnetic screening media, this expression simplifies: $Z_{in} = Z_0\,(\varepsilon' - i\varepsilon'')^{-1/2}\tanh(\gamma d)$. At that, a complex reflection coefficient is defined as: $\rho = (Z_{in} - Z_0)/(Z_{in} + Z_0)$. In practical applications, only the modulus of reflection coefficient is used: $R = 20\,\log|\rho|$. Basic formula for frequency dependence of reflection follows from above expressions; at that, thr reflection (*RL*) is measuring in the [nepers/m]:

$$RL = 20\log\left(\frac{\sqrt{\frac{\mu^*}{\varepsilon^*}}\tanh(\gamma d)-1}{\sqrt{\frac{\mu^*}{\varepsilon^*}}\tanh(\gamma d)+1}\right) = 20\log\left(\frac{\sqrt{\mu^*}\tanh(\gamma d)-\sqrt{\varepsilon^*}}{\sqrt{\mu^*}\tanh(\gamma d)+\sqrt{\varepsilon^*}}\right) \quad (6)$$

It is seen that a certain combination of permittivity and permeability makes it possible to realize such microwave absorber, which provides minimal reflection. For non-ferromagnetic media (considering only dielectric polarization and conductivity) the above expression simplifies: $RL = 20\ \log\ [(\tanh(\gamma d) - \varepsilon^{*1/2})/(\tanh(\gamma d) - \varepsilon^{*1/2})]$. The efficiency of microwave absorption is estimated as $MA = -RL$. In practice, to expand the frequency band of non-reflective coating, it is necessary to apply the multilayer covering onto metallic surface. These structures can be calculated using the data on conductivity, permittivity and permeability obtained by measurements.

Note that above formulas can be applied when measure parameters of both composites and fillers using the waveguide methods. The accuracy of measurement is especially increased, if the electrical length of a sample is the multiple of a quarter of wavelength in the studied substance. In the case of high reflection, it is advisable to use the dielectric quarter-wave transformers with a value of $\varepsilon = 2$–6 [4].

Microwave transmission through absorbent layer, in addition to expand the possibilities for measuring the parameters of materials used, represents mainly for microwave shielding designing, whose model is the same as in Fig. 2*b*, provided that instead of a metal, the medium ***3*** is dielectric, for example, air with a wave resistance Z_0, i.e., the absorbing layer *2* separates two semi-infinite air media ($Z_3 = Z_1 = Z_0$). The basic expression (4) in this case is converted to a formula:

$$Z_{in} = Z_0\sqrt{\frac{\mu^*}{\varepsilon^*}}\left(\frac{1+\tanh(\gamma d)\sqrt{\frac{\mu^*}{\varepsilon^*}}}{\tanh(\gamma d)+\sqrt{\frac{\mu^*}{\varepsilon^*}}}\right) = Z_0\sqrt{\frac{\mu^*}{\varepsilon^*}}\left(\frac{\sqrt{\varepsilon^*}+\tanh(\gamma d)\sqrt{\mu^*}}{\sqrt{\mu^*}+\tanh(\gamma d)\sqrt{\varepsilon^*}}\right). \quad (7)$$

This ratio relates the effectiveness of shielding with known (usually effective) parameters of applied composite material. In turn, the parameters of composite used in expression (7) should be designed on the basis of parameters of polymeric (or rubber) matrix with considering the parameters of used fillers and their volume concentration. In the non-ferromagnetic media, only the losses from dielectric polarization and conductivity should be considered, so expression (7) can be simplified:

$$Z_{in} = \frac{Z_0}{\sqrt{\varepsilon^*}} \left(\frac{\sqrt{\varepsilon^*} + \tanh(\gamma d)}{1 + \tanh(\gamma d)\sqrt{\varepsilon^*}} \right). \quad (8)$$

The complex reflection ρ and complex transmission coefficient τ of given structure (necessary to evaluate for protective layer effectiveness) are $\rho = (Z_{in} - Z_0)/(Z_{in} + Z_0)$ and $\tau = 2\ Z_{in}/(Z_{in} + Z_0)$. In practice, to calculate the transmission modulus T, the reflection modulus R and absorption modulus A in their logarithmic forms are used:

$$R = 20\lg\left(\left|\frac{Z_{in} - Z_0}{Z_{in} + Z_0}\right|\right), \quad T = 20\lg\left(\left|\frac{2Z_{in}}{Z_{in} + Z_0}\right|\right), \quad A = 20\lg\left(\sqrt{1 - \left(\frac{Z_{in} - Z_0}{Z_{in} + Z_0}\right)^2 - \left(\frac{2Z_{in}}{Z_{in} + Z_0}\right)^2}\right).$$

The R factor characterizes the decrease of reflected signal relatively to the incident signal: if R = 0 dB, the incident EM wave is fully reflected; if R = – 3 dB, the 50% of a signal is reflected, etc. Coefficient T shows the relative decrease in energy of transmitted though material EM wave as compared with incident signal: if T = 0 dB, the entire signal has passed; if T = – 3 dB only 50% of signal passed, etc. The coefficient A is the measure of attenuation of EM signal: at that, the transmitted EM energy is compared with incident signal. If A = 0 dB, full signal energy is absorbed; if A = – 3 dB, the 50% of signal energy is absorbed, etc. The difference between T and A is that the first characterizes the full air-material-air system, while the second is only the characteristic of a material. Shielding efficiency is SE = –T.

6.4 Microwave absorption in metals

Metals are interesting for use in the microwave absorbent composites as fillers for two main reasons. Firstly, their high conductivity (σ) makes it possible to ensure the absorption of EM wave by the increase in imaginary part of permittivity $\varepsilon'' = \sigma/\varepsilon_0\omega$, since from Maxwell's equation: rot H = j + ∂D/∂t it follows that losses caused by the delay of polarization (∂D/∂t) and the conductivity losses (j = σE) are indistinguishable for EM wave. Secondly, several metals are the ferromagnets, and thus due to a significant reduction in EM reflection (μ' > 1) and to additional magnetic absorption (μ') such a filler can significantly improve the absorbing composite.

It is quite obvious that the metal should be included in the composite only in the form of fine fraction (micro- or nano-particles). However, in this case, it is

impossible to use the macroscopic parameter σ of a metal, but the losses generated by metal particles can be predicted on the basis of a knowledge about the EM properties of metal in the frequency range, where σ(ω) undergoes dispersion, Fig. 6.3.

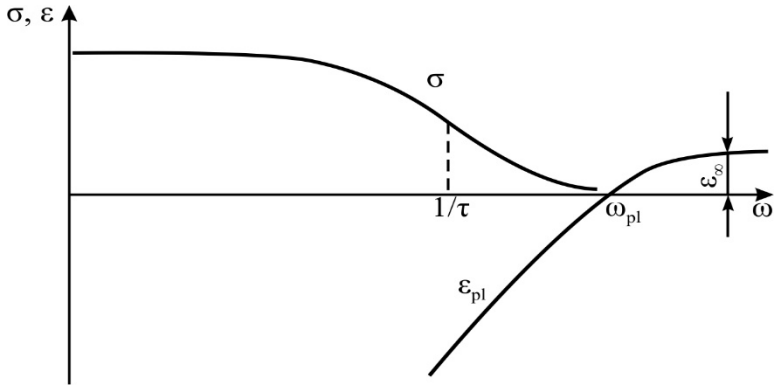

Fig. 6.3. Frequency dependence of conductivity σ and plasma contribution to effective permittivity ε_{pl} in vicinity of plasma resonance in metals (in ultraviolet part of spectrum)

Metals are characterized by the high reflectivity (R), which is due to their large conductivity, and, therefore, the part of incident EM energy (I), absorbed in metal (A), is small, since the energy of incident EM wave is the sum: I = R + A. At that, any transmission (T) of EM wave is possible only in the exceptional cases (mentioned below). From the microscopic point of view, when explaining possible cases of metal interaction with EM waves, it is important to consider that in a metal the valence band of electronic spectrum overlaps with conduction band, but they are separated by Fermi level, below of which the energy states are located for most electrons, which fast reaction explains the interactions of a metal with the EM field. However, this mechanism of EM wave interaction strongly changes in the small metallic particles.

The macroscopic consideration of conducting materials consists in applying the laws of electromagnetism to studied substance with a set of macroscopic parameters σ, ε and μ (or ε* and μ*). Note that at high frequencies, when the EM wave only partially penetrates conductor, some complex phenomena occur: reflection, attenuation and transmission. The reflection of EM waves incident on a metal occurs because the EM wave, when its amplitude, first increasing in time, excites the electrons inducing their transition to the higher energy levels (above the Fermi level). When the amplitude of exciting EM wave next decreases in time, previously excited electrons return to their equilibrium position below the Fermi level, which is followed by the emission of reflected EM waves. It should be noted that at very high frequencies (in ultraviolet part of spectrum) a significant contribution to the light reflection is also made by the excitation of electronic shells

of ions that is accompanied by the vibrations of ionic lattice and gives the input to permittivity ε_∞.

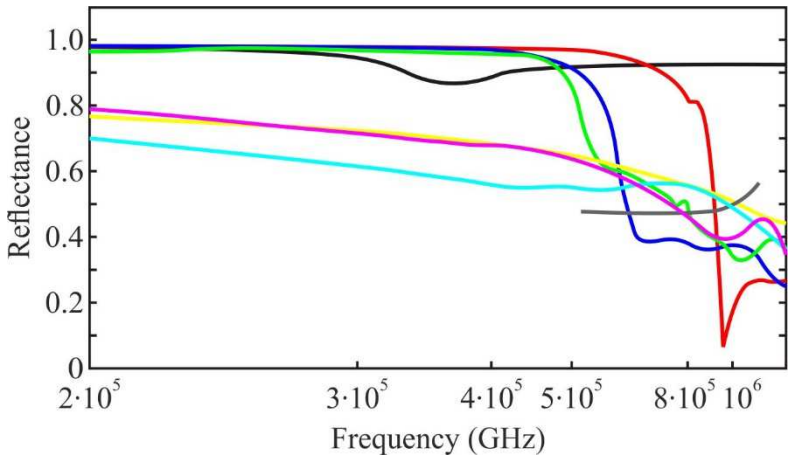

Fig. 6.4. Reflectance spectra of metals by lines: aluminum (black), silver (red), gold (blue), copper (green), beryllium (grey), cobalt (yellow), iron (cyan) and nickel (magenta) [5]

The reflectance coefficient can be defined as the efficiency of a material to reflect the incident light. This value depends only on complex refractive index (n) and damping constant (k) that is seen in equation: $R = [(n-1)^2+k^2]/[(n+1)^2+k^2]$. The study of metallic reflectance shown in Fig. 6.4 indicates that the process of $\sigma(\omega)$ dispersion not nearly as simple as the elementary theory predicts. Conductivity frequency dispersion $\sigma(\omega) = ne\upsilon = ne^2\tau/m$ is actually a dispersion of drift velocity $\upsilon = -eE\tau/m$ of metal electronic gas ($\tau \sim 10^{-14}$ s is the time between electrons collisions during their chaotic motion with the speed ~10^6 m/s, when electrons free path length is $l \sim$ 1–100 microns that is thousands of times higher than a crystal lattice parameter. Note that the sizes of the particles used in the absorbing microwave composites are commensurate or even smaller than this mean free path of electrons. It is also important to mention that at drift-movement of the electronic gas, not the acceleration but the electrons velocity is proportional to the electrical field. That is why, the conductivity is proportional not to the charge of electron, but to its square ($\sigma \sim e^2$) while the drift deceleration is $m\upsilon/\tau$ and can be described by the equation: $md\upsilon/dt = -m\upsilon/\tau + eE(t)$, the solution of which is shown in Fig. 6.3 as the conductivity frequency dispersion $\sigma(\omega) = \sigma_0/(1+i\omega\tau)$, or:

$$\sigma'(\omega) = \frac{\sigma_0}{1+\omega^2\tau^2}; \quad \sigma''(\omega) = -\frac{\sigma_0\omega\tau}{1+\omega^2\tau^2}, \quad \sigma_0 = \frac{ne^2\tau}{m}. \qquad (9)$$

The conductivity (being proportional to drift velocity of electrons) decreases with frequency, since during the acceleration of the electron along its free path (before collision and scattering), the direction of the high-frequency electrical field has no time to change. Far from the region of a dispersion, when $\omega\tau << 1$, the real

part of conductivity $\sigma'(\omega) \approx \sigma_0$ remains frequency constant, while its imaginary part, remaining rather small, increases linearly with frequency: $\sigma''(\omega) \approx \sigma_0\omega\tau$.

Plasma frequency of electrons in the conductors (which determines the quasi-particle plasmon) is an important parameter as for metals so for semiconductors; it characterizes the dynamic properties of the gas of almost-free electrons. The decrease in the real part of conductivity, Fig. 3b, is due to the delay in the electrons drift motion, and that's it which leads to the negative permittivity $\varepsilon'(\omega) = \sigma''(\omega)/(\varepsilon_0\omega)$, connecting with the imaginary part of conductivity. It is generally accepted that at certain frequency, called the plasma frequency (ω_{pl}), the permittivity vanishes $\varepsilon'(\omega) = 0$, crossing the abscissa axis and next reaching the value ε_∞, which for different metals can have a value of 4–8. This behavior of free electrons gas in metals in the high-frequency EM field requires the introduction the plasma frequency concept. Under approximate assumption that limiting permittivity of metal is $\varepsilon = 1$, the plasma frequency can be estimated by the value $\omega_{pl} = (Ne^2/m\varepsilon_0)^{1/2}$.

From one of Maxwell equations $\{\text{rot } H = j + \partial D/\partial t)\}$, it is seen that the current density $j = \sigma^*E$ and the time derivative of electrical displacement $\partial D/\partial t = i\omega\varepsilon_0\varepsilon^*E$ are the additive quantities, so the $\sigma^*(\omega) = \sigma'(\omega) + i\sigma''(\omega)$ is connected to complex permittivity $\varepsilon^*(\omega) = \varepsilon'(\omega) - i\varepsilon''(\omega)$:

$$\varepsilon'(\omega) = \frac{\sigma''(\omega)}{\varepsilon_0\omega}; \varepsilon''(\omega) = \frac{\sigma'(\omega)}{\varepsilon_0\omega}; \varepsilon^*(\omega) = -\frac{ne^2/m\varepsilon_0}{\omega^2 - i\omega\gamma} = -\frac{\omega_{pl}^2}{\omega^2 - i\omega\gamma}, \quad (10)$$

where the $\varepsilon^*(\omega)$ is expressed in the terms of plasma frequency ω_{pl} and the damping factor of plasma oscillation: $\gamma = 1/\tau$. Measurements at microwaves show that the negative permittivity of the highly conductive metals is close to several thousand while in the low-conductive magnetic metals it is only several hundreds.

Given description of plasma oscillations and associated dispersion $\sigma^*(\omega)$ needs to be clarified, because the microwave properties of small metallic particles, used as the fillers in the absorbent composites, are to be predicted. The point is that the plasmons in the nanoparticles, starting from their certain size, are no longer registered. Experimental data on reflectance spectra of the metal [5] indicate the nature of given description of $\sigma^*(\omega)$ dispersion. The metal reflectance is related to the conductivity in accordance to formulas (9, 10): good conductive metals have higher reflectance. But at a very higher frequency a sharp decrease in $R(\omega)$ is seen, Fig. 4. The fact is that in different metals the external electronic shells of metallic ions interact differently with the free flying electrons during their free path, due to

which the drift of electrons and their conductivity are created. At that, the direction of fast variable EM field changes during this free motion of electrons which do not have time to make a collision, as the EM field already changes direction, so the free flying electrons cannot acquire drift velocity. It is at this time, when the influence of ions, having external configuration of inert gas, becomes very important (Au^{+1} repeats the Rn shell, $Cu^{+2} \Rightarrow$ Kr shell, $Ag^{+1} \Rightarrow$ Xe shell, and $Al^{+3} \Rightarrow$ Ar shell). But in the 3d and 4f metals, electronic configurations of ions contain uncompensated spins, which by their magnetic moment affect the dynamics of electronic gas drift motion. That is why, the reflection EM waves and the conductivity of ferromagnetics much less than in other metals.

It should be noted that the reflection spectra of metallic elements change significantly with decrease in the size of metallic particles, especially when going to the nano-sizes. At that, the conductivity drops sharply and plasma oscillations do not appear: the nano-particles of metallic elements are no longer metals. At first, they exhibit the "semiconductor" and then even "dielectric" properties. It is obvious that at these stages a wide range of electromagnetic properties of nano-particles can be obtained, especially if using different technological methods to obtain agglomerates of particles, having quasi-one-dimensional or quasi-two-dimensional configurations. Obviously, in the absence of screening property given by the electronic gas (peculiar to bulk metal), the role of electronic shells of ions in the metal-elements nanoparticles increases significantly. Therefore, the nano-technologies make it possible to control EM properties of a substance. Absorbing and transmittance characteristics change especially strongly when going to the nanosize metals.

The absorption of that part of incident EM radiation, which nevertheless penetrates into metal, from microscopic point of view, occurs mainly because the electrons of metal, exciting by the EM radiation as during their transition to the higher energy levels above the Fermi level so at their subsequent return in the equilibrium state (accompanied by secondary emission of EM waves) interact with the ionic lattice exciting its oscillations, i.e., convert some of EM energy into a heat. From the macroscopic point of view, the phase velocity of EM wave, penetrating into a conductor, is sharply reduced in comparison with its velocity in a vacuum, so much so that the length of EM wave in the conductor (λ_m) becomes hundreds of times shorter than its wavelength in vacuum, Fig. 6.3a. This occurs due to the large conductivity, which in the electrodynamics corresponds to $\varepsilon''(\omega)$. (Note that the reduction of EM wavelength in a substance occurs in $|\varepsilon^*|^{1/2}$ times). Without a doubt, due to the huge step in the impedance in "vacuum-metal" interface, as well as very small phase velocity

of EM wave in conductor, any EM wave falling on the conductor (even in case of grazing incidence) refracts practically in the direction perpendicular to the conductor's surface.

The transmittance of a part of incident on conductor EM radiation is possible only in the case of a very thin metal layer, and, of course, when the frequency of EM radiation is sufficiently high. Analysis shows that the intensity of incident wave (I_0) decreases exponentially while it propagates through a metal, Fig. 3a, that leads to much lower intensity of the transmitting wave. This happens because the metal strongly damp the initial intensity of TM wave. It is obvious that the decrease of wave intensity is related also to the thickness of metal layer, so extinction coefficient equals $I(x) = I_0\exp(-4\pi kx/\lambda)$, where k is the damping constant. In connection with the attenuation and transmission of EM wave in a metal, the parameter penetration depth due to the skin effect becomes especially important.

The skin effect manifests itself only in the alternating electrical field and consists in the redistribution of current density in a conductor: it becomes maximal near the surface of conductor, and exponentially decreases with the increase of distance x from metal surface. In near-surface region the current density j_0 exponentially falls describing as: $j(x) = j_0\exp(-x/\delta)$, where δ is called the skin layer (or penetration depth), at which the surface current decreases to "1/e" of its initial value (i.e., consists 0.37). As a result, skin effect increases effective resistance of a conductor that is radically different from direct current, which is distributed evenly over a conductor. The skin effect is due to the opposing eddy currents, caused by change of magnetic field. At frequency of 10 GHz, when EM wavelength in vacuum is $\lambda_0 = 3$ cm, the depth of skin layer in good conductors is only $\delta = 0.6–0.8$ μm. General formula for the skin depth is:

$$\delta = \sqrt{\frac{2\rho}{\omega\mu_0\mu}\left[\sqrt{1+\left(\rho\omega\varepsilon_0\varepsilon\right)^2}+\rho\omega\varepsilon_0\varepsilon\right]}\,, \qquad (11)$$

where $\rho = 1/\sigma$ is the resistivity. At low frequencies, when $\rho\omega\varepsilon_0\varepsilon << 1$ (i.e., when conductivity is big: $\omega\varepsilon_0\varepsilon << \sigma$), the quantity inside brackets is close to unity, so formula (11) is more usually given as: $\delta = (2\rho/(\omega\mu_0\mu))^{1/2}$. However, in the case of lower-dimension metallic particles (i.e., for 0D, 1D and 2D nano-particles), which at microwaves becomes the poor conductors, factor inside brackets in formula (11) increases. As a result, at the frequencies much higher than $\omega \sim 1/\rho\varepsilon_0\varepsilon$, the skin depth, rather than continuing to decrease, approaches asymptotic value: $\delta \approx 2\rho(\varepsilon_0\varepsilon/\mu_0\mu)^{1/2}$. This difference from the usual formula only applies for the low conductivity materials and for such frequencies, at which the EM wavelength is not much larger

than skin depth itself. Just this case corresponds to the nano-scale metallic particles as well as for the heavily doped semiconductors. At the same time, for usual dielectrics and non-doped semiconductors, the skin effect doesn't need to be taken into account in most practical situations. But in the opposite case of extremely high conductivity of a material the mean free path of charge carries increases. Under these conditions, the anomalous skin effect arises, so mechanisms described above and leading to formation of usual skin effect no longer works: the thickness of a layer, in which the current is concentrated, changes under other laws. At normal temperatures, such phenomenon is expected in 2D graphene (which has no forbidden zone) and in the 1D nanotubes (where the ballistic mechanism of charge transfer is seen).

When discussing the possibility of using metallic elements as fillers for the absorbent composites, one cannot ignore the ferromagnetic metals. It is they that are of greatest interest, since in them the $\sigma^*(\omega)$ dispersion is manifested in a special way due to the influence of intrinsic magnetic moment of the lattice ions with spins of free electrons. Besides, this fillers can provide the increased permeability, determined by the gyromagnetic resonance, which occurs in the magnetic particles of metals imbedded in the polymeric matrix. This resonance manifests itself as a selective absorption of the EM wave energy in the frequency range, which coincides with natural frequencies of magnetic moments precession in a given ferromagnetic. The shape and width of absorption maximum are determined by collective spin-lattice nature of a magnetic. Moreover, in case of magneto-dielectrics composites, in which ferromagnetic particles are separated by the dielectric layers, the many-resonance processes start that is greatly blurred in the frequency range.

For effective absorbance of the EM waves, it is important that the composite would have close values of effective permittivity and effective permeability. Experiment shows that at frequency of 3 GHz for the nickel-filled epoxy rubber the parameters of composite with nickel concentrations of 10–40 % are: $\varepsilon' = 10–30$ and $\mu' = 2–6$. When content of nickel particles is changed from 10 to 40 volume percents, reflection coefficient of EM energy from composite is within 15–20 dB/cm [1]. Successful combination of dielectric and magnetic properties would be in the case of filler small concentration, i.e., at low percolation. In case of long nanotubes possessing high conductivity, the low percolation threshold can be achieved that contributes to composite flexibility. Moreover, the filling of nanotubes by magnetic elements significantly increases the magnetic permeability of a composite, which improves the condition for impedances matching [2]. To decrease the threshold of percolation, the iron oxide particles were prepared in a stick-like shape for use as

filler for microwave shielding composites [6]. In this case, magnetic iron oxide of various shapes, coated by reduced graphene oxide, are studied in frequency range of 12–18 GHz. The effective permittivity of the composite was $\varepsilon' = 25–15$ and $\varepsilon'' = 20–13$ with increased effective μ^*.

6.5 Absorption mechanisms in semiconductors

As known, the semiconductors are a large class of solids, which conductivity σ occupies intermediate position between conductors and dielectrics (at room temperature in the metals $\sigma > 10^5$ S/m while in the dielectrics $\sigma < 10^{-10}$ S/m). Like dielectrics, semiconductors show the exponential increase of conductivity with temperature: $\sigma = \sigma_0 \exp(-E_g/2k_BT)$, where E_g is the activation energy of electrons (band gap). As seen from this formula, near the absolute zero (when $T \approx 0$) semiconductor shows the property of insulator: $\sigma \approx 0$. The ability to manage conductivity in a wide range by the electrical and magnetic fields influence and by the temperature change is a basis of many and varied applications of semiconductors.

In the microwave range, the semiconductors show mainly their dielectric properties, since the influence of conductivity on the microwave absorption decreases proportional to frequency increase. Therefore, the electro-dynamic high-frequency properties of semiconductors and dielectrics are further discussed together.

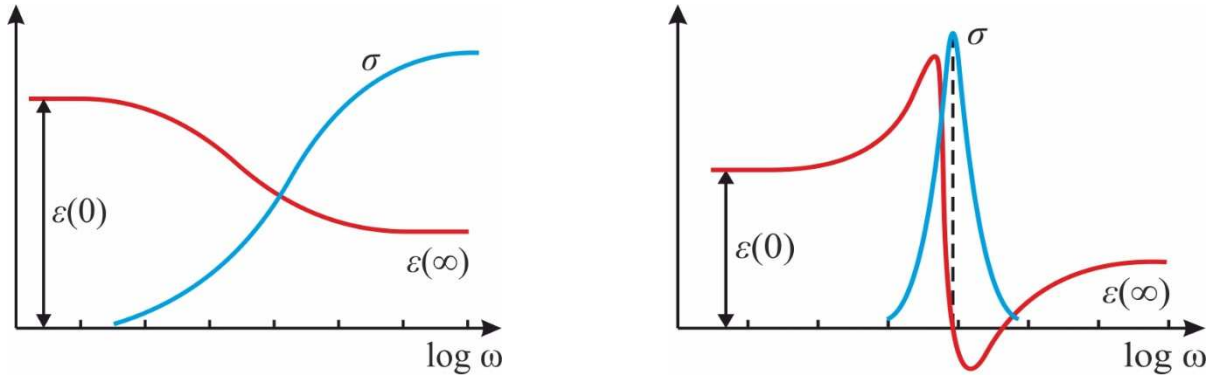

Fig. 6.4. Permittivity and effective conductivity frequency dependence comparison for two main models describing permittivity dispersion: a – relaxation, b – resonance

In accordance with charge carrier physical nature and depending on the properties of studied material, the effective electrical conductivity can increase or decrease with frequency growing and might have a maximum at certain frequency. Two typical cases of interdependent frequency variations of permittivity and

effective conductivity in the dielectrics and semiconductors are shown in Fig. 6.5; at that, it is assumed that the intrinsic conductivity (seen at a constant voltage) is so small that it can be neglected.

The increase of effective $\sigma(\omega)$ is usually caused by the delay of polarization mechanism. This effect is conditioned by a close physical connection between the processes of polarization and conduction, which, in principle, can be completely separated only at the direct voltage.

The *relaxation* dispersion of permittivity, Fig. 5*a*, consists in the $\varepsilon'(\omega)$ gradual decrease from the initial value $\varepsilon(0)$ to its end value of $\varepsilon(\infty)$, when the dielectric contribution $\Delta\varepsilon = \varepsilon(0) - \varepsilon(\infty)$ of the relaxing polarization mechanism is completely delayed. At that, a gradual increase in the effective conductivity from almost zero to a constant value $\sigma'_{ef} \approx \varepsilon_0\Delta\varepsilon/\tau$ is seen (τ is the relaxation time). This dependence of conductivity in dielectrics and wide-gap semiconductors is observed in a very *broad* frequency range (10^{-5}–10^{8} Hz), at that, such dependences are typical for quite different structures and chemical compositions of a material. This common property of effective $\sigma(\omega)$ dependence can be described by a power law $\sigma \sim \omega^n$, where $0.7 < n < 1$. This law is fulfilled, when charged particles move in the local area in the structure of dielectrics or semiconductor under alternating electrical field influence.

The *resonant* dispersion of permittivity, Fig. 6.5*b*, is characterized by the fact that at first the derivative $d\varepsilon'/d\omega$ is positive, next at the resonance point it changes sign to the negative value but after anti-resonance ends the derivative $d\varepsilon'/d\omega$ again becomes positive. Therefore, dielectric permittivity passes through the maximum and minimum. In region of resonance dispersion of permittivity, effective conductivity is characterized by sharp maximum $\sigma'_{max} = \varepsilon_0\Delta\varepsilon\omega_0/\Gamma$, locating *exactly at the resonance frequency* of oscillator describing this dispersion; here ω_0 is the oscillator frequency, Γ is the relative damping factor while $\Delta\varepsilon = \varepsilon(0) - \varepsilon(\infty)$ is the dielectric contribution of oscillator which describes dispersion of permittivity.

Figure 6.6 shows our measurements of microwave parameters of silicon, which is a typical atomic semiconductor. Its permittivity is completely independent on frequency, since it is due to a very fast (electronic) mechanism of polarization. This polarization does not contribute to the microwave losses $\tan\delta(\nu,T)$, which are determined only by the electrical conductivity. That is why, the microwave absorption are felt at the beginning of microwave range: these losses are dependent as on the frequency so on the temperature:

$$\tan\delta(\omega,T)=\frac{\sigma}{\varepsilon_0\varepsilon\omega}\approx\frac{\sigma_0\exp\left[a(T-T_0)\right]}{\varepsilon_0\varepsilon\omega},$$

where σ_0 is the specific conductivity at certain temperature T_0, parameter ε_0 is the electrical constant and ε is the frequency independent permittivity, while a is peculiar parameter for given semiconductor. Exponential increase $\sigma(T)$ is in a good agreement with experiment; so the conductivity contribution to the losses might by important at rather high temperatures mostly.

On the contrary, in the polar semiconductors of gallium arsenide type microwave absorption linearly increases with frequency, Fig. 7, that is due to so called fast relaxation. In the non-centre symmetric (polar) crystals loss factor is governed by the very high frequency mechanism of losses which can be explained by quasi-Debye losses. Frequency and temperature dependences of these losses at the condition when $\omega\tau < 1$ can be described by formula:

$$\tan\delta\approx\frac{\omega}{2\nu_D}\exp\frac{U}{kT}\frac{\varepsilon(0)-\varepsilon(\infty)}{\varepsilon(0)},$$

where ν_D is the Debye frequency, k is the Boltzmann constant, U is the potential barrier. In this case, the loss factor increases as with frequency so with temperature. It is clearly seen that the nature of increased microwave losses of GaAs is not due to its conductivity. Therefore, as it follows from our data, as the microwave "dielectric substrate" at millimeter waves, it is better to use highly resistive silicone than gallium arsenide (in spite of its conductivity is thousands of times less than that of silicon).

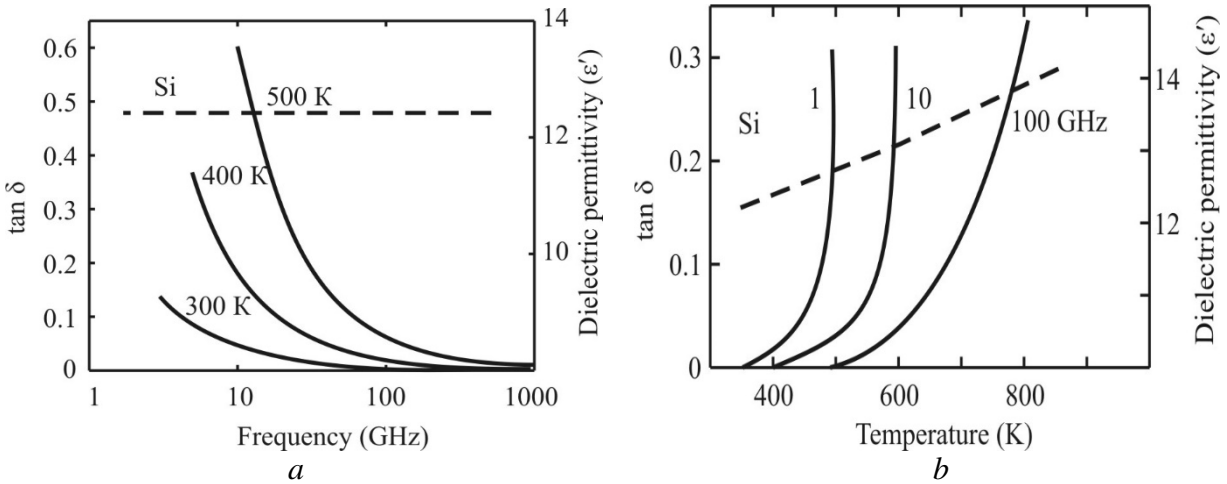

Fig. 6.6. Frequency (*a*) and temperature (*b*) dependences of microwave losses $\tan\delta$ (solid lines) and permittivity ε' (dotted lines) for the high-resistance silicon in the gigahertz range

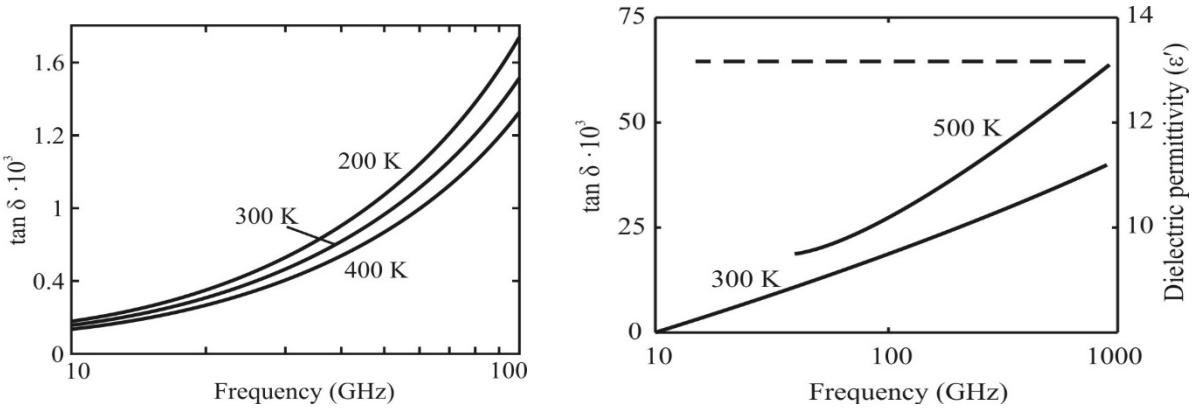

a *b*

Fig. 6.7. Loss tangent frequency dependence mechanism polar crystal GaAs: *a* – lower-frequency tail from loss maximum; *b* – impact of quasi-Debye mechanism (dotted line is permittivity)

Thus, the dispersion ε(ω) shown in Fig. 1b is the characteristic of covalent semiconductors possessing diamond structure. For this reason, semiconductors Ge and Si in far infrared range are the good-transparent crystals with high optical refractive index ($n_{Ge} \approx 4$, $n_{Si} \approx 3.5$). But in the visible optical range (OPT), the high transparency of these semiconductors disappears due to their fundamental optical absorption. Nevertheless, the sub-micron sized semiconductor particles could be served as fillers in the absorbing composites only if they are extremely alloyed by donors or acceptors.

6.6 Absorption mechanisms in dielectrics

As seen from Fig. 6.1, in the microwave range, only some dielectrics can transmit EM waves without significant absorption (they might have only a small absorption by structural defects on dielectric not shown in this figure). At that, in such dielectrics which have exclusively electronic (optical) polarization, in almost entire frequency range the EM waves can free penetrate material with the reflection coefficient $R \approx \{(\varepsilon^{1/2} - 1)/(\varepsilon^{1/2} + 1)\}^2$ that follows from equation (5) when $\mu = 1$. At that, the EM waves slow down their speed in $\varepsilon_{opt}^{1/2}$ times, but the fundamental absorption, accompanied by a reflection is observed in them only in the UV region, Fig. 1b. Next, as frequency rises, for sufficiently "hard" EM radiation the contribution from any polarization mechanism disappears: the refractive index becomes $n = \varepsilon^{1/2} \approx 1$, i.e., the dispersion law in any material gradually takes form $\omega = ck$ (as in vacuum). Most of polymers and rubbers, which are conveniently used in the microwave absorbing composite materials, belong to these dielectrics. However,

in some polymers in addition to the electronic polarization, there is also relaxation polarization, but this mechanism is small to affect slowing down or reflection of microwave wave.

Figure 6.1c schematically shows fundamental reflection and absorption of important kind of dielectrics, namely, those crystals, in which the lattice polarization mechanism (usually being characteristic only for IR range) descends into microwave region. Such dielectrics with a big value of permittivity and very large microwave absorption can be considered as the potential fillers for absorbing microwaves composites, and, therefore, their absorption mechanism should be discussed more detail. Far infrared polarization is a characteristic of all ionic crystals: it manifests itself in IR range of EM waves due to a mutual displacement of cationic and anionic sub-lattices of crystal. Large EM absorbing is seen between the longitudinal ω_{LO} and transverse ω_{TO} lattice vibration frequencies, but in the ferroelectrics ω_{TO} shifts to lower-frequency and makes contribution to refraction and absorption of EM wave. Dispersion law below frequency ω_{TO} has a form: $\omega = ck/(\varepsilon_{opt} + \varepsilon_{ir})^{1/2}$, so the value of ε_{ir} in the ferroelectrics much exceeds the value ε_{opt} due to the significant role of ionic sub-lattices displacement.

The ferroelectrics of order-disorder type the microwave absorption is large (see Rochelle Salt characteristics in Fig. 6.8a), but the use of water-soluble crystals in absorbing composites is unpromising. In the polycrystalline ferroelectrics of displace type the mechanism of microwave absorption is due to their multi-domain structure, Fig. 6.8b. Even at the large distance down from the phase transition point the domain microwave dispersion yet is observed in the gigahertz range. In this case, the maximum of absorption in $PbTiO_3$ is seen near frequency 3 GHz with the attenuation equal 16 dB/cm. In widely used in electronics piezoelectric ceramics PZT = $PbZrTiO_3$ same absorption maximum also remains in the GHz range, and attenuation reaches ~ 100 dB/cm. Barium titanate ($BaTiO_3$) and its solid solutions are also promising fillers for the flexible microwave absorbing composites, Fig. 6.8b.

The broad maximum of microwave absorption in the ferroelectric $BaTiO_3$ ceramics is seen at frequency of 4 GHz [4] and leads to the specific attenuation of 80 dB/cm at 10 GHz. For comparison, it should be noted that in paraelectric $SrTiO_3$, which has approximately same permittivity but $\tan\delta = 0.02$, the specific attenuation is only 3 dB/cm. As seen in Fig. 6.8b, the solid solution $(Ba,Sn)TiO_3$ demonstrates absorption maximum at lower frequency: 0.8 GHz, but its attenuation is much higher: 250 dB/cm at frequency 10 GHz. Other ferroelectrics with diffused phase transition, namely, the solid solutions $(Ba,Sr,Ca)TiO_3$ and $Pb(Zr,Ti)O_3$, have similar

properties at microwaves. All these materials are characterized by broad ε(T) maximum, associated with random distribution of same-valence cations in the sub-lattices. Heterogeneity of composition in the micro-regions is accompanied by the fluctuation of Curie temperature that leads to the diffused ε′(T) maximum. The nature of dielectric absorption for all mentioned compositions is similar to the ferroelectric $BaTiO_3$ but their microwave absorbing lies within 100 – 300 dB/cm.

The broad maximum of microwave absorption in the ferroelectric $BaTiO_3$ ceramics is seen at frequency of 4 GHz [4] and leads to the specific attenuation of 80 dB/cm at 10 GHz. For comparison, it should be noted that in paraelectric $SrTiO_3$, which has approximately same permittivity but $\tan\delta = 0.02$, the specific attenuation is only 3 dB/cm. As seen in Fig. 6.8b, the solid solution $(Ba,Sn)TiO_3$ demonstrates absorption maximum at lower frequency: 0.8 GHz, but its attenuation is much higher: 250 dB/cm at frequency 10 GHz. Other ferroelectrics with diffused phase transition, namely, the solid solutions $(Ba,Sr,Ca)TiO_3$ and $Pb(Zr,Ti)O_3$, have similar properties at microwaves. All these materials are characterized by broad ε(T) maximum, associated with random distribution of same-valence cations in the sub-lattices. Heterogeneity of composition in the micro-regions is accompanied by the fluctuation of Curie temperature that leads to the diffused ε′(T) maximum. The nature of dielectric absorption for all mentioned compositions is similar to the ferroelectric $BaTiO_3$ but their microwave absorbing lies within 100 – 300 dB/cm.

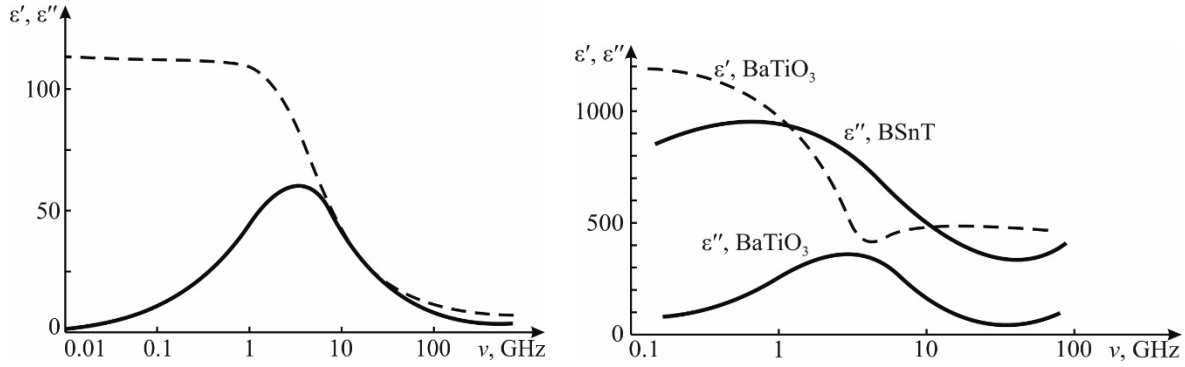

Fig. 6.8. Microwave permittivity dispersion and absorption in: a – order-disorder type ferroelectric Rochelle Salt, RS = $KNaC_4H_4O_6{\cdot}4H_2O$; b – displace type ferroelectrics barium titanate $BaTiO_3$ and its solid solution $Ba(Ti,Sn)O_3$

The relaxor ferroelectrics seem to be best candidates among the large-losses dielectrics as fillers for microwave absorbent composites (Fig. 6.9). In entire microwave range, these materials have highly absorbing properties. Crystal lattice of relaxor ferroelectrics is characterized by the cations of different valence, which randomly occupy similar structural sites. At that, the relaxor ferroelectrics might

have two different types of structural disordering. The PMN = $PbMg_{1/3}Nb_{2/3}O_3$ has (B^{+2}–B^{+5}) type of compositional disordering, while the potassium-lithium tantalate crystal (KLT = $K_{1-x}Li_xTaO_3$) has strongly disordered structure only for lithium ions, located in the non-central positions with various associations between them.

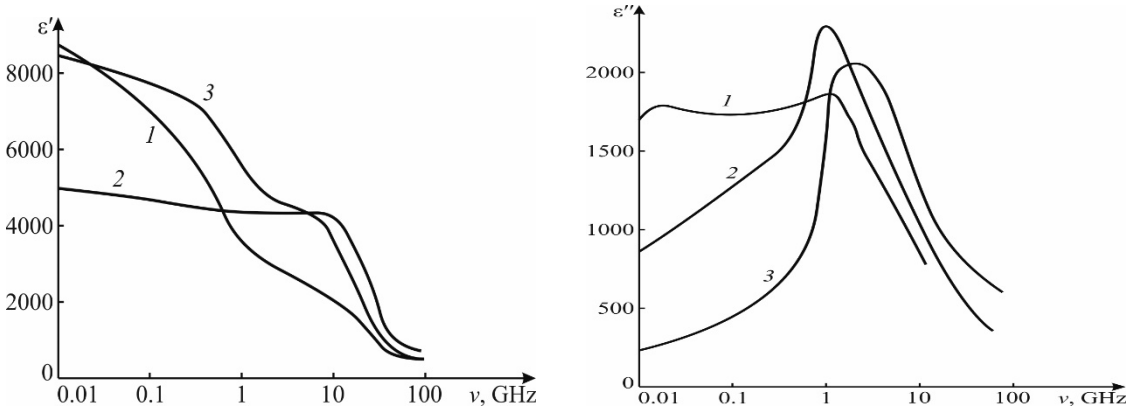

Fig. 6.9. Microwave dispersion in PMN = $PbMg_{1/3}Nb_{2/3}O_3$ at temperatures: *1* – 290 K; *2* – 300 K; *3* – 320 K; *a* – permittivity ε', *b* – loss factor ε''

The relaxor ferroelectrics have usual crystalline structure, in which, however, in them the "electrical disordering" is observed in a form of built-in quasi-dipole formations. They are easily amenable to orientation in alternating electrical field that leads to extremely high permittivity $\varepsilon \sim 10^4$, Fig. 6.9. Relaxation of clusters, having different sizes and formed from structural quasi-dipoles, occurs over a wide range of frequencies, including microwaves. Diffuse maximum of microwave absorption covers the entire microwave range that leads to attenuation of ~300 dB/cm.

Summing up, note, that in the decimetre and centimetre waves the flexible absorbing and shielding composites may use as fillers conductive materials and ferrite powders. At that, competitiveness in these frequency ranges dielectric absorbent fillers still needs to be proven. On the one hand, the size effect leads to the fact that in ferroelectric small particles as permittivity so microwave absorption sharply decrease. However, small ferroelectric particles retain and even increase their ability to the piezo-resonances that can be tailored precisely into the frequency range, where it is necessary to increase absorption of composites. Moreover, when frequency increases, absorbing ability of conductive and magnetic fillers decreases in proportion to the frequency grows, while the dielectric adsorbents, on the contrary, increase their absorption capacity. Therefore, the application of large loss dielectrics as fillers seems more perspective in the millimetre waves (in the range of 30–300 GHz), where many telecommunication, radio-astronomy and radar systems already work. Gigabit wireless communications has begun to spread to public welfare systems; for example, wireless gigabit communications utilizes

predominantly frequencies near 60 GHz. Moreover, the vehicle radars use several frequency intervals in the range of 60–80 GHz: these devises are used in advanced emergency-braking systems with autonomous emergency braking, and they are increasingly become international.

6.7 Microwave absorption in ferrites

Ideally, the microwave absorbing composites should not only provide the maximal absorption (otherwise, one could simply use the metalized polymeric film), but also to show a minimal reflection in order to really reduce the EM pollution of the surrounding area. Since all substances have this or that permittivity ($\varepsilon^* > 1$), the decrease in the reflection is only possible, if the absorbing composite includes the filler with noticeable permeability ($\mu^* > 1$). Theoretically, if $\mu^* = \varepsilon^*$ at certain frequency, then there will be no reflection of the EM wave. However, most substances are the diamagnets or paramagnets, in which $\mu^* = \mu \approx 1$, and only some magnetic materials are characterized by $\mu^* > 1$.

Realized microwave absorbents are the consequence of not only increased permittivity and conductivity of material, but also the result of increased permeability and magnetic losses. When developing such composites, not only the magnetic losses are important, but can play significant role the permeability. In fact, reflection coefficient R, formula (2), depends on the input impedance Z of material, while the impedance, in turn, depends on the ratio of permeability and permittivity. In known microwave composites the value of $\langle\varepsilon^*\rangle$ usually lies in range of 2–20, but the permeability of same value is difficult to obtain without ferromagnetic filler.

The nature of increased permeability and absorption of magnetic filler is determined by gyromagnetic resonance, which occurs in the magnetic particles of metals (like Fe, Ni, Co) or ferrites (like Fe_3O_4, Fe_2O_3, barium ferrite) imbedded in the polymeric matrix. Ferromagnetic resonance manifests itself as a selective absorption of EM wave energy in frequency range that coincides with natural frequencies of magnetic moments precession in a given ferromagnetic. The presence of multidomain structure in the ferromagnetic complicates the resonance process, leading to appearance of several resonance peaks, so that the resonant absorption of microwave energy is smeared to wide maximum. Moreover, in case of magneto-dielectrics composites, in which small ferromagnetic particles are separated by the dielectric layers, a many-resonance process becomes greatly blurred in frequency range.

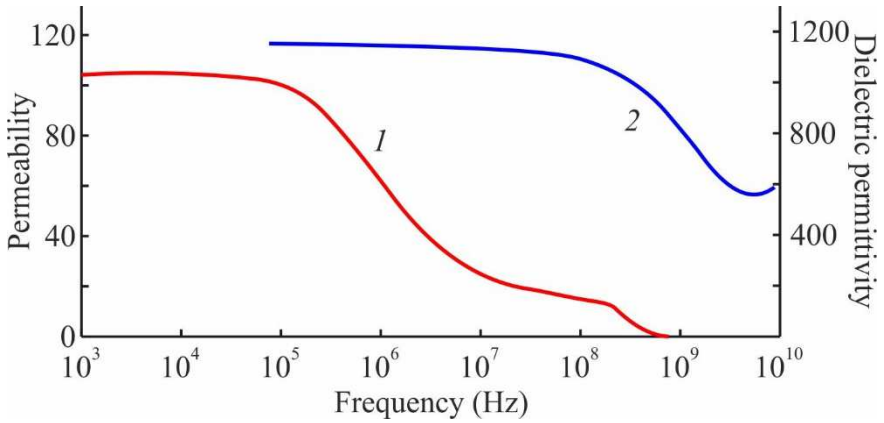

Fig. 6.10. Frequency dispersion of: *1* – permeability $\mu'(\omega)$ in ferrite yttrium iron garnet; *2* – permittivity $\varepsilon'(\omega)$ in ferroelectric barium titanate [4]

In the ferrites, main μ dispersion occurs in the megahertz range, since the large value of permeability is due to spin-orbital (i.e., electron-lattice) interaction generating magnons, which dispersion is similar to the acoustic lattice waves, which frequency thousands of times lower than frequency of optical waves. Nevertheless, at microwaves, in the most of magnets the "paramagnetic-type" spin contribution to the permeability is retained, which can provide μ = 1.5–2.5. This can essentially reduce the EM waves reflection in the absorbing composites.

For the magneto-active fillers in microwave absorbent composites, the use of size effects is highly desirable, i.e., the application of nano-sized powder fillers. The fact is that in the magnets just the spin-orbital interaction reduces the efficiency of spin magnetism. For example, the iron ions in a crystal, instead of $4\mu_B$ (Bohr magnetons), only $2.2\mu_B$ are effective, while in nano-particle magnetic spin efficiency increases to $3.2\mu_B$; in the nickel it rises from $0.6\mu_B$ for crystal to $1.1\mu_B$ in nano-particles; similar, in the cobalt from $1.2\mu_B$ rises to $2.2\mu_B$. As known, this effect is used also in the large permeability spin glasses.

6.8 Summary Chapter 6

Conclusions

In order to select the optimal materials for microwave absorbing composites, the various mechanisms of EM waves absorption in the main solid materials (fillers in composite) are considered. In the dielectrics possessing by electronic polarization only, any absorption is practically absent, but such polymers usually are good as the matrixes of composites. Metallic elements in the form of micro- and nano-particles have quite different properties than bulk metals, but can provide high microwave

absorption. From dielectrics possessing ionic polarization, only ferroelectrics have big microwave absorption, increasing with frequency rise, that serves as benefit for shorter wavelength absorbers. Magnetic fillers can not provide in composite big permeability, yet they reducing microwaves reflection of from composite.

Passing through the absorbing layer, electromagnetic wave loses its energy leading to absorber heating due to interaction of electromagnetic field with molecular and electronic structure of a material. To describe this process, two material's parameters are used: complex dielectric permittivity $\varepsilon^* = \varepsilon' - i\varepsilon''$ and complex magnetic permeability $\mu^* = \mu' - \mu''$. The real parts of permittivity and permeability (ε' and μ') characterize the energy *propagation* and *storage*, while the imaginary parts (ε'' and μ'') describe the *absorption* of electromagnetic energy by a medium.

For complete electromagnetic characterization of medium, in which electromagnetic wave propagates, the knowledge of ε', ε'', μ' and μ'' is sufficient, and they can be obtained by the dielectric spectroscopy. At that, in the lossless environment ($\varepsilon'' = \mu'' = 0$), the vectors of electrical and magnetic fields are changing with time *in phase*. However in the medium with losses, electrical field vector or lags behind magnetic field vector or it moves ahead – depending on the predominance of electrical or magnetic losses. In the ideal case of electric and magnetic losses *equality,* the changes in time of electrical and magnetic fields vectors going on in phase, as in the case of losses absence.

In the *non-magnetic* materials, electromagnetic energy dissipation is a result of dielectric relaxation or conduction mechanisms; in other words, through the damping forces acting on polarized atoms and molecules, and through the finite conductivity of material. In the *magnetic materials*, the cause of microwave absorption is the ferromagnetic resonance, in which the energy of spin waves excited by magnetic field is partially transferred to the acoustic vibrations of crystal lattice through the spin-lattice interaction.

Composite materials usually consist of two or more different substances with the interfaces between components. The constant interest in these materials is related to the fact that they represent a certain class of *artificial materials*, the properties of which can be deliberately set and vary within a very wide range by changing the matrix and filler materials, as well as by concentration and shape of inclusions. In particular, by varying different components, it is possible to obtain a material with predetermined conductivity – from good dielectric to good conductor. The greatest heterogeneity of electrical properties can be created exactly when dielectric and conductor are mixed.

References

[1] F. Kremer and A. Schönhals, *Broadband dielectric spectroscopy*. Springer, 2003.

ISBN 978-3-642-62809-2.

[2] M. T. Sebastian, *Dielectric materials for wireless communication*. Amsterdam: Elsevier, 2008. ISBN: 978-0-08-045330-9.

[3] J. Kruželák, A. Kvasničáková, K. Hložeková, and I. Hudec, *Progress in polymers and polymer composites used as efficient materials for EMI shielding*, Nanoscale Advances, vol. 3, no. 1, pp. 123–172, 2021. DOI: 10.1039/d0na00760a

[4] Y. Poplavko, *Electronic materials. Prinples and applied science.* ELSEVIAR, 2019.

ISBN 978-0-12-815789-0.

[5] M. J. Weber, *Handbook of Optical Materials*. Boca Raton: CRC Press, 2003.

ISBN 978-0-84933512-9.

[6] M. T. Sebastian, R. Ubic, and H. Jantunen, *Microwave materials and applications.* Hoboken, NJ: Wiley, 2017. ISBN 978-1-119-20852-5.

Questions

1. Why electronics need to create microwaves absorbant materials?
2. Explain main mechanisms of EM waves Interaction with solids.
3. Electromagnetic general description of microwaves absorption.
4. What is peculiar in microwave absorption in metals?
5. List main mechanisms of microwave absorption in semiconductors.
6. What is the nature of absorption mechanisms in dielectrics?
7. What is peculiar in microwave absorption in ferroelectrics?

CHAPTER 7. THERMAL DIFFUSION AND THERMAL DEFORMATION OF POLAR CRYSTALS

Contents

By measuring thermal conductivity and thermal diffusivity in the vicinity of ferroelectric phase transitions, the processes of polar bonds self-ordering and its forced-ordering by bias electrical field can be studied. Thermal energy transfer in polar crystals is inhibited, since responsible for heat transfer shortwave acoustic phonons interact with optical phonons. As a rule, such interaction retards the heat transfer due to optical phonons contribution scattering, which is revealed by a deep minimum in thermal diffusivity. But in the antiferroelectrics, it is found that optical-acoustic interaction may reinforce thermal diffusion, which is expressed as a large sharp maximum of diffusivity, because soft phonon frequency vanishes in the middle of Brillouin zone that promotes optical phonons participation in heat transfer together with acoustic phonons.

Physical nature of quite specific phenomenon of negative thermal expansion coefficient seen in the polar crystals is considered. Usually it is observed at low temperatures but is especially evident in the vicinity of ferroelectric phase transitions, when the non-polar structure replaces the polar one. The negative expansion is associated with fundamental nature of the non-central symmetric crystals caused by the difference in electronegativity of adjoined ions forming polar crystal. The negative thermal expansion is specified by the configurational entropy, conditioned by a self-ordering of polar bonds of pyroelectrics and ferroelectrics. This phenomenon corresponds to the case, when entropy grows with increasing pressure: this is a persuasive evidence of the configurational entropy, which is conditioned by the structural ordering of dynamically forming polar clusters. The negative thermal expansion can be applied in the thermal compensators to achieve minimal thermal deformations.

7.1 Basic concepts of heat transfer and thermal deformation

Thermal properties of material are caused by the internal energy of movement of molecules, atoms or electrons being strongly dependent on internal structure of material: the more stable bonds between atoms the more energy must be expended for atoms displacement. In other words, more stable interatomic bonds require more energy for their formation. Stabilization of any physical states in a given system occurs by its tendency to reach minimal energy. One consequence of this law is that electrons occupy orbits with lowest energies, except cases when they receive additional energy of excitation from the external sources. But over a time these excited electrons tend to return to more stable unoccupied orbits with lower energy; this happens thanks to thermal motion in crystals and is described by thermodynamics.

Thermal energy determines many properties of crystals. For example, the generation and recombination of charge carriers as well as their equilibrium concentration setting in the semiconductors are due to thermal motion in lattice. The ferromagnetic and ferroelectric phase transitions, the dielectric-to-metal transitions and such noticeable phenomena as pyroelectricity, electrocaloric effect, magnetic cooling, thermostriction and others directly relate to the thermal properties. However, this chapter is devoted only to two thermal phenomena in solids: *thermal conductivity* and *thermal expansion*. First it worth recalling some basic concepts of thermodynamics necessary for describing thermal properties.

The *potential energy* is a part of energy of a system that depends on the positions of particles and on external force fields. In solids the source of potential energy is the Coulomb forces that cause attraction of opposite charges and repulsion of same sign charges. The *kinetic energy* (energy of motion) also plays important role for description of substances properties. For example, gas pressure is due to kinetic energy of atoms or molecules. In solids atoms are not absolutely fixed in a lattice, but they continually oscillate as a result of thermal excitation. Such movement significantly affects basic properties of solids that will be discussed in following sections.

The state of a system is characterized by thermodynamic function called the *enthalpy A* (otherwise, it is the heat content in a system). As temperature increases from T_1 to T_2, enthalpy changes: $A_2 = A_1 + \int_{T_1}^{T_2} C_P \partial T$, where A_1 is enthalpy at initial

temperature T_1 while A_2 is enthalpy at final temperature T_2; at that, C_P is the *specific heat* under constant pressure P. As thermodynamic function, enthalpy can be defined in two ways. First method is based on determination of *internal energy* U and *work* PV, performed by material: $A = U + PV$, where P is pressure and V is volume of material. The second method is based on the Helmholtz conception about *free energy* F (or Gibbs free energy G), and on the parameter TS that is the energy conditioned by *internal disordering* in a matter: $A = F + TS + PV = G + TS$, where T is absolute temperature and S is *entropy* of material. In other words, entropy is the measure of system internal disordering (chaos). Typically, thermodynamic quantities are given in well-known Tables with values of entropy together with values of enthalpy and free energy.

The function $F = U - TS$ (that is called as Helmholtz free energy) is minimal energy of equilibrium state of system. When considering processes in solids, it is more convenient to control the volume of a system (not a pressure), and, therefore, it is necessary to use another thermodynamic function: Gibbs free energy $G = F + PV$. In this case minimum of G characterizes equilibrium of system at *constant volume* and *constant temperature*. In solids at atmospheric pressure condition of system equilibrium can be assessed using minimum F.

The enthalpy permanently increases with temperature, but the contribution of entropy TS increases *more rapidly*; therefore, Gibbs free energy *decreases* with increasing temperature. Since a concept of free energy is widely used in subsequent discussions in the context of solids properties and their stability, it is necessary to draw a few conclusions:

- At zero absolute temperature free energy equals enthalpy: $A = G$;
- Free energy that is used to characterize processes of structural change in a matter decreases with increasing temperature;
- The rate of free energy decrease with temperature is related to entropy.

Also, since the *entropy is always positive* and *obligatorily increases with temperature rise*, the slope of free energy curve continuously increases with temperature. At that, the value of free energy gives important information about given phase changing, so the lower free energy the more stable is a given phase. In connection with thermodynamic description and applications of solids in electronics (for example, in case of active dielectrics or ferromagnetics), it should be mentioned some basic concepts:

- The *heat* is energy of thermal motion of particles that form a body, in Gauss system it is measured in calories [cal] and in SI in Joules.

• The *absolute temperature* is thermodynamic quantity that characterizes the state of a body at its thermodynamic equilibrium; absolute temperature is denoted by T and measured in degrees of Kelvin [K]. Average energy of particles in a body is proportional to absolute temperature.

• The *heat capacity,* denoted C and measured in [J/deg] or in [cal/(deg·mol)], is a heat absorbed from outside when temperature increases. In active dielectrics and ordered magnetics heat capacity is dependent on mechanical and electrical boundary conditions of a crystal.

• The coefficient of *thermal conductivity*, being denoted λ and measuring in [W/(deg·m)] or [cal/(deg·sec·cm)], is characteristics property of heat-conducting material; numerically it is equal to amount of heat passing through unit area per unit time at unit temperature gradient.

• The coefficient of *thermal expansion* that is denoted α and measured in unit $[\text{deg}^{-1}] = [\text{K}^{-1}]$ represents alterations in solid body relative dimensions when temperature changes by 1 K.

The following discussion will focus on two thermal properties of solids: thermal conductivity and thermal expansion. These are properties that have greatest practical importance.

Thermal properties of solids are well researched [1], as well as the physics of ferroelectric crystals is largely described [2], but in thermal physics of ferroelectrics still a number of features remain which need clarification. Ferroelectrics belong to polar crystals, which are characterized by the mixed ionic-covalent bonds, possessing by a strong orientation, which may be considered as a main cause of these crystals low symmetry. (Indeed, purely ionic-bonded crystals so as purely covalent crystals belong to the central symmetrical classes, and, unlike polar crystals, they have no dedicated orientation in their inter-atomic bonding). The primary cause of the internal polarity, seen in some crystals, is the asymmetry in electronic density distribution along the inter-atomic bonds. In turn, this is conditioned by the difference in electronegativity of adjacent ions: the ion with increased electronegativity displace common electron pairs towards itself, so its operating charge is more negative, while the ion with lower electronegativity acquires, respectively, an increased positive charge. Together these ions create a polar bond with the inhomogeneous distribution of electronic density [3]. Such polar connection is strictly directed, which leads to the less-dense crystal structures possessing reduced coordination number. So it might be concluded that the intrinsic polarity in

some crystals arises due to the structural compensation of neighboring ions different electronegativity.

These features of polar crystals are clearly manifested in their thermal properties, in particular, in the mechanisms of thermal conductivity, which in ferroelectric materials is especially pronounced in the vicinity of phase transitions. At that, in addition to optical-acoustic interaction, the heat flow slows down by the fluctuations of polar bonds (as shown below, the applied electrical field can effectively control this effect).

As known, thermal conductivity characterizes the ability of a material to conduct the heat in the course of chaotic thermal movement of material's particles. Accordingly to Fourier's heat conductivity law, directed heat flux q is proportional to the temperature gradient: $q = -\lambda \cdot \mathrm{grad}T$ (in anisotropic crystals, vector $q_i = -\lambda_{ij}\nabla T_j$, where second rank tensor λ_{ij} is the thermal conduction coefficient). In the dielectrics, the thermal energy is transferred mostly by the short-length acoustic waves ("heat phonons"), which propagation velocity is much less as compared to the long-length "sound phonons". In the *covalent* crystals, the heat transfer is due to the fact that in them the heat carriers (short-wave acoustic phonons located near the boundary of Brillouin zone) nearly not interact with the optical phonons, so their thermal conductivity is rather big: λ = 50–150 W/(m·K). In the majority of *ionic* dielectrics, their thermal conductivity is much smaller: λ = 10–20 W/(m·K), because the inter-ionic bonding promotes the inhibition of thermal phonons spread through the mechanism of their interaction with the optical phonons. But this interaction even more enhanced in the *polar* (non-central symmetric) crystals, in which the intratomic bonding has the mixed ionic-covalent character, so the thermal conductivity in these crystals at normal temperatures usually is very small: λ = 1–10 W/(m·K) [3].

The deceleration of heat flow in the polar crystals by the ordering of polar bonds is convincingly shown in Fig. 7.1*a* as the dependence of thermal resistance of a material ($R = \lambda^{-1}$) on the squared coefficient of thermal expansion α (physical justification of this relationship will be will be given below). The group velocity of thermal phonons in the polar crystals is greatly reduced due to the fact that in them the acoustic phonons branch, when approaching the boundary of Brillouin zone, bends down by the acousto-optic interaction, Fig. 7.1*b*. Therefore, it is not surprising that in polar crystals, despite the low attenuation and high-velocity long (sound) waves, for the short (thermal) waves polar crystal looks like a turbid medium. But precisely for this reason the thermal resistance of such medium can be controlled by the electrical field, application of which leads to the forced ordering of dipole

clusters and, as a result, to increase their size, at the boundaries of which the thermal phonons scatter.

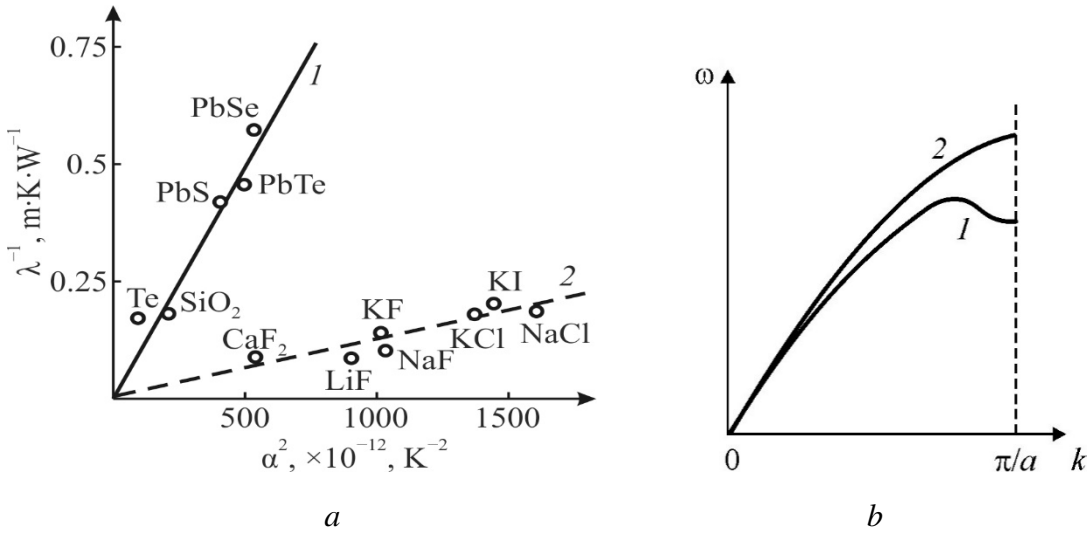

Fig. 7.1. Comparison: *a* – thermal resistance in polar (*1*) and non-polar (*2*) crystals; *b* – acoustic mode spatial dispersion in polar GaAs crystal (*1*) and in non-polar NaCl crystal (*2*)

To describe the heat transfer, two main parameters are usually used: thermal conductivity (λ) and thermal diffusivity (ξ). The first parameter is important mainly for the technical properties of materials (for example, to predict their overheating), while the second parameter is the best for heat transfer mechanism interpretation. As seen in Fig. 7.1*a,* in the polar crystals both these parameters are noticeably less than in the common dielectrics and semiconductors.

7.2 Thermal conductivity and thermal diffusivity comparison

Thermal conductivity λ [W/m·K] equals to the amount of heat passing through the unit area per unit time at unit temperature gradient. It depends on crystal specific heat *C,* average free path of phonons $\langle l \rangle$ and average velocity $\langle \upsilon \rangle$ of the phonons: $\lambda = (1/3)\cdot\upsilon\cdot l = (1/3)C\cdot\upsilon^2\cdot\tau$, where τ is the free path time. In turn, the free path $\langle l \rangle$ is determined by the square of anharmonicity coefficient. So, thermal conductivity λ relates to thermal expansion coefficient α, and in such a way that the inverse λ conductivity is proportional to the squared α. This ratio is confirmed experimentally: really, the correlation $1/\lambda \sim \alpha^2$ is seen in Fig. 7.1*a* as in non-polar so in polar dielectric and semiconductors, in both the phonon mechanism of heat transfer predominates. It follows from this, that, firstly, the crystals with larger thermal expansion have smaller thermal conductivity (since both parameters are determined by the anharmonicity of ions vibrations in the crystal lattice). And, secondly, it follows that in the polar crystals the thermal conductivity is much lower than that of

the non-polar crystals (again due to big difference in the magnitude of anharmonicity). Like specific heat $C(T)$ characteristic, thermal conductivity $\lambda(T)$ shows the temperature maximum located near $0.1\theta_D$ which is also connected with the minimum of thermal expansion coefficient [3].

Thermal diffusivity ξ [m^2/s] is defined as the thermal conductivity divided by the volumetric specific heat: $\xi = \lambda/C_p$. It characterizes the rate of heat transfer in a material from its hot side to cold side, being a measure of thermal inertia, determined by the average free path l and the average velocity υ of thermal phonons propagating in a crystal ($\xi \sim l \cdot \upsilon$). At low temperatures, the density of phonons is so small that they practically not interact, so their free path is large, depending mostly on the macroscopic-size defects. That is why, at very low temperatures, the $\xi(T)$ remains nearly constant, keeping its greatest value. However, as temperature rise, the $\xi(T)$ decreases hundreds of times. because due to anharmonicity the phonons collisions frequency increases, that describing by Grüneisen parameter γ: $\langle l \rangle \sim a/(\alpha \cdot \gamma \cdot T)$, where a is lattice constant. As temperature increases, thermal diffusivity falls very quickly: $\xi(T) \sim l \sim \exp(T^{-1})$, since the average free path of phonons is limited by the inter-phonon umklapp processes [1], which occur, when the phonons loss their quasi-momentum. Next, with subsequent increase of temperature (when $T > \theta_D$), in the temperature interval discussing below, the gradual lowering in $\xi(T)$-dependence follows Aiken law: $\xi(T) \sim T^{-1}$.

To identify the physical mechanisms of heat transfer, an analysis of $\xi(T)$ dependence seems much convincing than the analysis of thermal conductivity. For example, in the non-polar silicon crystal and in the polar quartz the speed of sound, determined by the spread of long-wave acoustic phonons, in both crystals is similar (~ 5000 m/s). However, the speed of shortwave (″heat") phonons differs in ~ 60 times (compare ξ_{Si} = 88 mm^2/s with ξ_{SiO2} = 1.4 mm^2/s at 300 K). Therefore, the coefficient of thermal diffusion is rather strong criterion for phonon movement investigation: it characterizes not a total heat flux but the kinetic characteristics of energy carriers. Their upper limit is determined by umklapp processes, while the lower boundary corresponds to the amorphous solids, where the energy transfer occurs only between the neighboring cells.

Methods of measurements. The thermal conductivity investigations were performed by the method of stationary heat flow, at that, the temperature gradient on a sample did not exceed 1 K. For study, near 1 mm thick samples were selected, being placed in a cryostat, which was an integral part of the automatic temperature control device [4]. The temperature was measured using the differential copper-

constantan thermocouple with the accuracy of not less than 0.01 K. The studies of thermal diffusivity were performed by the method of plane temperature waves in the mode of self-oscillation at a wave amplitude of ~ 0.1 K and with the rate of crystal temperature change ~ 200 mK/min [5].

7.3 Main thermal properties of ferroelectrics

When in polar crystals thermal properties investigation, the ferroelectrics can serve as the best example. In them, the thermal phonons are scattered by dynamically ordering polar clusters; therefore, by study of heat transfer it is possible as to trace the mechanisms of polar clusters self-ordering, so the their forced ordering under applied onto a crystal electrical field, obtaining amazing results in vicinity of phase transitions. It should be recalled, that main contribution in the heat transfer is given by the acoustic phonons, which group velocity slows down, when acoustic branch of spectrum approaches to the boundary of Brillouin zone, Fig. 1*b*. Main feature of polar crystals (as all of them are the piezoelectrics) is the interaction of acoustic phonons with optical phonons. At that, if optical phonons show essential spatial dispersion, they can make a significant positive contribution to the heat transfer. But in the most cases, their spatial dispersion manifests itself weakly, so the optical phonons give additional contribution only in the phonons scattering, which substantially decreases thermal conductivity. It is this reduction that explains the difference in the thermal conductivity of the polar and non-polar crystals shown before in Fig. 7.1*a*.

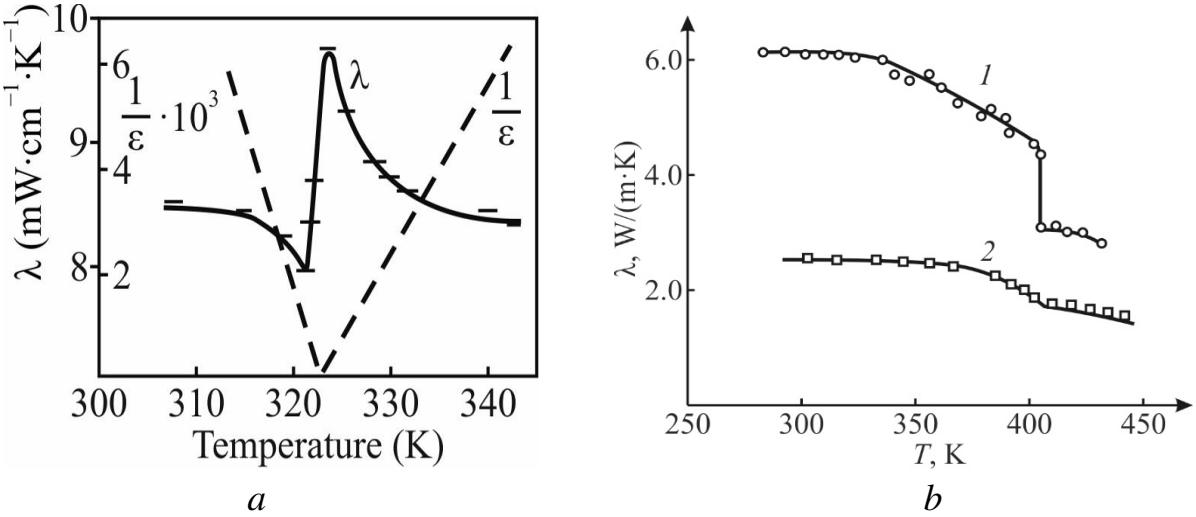

Fig. 7.2. Thermal conductivity (λ) temperature dependence: *a* – TGS crystal in [010]-direction with inverse value of permittivity ($1/\varepsilon$), while horizontal dashed lines show inevitable temperature gradient at measurements; *b* – barium titanate crystal (*1*) and ceramics (*2*)

Thermal conductivity is dependent on the degree of ordering of polar-sensitive bonds that is clearly seen with example of ferroelectrics. Moreover, as it could be expected, this effect is especially pronounced in the crystals with the order-disorder phase transition, but to a lesser extent in the crystals with the displacement-type transition. This can be seen in Fig. 7.2*a* on the example of TGS crystal, $(NH_2CH_2COOH)_3 \cdot H_2SO_4$, in which the Aiken's law $\lambda(T) \sim T^{-1}$ for thermal conductivity in the region of studied temperatures is not satisfied.

First of all, this is due to a small average free path of phonons, the scattering centers of which are commensurable with the order of lattice constant. Secondly, the temperature-variation of thermal conductivity partially follows the change in the specific heat, which has a maximum in Curie point [2]. But only in this case, the minimum of thermal conductivity would not be observed, since the main investment in the $\lambda(T)$ dependence is made by the change of specific heat. It is possible that phonons scattering in the vicinity of phase transition is due not only to the anharmonicity of lattice vibrations, but also to other additional phonon-scattering mechanisms, for example, the scattering on the structural heterogeneities.

It can be assumed that the minimum of thermal conductivity in phase transition region below Curie point is due to the phonon scattering, considering the interaction of acoustic and optical phonons. It is also possible, that an additional scattering of phonons on the domain walls exists. In the TGS-family crystals, the anomalies of thermal conductivity in the vicinity of phase transition are also observed in the [100] and [001] directions. However, as expected, the absolute values of thermal conductivity of TGS, TGFB and TGSel are of same order of magnitude [4]. The anisotropy of thermal conductivity is observed in all these crystals: largest value of $\lambda(T)$ is seen in the [100] direction, while the smaller ones are seen in [010] and [001] directions. At that, the anisotropy of thermal conductivity in the TGS crystal is consistent with the anisotropy of ultrasound propagation velocity.

It looks a little different the thermal conductivity change in the case of ferroelectrics of the displacement type phase transition, Fig. 2*b*. No maximum and no minimum of $\lambda(T)$ in the vicinity of phase transition are observed, since the phase transition is close to the first-order transition, at which transition temperature T_c is higher than critical Curie-Weiss temperature θ, so possible very intensive fluctuations of polarity are suppressed by the more rigid crystal lattice. According Fig. 7.2*b*, in the polycrystalline barium titanate the $\lambda(T)$ value in 2.5 times less than in the single crystal, both above and below Curie point ($T_c \approx 400$ K), because ceramics have macroscopically disordered structure. At that, in the $BaTiO_3$ crystal

and in its ceramics, in the ordered ferroelectric phase, the thermal conductivity almost doubles in comparison with microscopically disordered paraelectric phase.

As already mentioned, when study thr thermal conductivity anomalies in polar crystals, two important factors display simultaneously. First is the temperature maximum of heat capacity $C(T)$, seen at phase transition (that is a manifestation of latent heat of the transition). Second is the change in *average free path* of phonons $\langle l \rangle \sim \xi(T)$ due to a partial ordering of polar bonds below phase transition. As a result, it turns out that the heat transfer is determined by the product: $\lambda(T) = \xi(T) \cdot C(T)$. In order to avoid the influence of heat capacity while heat transfer analysis, and to separate out the process of phonons scattering, the thermal diffusion $\xi(T)$ should be measured, which indicates just the average free path of phonons without taking into account the heat capacity.

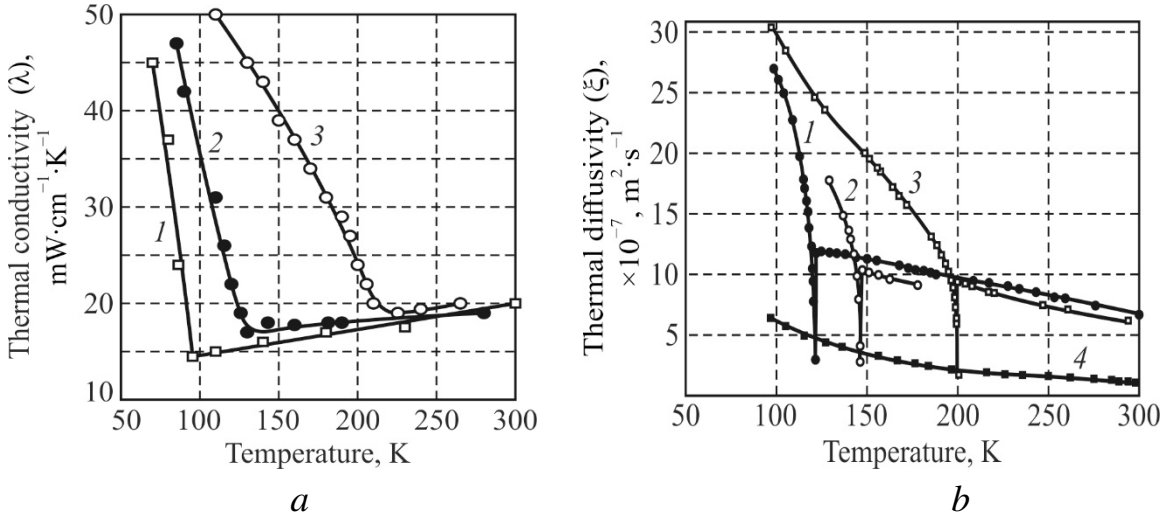

Fig. 7.3. Thermal conductivity λ and thermal diffusivity ξ in ferroelectrics: the phosphates *1* – KH_2PO_4, *2* – KH_2AsO_4, *3* – KD_2PO_4; and *4* – the Rochelle Salt $KNaC_4H_4O_6 \cdot 4H_2O$

Thermal diffusivity comparison with the thermal conductivity is shown in Fig. 7.3 on the example of the KDP group crystals in comparison with the Rochelle Salt. These dependences are significantly different. In the $\lambda(T)$ dependence, at the phase transition point, only a bend of $\lambda(T)$-dependence is seen, followed by its gradual increase below T_C due to the increase of polar bonds ordering. But in the $\xi(T)$ curves in KDP group crystals, a sharp minimums are observed, indicating a large shortening in the average wavelength of phonons in the vicinity of phase transition. Such difference between $\lambda(T)$ and $\xi(T)$ dependences is due to the fact that in the $\lambda(T)$-characteristic a large decrease in the phonons wavelength is compensated by the specific heat maximum. As above so below the Curie point, the acoustic vibration modes (phonons) in the polar crystals are mixed with the optical phonons; therefore, the optical phonons anyway participate in the heat transfer. The prerequisites for

heat transfer are provided by the spatial dispersion of optical modes. Iin other words, the process of heat transfer in the polar crystals is significantly influenced by optical phonons, since they are associated with acoustic phonons. Interaction of acoustic phonons with soft transverse optical mode (peculiar to ferroelectrics) leads to a decrease in the average free path of phonons which reduces to a possible minimal level in the point of phase transition. In the different crystals and at various T_C temperatures (and even in case of DKDP) this level remains almost same, Fig. 7.3*b*. It is established that in the wide temperature range just same very low level of thermal diffusion is seen in the Rochelle Salt crystal, where $\xi(T)$ sharp dips are not seen in Curie points.

On the basis of established lowest limit of the wavelength of thermal phonons (which, apparently, reaches the value of unit cell parameter of a crystal), one can come to the conclusion that in the disordered phase (above phase transition temperature) this wavelength still remains in order of magnitude larger and then continues to drop with temperature, as it is usual for all crystals. Below the phase transition temperature, the role of structural ordering of polar crystals becomes very noticeable (apart from Rochelle salt, in which a particularly complex structure makes it almost heat-impermeable (resembling glass). As temperature lowers starting from Curie point, a very fast increase of thermal phonons wavelengths is observed that indicates a substantial ordering in the polar-sensitive bonds. Since in this temperature range there are no noticeable anomalies in the specific heat, so same dependence is reproduced in the temperature dependence of thermal conductivity.

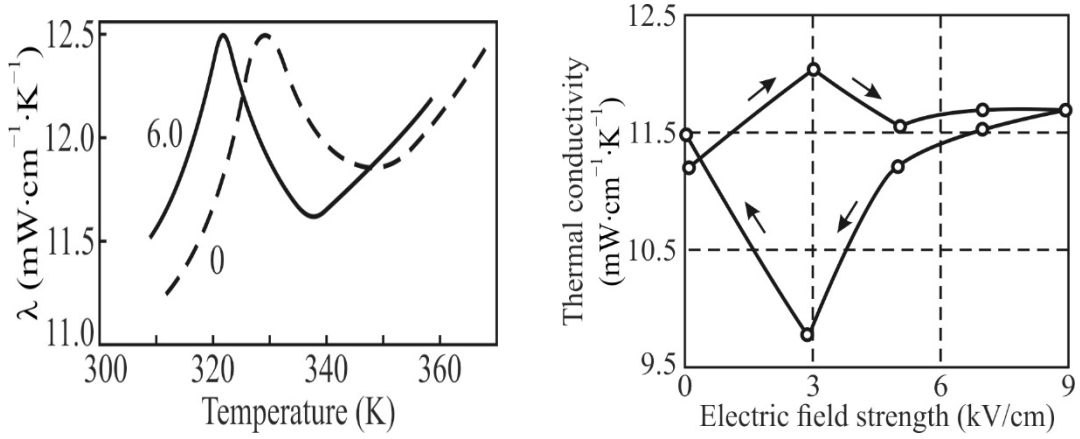

a *b*

Fig. 7.4. Influence of bias electrical field on thermal conductivity coefficient (λ) of nonlinear ferroelectric Ba(Ti,Zr,Sn)O_3 near its phase transition: *a* – λ temperature dependence at $E = 0$ and $E = 6.0$ kV/cm: *b* – λ-dependence on electrical field at 48 °C

Electrical control of heat transfer might have as scientific so technical interest. Firstly controlled heat transfer we stude with the polycrystalline

ferroelectric $Ba(Ti,Zr,Sn)O_3$, which has a diffuse phase transition and characterized by the electrically controlled dielectric permittivity up to ~ 0 times in the temperature interval. Measurements were carried out in the vicinity of the diffuse phase transition, and the results are shown in Fig. 7.4. When constant electrical field is applied, the maximum of thermal conductivity, seen in the region of phase transition, shifts by 5–8 degree towards lower temperatures. This corresponds to the $\lambda(E)$ increase the ferroelectric phase near the phase transition. However, for technical applications, such effect of thermal conductivity control seems to be too small. Moreover, a hysteresis in the $\lambda(E)$ dependence is observed, shown in Fig. 7.4*b,* indicating that phonons scattering is to some extent is due to the domain structure of ferroelectric.

Based on the previous results, it can be expected that $\lambda(E)$ control effect will be stronger in the order-disorder ferroelectrics. For this study, the TGS crystal is selected, because it most corresponds to the theoretical model for phase transitions of order-disorder type, and its phase transition is close to room temperature. The heat transfer peculiarities in the TGS crystal are shown in Fig. 7.5, and the greatest impact is seen along the polar axis, with a significant changes both in the $\lambda(T)$ and $\xi(T)$. The difference in thermal conductivity and in thermal diffusivity on the electrical displacement field is explained by the fact that this effect is due to a change in the frequency of optical phonons. For this reason, the minimum $\lambda(T)$ is accompanied by its maximum, which is shifted under the action of electrical field towards lower temperatures.

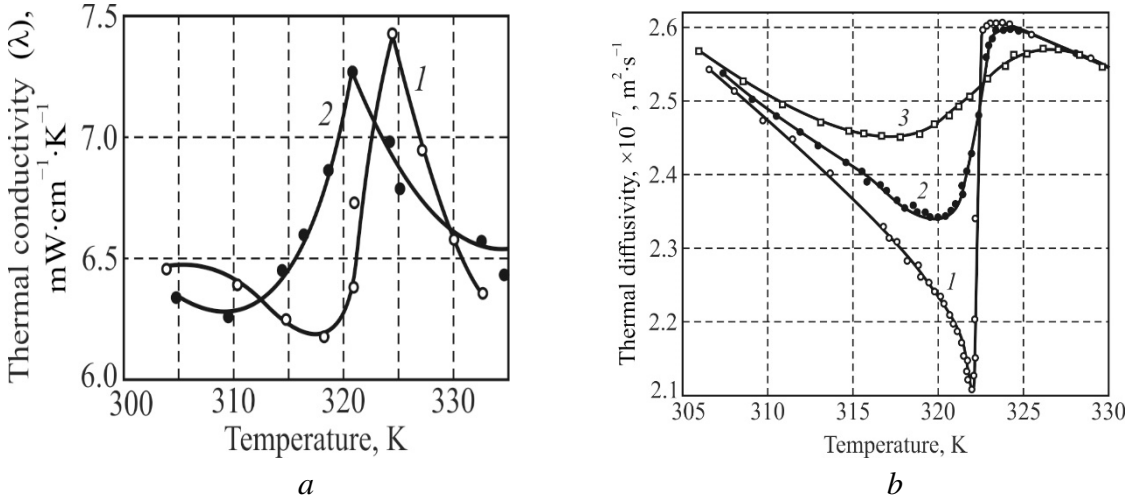

Fig. 7.5. Thermal conductivity (*a*) and diffusivity (*b*) in TGS crystal near Curie point under bias electrical field: *a* – E = 0 (*1*) and E = 6 kV/cm (*2*); *b* – E = 0 (*1*), E = 3.4 kV/cm (*2*) and E = 10 kV/cm (*3*)

It should be noted that heat transfer in the crystals depends not only on the conditions of phonon scattering, but also on the elastic properties of a crystal and its

heat capacity. In this case, in the region of phase transition, there is a large maximum of heat capacity and minimum of sound velocity, and both under the action of an electrical field shifts in temperature, decrease and become blurred. This makes it difficult to unambiguously interpret the changes in $\lambda(T)$, which is not reduced only due to change in mean free path of slow thermal phonons. During heat transfer in polar crystals, the optical phonons can influence this phenomenon in various ways. As a rule, since the group velocity of optical phonons is small, their influence on the thermal conductivity reduces only to the additional scattering of thermal phonons and increases thermal resistance. But it is impossible not to take into account, firstly, that when the boundary of Brillouin zone is approached, the group velocity of acoustic phonons essentially decreases, and, secondly, the fact that it is this region of phonon spectrum which determines the very nature of heat transfer.

On the other hand, in the polar crystal, the increased dispersion of optical phonons leads to their branch decrease near the boundary of the Brillouin zone. The optical-acoustic connection in polar crystals-piezoelectrics enhances the interaction of acoustic and optical phonons and increases their role in heat transfer processes. This is partially confirmed by the influence of electrical field on thermal conductivity and on thermal diffusion. In this case, the dual mechanism of participation of the optical phonons in heat transfer can compensate each other in the case of heat conduction, but not in the process of thermal diffusion. An increase of thermal diffusion coefficient in the ordered (ferroelectric) phase should be noted, which naturally indicates a greater ordering of the polar bonds (after all, it is their disorder that prevents heat diffusion). In the applied field, the $\xi(T)$ increases because the wavelength of thermal phonons increases.

Thus, the electrical field can indeed control the intensity of the heat flux within the limits of about 20%, but for practical purposes this effect turns out to be small and takes place only in a narrow temperature range. In the paraelectric phase of ferroelectrics (above Curie temperature), the thermal diffusion coefficient in the electrical field increases; i.e., the effect appears to be opposite, because the phase transition in the electrical field is smeared and shifted towards higher temperatures.

7.4 Thermal diffusion in antiferroelectrics

From a scientific point of view, the antiferroelectricity is a rather complex problem in the physics of ferroelectricity [2], and antiferroelectrics can only formally be related to the antiferromagnets. It is known, that when pressure increases, the antiferroelectric phase transition (in contrast to the ferroelectrics)

shifts toward higher temperatures. So the change in heat transfer in these substances looks of great importance for this phenomenon understanding. In the terms of technical application, the heightened interest in the features of thermal properties of antiferroelectrics is due, firstly, to the fact that they have simultaneously a high dielectric permittivity and increased thermal stability of properties with low microwave losses. Secondly, during phase transition between the ferroelectric and antiferroelectric states, a "giant" electrocaloric effect has recently been discovered, which might have great prospect for application [6], so the thermal properties of these substances are of particular importance.

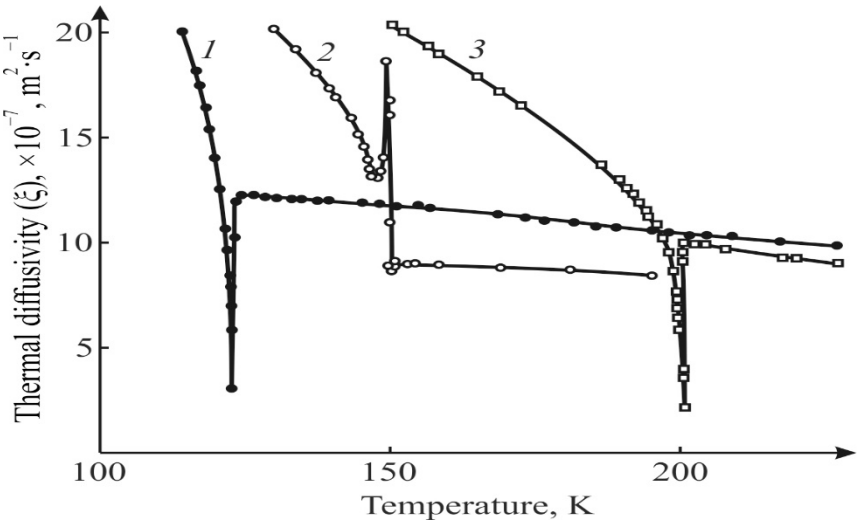

Fig. 7.6. Comparison of thermal diffusion in ferroelectrics KDP (curve *1*) and DKDP (curve *3*) and antiferroelectric ADP (curve *2*)

While study of heat transfer in the region of phase transitions, a grate advantage to investigate precisely the thermal diffusivity is obvious, because it makes possible to reveal the features of thermal phonons participation of in these process. And indeed, in antiferroelectric ammonium dihydrophosphate ADP = $(NH_4)(H_2PO_4)$ in the Curie point a sharp *maximum* of thermal diffusion is observed, instead of the usual deep minimum seen in the ferroelectrics. Such $\xi(T)$ dependence can only indicate that the optical phonons are actively involved in the heat transfer mechanism in vicinity of antiferroelectric phase transition. The point is that frequency of optical oscillation mode in the antiferroelectrics decreases critically not in the center (as in ferroelectrics) but at the boundary of Brillouin zone, mixing with the short-wavelength (thermal) acoustic phonons, providing heat transfer. That is why, the thermal diffusion coefficient rises sharply precisely at the Curie point, Fig. 7.6. In the ferroelectrics, this effect does not manifest itself, since the critical decrease of transverse optical oscillations frequency occurs in the region of long-wavelength phonons, i.e., in the center of Brillouin zone. On this reason in the

ferroelectric crystals a large maximum of dielectric permittivity is observed: in the KDP crystal: out measurements show that at frequency of 10 GHz (where any acoustic or relaxation processes can not manifest themselves) at Curie point $\varepsilon_{max} \approx$ 1000, while at same frequency in the antiferroelectric ADP $\varepsilon_{max} \approx$ 90.

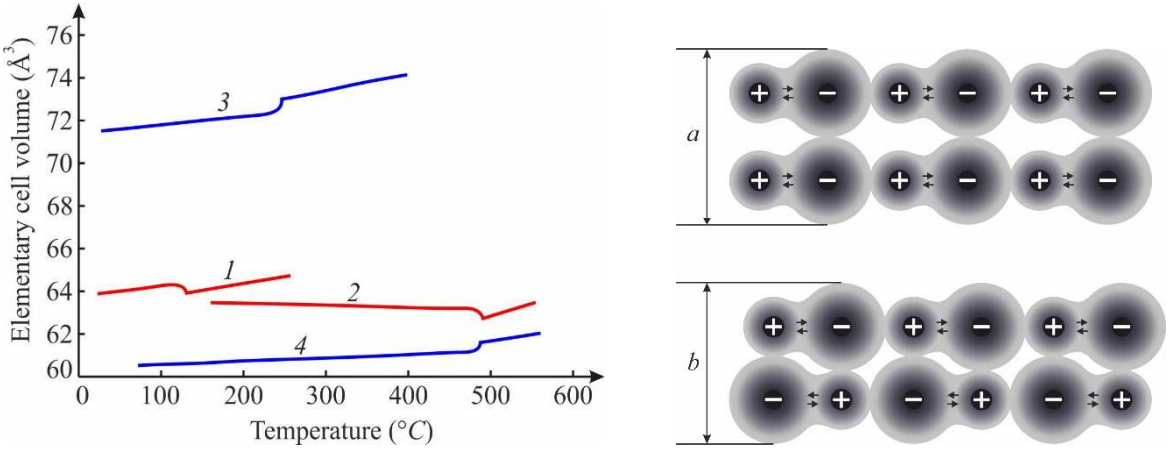

a *b*

Fig. 7.7. Ferroelectric and antiferroelectric phase transitions comparison: *a* – unit cells volume temperature dependence in ferroelectrics $BaTiO_3$ (*1*), $PbTiO_3$ (*2*) and antiferroelectrics $PbZrO_3$ (*3*), $NaNbO_3$ (*4*); *b* – simplified model of polar and antipolar structural ordering when *a* > *b*

In the antiferroelectrics, their phase transition from the no-npolar (paraelectric) to the anti-polar phase occurs with the decrease in volume, Fig. 7.7*a*, in contrast to the ferroelectrics, in which the volume of polar phase increases below phase transition. As a result, while antiferroelectric phase transition, the maximum of thermal expansion coefficient $\alpha(T)$ is seen, but not $\alpha(T)$ minimum, common for ferroelectric phase transitions. Simplified model representation of density increase in the anti-polar phase is shown in Fig. 7.7*b*.

It can be considered that this circumstance has been used recently to obtain the "giant" electrocaloric effect [6] during the transition from the anti-polar phase to the polar one. In general case, when phase transition is forced by an electrical field from the paraelectric phase to the ferroelectric phase, the jump in the volume leads to the change in temperature (this is clearly seen from relationship $PV = RT$: at constant P the change in V changes T). Usually this electrocaloric effect produces temperature change of about 1-2 degrees, that is not enough to be used in technology. However, electrically controlled volume jump at the transition antiferroelectric⇔ferroelectric at least doubles this temperature jump. Such electrocaloric effect in terms of technical application look as expedient. It is obvious,

that above studies of thermal physical properties in the region of antiferroelectric phase transition are topical.

Shown in Fig. 7.7*b* special arrangement of inter-atomic bonds in the anti-polar crystal leads not only to the promotion increased density of antiferroelectric, but also increases the probability of optical phonons participation in the thermal diffusion. An important factor is the fact that the antiferroelectric phase transition occurs with the multiplication of the crystal lattice parameter. This means that a spatial dispersion of optical phonons at the boundary of Brillouin zone is enhanced precisely because of critical decrease in their frequency.

7.5 Polar crystals peculiarities

Polar crystals are the solids characterized by the mixed ionic-covalent bonds, which may be considered as the main cause of low symmetry seen in these crystals. Thermal properties of solids [1] including ferroelectrics [2, 3] are good researched, but still some peculiarities seen in the thermal properties of polar crystals remain, which need clarification. One of these mysterious property is the negative coefficient of thermal expansion.

The primary cause of the internal polarity in crystal is the asymmetry in electronic density distribution along the inter-atomic bonds. In turn, this feature is conditioned by the difference in the electronegativity of adjoined ions: the ion with increased electronegativity displaces common electron pair towards itself, so its operating charge is more negative, while the ion with lower electronegativity acquires, respectively, the increased positive charge. Together these ions create the polar bond with a inhomogeneous distribution in the electronic density along the inter-ionic bond. Such polar connection is strictly directed, which leads to less-dense structure of crystal with reduced coordination number. Thus, it might be concluded that internal polarity, seen in centrosymmetrical crystals, arises due to a structural compensation of the different electronegativity of neighboring ions [4].

The polar bonds are a specific feature of both pyroelectrics and piezoelectrics, that explains a proximity of these crystals in manifestation of completely different properties:

1. During crystallization process, the density of polar crystals decreases in comparison to their melt: for example, growing GaAs crystal swims in its melt as the ice in a water. It may be deduced that the establishment of polar bonds expands the material, transforming its structure into the non-centre symmetric one (the example is ferroelectric phase transitions).

2. In their chemical properties, polar crystals exhibit the unipolarity on their surface: for instance, the etching of quartz occurs more rapidly at the "positive" end of polar *X*-axis, while the etching is more slow at the "negative" end of *X*-axis. Therefore, the etch patterns for quartz plates are very different for "+" and "–" surfaces [6]. In just the same way, in the cubic class polar GaAs crystal one can see a considerable distinction in chemical properties between two surfaces of the (111)-plate [4]; at last, the internal unipolarity is widely used while ferroelectric domains study [2].

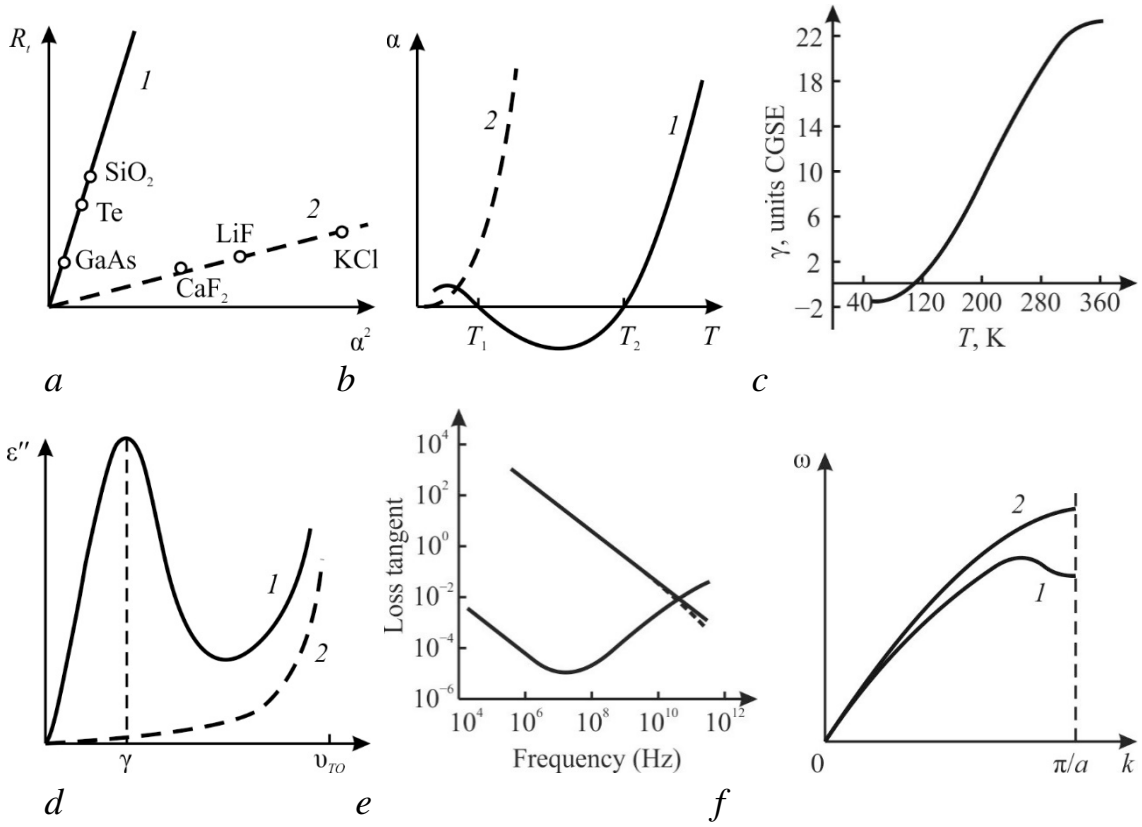

Fig. 7.8 Thermal physics and lattice dynamics properties of polar and non-polar crystals: *a* – thermal expansion coefficient α in polar (1) and in non-polar (2) crystals; *b* – thermal resistively coefficient R_t dependence on α^2 for polar (*1*) and non-polar (*2*) crystals; *c* – pyroelectric coefficient γ in polar crystal lithium sulfate Li_2SO_4-H_2O [6]; *d* – microwave absorption ε'' of quasi-Debye type; *e* – microwave losses in Si and GaAs crystals [4]; *f* – acoustic branch in Brillouin zone for polar (*1*) and non-polar (*2*) crystals

3. In their thermal properties, polar crystals resistance to the heat transfer far exceeds ones of the center symmetric crystals, Fig. 1*a*. Such increased thermal resistance of piezoelectrics is conditioned by the peculiarities of phonon dissipation process in these crystals. For that reason, the thermal diffusion intensity in the polar crystals is ten times lower than that of non-polar ones; for example, in the Si and SiO_2 (quartz) crystals, the speed of "short-wave" thermal phonons differs in them by

80 times (at that the sound speed in these crysral carrying by the "long-wave" phonons is almost same).

4. The thermal expansion coefficient $\alpha(T)$ in the polar crystals, in its temperature dependence, twice passes through a zero axis turning negative value at low temperatures, Fig. 1*b*, instead of showing its classical dependence of $\alpha \sim T^3$. It would be attributable to the assumption that the nature of inter-ionic attraction essentially changes at a small distance between ions. For the same reason, due to the negative thermal expansion, in some polar crystals their pyroelectric coefficient changes its sign at lower temperatures, Fig. 1*c*.

5. In the polar crystals, their fundamental high frequency absorption $\varepsilon'' = \varepsilon' \cdot \tan\delta$ vastly superiors this absorption in the center symmetric crystals [4]. Moreover, at microwaves, the dielectric losses $\varepsilon''(\omega)$ of piezoelectrics show an additional maximum of quasi-Debye type of absorption, Fig. 1*d,* due to interaction between optical and acoustical phonons. Our experimental evidence of this effect is shown in Fig. 1*e* as the comparison of microwave properties of two semiconductors: non-polar Si and polar GaAs.

6. The above mentioned special features of polar crystals correlate with their acoustic phonon spectrum near Brillouin zone boundary, where the acoustic mode has anomaly, as example, show for GaAs crystal in Fig. 1*f*. On the contrary, purely ionic-bonded crystals like NaCl, as well as the purely covalent crystals like Si usually belong to centre symmetrical classes of crystals, and, unlike polar crystals, they have no anomalies in acoustic or optical phonon modes dispersion (as well as dedicated orientation in their inter-atomic bonding and in many others properties).

7.6 Thermal expansion uniqueness for crystal research

The relative deformation of a solid is the dimensionless parameter, described by second-rank tensor: the mechanical strain x_{ij}. This deformation can occur not only when solid exposed by the mechanical stress X_{kl} (also second rank tensor), but under other external influences: electrical field described by polar vector E_k; magnetic influence described by axial vector H_k; scalar action – hydrostatic change of pressure δp; other scalar influences –change in temperature δT. In all listed cases, type and symmetry of parameters, which link various impacts (X_{kl}, E_k, H_k, δp, δT) and induced by these impacts response – the strain x_{ij} – are quite different:

$$x_{ij} = s_{ijkl}X_{kl}\,, \quad x_{ij} = d_{ijk}E_k, \quad x_{ij} = \varsigma_{ijk}H_k, \; x_{ij} = \xi_{ij}\delta p, \quad \boldsymbol{x_{ij} = \alpha_{ij}\delta T},$$

where s_{ijkl} is the elastic compliance (fours rank tensor), d_{ijk} is the piezoelectric module (third rank tensor), ς_{ijk} is the piezomagnetic module (third rank tensor), ξ_{ij} is the compressibility (second rank tensor), and α_{ij} is the coefficient of thermal expansion (second rank tensor) – exactly the parameter discussing here.

It is noteworthy that first three of above parameters characterize such properties of a crystal, which are obtained by external impacts in a form of various fields, which possess own t characteristics of symmetry, so the symmetry of a response-strain x_{ij} *composes* the symmetry of the impact and the symmetry of a crystal. Therefore, in case of multifaceted study of crystal properties, the tensors s_{ijkl}, d_{ijk} and ς_{ijk} only indirectly can characterize the nature of the internal bonds of atoms (or ions) in a crystal.

At the same time, the *scalar* actions on a crystal δp and δT, which have the symmetry of a *sphere*, gives such parameters ξ_{ij} and α_{ij}, which reflects intrinsic properties of exactly the inter-atomic bonds, directly seen in the response. However, of these two experimental possibilities for studying inter-atomic bonds, the hydrostatic pressure method is very difficult, so in following is considered only the easily measurable thermal expansion coefficient (α_{ij}), describing the action of scalar parameter = homogeneous change in temperature δT. At that, the response x_{ij} is the second rank tensor, which, depending in this case only on the symmetry of crystal, leads to great variety in different components of α_{ij} material tensor. This components reflect the anisotropy and magnitude of thermal expansion, characterizing just the properties of atomic bonds in a crystal. It can be argued that it is the internal polarity, which is one of reasons for both the anisotropy and one or the other thermal expansion coefficient when crystal temperature changes in a certain range.

Thermal expansion anisotropy is clearly seen from α_{ij} matrix representations shown in Fig. 7.9, where the various matrices for the crystals of different symmetry are presented.

$$\begin{pmatrix} \alpha_{11} & 0 & 0 \\ 0 & \alpha_{11} & 0 \\ 0 & 0 & \alpha_{11} \end{pmatrix} \quad \begin{pmatrix} \alpha_{11} & 0 & 0 \\ 0 & \alpha_{11} & 0 \\ 0 & 0 & \alpha_{33} \end{pmatrix} \quad \begin{pmatrix} \alpha_{11} & 0 & 0 \\ 0 & \alpha_{22} & 0 \\ 0 & 0 & \alpha_{33} \end{pmatrix} \quad \begin{pmatrix} \alpha_{11} & \alpha_{12} & 0 \\ \alpha_{12} & \alpha_{22} & 0 \\ 0 & 0 & \alpha_{33} \end{pmatrix} \quad \begin{pmatrix} \alpha_{11} & \alpha_{12} & \alpha_{13} \\ \alpha_{12} & \alpha_{22} & \alpha_{33} \\ \alpha_{13} & \alpha_{23} & \alpha_{33} \end{pmatrix}$$

a *b* *c* *d* *e*

Fig. 7.9. Matrices of thermal expansion coefficient in various symmetry: crystals *a* – cubic; *b* – hexagonal; *c* – rhombic; *d* – monoclinic; *e* – triclinic [6]

In most common ionic and covalent crystals, the coefficient of thermal expansion is isotropic, and can be represented by the scalar value $\alpha_{ij} = \alpha$; at that, all

components of tensor, located in the main diagonal of matrix α_{ij}, are same, Fig. 2*a*. The ball made of such crystal, being exposed by uniform heating or cooling, will change its radius but will not change its shape. It would be seem that in the hexagonal crystals, Fig. 7.9*b*, this ball will turn into the ellipsoid of rotation, and in the case of rhombic or monoclinic crystals the initial ball will be transformed into the three-axis ellipsoid. In lower symmetry crystals, their diagonal components α_{11}, α_{22} and α_{33} can have not only the different values, but also the different signs. Thus, the anisotropy of thermal expansion reflects a complex distribution of hybridized ionic-covalent inter-atomic bonds in the polar crystal, while the simple ionic or covalent bonds in crystal are characterized by the isotropic (scalar) thermal expansion coefficient. It can be seen from presented data that the nature of thermal expansion can be quite complex, but it is this parameter which reveals the structure of inter-atomic bonds. A detailed study of the α_{ij} matrix components can only be carried out individually for a particular crystal, however, there is the possibility of a generalized study in the form of a volume expansion coefficient, which is the subject of this work.

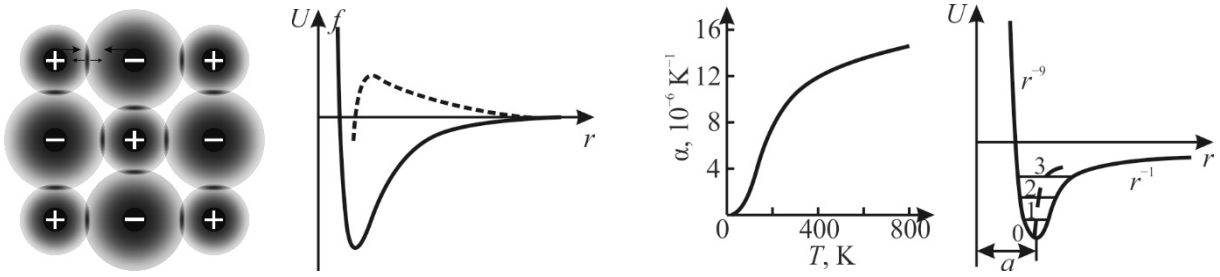

a *b* *c* *d*

Fig. 7.10. Thermal expansion modeling: *a* - two-dimensional image of electrical charge distribution in ionic crystal; *b* – ions attraction energy compensating by partial overlapping of electronic shells (dotted curve shows inter-ionic force) *c* – typical for solids $\alpha(T)$ dependence; *d* – increase in the amplitude of ions oscillations with temperature rise, shown by horizontals 0-1-2-3, leads to increase of lattice constant *a*, shown by dotted line (really this situation develops near the very bottom of energy minimum in the narrow interval of inter-ionic distance *r*)

Volumetric thermal expansion coefficient, defining as $\alpha_V = (1/V)\cdot(\Delta V/\Delta T)_p$, is a sum of the diagonal components of expansion tensor: $\alpha_V \approx \alpha_1 + \alpha_2 + \alpha_3$. The obvious reason of thermal expansion in the solids can be justified, for example, by the model of ionic crystal, Fig. 7.10*a*, to which belong almost all objects discussed below. The dependence of energy versus inter-ionic distance $U(r)$ always is characterized by the asymmetric minimum, Fig. 7.10*b*. At lowest temperature, the bottom of potential well looks like a symmetric parabola, so that, when temperature

changes near the absolute zero, $r = a$ (lattice parameter). This explains why the coefficient of thermal expansion for quite different solids in the region of absolute zero tends to zero, Fig. 7.10*c*. Next, when temperature rise, initially $\alpha(T) \sim T^3$ (like specific heat *C*) but then it goes to the saturation, repeating temperature dependence of specific heat.

The negative energy of ions attraction changes with the distance rather slowly (r^{-1}–r^{-4}), while the positive energy, conditioned by the electronic shells repulsion due their overlap, changes very rapidly (r^{-8}–r^{-12}). The forming total energy minimum is quite asymmetric, which leads to the anharmonicity of ions thermal vibrations, and, eventually, to the thermal expansion. Thus, thermal expansion is due to anisotropy of inter-ionic potential relief. In the case of small oscillations of ions around their equilibrium positions, the potential energy $U(x)$ may be presented by Taylor series: in terms of ions shift x from equilibrium position $x = a$: $U(x) = ½cx^2 - (1/3)bx^3$, where c characterizes elastic bonding, b is the coefficient of anharmonicity, and a is the lattice constant. If one would take into account only the first term of this expansion ($½cx^2$), the oscillations of ions will be harmonic, and no thermal expansion is expected. The thermal expansion is described by the second term $(1/3)bx^3$, i.e., by the anharmonicity in atoms vibrations. Acting between oscillating ions force $f = -\mathrm{d}U/\mathrm{d}x = -cx + bx^3$ vanishes at $r = a$, Fig. 3*b*. The role of anharmonicity becomes the more significant the greater displacement x, Fig. 7.10*d*..

Main features of thermal expansion phenomenon in solids are as follows:

1. Given above simple model can explain only the *positive* thermal expansion of solids. Average potential energy of thermal fluctuations ($½cx^2$) at a given temperature equals $½k_BT$, where k_B is the Boltzmann constant. One can show that average shift of ions in this model is $\langle x \rangle = (b/c^2)\cdot k_BT$, so the thermal expansion coefficient is defined as the ratio of average shift $\langle x \rangle$ to equilibrium inter-ionic distance a: $\alpha = k_Bb/ac$. It follows that in the absence of anharmonicity, i.e., if $b = 0$ thermal expansion coefficient is $\alpha = 0$.

2. The stronger inter-atomic bonds in a crystal the more difficult to change and wreck them, so the greater crystal melting temperature the smaller thermal expansion: $\alpha_V \sim 1/T_{\mathrm{melt}}$ [1]. And indeed, in the diamond $\alpha_V = +3\cdot10^{-6}$ K^{-1} while in the aluminum $\alpha_V = +70\cdot10^{-6}$ K^{-1}, in both cases, again the *positive* value of α_V is expected and seen.

3. The binding energy between atoms is characterized by Debye temperature θ_D, while the melting temperature of crystal is $T_m \sim \theta_D^2$. Comparing with (2), we have: $\alpha_V \sim \theta_D^{-2}$, from which one can make a conclusion that the coefficient α_V is awaited to be positive quantity.

4. From fundamental Grüneisen law, again the increase of $\alpha_V(T)$ follows. This law defines the state of equation for solids, considering the anharmonicity of inter-atomic forces and establishing the similarity of temperature dependence for α_V and specific heat C_V: $\alpha_V = \gamma C_V/3K$ [1], where K is the modulus of bulk elasticity (i.e., all-round compression modulus) and γ is the Grüneisen constant. Insofar as $C_V(T) \sim T^3$, positive α_V is expected with its temperature change $\alpha_V \sim T^3$.

5. It can be shown from the microscopic examination that α is the reciprocal of the slope for curve, which expresses the dependence of binding energy on the inter-atomic distance $(a+x)$ at the point corresponding to the time-average position of atom: $dU(a+x)/d(a+x) \sim 1/\alpha$ [4]. Thus, the $\alpha(T)$ dependence is determined by the middle profile of $U(r)$ dependence of crystal, where $U(r)$ is the sum of inter-atomic attraction and repulsion energies, Fig. 3*d*.

6. As the amplitude of thermal oscillations increases, the average inter-atomic distance (shown by dotted line in Fig. 3*d*) increases also: exactly this is the evident cause of thermal expansion. With temperature rise, the displacement of oscillating atoms to the left becomes less than their displacement to the right. As a result, the time-average equilibrium position of atom $(a+x)$ shown by the dotted line shifts to the right, and this effect becomes the stronger the higher is the energy of atoms oscillations. This concept of time-average displacement $\langle x \rangle$ of the vibrating atoms actually determines the $\alpha(T)$ dependence.

All previous reasoning (1–6) testifies to a positive coefficient of thermal expansion. Next task is to explain the possibility of the negative $\alpha(T)$ dependence.

7.7 Negative thermal expansion explanation

The possibility of negative thermal expansion existence can be substantiated even in a simple model, Fig. 4, considered mainly on the example of polar crystals, where authors have own experimental data. Insofar as in a certain temperature range $\alpha(T)$ takes negative value, so the dependency $\alpha(T)$ twice passes through zero line before it goes to usual for most crystals growing $\alpha(T)$ by the law: $\alpha \sim T^3$, Fig. 4*a*. For instance, hexagonal crystal ZnO has polar wurtzite structure of 6*m* symmetry and shows $\alpha_{min} = -1.2 \cdot 10^{-6}$ K^{-1} at $T_{\alpha min}$, = 75 K with saturation $\alpha_{sat} = +5 \cdot 10^{-6}$ K^{-1}, while cubic crystal HgTe has also polar but sphalerite structure (43*m* symmetry) with $\alpha_{min} = -4 \cdot 10^{-6}$ K^{-1} at $T_{\alpha min}$, = 25 K and $\alpha_{sat} = +6 \cdot 10^{-6}$ K^{-1}. Polar crystal InP shows $\alpha_{min} = -0.5 \cdot 10^{-6}$ K^{-1} at $T_{\alpha min}$, = 45 K with $\alpha_{sat} = +8 \cdot 10^{-6}$ K^{-1} while the fused quartz is characterized by $\alpha_{min} = -9 \cdot 10^{-6}$ K^{-1} at $T_{\alpha min}$, = 40 K and $\alpha_{sat} = +6 \cdot 10^{-6}$ K^{-1}.

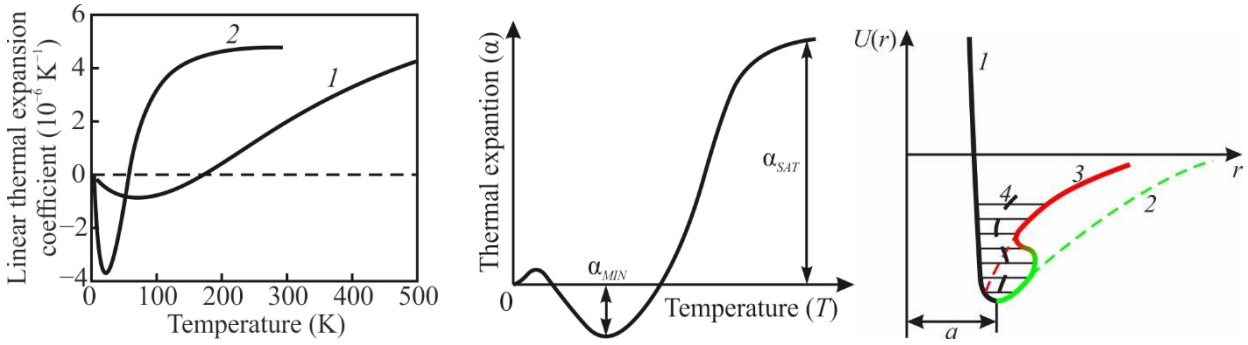

a *b* *c*

Fig. 7.11. Negative thermal expansion: *a* – in polar crystals ZnO (*1*) and HgTe (*2*), *b* – minimum and saturation in $\alpha(T)$ dependence; *c* – symbolic explanation of negative $\alpha(T)$: *1* – repulsion energy, *2* – polar bonds attraction energy, *3* – non-polar attraction energy, *4* – average dynamic position oscillating particles (shown situation develops only near the bottom of total energy minimum)

The explanation of negative $\alpha(T)$ is given in Fig. 7.11*c*. This behavior requires a special nature of ions attraction, peculiar in polar crystals, which occurs due to the hybridization of ionic and covalent bonds; as a result of which they become polar. It is this that leads to a specific profile of attraction energy, which in the polar crystal decreases much slowly with the inter-atomic distance r than usual for ionic crystals law ($U \sim r^{-1}$). Thus, at low enough temperature, the polar crystal is characterized by an additional attraction of a dipole-dipole type, which expands the bottom of total energy minimum. Therefore, the inter-ionic distance (curve *4* in Fig. 7.11*b*), describing anharmonic vibrations, become dependent on energy in a complex way. At that, with increasing temperature, the energy increases in accordance with the climbing steps of horizontal lines, Fig. 7.11*c*; at that, shown by curve *4* shift of average in time inter-ionic distance changes its sign. First it a little increases in those aria, where dipole-type attraction prevails, so the derivative $dr/dT > 0$ and $\alpha > 0$, Fig. 7.11*b*. Then, as dipole-type attraction weakens (due to the increase of inter-ionic distance), the thermal deformation, shown by curve *4,* changes its sign to the negative value: the derivative $dr/dT > 0$ because attraction becomes weakened (usual for any ionic crystal), so in aria of such transition $\alpha < 0$. All this occurs below Debye temperature, when the lattice vibrations obey quantum laws. In all the cases studied, $\alpha(T)$ minimum is observed at temperature of ~ 0.1 θ_D; apparently, at this temperature the thermal vibrations acquire sufficient intensity to prevent the self-ordering of polar bonds.

Negative thermal expansion is consequence of following circumstances:

(1) physical substantiation of polar crystals existence;

(2) matching negative thermal expansion with thermodynamic theory;

(3) explanation of special $\alpha(T)$ dependence which twice changing its sign when crossing temperature axis.

1. Thermal deformation of crystal is a feature of the internal connections of atoms, ions or molecules; at that, it depends on the energy of these bonds. Coefficient α reflects the peculiarities of inter-atomic bonds in a crystal; particularly, in polar dielectrics this is their polar-sensitive structure, which arises due to the structural compensation of atoms electronegativity. It determines the ability of atom to attract the binding pair of electrons. The electronegativity of atom depends not only on the charge of its nucleus, but also on the number and location of electrons in deep atomic shells. The further from the nucleus are the valence electrons, the less positive charge of nucleus affects them: both because of the increased distance from nucleus, and because of screening of valence electrons from the positively charged nucleus by the electrons located on deep orbitals. In the polar bond, the separation of charges between neighboring ions occurs due to cation is more positive while the anion is more negative that is expected from their formal valence. In atomic and metal crystal, consisting of particles with close in the value of electroneutrality, a highly symmetric (usually cubic) structure is formed with the maximal coordination number of 12. On the contrary, the crystals, consisting of ions with the noticeably different electroneutrality, are predisposed to polar bonds arising, and, accordingly, they have very complex low-symmetry structures with lower coordination numbers of 6–8.

Polar-sensitive structures manifest itself in the crystals as the ability to provide electrical (vector-type) response to the non-electrical scalar actions (or to more complicated tensor-type actions). The hybridized ionic-covalent bonding causes a reduction in the crystal symmetry, so the polar crystals always belong to the non-central symmetric classes. Moreover, exactly the presence of such bonds determines the non-central symmetric structure of crystals. Therefore, hybridized ionic-covalent bonding is a main cause of the pyroelectric and piezoelectric properties. Used in Fig. 7.11*c* model is based on the asymmetry in electronic density distribution along atomic bonds that ensures the ability of crystal to its polar (electrical) response onto the non-electrical action.

2. Thermodynamic explanation of negative $\alpha(T)$ is based on the concept of *configuration entropy*. In this case, in addition to traditional "kinetic" entropy, associated with individual particles movement, a such entropy is considered, which is caused by dynamics of the restructuring of various nanoscale configurations. The statistical probability of numerous intra-coordinated states stipulates the increase of

entropy. The configurational entropy arises as the part of total entropy of a system, which, in addition to the kinetic energy of particles, is characterized by the various *positions* of the groups of particles. Such contribution to the entropy corresponds to a number of ways of particles mutual arrangement, maintaining some overall set of specified system properties. At that, the change in configuration entropy corresponds to the same change in general entropy. A number of physical phenomena, observed while the self-ordering in polar dielectrics (and the spins in magnets), directly indicate a large role of configuration part of entropy: the *maximum* of heat capacity seen at phase transition from disordered phase to ordered phase, the *increase* in the volume of self-ordered phase (when it arises from disordered phase), the *decrease* of volume in the anti-polar phase at correspondent phase transition, the drastic decrease of the *heat transfer* given by the short-wave phonons scattering, etc.; but below only the *negative* coefficient of thermal expansion is discussed.

To explain the negative $\alpha(T)$ seen in a certain temperature range, the Gibbs function can be used, which is the isobaric-isothermal thermodynamic potential which shows how much of system total internal energy can be used at the transformations under the specified conditions. This potential is: $G = U + pV - TS$, where U is internal energy, p is pressure and S is entropy. The minimum of Gibbs potential corresponds to stable equilibrium of a system at fixed temperature, pressure and number of particles. In studied case of system with constant number of particles, the differential of Gibbs energy is expressed as: $\mathrm{d}G = -S\mathrm{d}T + V\mathrm{d}p$. Parameter $\alpha = (\partial V/\partial T)_p/V$ is defined at constant pressure; so, the change in volume of a system, defined through the Gibbs potential at constant temperature, is: $V = (\partial G/\partial p)_T$ that can be used to get following expressions:

$$\alpha = \frac{1}{V}\left(\frac{\partial\left(\partial G/\partial p\right)_T}{\partial T}\right) = \frac{1}{V}\left(\frac{\partial^2 G}{\partial T \partial p}\right),$$ by replacing variables $$\alpha = \frac{1}{V}\left(\frac{\partial\left(\partial G/\partial T\right)}{\partial p}\right) = \frac{-1}{V}\left(\frac{\partial S}{\partial p}\right)_T$$

Obtained formula means that entropy is the less the greater is pressure, and this correlation corresponds to the thermal expansion, normally observed in most of solids in which $\alpha > 0$. On the contrary, in the dynamically ordering systems, for example, the in polar crystals, a certain temperature interval exists, in which coefficient $\alpha < 0$. This means the increase of entropy with growing pressure. Such unusual phenomenon, being a characteristic of polar crystals, requires the concept of configuration entropy, arising due to the dynamic change in various microscopic configurations (polar clusters). It is believed that certain arrangement of particles, which are characterized by average quantities, is a *macrostate*, while the individual

arrangement, defining properties of all particles for a given macrostate, are the *microstates*. Entropy is such only function, which shows the *direction* of the thermodynamic processes. During ideal reversible process, the entropy does not change, while the irreversible process always increases total entropy. Thus, in connection with the study of dynamically ordering polar clusters in crystals, the separation of entropy into the "vibrational" and the “configurational” becomes important. The vibrational entropy is the number of microstates, through which the thermal energy share between particles. The higher temperature, the greater vibrational entropy, but with increasing pressure it becomes smaller, since the binding energy of particles increases. Thus, with pressure increase, the vibrational entropy decreases. The configurational entropy is those part of system entropy, which is due to various positions of some parts of a system, and this rule is applicable to all possible configurations of a system. With pressure increase, the possibilities of partial ordering of dynamic nanoscale clusters collapses, and a mutual chaos increases. That is why, a distinctive feature of the configurational entropy is its growth with increasing pressure.

Correlation in the temperature expansion coefficient and the crystal’s compressibility ($\alpha \Leftrightarrow K$) is due to the fact that both of these phenomena shows the deformation of a crystal under the uniform scalar actions (temperature or hydrostatic). Therefore, corresponding reaction of a crystal (its strain), being the second rank tensor, in both cases relates to the internal *elastic properties* of a crystal, reflecting its internal atomic bonds peculiarities. Therefore, it is not surprising that, during discussion about the nature of negative $\alpha(T)$, this property is compared with the modulus of crystal bulk elasticity K, which characterizes the response of a crystal to the hydrostatic compression. When discussing the relationship of entropy and pressure, the Le Chatelier’s principle can be applied: the ordering of polar bonds leads to the decrease in entropy and to the increase in volume; therefore, the increase in pressure (which decreases the volume) should lead to the disordering of polar bonds, and, accordingly, to the increase in entropy. And vice versa: negative $\alpha(T)$ indicates the presence of some self-ordering-disordering processes in crystals. Therefore, when description of polar crystals properties, the phenomenon of negative $\alpha(T)$ needs the account of configurational entropy.

3. Anomalous dependence of deformation on temperature in various crystals manifests itself in different ways, which is considered below. In connection with negative $\alpha(T)$, which is seen at low temperatures in the polar crystals, it is important to keep in mind the well known cases of negative thermal expansion. Primarily, the example of configurational entropy change with pressure is the phase transition in

H_2O at 273 K: freezing of a water leads to ice formation, which has increased volume, but externally applied pressure returns the H_2O into disordered structure of a water with pronounced configurational entropy due to fluctuations of polar clusters.

In solids, the discussion about negative $\alpha(T)$ should be started with thermal deformation of ferroelectrics and antiferroelectrics which show the opposite $\alpha(T)$ anomaly in the vicinity of phase transitions T_c, Fig. 5*a*. In ferroelectrics, the volume of lower-temperature partially ordered phase becomes greater in comparison with the volume of higher-temperature *disordered* paraelectric phase. In their polar tetragonal structure previously cubic crystals $BaTiO_3$ and $PbTiO_3$ elongate along the *c*-axis but shorten along two *a*-axes; however, the volume of these crystals increases. Dynamical structural disordering in the $BaTiO_3$, which have as a basic cubic structure, internal polarity intensive fluctuations exist along four axes of [111]-type.

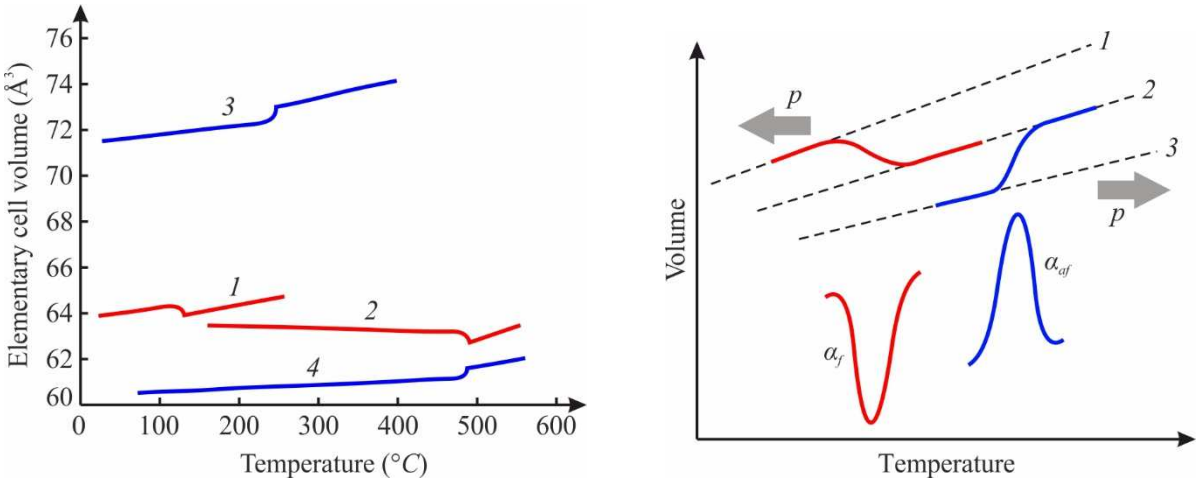

Fig. 7.12. Temperature expansion in ferroelectrics: *a* – unite cell volume in ferroelectrics $BaTiO_3$ (*1*), $PbTiO_3$ (*2*) and in antiferroelectrics $PbZrO_3$ (*3*), $NaNbO_3$ (*4*); *b* – anomalies in volume $V(T)$ and $\square(T)$ during phase transitions: $2 \Rightarrow 1$ – paraelectric-ferroelectric: $2 \Rightarrow 3$ – paraelectric-antiferroelectric. Designations: *1* – $V(T)$ dependences for polar phase, *2* – $V(T)$ for non-polar phase, *3* – $V(T)$ for antipolar phase, $\square_f$ – coefficient at ferroelectric transition, $\square_{af}$ – at anti-ferroelectric transition, arrows indicate direction of T_c displacement with increasing pressure *p*

The hydrostatic pressure, applied to $BaTiO_3$ below its Curie point (i.e., in the polar phase), returns this crystal into the paraelectric non-polar phase, in which, naturally, the configurational entropy is larger. Shown in Fig. 5*b* the T_c decrease with increasing pressure occurs with rate 5 K/kbar [2]; as a result, at the pressure of 30 kbar at room temperature the polar phase in $BaTiO_3$ already disappears: it is "squeezed out" (in ferroelectric $PbTiO_3$ the rate of T_c decrease is 8 K/kbar [2]). Figure 5*b* explains symbolically these processes that are fully consistent with the concept of configurational entropy. Naturally, that the increase in polar phase

volume during the ferroelectric transition is accompanied by a minimum of the thermal expansion coefficient, Fig. 7.13.

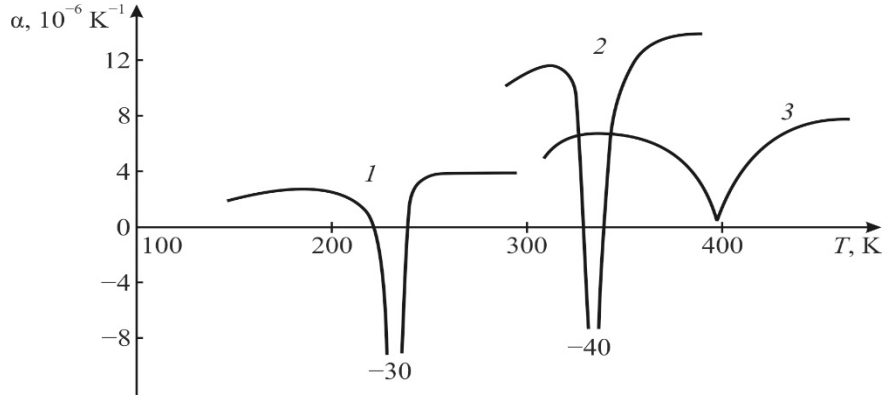

Fig. 7.13. Typical for ferroelectric $\alpha(T)$ dependence: *1* – KDP crystal (KD_2P0_4); *2* – TGS crystal $(NH_2CH_2COOH)_3 \cdot H_2SO_4$); *3* – $BaTiO_3$ ceramics

On the contrary, in the case of antiferroelectrics, the volume of antipolar phase decreases at T_c; correspondingly, in the phase transition $\alpha(T)$ shows big maximum. As shown in [4], the density of antiferroelectric does not decrease (as in case of polar crystals) but it increases, so the entropy in the antipolar phase decreases also. Accordingly, the hydrostatic pressure shifts the T_c to the high-temperature region: for $PbZrO_3$ with the rate of + 4.5 K/kbar [2].

7.8 Negative thermal expansion in different crystals

It is pertinent to note that just polar semiconductors are the *direct-band* semiconductors, while the atomic semiconductors with diamond symmetry are the *non-direct band* semiconductors. This means that polarity of a structure significantly affects the fundamental nature of electronic spectrum of semiconductors. At that, it should be noted that at low temperatures, where the negative $\alpha(T)$ is sometimes seen, the concentration of free charge carriers in the semiconductors is such small that they do not screen possible polar fluctuations in structure.

Discussing the polarity of semiconductors, first of all, it should be noted that the negative $\alpha(T)$ dependence is observed among the crystals, which have the chain or layered structures. Typical examples of chain crystals are the rhombohedral tellurium and selenium, which refers to the piezoelectrics of polar-neutral class 32 (same as quartz). For instance, in the Te crystal, transversal thermal expansion coefficient is positive: $\alpha_1 = \alpha_2 = + 27 \cdot 10^{-6}$ K^{-1}, but along the chains it is negative: $\alpha_3 = - 1.6 \cdot 10^{-6}$ K^{-1}. In the Te and Se crystals, the helical chains Te–Te (or Se–Se) are elongated parallel to axis *3*. Pronounced anisotropy and negative value of α_3 are due

to the fact that inter-atomic bonds along chains are much stronger than the interaction between chains. With heating, the crystal contracts in direction *3* but expands in perpendicular directions.

The example of layered crystal is hexagonal graphite, in which in the direction perpendicular to the plane of layers (where inter-atomic bonds are weak), usual positive thermal displacement of atoms is observed with $\alpha_3 = +30 \cdot 10^{-6}$ K^{-1}. However, along the layers of a graphite (where atomic bonds are very strong) at low temperatures a negative thermal expansion coefficient is seen: $\alpha_1 = \alpha_2 = -5 \cdot 10^{-6}$ K^{-1}. In the graphite layers, covalent bonds are so strong that at low temperatures atoms thermal vibrations can be excited mostly perpendicularly to the rigid layers (along *3* axis). At low temperatures (up to about 300 K) in graphite layers, the transverse acoustic vibrations dominate, being polarized perpendicularly to layers of carbon: just this corresponds to negative expansion, Fig. 7*a*. Only at temperature of 650 K coefficients $\alpha_1 = \alpha_2$ acquire positive value – when the intensity of thermal movement becomes big enough. Note, that large negative coefficient of thermal expansion is seen also in the graphene and nanotubes.

Thus, through the temperature dependence of thermal expansion, the features of crystal inter-atomic bonds are manifested. In the layered crystals, the positive thermal displacements of atoms is seen perpendicularly to the planes of layers, while in the chain crystals – perpendicularly to the axis of chains. In both cases, in the directions of strong bonds, the $\alpha(T)$ is negative. The conclusion is obvious: the stronger inter-atomic bond, the less thermal expansion coefficient – down to its negative value.

Many semiconductors are the polar crystals: the $A^{III}B^{V}$ compounds have sphalerite (piezoelectric) structure, while to the wurtzite (pyroelectric) symmetry belong $A^{II}B^{VI}$ compounds. However, how can one explain the fact of negative temperature expansion in the atomic semiconductors of diamond type, Fig. 7*a*: in the germanium $\alpha_1(T)$ is seen at temperature 35 K, i.e., at ~ 0.1 θ_D, while in silicon this minimum is seen at 60 K, also ~ 0.1 θ_D. It is pertinent to note, that in graphite the negative minimum of $\alpha_1(T)$ is observed at 230 K, again at ~ 0.1 θ_D. Apparently, it is at this temperature, when the intensity of thermal motion decreases so much that the self-ordering of existing polar bonds begins to manifest itself. This means that there is a reason to suspect that these crystals somehow have the tendency to polar ordering, possibly due to the fluctuating polar motive, emerging at low temperatures.

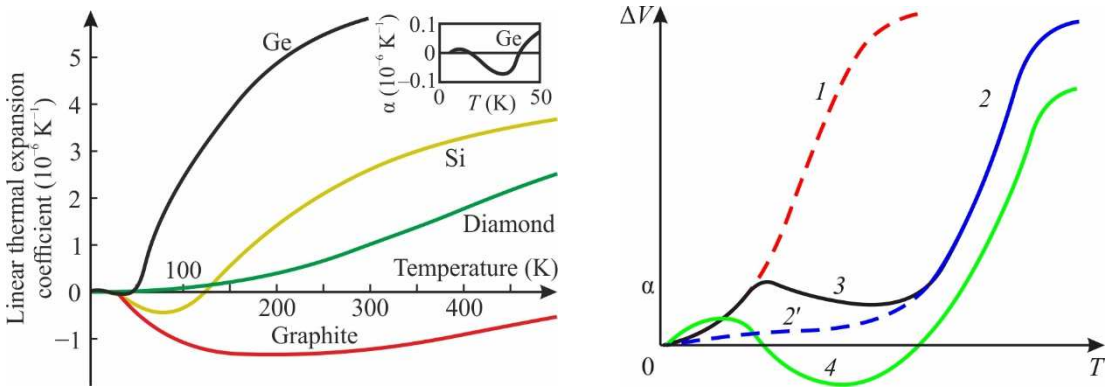

a *b*

Fig. 7.14. Thermal expansion: *a* – in Ge, Si, C-diamond and C-graphite; *b* – explanation of $\alpha(T)$ minimum in polar crystals, ΔV – volume increment peculiar for: *1* – polar bonding, *2* – non-polar bonding , *3* – transition section; *4* – thermal expansion coefficient α

Obviously, that it is necessary to indicate, which kind of ordering process would be possible in the crystals of diamond type. In might be supposed that the reason of negative $\alpha(T)$ in Si and Ge are fluctuating partial ordering of hexagonal (wurtzite) polar clusters formed due to the triple bonds of Si≡Si type randomly formed in a structure instead of usual double Si=Si bonds. This assumption is based on the fact of wurtzite form of diamond existing in a nature: initially it was discovered in the meteorites, but later was synthesized in the laboratory as well [1]. In ordinary diamond, which has an extremely rigid structure (θ_D ~ 1900 K and T_{melt} ~ 4000 K), any fluctuation of such a phase does not cause negative $\alpha(T)$. However, in less hard crystals Si (θ_D ~ 600 K and T_{melt} ~ 1700 K) and Ge (θ_D ~ 360 K and T_{melt} ~ 1200 K) crystals, weak self-ordering effects apparently can arise when leading to the negative expansion at low temperatures. It is pertinent to note that these crystals in a natural way grow from their melt just in the polar [111]-direction, and they can float in their own melt that indicates the decrease in material density during crystallization. The same property is seen, for example, in polar GaAs crystal. Note also that hexagonal type structural feature, arising in the wurtzite-diamond and possibly fluctuating in the silicon and germanium, is fully implemented in the graphite and graphene, which cellular plane is characterized by the negative $\alpha_1 = \alpha_2$ with clarly explicit minimum at temperature ~ 200 K, Fig. 7*a*. Crosswise to the layers of graphite α_3(T) is positive.

Shown in Fig. 7.14*b* is the simplified representation as to the mechanism of negative expansion in the polar crystals and "slightly-polar" crystals, in which structure there is a tendency (sometimes, even very weak) to the self-ordering of polar bonds although this is strongly prevented by the thermal chaotic motion. As

known [1], the thermal expansion coefficient is an extremely sensitive parameter: in various solids it can differ by dozens of times. As already established, at low temperature the crystal density is reduced due the polar bonds partial ordering, which increases the susceptibility of crystal to thermal expansion. Accordingly, the increment to volume $\Delta V(T)$ increases with temperature rise, as seen by *curve 1* in Fig. 7.14*b,* and adequate parameter $\alpha(T)$ is positive, as shown by *curve 4*. But with a further growing of temperature and thermal vibrations intensity rising, the disorder in the polar bonds also gains, so that increment $\Delta V(T)$ slows down, because it cannot follow the *curve 1* in Fig. 7.14*b*, which is only potentially possible for the ordered structure. The termination of $\Delta V(T)$ growing affects its derivative with respect to temperature: $\alpha(T)$ decreases until it enters the negative region, *curve 4* in Fig. 7.14*b.* In the disordered, more denser and more rigid structure, the potential temperature dependence of volume increment $\Delta V(T)$ would be described by the *curve 2'* in Fig. 7.14*a.* Subsequently, as temperature rises, the increment $\Delta V(T)$ changes according to the *curve 2,* so the usual growth of $\alpha(T)$ is observed, which is proportional to the cube of temperature Thus, it is the transition region *3* in Fig. 8*b,* which corresponds to the negative $\alpha(T)$.

Summing up, note that in the polar-sensitive crystals, when temperature decreases and thermal chaotic motion gradually freezes, the opportunity opens for partial self-ordering of polar bonds. As a result, with decreasing temperature, the volume of a crystal somewhat increases, but not abruptly, as in the case of ferroelectric phase transition, but very gradually. At that, the configurational entropy decreases, demonstrating the $\alpha(T)$ minimum, but a very shallow, not as deep as in the ferroelectrics. The foregoing makes it possible to affirm that the negative value of thermal expansion coefficient at low temperatures in the polar crystals is due to the partial ordering of their polar-sensitive bonds.

Negative thermal expansion of a particular material can be used in the combination with a material with positive expansion to obtain a composite material with zero or a given coefficient of thermal expansion. Thus, negative and positive thermal expansion cancel each other up to a certain value as the temperature changes. Adjusting the overall coefficient of thermal expansion to a certain value can be achieved by varying the volume fraction of various materials that promote thermal expansion of the composite.

Another application of controlled thermal deformations in polar crystals is the lattice strain engineering realizable with epitaxial films and based on the mismatch of thermal expansion between the substrate and film [9]. The anisotropic change of

crystal lattice is achieved through film elongation along the axis of potential polarization and its compression in the perpendicular direction (at that, the volume of ferroelectrics increases but in anti-ferroelectrics it decreases). This is a mechanical control by polar film parameters possible only in the epitaxial thin films, which allow large biaxial (plane) deformations without film destruction [10]. The highly perfect ferroelectric thin films, which are synthesized on the suitable substrates, demonstrate that strained ferroelectric thin films can exhibit properties, which are greatly superior the possibilities of their bulk crystals.

7.9 Summary Chapter 7

Conclusions

In ferroelectrics, as well as in other dielectrics, in process of heat transfer the phonon mechanism dominates, at which the speed of short-wavelength longitudinal acoustic waves ("thermal phonons") is small as compared to long-wavelength "sound phonons". It is stated that in the case of polar crystals the phonon acoustic branch bends down while approaching to boundary of Brillouin zone. This effect is due to the acoustic-optical interaction, which reduces group velocity of phonons decreasing thermal conductivity. These effects are especially noticeable in the ferroelectrics near phase transitions, since in them the wavelength of thermal phonons becomes comparable with size of fluctuating polar clusters, whose activity, however, can be suppressed by the electrical field opening up the possibility of electrical control by heat flow. It has also been established that when studying heat transfer the thermal diffusion is a more sensitive factor than thermal conductivity. Indeed, in the ferroelectrics, phase transition point a sharp minimum of thermal diffusivity is found, which is due to the decrease in the wavelength of thermal phonons which are affected by polar bonds self-ordering increasing phonons scattering. On the contrary, in antiferroelectric phase transition, a sharp and big maximum of thermal diffusion is found, explained by the active participation of optical phonons in heat transfer in the vicinity of phase transition.

The thermal expansion coefficient of polar crystals in some interval of its temperature dependence becomes negative, which is unusual property inherent in the structurally ordering crystals. At that, the coefficient of thermal expansion in the polar crystals at low temperatures changes its sign twice, forming the region of its negative value. It is shown that in any case $\alpha(T)$ is the reciprocal of a slope of the curve, which expresses the dependence of binding energy on inter-atomic distance

at the point corresponding to time-average position of an atom. It is supposed that the polarity in some crystals arises due to the structural compensation of different electronegativities inherent to neighboring atoms. It is established that negative value of $\alpha(T)$ corresponds to such a case, when the entropy grows with increasing pressure: this is a characteristic of the configurational entropy. It is argued also that interval of negative thermal expansion is due to self-ordering of the polar bonds, which creates the increase in crystal volume. The volume of polar phase in the ferroelectrics increases in comparison with their paraelectric phase, so $\alpha(T)$ shows deep minimum while the phase transition shifts to low temperature when the pressure grows. On the contrary, in antiferroelectrics the volume of antipolar phase decreases as to the paraelectric phase, so $\alpha(T)$ shows a big maximum, while under pressure phase transition shifts to higher temperature. The proposed concept is extending to the semiconductors, in which $\alpha(T)$ minimum might be seen: it can be assumed that some polar tendencies, fluctuating in their structure, become consolidated at lower temperatures. In electronics, negative thermal expansion can be applied in the thermal compensators as well as in thin films technology to achieve certain characteristics.

References

[1] C. Kittel, Introduction to solid state physics, 5th ed. New York: John Willey, 1976.
[2] M.E. Lines and A.M. Glass, Principles and application of ferroelectrics and related materials, Clareton Press, Oxford, 1977.
[3] Y.M. Poplavko, Electronic materials. Principles and applied science. ELSEVIER, 2019.
[4] E.N. Dimarova and Yu.M. Poplavko, "Electrical bias field influence on ferroelectrics thermal conductivity," Izvestia AN SSSR, Serial Phys. 31 (11), pp. 1842, 1967 (in Russian).
[5] V.F. Zavorotnii, Yu.M. Poplavko, "Plane temperature waves method for thermal diffusion study," Pribori e Technika Experimenta, Vol. 5, p. 189, 1984 (in Russian).
[6] W.O. Cady, Piezoelectricity, Amazon com, New York, 1946.
[7] I.S. Jeludev, Basics of ferroelectricity, Atomizdat, Moscow, 1973.

Questions

1. What is reasons of heat transfer and thermal deformation?
2. Compare thermal conductivity and thermal diffusivity.
3. List main thermal properties of ferroelectrics.
4. What is peculiar in antiferroelectrics thermal diffusion?
5. List main peculiarities of polar crystals.
6. Why thermal expansion method is important for crystal research?
7. Explain formally the possibility of negative thermal expansion.

CHAPTER 8. TRAINING IN APPLIED PROBLEMS SOLVING

Contents

Many material science problems can be solved by thermodynamic calculations. The solution of these problems is widely covered in the scientific and educational literature, and some of these solutions are given in the first three paragraphs. Having become familiar with these techniques, the reader can practice such solutions on his own, which is detailed in the following sections.

8.1 Basics of applied thermodynamics

The description of a thermodynamic state in any system or material (particularly, in dielectrics) is dependent on the purpose of theory application, i.e., what kind of physical properties of a substance needs to be predicted or explained. In the case of dielectric, the thermodynamics allows to describe processes of dielectrics polarization as well as many other properties and features in the terms of *energy*: the dielectric is regarded as the thermodynamic system, which equilibrium state can be changed as by the electrical field application so due to many other factors [1].

At that,

- Thermodynamic *state* is determined by combination of thermodynamic parameters, and it is characterized by the internal energy of a system;
- Thermodynamic *parameters* are temperature (T), pressure (p), volume (V) and others;
- Thermodynamic *process* is the change in the state of a system, depending on the conditions (the constancy of certain parameters); this process can be isothermal ($T = const$), adiabatic ($\delta Q = const$), isobaric ($p = const$), and isochoric ($p = const$);

• *Absolute temperature T,* measured in [K] (Kelvin degree), characterizes the state of a body at the thermodynamic equilibrium (this temperature is proportional to the average kinetic energy of particles);

• *Heat Q,* measured in [J[(joule), is the energy, absorbed by a system when its temperature increases when system does not perform work (heat represents energy of thermal motion of particles forming a body);

• *Specific heat C,* measured in [J/deg] or in [cal/(deg·mol)], is the absorbed (or released) heat when temperature changes: it is the ratio of heat given to a body from outside to corresponding increase in temperature.

• *Potential energy* is a part of the energy of asystem or body that depends on the positions of particles in the force fields. In solids, the sources of potential energy are Coulomb forces that cause the attraction of opposite sign charges and the repulsion of same sign charges.

• *Kinetic energy* (or energy of particles motion in solids) is due to the fact that atoms and ions continuously oscillate due thermal excitation.

• *Internal energy* (*U*) is that part of the total energy of a thermodynamic system, which does not depend on the choice of the frame of reference, but can change within the framework of the problem under consideration. Internal energy is a collection of those variable components of the total energy of system that should be taken into account in a particular situation. Therefore, the internal energy is an additive quantity, that is, the internal energy of system is equal to the sum of internal energies of its subsystems, i.e., internal energy of system includes the energy of various types of motion and interaction of particles included in the system: the energy of translational, rotational and vibrational movements of atoms and molecules, the energy of intra- and intermolecular interactions, the energy of the electronic shells of atoms, etc. When temperature rises, the internal energy increases, and when temperature decreases, it decreases, but the constancy of the temperature of a system does not mean the invariability of its internal energy, for example, the temperature of the system is unchanged during phase transitions, but the energy changes.

• *Enthalpy* (*H*) is the isobaric-isentropic potential, the thermal Gibbs function, which determines the heat content of system by doing constant pressure and corresponds to the amount of energy that is available for conversion into heat at a certain temperature and pressure. Enthalpy is the extensive quantity, i.e., for a composite system, it is equal to the sum of the enthalpies of system's independent parts; in this case, like the internal energy, the enthalpy is determined up to arbitrary constant term. Being general energetic function, the enthalpy is such a property of

thermodynamic system that is defined as the sum of system's internal energy and the product of pressure p on volume V. As temperature increases from T_1 to T_2, the enthalpy increases: $H_2 = H_1 + \int_{T_1}^{T_2} C_P \partial T$, where H_1 is the enthalpy at initial temperature T_1, and H_2 is the enthalpy at final temperature T_2 and C_p is the specific heat under constant pressure p. The enthalpy can be defined in two ways. The first method is based on the *internal energy U* and the *work pV* performed by a system relatively to the environment: $H = U + pV$, where P is the *pressure* and V is the *volume* of a material. The second method of enthalpy definition is based on the Helmholtz free energy F : $H = F + pV + TS$, where $F = U – TS$, or on the Gibbs free energy G: $H = G + TS$, where $G = F + pV$ (or $G = H – TS$) while TS represents the energy conditioned by internal disordering in a matter, i.e., the energy assessment of a chaos.

It is appropriate here to clarify some of introduced concepts:

- *Helmholtz free energy* ($F = U – TS$) is the isothermal-isochoric thermodynamic potential that measures useful work obtainable from thermodynamic system at constant temperature (isothermal processes) and constant volume (isochoric processes). Note that at constant temperature and in the equilibrium state Helmholtz free energy is minimized.

- *Gibbs free energy* ($G = F + pV$), i.e., isobaric-isothermal thermodynamic potential is a quantity whose change in the course of transformations is equal to the internal energy change of a system. The Gibbs energy shows what part of the total internal energy of a system can be used for the transformations (or obtained as a result of them) and makes it possible to establish the fundamental possibility of thermodynamic process under specified conditions. Mathematically, this is a thermodynamic potential of the following form: $G = H – TS = U + pV – TS$.

The spontaneous course of this isobaric-isothermal process is determined by two factors: the enthalpy, associated with its decrease in system, and due to increase in its entropy (system disordering). It is the difference of these thermodynamic factors that is a function of the state of the system, called the isobaric-isothermal potential or Gibbs free energy. In solids, when thermodynamic processes studying, the more expedient is to take into account not a pressure, but the *volume* of a system, so the preference is given to the Gibbs free energy, $G = F + PV$. Its minimum corresponds to the equilibrium state of a system, changing at *constant temperature* and *constant volume*. The enthalpy in all cases increases with temperature, but the value of entropy (TS) *increases faster*. Consequently, the Gibbs free energy

decreases with temperature rise. Since it is the *free energy* that used in subsequent discussions below, it should be noted that at zero absolute temperature the Gibbs free energy equals enthalpy: $G = H$. At the same time, the free energy decreases with temperature increase, but the rate of free energy decrease is associated with the entropy

• *Entropy* (S) is the meaningful property of thermodynamic system denoting the measure of irreversible energy dissipation using to describe the *equilibrium* (reversible) processes. Besides, in the nonequilibrium (irreversible) processes, the entropy serves as a measure of the proximity of the state of a system to equilibrium: the greater the entropy the closer the system to the equilibrium; it is obvious that in the state of thermodynamic equilibrium the entropy of system has maximum. The physical meaning of entropy is the logarithm of the number of available microstates of the system; entropy dimension in SI units is $[kg \cdot m^2 \cdot s^{-2} \cdot K^{-1}]$ or the "joules per kelvin", $[J \cdot K^{-1}]$. Entropy is defined as function of the state of a system; the difference of entropy in two equilibrium states 1 and 2 equals to the reduced amount of heat $\delta Q/T$, which system needs to give in order to be transformed from state 1 to state 2 along any but quasi-static path: $\Delta S = S_2 - S_1 = \int \delta Q/T$. Since the entropy is determined as to arbitrary constant, then in initial state it is possible to set $S_1 = 0$, then $\Delta S = \int \delta Q/T$, This integral is taken for the arbitrary quasi-static process. The *differential function* of the entropy has a form $dS = \delta Q/T$. Also, since the entropy is always *positive* and increases with temperature rise, the slope of free energy plot on temperature continuously increases as seen in Fig. 1.1A, where no phase transformations are implied in a given substance. However, when in the studied material the *different phases* are possible, the value of free energy shoes anomalies which gives important information about correspondent phase transformation, at that, the lower is the free energy the more resistant is the phase.

8.2 Piezoelectric effect thermodynamic description

Simplified description of piezoelectric effect is necessary for further application of given in the following paragraphs of calculations [2, 3]. These data can be viewed also in Section 4.1.

In the thermodynamic theories (as opposed to microscopic theories) the atomic structure of matter are not taken into account but it is regarded as a continuum that has certain properties. In the case of piezoelectricity this continuum is anisotropic: its

electrical, thermal and elastic properties depend on the direction of the applied forces and fields.

Need thermodynamic potentials. It is assumed that the thermal, elastic and electrical properties of piezoelectricity can be described by the six parameters: two thermal (T – temperature, S – entropy), two mechanical (X – stress, x – strain) and two electric (E – electric field, D – electric induction). If dielectric gets a small amount of heat dQ, the change in its internal energy dU, according to the first principle of thermodynamics, is described by the expression:

$$dU = dQ + dW = dQ + Xdx + EdD, \quad (8.1)$$

where dW – work carried out by electrical (EdD) and mechanical (Xdx) forces. As the only reversible processes are reviewed (this includes both electric polarization and mechanical strain), then d$Q = T$dS – in accordance with the second principle of thermodynamics. As a result, the change in the internal energy (2.2.1) can be represented as a function of the six basic parameters of the dielectric:

$$dU = TdS + Xdx + EdD, \quad (8.2)$$

where selected basic parameters are S, x and D. The remaining parameters – T, X and E – are defined as derivatives of the internal energy U on the entropy S, strain x, and electric induction D. During differentiation, one parameter is assumed as a constantcy of the other two parameters denoted by the corresponding indexes:

$$T = (\partial U/\partial S)_{x,D};$$
$$X_n = (\partial U/\partial x_n)_{S,D}; \quad (8.3)$$
$$E_i = (\partial U/\partial D_i)_{S,x}.$$

These ratios in the brief form are essentially three dielectric equation of state – thermal, elastic and dielectric. For piezoelecrics, a variety of boundary conditions are pointed – electrical, mechanical and thermal. Of the three pairs of related parameters: $T – S$, $X – x$ and $D – E$, three independent parameters can be chosen, obviously, by the eight ways. The objectives of different boundary conditions describing thermal, elastic and electrical properties of polar crystals determines the choice of eight different thermodynamic functions (potentials), with which one can express the basic equation of state of piezoelectricity. Obtained above equation (8.1) is just one of them:

$$dU = TdS + Xdx + EdD;$$
$$dH = TdS – xdX – DdE;$$
$$dH_1 = TdS – xdX + EdD;$$
$$dH_2 = TdS + Xdx – DdE; \quad (8.4)$$
$$dA = – SdT + Xdx + EdD;$$
$$dG = – SdT – xdX – DdE;$$
$$dG_1 = –SdT – xdX + EdD;$$
$$dG_2 = – S\mathrm{d}T + X\mathrm{d}x – D\mathrm{d}E,$$

where H – enthalpy, H_1 – elastic enthalpy, H_2 – electric enthalpy, A – Helmholtz free energy; G – Gibbs free energy, G_1 – elastic Gibbs energy, G_2 – electrical Gibbs energy. Indexes at the vector and tensor parameters are omitted for simplicity.

From the equation (8.2) three equations of state were obtained (2.2.3). With an increasing number of thermodynamic functions up to eight, the number of equations of state also increases. For example, if the independent variables would be selected the electric induction D, strain x and temperature T, then thermodynamic potential should be nominated the Helmholtz free energy, and the equation of state of the dielectric is differ from the equations (2.2.3):

$$-S = (\partial A/\partial T)_{x,D};$$

$$X_m = (\partial A/\partial x_m)_{T,D};$$

$$E_i = (\partial A/\partial D_i)_{T,x}\,.$$

The equation of state can be written as linear differentials of the independent variables:

$$dS = (\partial S/\partial T)_{D,x}dT + (\partial S/\partial x_m)_{D,T}dx_m + (\partial S/\partial D_i)_{x,T}dD_i\,;$$

$$dX_n = (\partial X_n/\partial T)_{D,x}dT + (\partial X_n/\partial x_m)_{D,T}dx_m + (\partial X_n/\partial D_i)_{x,T}dD_i; \quad (8.5)$$

$$dE_j = (\partial E_j/\partial T)_{D,x}dT + (dE_j/\partial x_m)_{D,T}dx_m + (dE_j/\partial D_i)_{x,T}dD_i\,.$$

As the number of potentials is eight, then all number of such equations is 24. Coefficients in these equations are the generalized state of compliance – they define the various fields (electrical, mechanical and thermal). The most important ones are mentioned earlier in connection with the description of piezoelectric: second rank tensors (ε_{ij}, α_{ij}), tensors of the third rank (d_{in}, e_{im}, h_{jn}, g_{jn}, the fourth rank tensors (c_{mn} and s_{mn}). Here the indices are $i, j, k = 1,2,3$; $m, n = 1,2, ..., 6$, and they are used for matrix presentation of parameters.

Thermodynamics of piezoelectricity. Thermodynamic potentials (8.4), including the Helmholtz free energy, are responsible to describe not only the piezoelectric effect, but the pyroelectric effect, ferroelectrics, and other phenomena. To describe only the piezoelectric event, a negligible changes need to be done considering primary four potentials from the equations (8.4) as the adiabatic ones ($dS = 0$), and the following four potentials as isothermal ($\mathrm{d}T = 0$) ones. Specifically, with this example – Helmholtz free energy – the last two equations of state (8.5) based on $\mathrm{d}T = 0$ are available for piezoelectric from:

$$\mathrm{d}X_n = c^D{}_{mn}\mathrm{d}x_m - h_{in}\mathrm{d}D_i\,;$$

$$\mathrm{d}E_j = -h_{jm}\mathrm{d}x_m + (\beta^x{}_{ij}/\varepsilon_0)\mathrm{d}D_i,$$

in which the coefficients are: $c^D{}_{mn} = (\partial X_n/\partial x_m)_D = (\partial^2 A/\partial x_n \partial x_m)_D$ – elastic stiffness that are determined at the constant induction (see section 1. ....), while parameter

$(\beta^x_{ij}/\varepsilon_0) = (\partial E_i/\partial D_j)_x = (\partial^2 A/\partial D_i \partial D_j)_x$ is the inverse permittivity of clamped crystal. Parameter h_{jm} is one of four piezoelectric coefficients that also refer to one of the generalized compliances:

$$h_{jm} = -(\partial X_n/\partial D_j)_x = -(\partial E_i/\partial x_n)_D = -(\partial^2 A/\partial x_n \partial D_i).$$

Thus, one of four piezoelectric coefficients (*d, e, g, h*) is possible to consider as discovered. The same pair of equations can be obtained from the free energy expression (8.2), and from other thermodynamic potentials (8.5), the number of which in the terms of $dS = 0$ and $dT = 0$ is reduced to 4. As a result of the thermodynamic relations, four pairs of basic equations of piezoelectric effect follow as:

$$D_i = d_{in}X_n + \varepsilon_0\varepsilon_{ij}E_j;$$
$$x_m = s^E_{mn}X_n + d_{jm}E_j;$$
$$D_i = \varepsilon_0\varepsilon^x_{ij}E_j + e_{im}x_m;$$
$$X_n = c^E_{nm}x_m - e_{jn}E_j;$$
$$E_j = (\beta^x_{ji}/\varepsilon_0)D_i - h_{jm}x_m;$$
$$X_n = c^D_{nm}x_m - h_{in}D_i;$$
$$E_j = (\beta^x_{ji}/\varepsilon_0)D_i - g_{jn}x_n;$$
$$x_m = s^D_{mn}X_n - g_{im}D_i.$$

Therefore, all four piezoelectric coefficients is possible to consider as discovered.

Electromechanical coupling coefficient also to find from thermodynamics; it is possible to use several expressions for this:

$$K^2_{EM} = d^2_{jn}/(\varepsilon_0\varepsilon^x_{ij}\, s^E_{mn}) = e^2_{jm}/(\varepsilon_0\varepsilon^x_{ij}\, c^E_{mn}),$$
$$K^2_{EM} = \varepsilon_0\, h^2_{jm}/(\beta^x_{ij}\, c^D_{mn}) = \varepsilon_0\, g^2_{im}(\beta^X_{ij}\, s^D_{mn}).$$

Two pairs of these correlations were obtained and examined in the previous section, and with their help it has been found the expressions for the electromechanical coupling factor: eqs. (8.1) and (8.3). From the remaining piezoelectric equations another two expressions for K^2_{EM} can be derived.

If thermal effects are neglected, the internal energy is the sum of piezoelectric elastic and electric energies:

$$U = \tfrac{1}{2}\, x_m X_n + \tfrac{1}{2}\, D_j E_i.$$

Using the first pair of piezoelectric equations, this formula can be transformed as:

$$U = \tfrac{1}{2}\, X_n s^E_{mn} X_n + \tfrac{1}{2}\, X_n d_{in} E_i + \tfrac{1}{2}\, E_i d_{in} X_n + \tfrac{1}{2}\, \varepsilon_0\varepsilon_{ij}E_jE_i = W_E + 2W_{EM} = W_M.$$

Thus, the electromechanical coupling factor can be found as

$$W_{EM}^2/(W_M \cdot W_E) = K^2_{EM}, \quad (8.6)$$

where $2W_{EM} = d \cdot X \cdot E$ – mutual energy, $W_M = ½\ sX^2$ – mechanical (elastic) energy; $½\varepsilon_0\varepsilon E^2$ – electrical energy.

This definition holds true for the third pair of the piezoelectric equations.

However, the second and fourth pairs of equations are just another expressions:

$$W_{EM}^2/(W_M \cdot W_E) = K^2_{EM}/(1 - K^2_{EM}) . \quad (8.7)$$

Only for small values of coupling coefficients ($K_{EM} < 0.3$) it is possible to assume that the formulas (8.6) and (8.7) are approximately the same.

Thus, thermodynamic (phenomenological) theory allows without clarifying the molecular mechanisms get all the basic equations that describe the direct and inverse piezoelectric effect at the macroscopic level. These equations are used in engineering calculations, and parameters of these equations can serve as a basis for comparing the properties of various piezoelectric materials. Mechanical (elastic), electrical and thermal properties of crystals can be described by six parameters: two mechanical, two electric and two thermal parameters. Thermal parameters must be considered for further thermodynamic analysis of the pyroelectric effect and explain under what conditions pyroelectric effect can appear in the piezoelectric.

The objectives of different boundary conditions to describe elastic, electrical and thermal properties of polar crystals determines the choice of eight different thermodynamic functions (potentials), with which it is possible to express the basic equation of state of piezoelectricity. Most appropriate for the piezoelectricity analysis is the election of thermodynamic potential "Helmholtz free energy". From this analysis received eight basic equations of the piezoelectric effect and the basic formulas for the coefficient of electromechanical coupling.

8.3 Pyroelectric effect thermodynamic description

Simplified mechanism of pyroelectric effect is very necessary for further application of given below theory [3, 4]. These data can be viewed in Section 4.1.

Pyroelectric effect is defined as spontaneous polarization P_S change in the electrically and mechanically free crystal under the uniform change of crystal temperature T. This change is characterized by the pyroelectric coefficient $\gamma^{X,E} = \partial P_S/\partial T$ where the indices indicate electric field strength E_i and mechanical stress X_m permanency while $\gamma^{X,E}$ is determining. As from the simple model of pyroelectricity shown in Fig. 1.5 so from the strict thermodynamic analysis follows

phenomenological division of pyroelectric effect into primary and secondary ones with the coefficients $\gamma^{(1)}$ и $\gamma^{(2)}$ correspondingly:

$$\gamma_i^{X,E} = \gamma_i^{(1)} + \gamma_i^{(2)} = \gamma_i^{x} + d_{im}{}^{T} c_{mn}{}^{X,E} \alpha_n^{X,E}, \qquad (8.8)$$

$$i = 1, 2, 3; \quad m, n = 1, 2, \ldots 6.$$

The contribution of the primary pyroelectric effect in principle can be found during clamped crystal study when strain is absent ($x_n = 0$), i.e. $\gamma^{(1)} = \gamma_i^{x}$. The contribution of secondary effect corresponds to the difference in the pyroelectric coefficients of free and clamped crystal: $\gamma_i^{(2)} = \gamma_i^{X,E} - \gamma_i^{x}$ and can be calculated by the formula (1) with known components of piezoelectric modulus d^{T}_{im}, elastic stiffness $c_{mn}{}^{X,E}$, and thermal expansion coefficient $\alpha_n^{X,E}$. In the linear pyroelectrics parameter $\gamma = 10^{-7} \ldots 10^{-5}$ C·m^{-2}·K^{-1} while in ferroelectrics $\gamma = 10^{-5}$–10^{-3} C·m^{-2}·K^{-1}.

Symmetry requirements permit both primary and secondary pyroelectric effects only in the 10 of the 20 piezoelectric classes of crystals. In pyroelectric there is a "peculiar polar direction" along which pyroelectric response is maximal. In the remaining 10 piezoelectric but not pyroelectric classes of crystal any scalar (homogeneous) influence, including temperature, can not lead to a vector (electric) response under homogeneous boundary conditions, i.e., if the crystal is completely free, fully mechanically clamped, etc. In order to excite the electric response in the piezoelectrics by thermal influence the temperature gradient or inhomogeneous boundary conditions are needed.

Pyroelectric is a transducer of thermal energy into electrical energy. When using the electro-calorific effect that is the inverse effect to the pyroelectric one, electrical energy is converted into heat. The efficiency evaluation as to thermal energy conversion into electrical energy and vice versa (electric heat to thermal enegy) is the coefficient of electro-thermal bonding $k_{te} = k_{et}$. Square of the thermoelectric conversion k_{te}^2 shows what part of thermal energy dW_{T} delivered to a reformative element is converted into electrical energy dW_E:

$$K_{ET}^2 = dW_E/dW_T. \quad (8.9)$$

In view of the difficulties associated with determination of k_{ET} in the dynamic elements routine of work, thermoelectric conversion efficiency is usually estimated using the quasi-static thermodynamic relations derived on the basis of the Gibbs thermodynamic potential (G) or on the basis of the electric potential of the Gibbs (G_2), which describe the equilibrium properties of crystals. There are 8 thermodynamic potentials, corresponding to the 8 combinations of conjugate thermodynamic variables D and E, X and X, S and T, three of which are selected as dependent, and the remaining three – as independent variables.

Potential G independent variables are stress (X), the electric field (E), temperature (T), and dependent variables are strain (x), the electric displacement (D) and entropy (S). Potential G_2 independent variables are the strain (x), the electric field (E), temperature (T), while dependent variables are stress (X), the electric displacement (D) and entropy (S). Increment of thermodynamic potentials determined by the work done by the reformative element under certain boundary conditions on the functional specificity of the element:

$$dG = - x_i\, dX_i - D_n\, dE_n - S\, dT\,,$$

$$dG_2 = X_i\, dx_i - D_m dE_m - S\, dT,$$

where $x_j = - \delta G / \delta X_j$; $D_m = - \delta G / \delta E_m$; $S = - \delta G / \delta T$,

and correspondingly,

$$X_j = - \delta G_2 / \delta x_j \; ; \; D_m = - \delta G_2 / \delta E_m ; \quad S = - \delta G_2 / \delta T \; ;$$

where: $i, j = 1,..3$ while $n, m = 1, 2,\ldots 6$.

The choice of potential (of a possible 8) to estimate the work carried out by a thermodynamic system is determined by the mechanical, electrical and thermal boundary conditions under which the element of the device works. The change of independent variables (X, E, T) corresponds to the equation of state for the dependent variables (x, D, S), where the superscripts X, E, T denote the so-called boundary conditions, which must be invariable while crystal` parameters are measured:

$$dx_i = s_{ij}^{E,T}\, dX_j + d_{in}^{X,T}\, dE_n + \alpha_i^{X,E}\, dT;$$

$$dD_n = d_{nj}^{E,T}\, dX_j + \varepsilon_{nm}^{X,T} dE_m + \gamma_n^{X,E}\, dT; \quad (8.10)$$

$$dS = \alpha_j^{X,E} dX_j + \gamma_n^{X,T}\, dE_n + C^{X,E}\, dT/T.$$

In the above expressions (8.10), the following notations are:

$$s_{ij}^{E,T} = \delta x_i / \delta X_j = - \delta^2 G / \delta X_i \delta X_j$$

– elastic stiffness, fourth rank tensor;

$$d_{nj}^{X,T} = d_{nj}^{T} = \delta x_j / \delta E_n = \delta D_n / \delta X_j = - \delta^2 G / \delta X_j \delta E_n$$

– piezoelectric modulus, third rank tensor;

$$\varepsilon_{nm}^{X,T} = \delta D_n / \delta E_m = - \delta^2 G / \delta E_n \delta E_m$$

– permittivity tensor, second rank tensor;

$$\alpha_j^{X,E} = \alpha_{j'}^{E} = \delta x_j / \delta T = - \delta^2 G / \delta T \delta X_j$$

– thermal expansion tensor free crystal, second rank tensor;

$$\gamma_n^{X,E} = \gamma_{j'}^{E} = \delta D_n / \delta T = \delta S / \delta E_n = - \delta^2 G / \delta T \delta E_n$$

– pyroelectric coefficient, tensor of the first rank;

$$C^{X,E} = T \delta S / \delta T = - T\, \delta^2 G / \delta T^2$$

– specific volumetric heat capacity, scalar (tensor of zero rank).

The piezoelectric strain tensor transformations are: $e_{nj}^{x,T} = e_{nj}^{E,T} = e_{nj}^{E}$.

Provided that the shape and volume of crystal element does not change (x = 0, i.e. crystal is mechanically clamped), from the above equations in the case of E = 0 it is possible to obtain a factor of the *primary* pyroelectric effect:

$$dP_n = \gamma_n^x \, dT, \qquad (8.11)$$

where $\gamma_n^x = \gamma^{(1)}$.

Equations (8.11) allow also find piezoelectric contribution to the pyroelectric coefficient, as well as the dielectric constant and the volumetric specific heat of the crystal. Pyroelectric measurements are usually carried out at the condition E = 0. When using equations (8.3) and (8.11) it is possible to obtain the following relationship between pyroelectric coefficient of free (X = 0) and mechanically clamped (x = 0) crystal):

$$\gamma_n^X = \gamma_n^x + e_{mj}^T \alpha_j^E,$$

that means $\gamma = \gamma^{(1)} + \gamma^{(2)}$, because the expression $e_{mj}^T \alpha_j^E = \gamma^{(2)}$ describes the contribution of the secondary pyroelectric effect.

At the constant temperature, the dielectric constant of mechanically free $\varepsilon_{nm}^{X,T}$ and clamped $\varepsilon_{nm}^{x,T}$ crystal are related as follows:

$$\varepsilon_{nm}^{X,T} = \varepsilon_{nm}^{x,T} + d_{nj}^T e_{mj}^T, \qquad (8.12)$$

where $d_{nj}^T e_{mj}^T$ is piezoelectric contribution to the permittivity.

For the heat capacity of electrically short-circuited (E = 0) and mechanically free pyroelectric crystal the following relation holds:

$$C^{E,X} = C^{E,x} + T\alpha_i^E c_{ij}^{E,T}.$$

Note that the difference between the $C^{E,X}$ and $C^{E,x}$ is small, so that in the notation of volume specific heat is often kept only one superscript: C^E.

From the equation (8.5) it follows that the use of the pyroelectric element in the absence of mechanical stress (X = 0) when electric field is absent (E = 0), the accumulation of electrical energy in the pyroelectric element dW_E is described by the potential G, that in a given boundary conditions corresponds to the expression:

$$dW_E = D_n \, dE_n = (dP_s)^2/\varepsilon_o \varepsilon_{nm}^{X,T} = (\gamma_n^{X,E})^2 (dT)^2/\varepsilon_o \varepsilon_{nm}^{X,T}, \quad (8.13)$$

where $dP_s = dD_n$ and dW_E is the desired quantity of electrical energy.

Thermal energy dW_T that is spent on energy storage in a crystal, by a definition equals $dSdT$; under the given boundary conditions it corresponds to the expression:

$$dSdT = (\alpha_j^{X,E} dX_j + \gamma_n^{X,T} dE_n + C^{X,E} dT/T)dT,$$

where the increments dX_j and dX_j respectively represents the appearance of the spontaneous stress and coercive electric field in the free crystal. The estimation of the amount

$$(\alpha_j^{X,E} dX_j + p_n^{X,T} dE_n)$$

in different pyroelectric crystals shows that it does not exceed a fraction of a percent of the value ($C^{X,E}$dT/T), so

$$dW_m = C^{X,E} (dT)^2/T_p, \quad (8.14)$$

where $T_p = T$ – operating temperature of element and $dW_т$ is desired quantity of thermal energy.

Thus, when the crystal element is mechanically *free* ($X = 0$), the equation (8.2) after the substitution of the equations (8.8) and (8.9) can be written as follows:

$$K_{ET}^2 = [(\gamma_n^{X,E})^2 (dT)^2/\varepsilon_o \varepsilon_{nm}^{X,T}]/[C^{X,E}(dT)^2/T_p] = (\gamma_n^{X,E})^2 T_p /\varepsilon_o \varepsilon_{nm}^{X,T} C^{X,E}.$$

Similarly, the factor of electro-thermal conversion for mechanically clamped crystal element is:

$$k_{ET}^2 = [(\gamma_n^{x,E})^2 (\mathrm{d}T)^2/\varepsilon_o \varepsilon_{nm}^{x,T}]/[C^{x,E}(\mathrm{d}T)^2/T_p] = (\gamma_n^{x,E})^2 T_p/\varepsilon_o \varepsilon_{nm}^{x,T} C^{x,E}.$$

Relatively low efficiency of the thermoelectric conversion is due to the physical nature of this phenomenon in dielectric crystals that are "electrically hard" in relation to external influences. Note in this regard that the efficiency of energy conversion is much higher in the case of the piezoelectric effect. Corresponding electromechanical coupling coefficient K_{EM} much exceeds the pyroelectric K_{ET}. The value of K_{EM} sometimes reaches ~ 0.95, and in case of piezoelectric resonance in crystals with high electro-mechanical quality this coefficient increases to almost 1.

In spite of low efficiency, pyroelectric effect is used primarily for the detection and measurement of heat flow, and, under certain conditions, for direct transition of thermal energy into electricity. The "direct" conversion of heat into electricity is used in thermal imaging and highly sensitive temperature sensor.

Inverse to the pyroelectric effect is the *electrocaloric effect* that affects to the value of the permittivity of a polar crystal. When thermal equilibrium has enough time to be established at the applied electric field frequency, the crystal completely absorbs applying an electric energy converted to a heat (as well as to return this energy). On the part of the electrical circuit this process increases the electrical capacity that looks like the increase of crystal permittivity ε_{nm}^T (isothermal permittivity). At higher frequencies, the electric field has no time for thermal energy exchange (thermal equilibrium cannot be set). It looks like a decrease in the capacitance of pyroelectric element, so at the increased speed of process the adiabatic permittivity ε_{nm}^S is measured. The difference $\Delta\varepsilon_{EC} = (\varepsilon_{nm}^T - \varepsilon_{nm}^S)$ is the electrocaloric part of low frequency permittivity; it is possible in the pyroelectrics only and depends on the value of the specific heat and on the pyroelectric coefficient: $\Delta\varepsilon_{EC} = (\gamma_n^2 T)/(\varepsilon_0 C^{x,E})$.

Electrocaloric effect in which electrical energy is linearly converted into a heat, enables crystal cooling due to the applied electric field to it a certain polarity. "Inverse" transformation in the form of cooling by the solid body is promising for a new type of refrigerators that do not have the environmentally harmful freon gas and electric motors (machinery). Electrocaloric effect can be applied also to an electrically controlled decrease of temperature (for example, to achieve a better cooling in cryogenic).

8.4 Thermodynamic description of artificial pyroelectric effect

A conception of the artificial pyroelectric effect (APE) is introduced as an effect that is induced by the homogeneous heating of non-central symmetric crystal, in a polar cut of which the part of thermal strain is artificially restricted. Correspondent equations ratio are found that allows to determine the APE-coefficient (that is similar to the pyroelectric coefficient) for various classes of non-central symmetric crystals using components of piezoelectric tensor, elastic compliance and thermal expansion coefficient [5-7].

As already is mentioned, usually the pyroelectricity is defined as the change of spontaneous polarization P_S of electrically and mechanically free crystal with an uniform change in its temperature T. The pyroelectric effect consists of primary and secondary effects $\gamma_i^{X,E} = \gamma_i^{(1)} + \gamma_i^{(2)}$. Contribution of the primary effect is determined by study of completely clamped crystal, which has no strain ($x_n = 0$), i.e. $\gamma^{(1)} = \gamma_i^{x}$. Contribution of the secondary effect corresponds to the difference of the coefficients $\gamma_i^{(2)} = \gamma_i^{X,E} - \gamma_i^{x}$.

In piezoelectric materials, the thermoelectric response might be obtained either under inhomogeneous influence (temperature gradient over the sample) or in the case of inhomogeneous boundary conditions. It is for a long time known that the non-uniform thermal impact causes the polar response in piezoelectric. In early studies, this phenomenon was called as actinoelectricity. Later it was identified as the tertiary pyroelectricity. Tertiary effect might be more clearly defined as the temperature variation of piezoelectric material polarization which is induced by the thermal stress:

$$dP_i = d^T{}_{im} c_{mn}{}^{X,E} \cdot (x_n - \alpha_n^{X,E} dT).$$

Here it is shown that under uniform thermal excitation of piezoelectric (when grad$T$ = 0) the polar response also can be obtained, if such a condition is created which excludes the part of thermal strains. In this case, the permissible thermal strain induces piezoelectric polarization which is due to the *partial clamping* of the crystal

and can not be compensated. At this the state crystal is the same at all his points, but it is uniformly stressed. In the experiment, the anisotropic thermal deformation limiting can be implemented in different ways: an artificial fixing piezoelectric thin plate on a rigid substrate or by the natural limitation of the radial deformation of a thin disk above the frequency of electromechanical resonance, etc.

Thus, the artificial pyroelectric effect is defined as induced by mechanical stress polarization in the electrically free, but mechanically partially clamped piezoelectric under *uniform* thermal exposure. Partial clamping is provided by the inhomogeneous boundary conditions which *anisotropically* limit the thermal strains of non-central symmetric crystal, so it is homogeneously but anisotropically stressed. The artificial pyroelectric effect maximally manifests itself in the direction of any of polar axes of the piezoelectric crystal. This axis, under the influence of stress, is transformed into a peculiar polar axis in accordance with the Curie principle.

Effective pyroelectric coefficient that characterized APE depends on the piezoelectric, elastic and thermal properties of the crystal, as well as on the method of thermal deformations limiting:

$$\gamma^*_{APE} = \gamma_k^{Xk,E} = d^T_{km}\,\lambda^*_m,$$

where λ^*_m is thermo-elastic coefficient of partially clamped crystal. Index at the APE coefficient γ_k indicates that only a part of the elastic stress tensor components X_k are zero. For various piezoelectric the coefficient $\gamma^*_{APE} = 10^{-6} = 10^{-4}\ C \cdot m^{-2} \cdot K^{-1}$, i.e., the effect is comparable in magnitude to the pyroelectric coefficient of usual pyroelectrics and ferroelectrics. The dimension of the APE coefficient corresponds to usual pyroelectric coefficient $\gamma_i^{X,E}$ dimension because partial clamping turns the piezoelectric into the artificial pyroelectric. This effect could be classified as a "secondary" effect in view of the similarity in the calculation methods. However, this definition is incorrect as the secondary pyroelectric effect is manifested in the mechanically free crystals while the artificial pyroelectric effect is observed in the partially clamped crystals only.

It is important to compare the artificial pyroelectric effect with the so-called "tertiary pyroelectric effect." In accordance with known definition, as tertiary effect so the APE are due to thermal stresses in the piezoelectrics. However, in the case of the tertiary pyroelectric effect these stresses are caused by spatial heterogeneity of crystal temperature. The the APE as the conventional pyroelectric effect, occurs at a uniform heating or cooling of the crystal. It appears under the restriction of certain strains of the crystal, i.e., it arises as result of inhomogeneous boundary conditions, that in traditional pyroelectric lead to a ban of the secondary pyroelectric effect.

In all cases, induced in the piezoelectric APE can be regarded as a consequence of the superposition of the crystal symmetry and the impact on him. The most accurate (but not brief) definition of the APE physical effect would be "Pyroelectricity in partially clamped piezoelectrics", but using here term “Artificial pyroelectric effect” also briefly and quite clearly indicates the physical mechanism of the phenomenon under discussion.

In previous section, equation (8.8) was obtained for the pyroelectric coefficient of crystals with special polar direction using Gibbs thermodynamic potential. when the independent variables *X, E* and *T*, while the dependent values are strain *x*, electrical displacement *D* and entropy *S*. In this case, the equation of state of a pyroelectric can be written as follows:

$$dx_m = s_{mn}^{X,E} dX_n + d^T_{mi}\, dE_i + \alpha^{X,E}_m dT,$$
$$dD_j = d^T_{jm}\, dX_m + \varepsilon^{X,T}_{ij}\, dE_i + p_j^X dT,$$
$$dS = \alpha_m^E dX_m + p^X_j\, dE_j + C^{E,T}\, dT/T,$$

where $s_{mn}^{X,E}$ is tensor of elastic compliance and $C^{E,T}$ is heat capacity. For piezoelectrics, in the simplest experimental situation, when the crystal is electrically free (i.e., short-circuited, $E = 0$ and $D = P$), and in the absence of spontaneous polarization $P_j^X = 0$, the equations (8.20) get the form:

$$dx_m = s_{mn}^{X,E} dX_n + \alpha^{X,E}_m dT,$$
$$dP_j = d^T_{jn}\, dX_n,$$
$$dS = \alpha_m^{X,E} dX_m\ C^{E,T}\, dT/T,$$

where *S* is entropy. Superscripts indicating the thermodynamic state of the crystal, at further analysis are omitted; so the change of entropy is not considered. Since it is assumed the constancy of *E* and *T*, then in the partially clamped piezoelectrics the isothermal current pyroelectric coefficient $\gamma_{\text{ТПЭЛ}} = \partial P_i/\partial T$ is calculated.

Above equations should be specified in accordance with boundary conditions. It is assumed that while experimental studies or practically applications the pyroelectric devices constitutes the "endless" thin piezoelectric plate "ideally" fixed on a thick rigid substrate that has zero thermal expansion coefficient ($\alpha_n = 0$). The thickness of this plate *h* must be substantially less than the depth of penetration of the temperature wave $l = (2a/\omega)^{1/2}$ where *a* is temperature conductivity and ω is heat flow modulation frequency. At these conditions the temperature gradient in the piezoelectric can be neglected, and the substrate under the influence of the temperature wave will not flex (because $\alpha_n = 0$).

As a result, the tangential deformation of piezoelectric completely suppressed, and the only on the deformation of the plate thickness in the direction of the free

surface is permitted. Shear deformations under the uniform heat flux are not excited, while the "infinitely large" area of the plate allows neglect by the boundary effects in this model. The normal to the plate is oriented to one of the polar directions of piezoelectric crystal, which, because of the limitations in planar piezoelectric strains becomes a special polar axis in accordance with the Curie principle of superposition.

Solution of above equations depends on the crystal symmetry [3].

8.5 Artificial pyroelectric effect in quartz

As the most simple case, consider the class of the crystals 32, to which belong the well-studied piezoelectric quartz. In the basic setting, 32 class crystals are characterized by longitudinal piezoelectric module d_{11} transverse module $d_{12}= -d_{11}$ and shear modules d_{14}, d_{25} и d_{26}. Thin quartz plate must be cut perpendicular to the axis 1 (this is a *X*-cut or Curie slice). Rigid substrate prevents deformation in the cutting plane: $dx_2= dx_3 = 0$, , so that only allowed deformation is dx_1 (shear deformations, according to the model, are not excited). Electrodes cover the surface (100) so $E_1= 0$, moreover, $X_1= 0$ because the strain x_1 is permitted; elastic compliances $s_{11} = s_{12}$, $s_{13} = s_{33}$, thermal expansion coefficients $\alpha_1 = \alpha_2 \neq \alpha_3$,. Under these conditions, equations (8.20) take the form

$$dx_1= s_{11}dX_2 + s_{12}dX_3 + \alpha_1 dT,$$
$$dx_2= s_{22}dX_2 + s_{23}dX_3 + \alpha_2 dT = 0,$$
$$dx_3= s_{32}dX_2 + s_{33}dX_3 + \alpha_3 dT,$$
$$dP = d_{12}dX_2. \quad (8.14)$$

From the equations (8.15) an expression for the pyroelectric coefficient of partially clamped crystal class can be obtained as

$$\gamma_{1APE} = dP/dT = d_{11}(\alpha_1 s_{33} - \alpha_3 s_{13})(s_{11}s_{33} - s_{13}^2)^{-1}. \quad (8.15)$$

For the quartz (SiO_2) crystal X-cut at temperature 300 K the APE coefficient is $\gamma_{1APE}= 2.5\ \mu C \cdot m^{-2} \cdot K^{-1}$. For other crystals of the 32 symmetry class the calculations show: berlinite crystal ($AlPO_4$) $\gamma_{1APE}= 5.7\ \mu C \cdot m^{-2} \cdot K^{-1}$, calomel crystal ($Hg_2Cl_2$) the $\gamma_{1APE}= 8.7\ \mu C \cdot m^{-2} \cdot K^{-1}$, and tellurium crystal (Te) shows $\gamma_{1APE}= 10\ \mu C \cdot m^{-2} \cdot K^{-1}$.

First *two-dimensional* structural arrangement of the polar-sensitive bonds will be considered. In actual (“exclusive”) piezoelectric, the primary pyroelectric effect is always absent ($\gamma_i^{(1)} = 0$) and in mechanically clamped condition the secondary pyroelectric effect also looks to be impossible ($\gamma_i^{(2)} = e_{im}\alpha_m = 0$). However, in the *partial clamping conditions* any piezoelectric is liable to show “secondary type”

pyroelectric effect, because the sum $e_{im}\alpha_m \neq 0$. Just this is the "*artificial* pyroelectric effect".

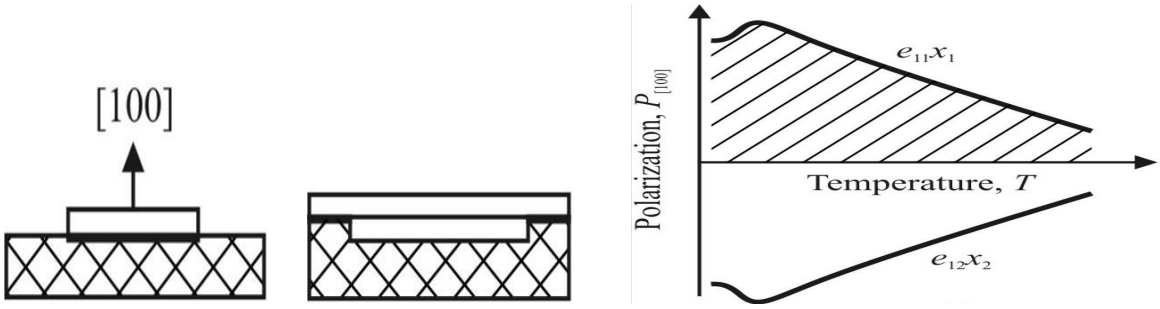

a b c

Fig. 8.1. Partially clamped quartz samples: *a* – tangential strain in thin plate is forbidden by plate soldering to substrate; *b* – membrane variant of partial clamping; *c* – thermally induced polar response conditioned by piezoelectric effect

From 10 classes of "exclusive" piezoelectrics, exactly the quartz is simplest example for explanation of internal polarity nature. Trigonal α-quartz, which belongs to 32 class of symmetry, is electrically active only in the [100]-type directions that corresponds to (100)-plate of quartz, which is known as a "Curie cut". This cut should be prepared perpendicularly to any one of three two-fold polar axes: *1*, *1′* or *1″* (distribution of polar activity in quartz crystal was presented in Chapter 4).

Further it will be shown how it is possible to measure the components of the polar-sensitivity in the polar-neutral crystal.

In the standard crystallographic setup of quartz crystal the matrix of piezoelectric coefficients e_{im} consists of one longitudinal (e_{11}), one transverse (e_{12}) and three share components of piezoelectric strain modulus (e_{14}, e_{25} and e_{26}):

$$e_{im} = \begin{bmatrix} e_{11} & e_{12} & 0 & e_{14} & 0 & 0 \\ 0 & 0 & 0 & 0 & e_{25} & e_{26} \\ 0 & 0 & 0 & 0 & 0 & 0 \end{bmatrix}.$$

Transverse component e_{12} equals to longitudinal one but has opposite sign: $e_{12} = -e_{11}$. Besides, only one of share piezoelectric modules (e_{14}) is independent, others share components are $e_{25} = -e_{14}$ and $e_{26} = 2e_{11}$. So the only two components of given matrix are independent.

Before proceeding further, it is necessary to show that *any* homogeneous influence (uniform change of temperature or hydrostatic pressing) can not induce the electrical response in a specimen of quartz even being taken from the Curie cut.

First of all, any share strain cannot be excited in a sample, if external influence has the scalar type. So only the longitudinal and the transverse electrical response should to be taken into account. In the non-clamped quartz sample (i.e., in free-stress state) the longitudinal piezoelectric effect ($e_{11}x_1$) and the transverse effect ($-e_{12}\,x_1$) *compensates* each other. It is illustrated in the Fig. 8.1*c*, which characterises uniform thermal influence on quartz sample: one part of piezoelectric response ($e_{11}x_1$) induced by thermal deformation x_1 equals to another part ($e_{12}x_1$) but with opposite sign.

Since a rather complex phenomenon is discussed here, it makes sense to give the additional proof that any electrical response in actual piezoelectric really is compensated in the case of scalar influence, as shown in Fig. 8.1*c*. First of all note that from the matrix for piezoelectric strain modulus e_{im} it follows that polarization component $P_3 = 0$ (in $Z = 3$ direction quartz shows no piezoelectric effect) as well as for component $P_2 = 0$, because shear strains e_{23} and e_{26} can not be excited by the uniform action. It remains to analyze the polarization component P_1.

Induced mechanically (by direct piezoelectric effect) this component of electrical polarization can be given by

$$P_1 = e_{1m}x_m = e_{11}x_1 + e_{12}x_2 + e_{13}x_3 + e_{14}x_4 + e_{15}x_5 + e_{16}x_6 = e_{11}x_1 + e_{12}x_2.$$

This sum depends on mechanical boundary conditions, in which crystal is located:

(i) In case when crystal is totally clamped, any mechanically induced polarization is impossible: $P_1 = 0$ due to $x_m = 0$.

(ii) It is essential to show that in case of free-stress condition (when quartz crystal can be deformed) any polar response is also absent ($P_1 = 0$).

Firstly, many components of the piezoelectric strain module of quartz crystal are zero: it is seen from the above matrix that $e_{13} = e_{15} = e_{16} = 0$. Secondly, in the above equation the share strain $x_4 = 0$ because any share strain should be absent in the case when external action is uniform.

Thirdly, in free-stress quartz crystal the strains x_1 and x_2 in the (100)-plane are equal: $x_1 = x_2$. In fact, that in case of uniform thermal action ($x_m = \alpha_m dT$) these strains are equal due to the parity of correspondent components of quartz thermal expansion coefficients: $\alpha_1 = \alpha_2$ (however, $\alpha_1 \neq \alpha_3$).

In fourth, in the event of uniform stretching (or compression), again, the strains $x_1 = x_2$ due to the equality of correspondent quartz elastic stiffness components: $c_{11} = c_{22}$. Strains could be calculated from the equation $x_m = c_{mn}X_n$, where X_n is the uniform (hydrodynamic) stress. Thus, excitation in the actual piezoelectric the homogeneous deformation (by thermal or elastic way) does not lead

to its polar response, since the piezoelectric contributions from strains $e_{11}x_1$ and $e_{12}x_2$ into the polarization P_1 compensate each other, Fig. 8.1*c*.

(*iii*) However, in the *partially clamped* quartz crystal the thermally induced polarization will not be zero ($P_1 \neq 0$), and just this circumstance is used here to examine internal compensated (latent) polarity that, in principle, makes possible the use partially clamped quartz (and others polar-neutral piezoelectrics) in the thermal or pressure sensors.

The fundamental idea is that artificial limitation (by mechanical boundary conditions) of any one of strain (x_1 or x_2) should transform the plate of piezoelectric quartz into the artificially created "pyroelectric" crystal [14].

Suppose that one of two types of deformations can not be realized in the piezoelectric plate. For example, it is possible to suppress the tangential strains ($x_2 = 0$ and $x_3 = 0$), if piezoelectric plate is firmly fixed on the massive incompressible substrate with zero coefficient of thermal expansion (in given case as substrate the fused silica in which $\alpha \approx 0$, Fig. 8.1*a*). In this case the uniform heating or cooling (as well as hydrostatic compression) will lead to the polar response appearance: $P_{[100]} = e_{11}x_1$. Similarly, the prohibition on the normal strain ($x_1 = 0$) with a possibility of tangential strain would cause the response of opposite polarity: $P_{[100]} = e_{12}x_2$, but experimental realization of second case is more difficult.

In practice, it is easier to limit the plane strain x_2, if piezoelectric plate soldered onto a fused silica. The only deformation that can be realized in this case is the thickness strain x_1 directed along polar-neutral axis "1", which by this way is turned into the single polar axis. Therefore, substantial reducing of one type of deformations transforms piezoelectric crystal into artificial pyroelectric. This effect can be defined also as the polarization of partially clamped actual piezoelectric by the uniform change of its temperature. Partial clamping is provided by the non-uniform mechanical boundary condition, limiting some of thermal strains of a crystal, which becomes uniformly but anisotropic stressed.

Artificial thermo-piezoelectric effect can be characterized by the coefficient γ^* which is equivalent to the pyroelectric coefficient, which depends on electrical, elastic and thermal properties of the non-central crystal, as well as on the way of its deformation limitation:

$$\gamma^* = d_{im}\lambda^*_m, \quad (8.16)$$

where d_{im} is piezoelectric modulus and λ^*_m is effective thermo-elastic coefficient of partially clamped crystal.

The spatial distribution of the sensitivity of artificial pyroelectric effect in the crystals of quartz type symmetry (such as berlinite ($AlPO_4$), cinnabar (HgS),

tellurium (Te), etc.) can be found similarly to quartz crystal. It is possible to find "pyroelectric coefficients" in these crystals, even in any slanting plates. The spatial distribution of $\gamma^*(\theta,\varphi)$ that characterizes artificial pyroelectric coefficient in the quartz type crystals can be presented in polar coordinates: $\gamma^*(\theta,\varphi) = \gamma^*_{max}\sin^3\theta\cdot\cos 3\varphi$, where θ is azimuth angle and φ is plane angle. This spatial pattern is equivalent to longitudinal piezoelectric modulus distribution that was shown in Fig. 1.13A. Through the radius vector directed from the center of this figure it is possible to determine the size of the artificial effect in any cut of quartz-type crystals. It is obvious that maxims of the effect occur along any of three *X*-axes.

In order to get effective pyroelectric coefficient $\gamma^* = dP_i/dT$, the thermodynamic equations for the non-centrosymmetric (but not pyroelectric) crystal should be used. With assumption that crystal is short-circuited ($E = 0$), the exact solution is given below:

$$dx_n = s_{nm}\,dX_m + \alpha_m\,dT;$$
$$dP_i = d_{im}\,dX_m,$$

where s_{nm} is components of elastic compliance tensor. Solving equations (2.5) for trigonal crystal class (which include quartz crystal) leads to following expression:

$$\gamma^*_{100} = d_{11}(\alpha_1 s_{33} - \alpha_3 s_{13})\,[s_{11}\cdot s_{33} - (s_{13})^2]^{-1}. \quad (8.17)$$

For quartz crystal one can obtain $\gamma^*_{100} = 2.6$ μC/m^{2}K, in others crystals of 32 symmetry class this parameter is bigger: $\gamma^*_{100} = 2.7$ μC/m^{2}K in berlinite, 8.7 μC/m^{2}K in cinnabar, and 10 μC/m^{2}K for tellurium crystal. This parameter is not very small, because the first known pyroelectric tourmaline has pyroelectric coefficient $\gamma = 4$ μC/m^{2}K, while in wurtzite crystal (ZnS) usual pyroelectric response is characterized by $\gamma = 0.3$ μC/m^{2}K.

In quartz, as in other piezoelectrics the thermomechanically induced pyroelectric effect was studied by a quasistatic method, in which the pyroelectric coefficient is determined by the time during which the pyroelectric current charges the measuring capacitor. Electronic equipment includes the Peltier element used for heating and cooling. Samples, having a plate shape about 100 microns thick and the area of ~ 1 cm^2 with copper electrodes, soldered onto silica glass substrates were investigated.

Temperature dependence of artificial pyroelectric response of partially clamped in the (100)-cut of quartz crystal is shown in Fig. 8.2 along with the rest of the key parameters. Investigation shows that artificial pyroelectric coefficient γ^*_{100} changes with temperature very slowly while the alteration of some others components of tensors might be very complicated. In a wide temperature range

artificial "pyroelectric" coefficient $\gamma^*_1$is almost constant, but it is seen a tendency to it decrease at low temperatures, perhaps due to reduction of thermal expansion coefficient. In vicinity of quartz $\alpha \rightarrow \beta$ phase transition at temperature $\theta_1 \approx 850$ K the γ_1^* breaks off. It is remarkable that for thermally induced polarity $P_{[100]} = \Delta P_1 = \int \gamma^*_1 dT$ the simplest linear temperature dependence is observed: $\Delta P_1 \sim (\theta - T)$ with a critical index $n = 1$.

It should be noted that piezoelectrics of quartz symmetry (SiO_2 and $AlPO_4$), in addition to $\alpha \rightarrow \beta$ phase transition have the second high-temperature transformation between their β and γ phases.

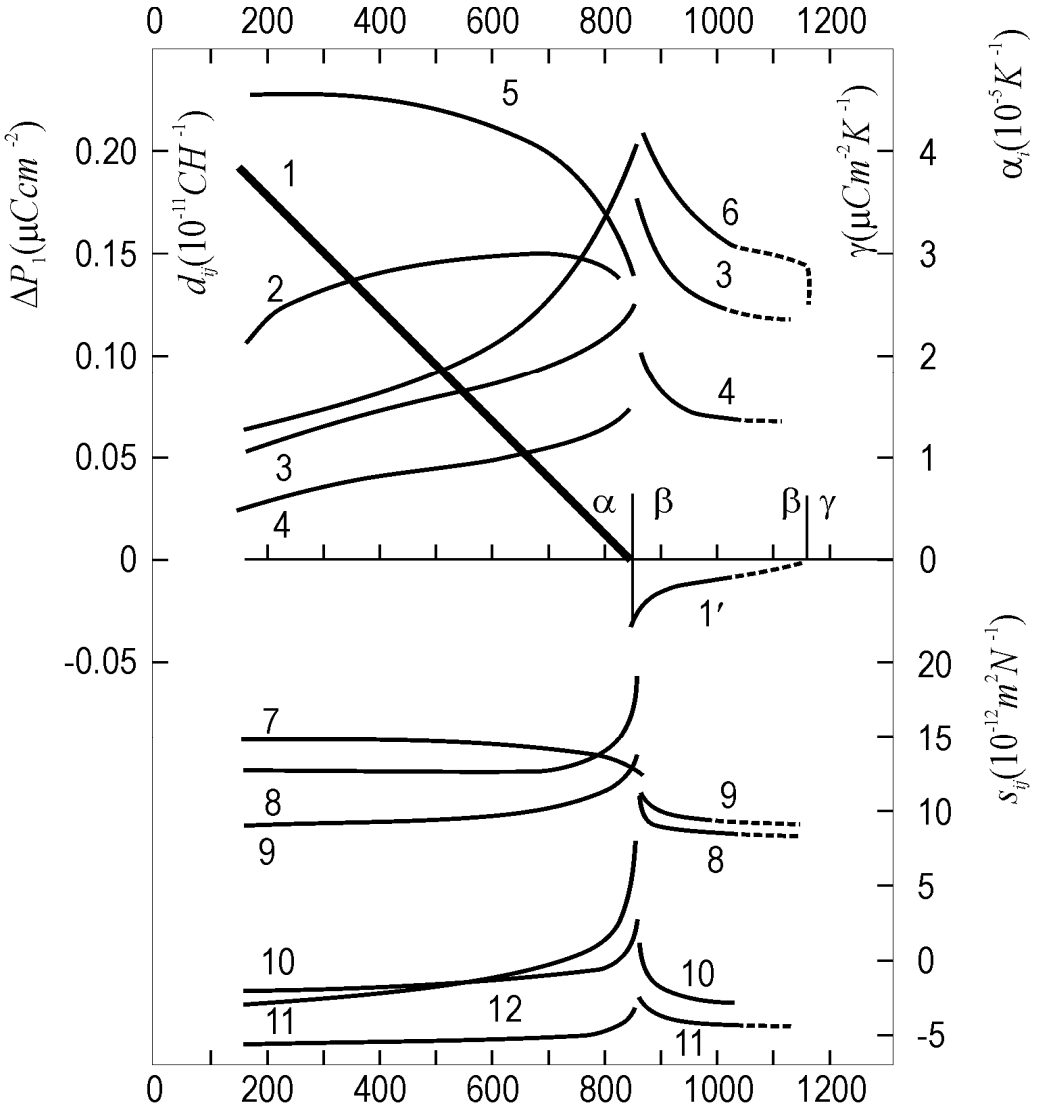

Fig. 8.2. Latent (hidden) intrinsic polarity temperature dependence for quartz (curve 1) in comparison with dependences of other thermal and elastic parameters of this crystal: *1* – ΔP_1 found in [100]-cut thin plate of quartz in α-phase; 1`– ΔP_1 found in [110] oriented rod in high-temperature β-phase of quartz; 2 – artificial pyroelectric coefficient $\gamma_1^*$of partially clamped [100]-cut of quartz in α-phase; 3, 4 – thermal expansion coefficients α_1 (3) и α_3 (4) of quartz crystal; 5, 6 – piezoelectric modulus d_{11} (5) и d_{14} (6) of quartz α-phase; 7–12 – elastic compliance components: $0{,}5 \cdot s_{66}$ (7), s_{11} (8), s_{33} (9), s_{12} (10), s_{13} (11), s_{44} (12)

Temperature dependence of artificial pyroelectric response characterises quartz in its β-phase with temperature dependence of 3D moment M_{ijk}. It is described by another equation; $P_{13} \sim (\theta_2 - T)^2$ with $\theta_2 = 1140$ K. As seen from Fig. 8.2 (curve *1'*), this electrical moment vanishes at the $\beta \rightarrow \gamma$ phase transition. In the quartz crystal high-temperature γ-phase is non-polar. Again, it is necessary to note that the study of volumetric piezoelectric effect needs the non-compressible substrate, so only theoretical estimation on this effect can be provided.

8.6 Artificial pyroelectric effect in gallium arsenide

Among possible practical applications of artificial pyroelectricity, the most promising are the semi-insulated (*s/i*) semiconductors of GaAs group ($A^{III}B^{V}$). The point is that they might be used as the pyroelectric converters in the upper layer of a sandwich composition, which can be integrated with the amplifiers (in bottom layer) using semiconductor with the high-mobility electrons.

These crystals have sphalerite structure which belongs to polar-neutral $\bar{4}3m$ group of symmetry. In specially oriented plates and by using the *restriction* of part of thermal deformations, the $A^{III}B^{V}$ crystal is capable to produce pyroelectric signal. At that, the voltage sensitivity of *s/i*-GaAs, for instance, is close to the pyroelectric ceramics: GaAs plate with thickness of 100 microns at temperature change of several degrees shows the electrical potential 2 B. This can be of interest for implementation in the multi-element planar integral thermal far-IR detectors. It is assumed that in a special way oriented semi-insulating layers or micro-regions, embedded in gallium arsenide integrated circuit together with amplifiers and switching devices, may form a mosaic microstructure of non-selective and highly sensitive infrared detectors.

Polar-sensitive bonds in the piezoelectric-active $A^{III}B^{V}$ type semiconductors of sphalerite structure are directed along each of four threefold axes of the cubic crystal. However, polar-sensitivity in such crystal is completely compensated; therefore, any scalar influence to it, including the uniform temperature change, can not produce any electrical response. Nevertheless, natural compensation of electrical polarity can be broken in the specially oriented plates (or layers), in which part of thermal deformations are limited. As a result, along one of threefold polar axis the electrical response appears, just that is *artificial pyroelectric effect.*

High-symmetry cubic crystals of $\bar{4}3m$ class is characterized by the isotropy of thermal expansion coefficient: $\alpha_m = \alpha$ (in GaAs $\alpha = 2.8 \cdot 10^{-6}$ K^{-1} at 300 K). In these crystals, the elastic compliance $s_{mn}^{E,T}$ tensor is reduced to three independent

components (in GaAs $s_{11}^{E,T} = 12 \cdot 10^{-11}$, $s_{12}^{E,T} = -4.6 \cdot 10^{-11}$ and $s_{33}^{E,T} = 17 \cdot 10^{-11}$ m^2/N). In its main installation, the piezoelectric properties of $A^{III}B^{V}$ crystal are described by the matrix:

$$d_{im} = \begin{bmatrix} 0 & 0 & 0 & d_{14} & 0 & 0 \\ 0 & 0 & 0 & 0 & d_{25} & 0 \\ 0 & 0 & 0 & 0 & 0 & d_{36} \end{bmatrix}, \quad (8.18)$$

This matrix represents the third rank tensor of piezoelectric coefficients. In main installation of such crystal, for (100), (010) and (001) crystal plates all longitudinal (d_{11}, d_{22}, d_{33}) as well as all transverse (d_{12},, d_{13}, d_{21}, d_{23}, d_{31}, d_{23}) piezoelectric modules are zero. Therefore, usually used in the electronics and in the most of experiments the [100]-oriented plates of $A^{III}B^{V}$ semiconductors are *non-sensitive* to any homogeneous mechanical influence (except shear action correspondind to share modules $d_{14} = d_{25} = d_{36}$). It is obvious from the matrix (8.18) that no electrical response is possible, if external influence on crystal has scalar character. In other words, being applied to the standard (100)-plates of $A^{III}B^{V}$ crystals, any partial clamping cannot invoke any polar response. Meanwhile, the crystal plates of the (100) orientation are conceptually the sole chips using for GaAs type devices. Therefore, it is not improbable that this is the main reason for mentioned polar effects previously were out of consideration.

Due to cubic symmetry of crystal, in its standard installation piezoelectric module components are equal: $d_{14} = d_{25} = d_{36}$ and, therefore, they might be denoted simply as d. In gallium arsenide $d = 2.7 \cdot 10^{-12}$ C/N, i.e. it surpasses even quartz piezoelectric module ($d_{SiO2} = 2.4 \cdot 10^{-12}$ C/N). From above equations one cannot see any opportunity of artificial pyroelectric effect in the GaAs, since the piezoelectri matrix contains only shear c components which can not be excited by the homogeneous heat exposure. As shown before, the artificial pyroelectric effect, generally, occurs due to the *de-compensation* of contributions from longitudinal and transverse piezoelectric effects, described by the left half of piezoelectric matrix. But in this case (in the *standard installation* of $A^{III}B^{V}$ crystal) all components of longitudinal and transverse piezoelectric module are zero.

However, in another orientation of crystallographic axes, to which standard matrix (8.18) can be converted, both longitudinal and transverse components of piezoelectric module appear. These components are maximal in such slices of a crystal, which are oriented perpendicularly to the axis of a third order (which are the spatial diagonal of a cube), since greatest polar-sensitivity in $A^{III}B^{V}$ crystal coincides with these directions. This polarity is due the mixed ionic-covalent bonding between

A—B ions, and the anisotropy of electronic density distribution is such a way that the density is increased in a vicinity of B-ion.

When describing effect of partial limitation of deformations on piezoelectric properties of polar crystal, sometimes it is more convenient to use not the piezoelectric modulus d, (describing the relationship between mechanical stress X and induced by it polarization: $P_i = d_{in}X_n$) but the piezoelectric constant e, which relates the deformation x to the polarization: $P_i = e_{in}x_n$, where $e_m = d_{in}c_{mn}$ and c_{mn} is the elastic stiffness. The matrix of piezoelectric constant for main crystal installation corresponds to the piezoelectric modulus

$$e_{im} = \begin{matrix} 0 & 0 & 0 & e_{14} & 0 & 0 \\ 0 & 0 & 0 & 0 & e_{15} & 0 \\ 0 & 0 & 0 & 0 & 0 & e_{36} \end{matrix}$$

This matrix represents the third rank tensor of piezoelectric coefficients. In this instance, for (100) = (010) = (001) crystal plates as longitudinal (e_{11}, e_{22}, e_{33}) so transverse (e_{12}, e_{13}, e_{21}, e_{23}, e_{31}, e_{23}) modules are zero. That is why (100) type of GaAs plate is not sensitive to any mechanical strains except the twist ones. The lasts corresponds to share modules $e_{14} = e_{25} = e_{36}$ but they could not provide any response under the *homogeneous* influences. Partial clamping is also useless, if it is applied to the standard (100) plates of III-V crystals.

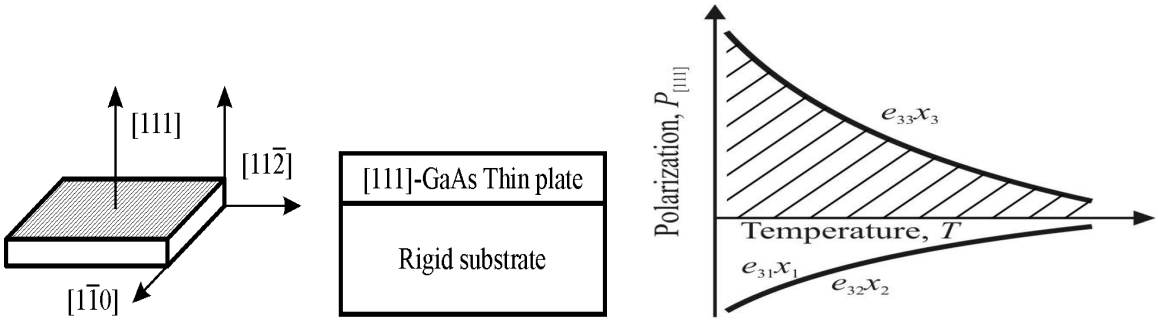

Fig. 8.3. Partial (in plane) clamping realization: *a* – orientation of *s/i*-GaAs [111]-cut; *b* – plate soldered to rigid substrate, *c* – internal polarity change decompensated by partial clamping

Figure 8.3 *a* and *b* shows such orientation of the $A^{III}B^{V}$ crystal, which should be prepared to invoke its polar response. Polar cut of $A^{III}B^{V}$ crystal should be oriented by such a way, at which the [111]-axis is perpendicular to studied plane. In case of volumetric piezoelectric effect investigation, this (111)-plate has to be fixed onto the "ideally hard" substrate (in trial experiments the hard steel might be used, but in the microelectronic piezoelectric sensors it is expedient to use the membrane, clamped along its boundaries). In similar fashion, the *s/i*-GaAs (or GaN) crystalline (111)-plate could be activated for the "pyroelectric" response, if a rigid substrate,

shown in Fig. 8.3*b,* would have very small thermal expansion coefficient ($\alpha \sim 0$). In our first experiments the fused silica was used as a substrate, but in the microelectronic practical devices, the pyro-active *s/i* (dielectric) layer of Ga(AsP) or (GaAl)As layer can be directly deposited on the substrate made of GaAs crystal, followed by the etching and forming the membrane clamped along its boundaries.

Such partial clamping makes impossible the plane strains ($x_1 = x_2 = 0$), so the electrical response from uniform pressure (or thermal deformation) can be realized only perpendicularly to the plane: $M_3 = e_{33}x_4$. It is obvious that created artificially composite structure (Fig. 8.3*a*) can be used for investigation of volumetric piezoelectric effect (or to study the artificial pyroelectric response).

In the any form of free-stress sample, the longitudinal piezoelectric effect (e_{33}) and *two* transverse effects (e_{31} and e_{32}) compensate each other: $e_{31} + e_{32} = -e_{34}$. It is illustrated in Fig. 8.3*c*, which describes thermal investigation of GaAs (111)-plate: one part of piezoelectric polarization ($e_{33}x_3$, induced by thermal deformation x_3) equals to other parts ($e_{31}x_1 + e_{32}x_2$) but with opposite sign (in this case, index "3" corresponds to the [111]-axis). Strain components in free-stress cubic crystal are equal: $x_1 = x_2 = x_3$, because the excitation is homogeneous. That is why, in the non-pyroelectric crystal, the sum of piezoelectric coefficients of transverse and longitudinal piezoelectric coefficients is zero:

$$e_{31} + e_{32} + e_{33} = 0 \qquad (e_{31} = e_{32} = -\tfrac{1}{2}\, e_{33}).$$

As a result, the piezoelectric effect, produced by the longitudinal strain component $x_3 = \alpha \mathrm{d}T$ is compensated by the effect of two transverse strain components $x_1 = x_2 = \alpha \mathrm{d}T$; therefore no electrical response is possible. Consequently, free-stress polar (111)-plate of GaAs type crystals is not sensible to the homogeneous excitations.

However, the artificial limitation of any one of mentioned strain components (x_3 or $x_1 + x_2$) can transform the piezoelectric (111)-plate of GaAs type crystal into an artificially created "pyroelectric". In practice, it is easier to limit the plane strain ($x_1 + x_2$) by a simple mechanical design. In this case, the only thickness strain x_3 can be excited, and just in the direction of polar axis "3" ([111]-direction), which is transformed into a "peculiar" polar axis. This effect is impossible as in the free-stress so in the free-strain crystals: both artificial effects are the result of the non-isotropic partial clamping. Only partially clamped piezoelectric crystal manifests the artificial pyroelectricity or volumetric piezoelectric effect.

Partial clamping violates the polar neutrality ($e_{31}x_1 + e_{32}x_2 = 0$) and makes it possible to manifest the artificial pyroelectric effect as $M_i = e_{33}x_4$. Greatest effect in the crystals of $\bar{4}3m$ class of symmetry can be achieved in such a special installation,

in which one of new axis *3′* coincides with polar-neutral axes of [111]. With this new installation, the axis *1′* should be directed normally to the axis passing through the *3′* plane of symmetry of a cube, while orientation of new axis *2′* is predetermined by Descartes coordinate system.

For further calculations, it is expedient to return to the matrix of piezoelectric module. After above procedure application, the matrix of piezoelectric module for $\bar{4}3m$ crystal in new installation is:

$$d_{i'm'} = \begin{bmatrix} 0 & 0 & 0 & 0 & -\frac{d}{\sqrt{3}} & \frac{2d}{\sqrt{6}} \\ \frac{d}{\sqrt{6}} & -\frac{d}{\sqrt{6}} & 0 & -\frac{d}{\sqrt{3}} & 0 & 0 \\ -\frac{d}{2\sqrt{3}} & -\frac{d}{2\sqrt{3}} & \frac{d}{\sqrt{3}} & 0 & 0 & 0 \end{bmatrix}. \qquad (8.19)$$

All components of this new matrix are expressed in the terms of shear module *d*, taken from the basic installation of the crystal (6.6). The third row of the matrix (8.19) characterizes the piezoelectric properties of such crystal plate, which is cut perpendicularly to the axis *3′* = [111] and characterized by the longitudinal piezoelectric module $d_{3'3'} = d/\sqrt{3}$ and by transverse effect $d_{3'1'} = d_{3'2'} = -d/2\sqrt{3}$. Piezoelectric shear components in third row of this matrix are absent.

Thus, in the ideal conditions, the determination of artificial pyroelectric coefficient $\gamma_{APE} = \mathrm{d}Mi/\mathrm{d}T$ is possible, when the thermo-electrical response from the tangential strain is completely suppressed by a rigid substrate: $\mathrm{d}x_1 = \mathrm{d}x_2 = 0$. At the uniform change of temperature, the only allowed strain is the $\mathrm{d}x_3$ (hereinafter for simplicity there is no indexes). Since the thermal deformation is allowed only in the direction "3", the corresponding component of mechanical stress tensor X_3 is zero. Another boundary condition is the $E_3 = 0$, i.e. crystal is assumed electrically free (close-circuited), as usually supposed at thermodynamic analysis of piezoelectric and pyroelectric effects. Corresponding equations are presented below:

$$dx_n = s_{mn}^{E,T}\, dX_m + \alpha_n^E\, dT,$$
$$dM_i = d_{in}T\, dX_n. \qquad (8.20)$$

Here x_n and X_m are the strain and stress tensor components, parameters $s_{mn}^{E,T}$ is the elastic compliance, d_{in}^T is the piezoelectric module and α_n^E is the thermal expansion, indices *E* and *T* indicate that parameters assume constancy of electrical field and temperature. For crystals of $\bar{4}3m$ group at chosen boundary conditions equations (2.11) can be specified:

$$dx_1 = s_{11}^{E,T}\, dX_1 + s_{12}^{E,T}\, dX_2 + \alpha dT = 0,$$
$$dx_2 = s_{12}^{E,T}\, dX_1 + s_{22}^{E,T}\, dX_2 + \alpha dT = 0,$$

$$dx_3 = s_{31}^{E,T} dX_1 + s_{32}^{E,T} dX_2 + \alpha dT ,$$
$$dM_3 = d_{31}^{T} dX_1 + d_{32}^{T} dX_2 .$$

It is necessary to take into account that in the cubic crystals $s_{11}^{E,T} = s_{22}^{E,T}$ and $X_1 = X_2$; for artificial piezoelectric coefficient in a new installation of a crystal (and return back to broken indexes) it is possible to obtain

$$\gamma_{3'} = dM_3/dT = 2 d_{3'1'} \alpha/(s_{1'1}^{E,T} + s_{1'2}^{E,T}).$$

After conversion of incoming in formula parameters, all tensor components should be presented in the standard installation of a crystal (which is usually listed in the reference books):

$$\gamma_{111} = 2\sqrt{3}\, d_{14}\alpha/(4s_{11}^{E,T} + 8s_{12}^{E,T} + s_{44}^{E,T}). \quad (8.21)$$

For gallium arsenide this coefficient is $\gamma_{111} = 1.5$ μC·m^{-2}·K^{-1} (estimates show that in the gallium nitride this coefficient is much higher). It should be noted that similar calculation of artificial pyroelectric coefficient for quartz crystal results in the $\gamma_{100} = 2.6$ μC·m^{-2}·K^{-1} and can be observed along three polar-neutral axes, while in the well-known pyroelectric tourmaline its pyroelectric coefficient is 4 μC·m^{-2}·K^{-1} and the maximum effect is possible only along one particular polar axis. In the gallium arsenide artificial pyroelectric effect in the directions of basic axes [100], [010] and [001] is impossible. The maximum of this effect in the $A^{III}B^{V}$ crystals corresponds to four [111]-type polar-neutral axes.

Indicatory surface of $\gamma(\theta,\varphi)$ for polar-neutral cubic crystals constitutes of eight identical surfaces which start from the centre of a cube to its vertices at the angle of 109.2°, Fig. 8.4*a* It is possible to find $\gamma(\theta,\varphi)$ in any direction for crystal of gallium arsenide group: the magnitude of "pyroelectric" coefficient can be determined as a radius-vector emanating from centre of cube to the intersection with indicatory surface. Being compared with quartz, the indicative surface of gallium arsenide crystals group is more complicated, because it characterizes the artificial pyroelectric effect along four polar-neutral axes (and each has two possible directions).

With temperature increase the internal polar-sensitivity decreases in all studied piezoelectrics. It should be recalled that in the quartz this polarity vanishes at the temperature of $\alpha \rightarrow \beta$ transition , Fig. 8.2, while in the KDP crystal γ_{100} also vanishes at high-temperature phase transition. It can be assumed that in the piezoelectric crystals of gallium arsenide group, their internal polar sensitivity disappears at the melting point. In Fig. 8.4*b*, the temperature dependence of polar moments M_{111} of GaAs and GaP crystals and component M_{100} of internal polarity of quartz crystal is compared. In the molten state, any stable polar formations are impossible, but it is noteworthy that the growth of polar crystal from a melt forms

the polar bonds which lead to an increase in the volume of material and, accordingly, a lower crystal density compared to its melt density.

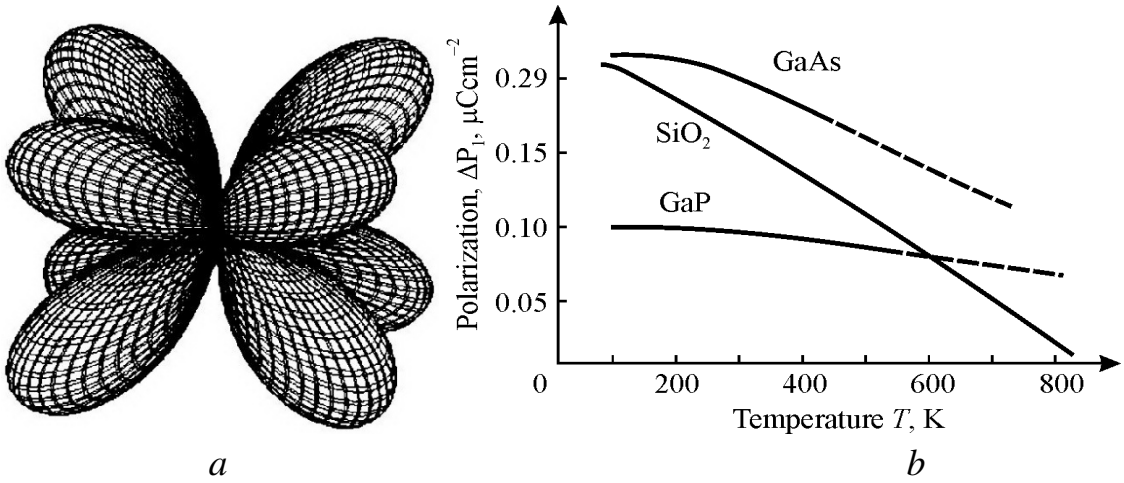

Fig. 8.4. Indicatory surface (*a*) and temperature dependencies (*b*) of component M_{111} for GaAs and GaP crystals in comparison to M_{100} of SiO_2 (α-quartz) crystal

Polar crystals are substances with mixed ionic-covalent bonds. Just this peculiarity causes low symmetry of polar crystals, and most of them belong to the non-central symmetric groups of crystals. On the contrary, purely ionic bonded crystals as well as the purely covalent bonded crystals are the non-polar ones. They belong to the centre symmetric classes of crystals. In most cases of the ionic crystals a full symmetry exists, and usually there is no special orientation in the bonding. In the same way, in the simple covalent crystals, each atom provides one unpaired electron, but formal charges of all atoms remain unchanged, so the atomic bonds have socialized electron pair. That is why, they usually are centrosymmetric ones. The primary cause of the polarity in crystals is the asymmetry in the electron density distribution along the atomic bonds. This is conditioned by the differences in the electro-negativity of atoms. Sometimes the distinction of electronegativity in different atoms might be large (on Poling' scale). Atom with higher electro-negativity strongly attracts the electron-pair bond, so his true charge becomes more negative. Atom with a lower electro-negativity acquires, respectively, the increased positive charge. Together these atoms create a polar bond.

Consequently, in the polar crystals a system of build-in polar moments exists. In the tree-dimension crystal the structure and symmetry of polar bonds might be rather complicated but its distinctive feature is the absence of central symmetry. It has an influence on many physical properties of polar crystals: on the electrical, mechanical, thermal and chemical features. Moreover, polar bonds cause essential mutual relations between these features. As a consequence of this interdependence the electromechanical, electro-thermal and other interrelations appear. For example,

in the case of mechanical influence to polar crystal an electrical response arises (piezoelectric effect). The point is that reciprocal displacement of the atoms constrained polar bonds generates electricity on the crystal surface (polarization). On the contrary, if the atomic bonds are non-polar, no electric response possible to any mechanical perturbation.

Non centre-symmetric arrangement of electrical charges in the polar crystals can be characterized by different structural motives, such as the imaginary dipole, or sextuple, or octopole. The simplest event is a dipole structural motive that corresponds to the spontaneous polarization P_s in crystal. It might be represented by the polar vector "built into the crystal structure" that is, in other words, a polar tensor of the first rank. This internal polarization results in the vectorial response to any external scalar action on the crystal: to the volumetric piezoelectric effect in the case of all-round (hydrostatic) pressure, and to the pyroelectric effect to uniform heating or cooling. Crystal possessing spontaneous polarization (i.e., with dipole-type polarity) regards to the pyroelectrics. However, many others polar crystals are not pyroelectrics, but piezoelectrics. Respectively, in the piezoelectrics, the imaginary sextuple or octopole electric moments (correspondingly, tensors of the second or the third rank) are also possess the internal polarity but it is a latent (totally compensated) polarity. Therefore, an arbitrary scalar action (hydrostatic pressure or uniform heating) can not "awake" in such a crystal any vectorial response. The only outer tensorial actions: such as mechanical stress X_{ij} (second rank tensor) or temperature gradient (vector grad T) are capable to provoke the hidden polarity to a vector response (that is, to induce voltage or electric current).

Electrical, elastic and thermal properties of polar crystals are interrelated. Moreover, even in the case of only electric effects investigation (for instance, polarization) its electrical parameters depend on the mechanical and thermal boundary conditions. For instance, the permittivity of mechanically free crystal (ε^X) differs from the permittivity of clamped crystal (ε^x), at that $\varepsilon^X > \varepsilon^x$. Likewise if polar crystal is exposed to alternating electric field in the adiabatic conditions (when there is no time to exchange energy between crystal and environment) the permittivity ε^S is less than the ε^T obtained under isothermal conditions.

Mechanical properties of piezoelectric such as its elastic stiffness c (or its elastic compliance s) is dependent on the electrical state of the crystal (close-circuited, $E = 0$, or open-circuited, $D = 0$), and sometimes the c^E differs from the c^D in several times. Similarly, adiabatic elastic parameters c^S or s^S differ from the isothermal c^T or s^T. In the same way, when seemingly "pure thermal" experiment is provided, for example, the measuring of specific heat capacity C, one can see a

significant differences between C^E and C^D (that is to say, when the electrodes deposited on the test sample are shorten ($E = 0$) or opened ($D = 0$). Similarly, different specific heat capacity is observed for mechanically free ($X = 0$) and mechanically clamped ($x = 0$) crystals: $C^X \neq C^x$.

Pure ionic, as well as pure covalent crystals are defined by the centre-symmetric structure and do not show piezoelectric effect. Therefore, non centre-symmetric crystalline structure is the only manifestation of a mixed ionic-covalent bonding of its atoms. This bonding is exactly directional, and therefore it leads to the different manifestations of the asymmetry and complexity of polar crystal structure. Since polar crystal formation from charged ions (in initially liquid or vapour state of material) a polar structure of non centre symmetric crystals is spontaneously formed. In this book it is simplistically described by a combination of imaginary dipoles, which leads to the electric moments, describable by the tensors of different ranks.

8.7 Summary Chapter 8

Conclusions

A conception is discussed that any piezoelectric possesses an intra-crystalline polar moment, even though this crystal is not belongs to pyroelectric symmetry. In line with this assumption, an internal polarity of piezoelectric crystals is described by the different types of high-rank multiple moments. Octopole–sextuple–dipole moments correspond to three–two–one dimension arrangement of the intra-crystalline polarity. Dipole (1D) polarity is the pyroelectric spontaneous polarization that is a vector (first rank tensor). The 2D sextuple moment is arranged in a plane non-center symmetric configuration of three dipoles, and it is described by the second rank polar tensor. The octopole moment is the non-center symmetric spatial (3D) conformation of four dipoles that is described by the third rank tensor.

Temperature dependence of intra-crystalline polar moment components show a critical law $P \sim (\theta - T)^n$ and vanishes at the phase transition temperature θ. The critical parameter equals to $n = 1$ if all components of intrinsic polarity are flatness arranged (two-dimensional case, 2D). For the spatial (3D) arrangement of the latent polarity components this exponent is $n = 2$. These result differ essentially from 1D ferroelectric spontaneous polarization that shows $P_S(T)$ the critical law with $n = 0.5$.

For technical application, it means that under the anisotropy of boundary conditions any high-gap $A^{III}B^{V}$ semiconductor-piezoelectric shows a behaviour of

pyroelectric crystal. It is important that such a crystal might be used as far infrared sensor or as a volume-piezoelectric effect sensor integrated with amplifier in one $A^{III}B^{V}$ crystal. On the other hand, any device based on $A^{III}B^{V}$ semiconductor that has erroneous orientations of a crystal can generate polarization noises due to vibrations or thermal fluctuations.

References

[1] Yu.M. Poplavko, S.O. Voronov, Yu.I. Yakymenko. Selected problems of materials science. Науковий посібник (in English), 2021, 410 pages; Ukraine, Kiev, NTUU "Igor Sikorsky KPI", Затверджено Методичною радою НТУУ КПІ (протокол №12 від 14.05 2021 р.).

[2] Yu. M. Poplavko. Electronic materials. Principles and applied science. 2019, 683 pages. Edited by ELSEVIER, USA.

[3] Yu.M. Poplavko, Yu.I. Yakymenko. Functional dielectrics for electronics. Fundamentals of conversion properties. 2020, 294 pages. Edited by ELSEVIER, USA.

[4] Yu. M. Poplavko. Dielectric spectroscopy of electronic materials. Applied physics of dielectrics, 345 pages, 2021, Edited by ELSEVIER, USA.

[5] Yu. Poplavko, "Spontaneous Polarization as Polar-Sensitive Structure Manifestation," 2021 IEEE International Symposium on Applications of Ferroelectrics (ISAF), 2021, pp. 1-4, DOI: 10.1109/ISAF51943.2021.9477391.

[6] Yu. Poplavko, "Polar Bonds Self-Ordering and Negative Thermal Expansion," 2021 IEEE International Symposium on Applications of Ferroelectrics (ISAF), 2021, pp. 1-4, DOI: 10.1109/ISAF51943.2021.9477345.

[7] Yu. Poplavko, Yu.V. Didenko. "Spontaneous polarization or manifestation of peculiar internal structure?" The Third International Conference on Information-Telecommunication Technologies and Radio Electronics (UkrMiCo'2018): Proc. of Int. Sci. Conf. (September 10–14, 2018, Odessa, Ukraine). – Kyiv: Igor Sikorsky Kyiv Polytechnic Institute, 2018. pp. 1–6. DOI: 10.1109/UkrMiCo43733.2018.9047562.

Questions

1. What thermodynamic parameters are convenient to use when describing the polarization of dielectrics ?
2. What are the main result of thermodynamic description of piezoelectric effect?
3. What are the main result of thermodynamic description of pyroelectric effect?
4. How is it different of artificial pyroelectric effect from usual pyroelectric effect?
5. How is it different of artificial pyroelectric effect from piezoelectric effect?
6. What technical applications can artificial pyroelectric effect have in semiconductors such as gallium arsenide?

GENERAL REFERENCES

References Chapter 2

[1] L.H. Van Vlack, Materials science for engineers, Addison-Wesley Publishing Co., 1975.
[2] C. Kittel, Introduction to solid state physics, fifth ed., John Willey, New York, 1976.
[3] N.W. Ashcroft, N.D. Mermin, Solid state physics, Holt and Winston, New York, 1976.
[4] Y.M. Poplavko, Polar crystals: physical nature and new effects, Lambert Academic Publishing, Saarbrucken, 2014.
[5] S.A. Voronov, Y.I, Yakymenko, L.P. Pereverzeva, Y.M. Poplavko, Materials science physics, Kiev Polytechnic Institute Ed., 2004.
[6] R. Waser (Ed.), Nanoelectronics and information technology: Advanced electronic materials and novel devices, Weinheim: Wiley-VCH, 2005.
[7] H.S. Nalva (Ed.), Nanostructured materials and nanotechnology, Academic Press, New York, 2002.

References Chapter 3

[1] Yu. M. Poplavko, *Electronic materials. Principles and applied science,* ELSEVIAR, 2019.
[2] R. E. Newnham, *Properties of materials: anisotropy, symmetry, structure*, Oxford University press, Oxford, 2004.
[3] L. Levinson, H.R. Philip, *Zinc oxide varistors*, American Ceramic Society Bulletin 65(4), 639. 1986.
[4] A. P. Ramirez, *Colossal magnetoresistance*. Journal of Phys: Condensed matter. 9 (39): 8171. 1997.
[5] Yoon-Bong Hahn, *Zinc oxide nanostructures and their applications*, Korean J. Chem. Eng., 28(9), 1797, 2011.
[6] A. Von Hippel, Dielectrics and waves, Jon Wiley, New York. 1954.
[7] C. Kittel. Introduction to solid state physics. John Willey & Sons. New York. 1975.
[8] A.K. Jonscher, Dielectric relaxation in solids. Chelsea Dielectrics Press, London, 1983.
[9] M. J. Weber, Handbook of Optical Materials. Boca Raton: CRC Press, 2003.

References Chapter 4

[1] C. Kittel, *Introduction to solid state physics*, 5-th ed. New York: John Willey, 1976.
[2] M.E. Lines and A.M. Glass, *Principles and Applications of Ferroelectrics and Related Materials,* Clarendon Press, Oxford, 2009.
[3] Yu. M. Poplavko, *Electronic mfterials. Princeples and applied science*, ELSEVIAR, 2019.
[4] R.D. King-Smits, D. Vanderbilt, *Theory of polarization of crystalline solids,* Phys. Rev. B 47, 1651, 1993.
[5] R. Resta, *Manifestation of Berry phase in molecules and condensed matter*,

J. Phys. Condensed Matter, 12, R107, 2000.
[6] W.O. Cady, *Piezoelectricity*, Amazon com, New York, 1946.
[7] I.S. Jeludev, *Basics of ferroelectricity*, (in Russian) Atomizdat, Moscow, 1973.
[8] Yu.M. Poplavko. *Dielectric spectroscopy of electronic materials. Applied physics of dielectrics*. ELSEVIAR, 2021.
[9] Fansping Zhuo, Qiang Li, Huimin Qiao et. al. *Field-induced phase transitions and enhanced double negative electrocaloric effects in (Pb,La)(Zr,Sn,Ti)O_3 antiferroelectric single crystal.* Appl. Phys. Lett., 2018, 112, 133901.
[10] Yu.M. Poplavko, L.P. Pereverzeva, I.P. Raevskiy, *Physics of active dielectrics* (in Russian), South Federal University of Russia, Postov-na-Donu, 2009.
[11] L.P. Pereverzeva, I.Z. Pogosskaya, Yu.M. Poplavko, I.S. Res, *Dielectric anomalies in crystals KH_2PO_4, KD_2PO_4, RbH_2P0_4 at high temperatures*, Phys. Tverdogo Tela, 1973, Vol.15, N° 4, p. 1250.
[12] Yu.M. Poplavko, L.P. Pereverzeva, N.I. Cho, Y.S. You. Feasibility of microelectronic quarz temperature ans pressure sensors. Jpn. J. Appl. Phys., Vo7.37,1998, p.4041.
[13] Yu.M. Poplavko, L.P. Pereverzeva, *Polar properties of non-isotropically clamped piezoelectrics* (in Russian) Ukrainskii Physichaskii Jurnal, 1993, Vol 38 p. 1383.
[14] D.G. Schlom, L.-Q. Chen, Ch. Eom, K.M. Rabe, S.K. Streifer, and J.M. Triscone, *Strain tuning of ferroelectric thin films*, Annu. Rev. Mater. Res., vol. 37, pp. 589-626, 2007.

References Chapter 5

[1] M. T. Sebastian, *Dielectric materials for wireless communication*, ELSEVIER, 2008.
[2] M.T. Sebastian, R. Ubic, H. Jantunen, *Microwave materials and applications*, Wiley, 2017
[3] Yu.M. Poplavko, *Physics of dielectrics* (in Russian), Ed. Vischa shoola, Ukraine, Kiev. 1980.
[4]Yu. M. Poplavko, *Nature of dielectrics thermal stability in microwave range* (*in Russian*). Izvestia Akad. Nauk, Seria Physicheskay, 1996, 60, 10, pp. 167–172.
[5] Yu. M. Poplavko. *Dielectric spectroscopy of electronic materials*. *Applied physics of dielectrics*. ELSEVIAR, 2021.
[6] Yu. M. Poplavko, Yu. V. Didenko, *Polarization mechanisms in thermal stable microwave BLT ceramics*, Electronics and Electronics and Communications, 2015, 20, 1, pp. 18–22.
[7] Yu. M. Poplavko, *Nature of dielectrics thermal stability in microwave range* (*in Russian*). Izvestia Akad. Nauk, Seria Physicheskay, 1996, 60, 10, pp. 167–172.
[8] Yu.M. Poplavko, V.A. Kazmirenko. *Ferroelectric thin film microwave examination*. Ferroelectrics. 2003. Vol. 286. pp. 353–356.
[9] Yu.M. Poplavko, V.A. Kazmirenko, Yu. V. Prokopenko. *Measurement of bulk and film ferroelectric materials properties at microwaves* Microwaves, Radar and Wireless Communications, 2002. MIKON-2002. 14th Intern. Conference, Vol. 2, 2002, pp. 397–400.
[10] Yu.M. Poplavko,V.A. Kazmirernko, M. Kim, S. Baik, *Electrode-less technique of ferroelectric film study at microwaves,* 10th Europ. Meet. on Ferroelectricity. 2003, Cambridge UK, p. 178.

[11] Yu.M. Poplavko,V.A. Kazmirernko, M. Kim, S. Baik, *Contemporary waveguide technique of ferroelectric materials study by vector network analyzer*. Intern. Microwave Symposium, June 13, 2003, Philadelphia, ARF-61-14, P. 437–440.

[12] Yu.M. Poplavko, B. Kim, V. Kazmirenko, Y. Prokopenko, Non-resonant electrode less method for measurement the microwave complex permittivity of ferroelectric films, Measurement Science and Technology, Vol. 16, 2005, pp. 1792-1797,

[13] E. Furman, M, Lanagan, I. Golubeva, Yu. Poplavko. Piezo-controlled microwave frequency agile dielectric devices, IEEE International Frequency Control Symposium and Exposition, Montréal, Canada, Aug. 2004, P.266 – 271.

[14] Yu.V. Prokopenko, Yu.M. Poplavko, N. Ruda, Dielectric-Air structure as component of electromechanically controlled microwave devices, Int. Conf. Mathematical Methods in Electromagnetic Theory, 2010, Kiev, pp. 71-75.

References Chapter 6

[1] F. Kremer and A. Schönhals, *Broadband dielectric spectroscopy*. Springer, 2003.

ISBN 978-3-642-62809-2.

[2] M. T. Sebastian, *Dielectric materials for wireless communication*. Amsterdam: Elsevier, 2008. ISBN: 978-0-08-045330-9.

[3] J. Kruželák, A. Kvasničáková, K. Hložeková, and I. Hudec, *Progress in polymers and polymer composites used as efficient materials for EMI shielding*, Nanoscale Advances, vol. 3, no. 1, pp. 123–172, 2021. DOI: 10.1039/d0na00760a

[4] Y. Poplavko, *Electronic materials. Prinples and applied science.* ELSEVIAR, 2019.

ISBN 978-0-12-815789-0.

[5] M. J. Weber, *Handbook of Optical Materials*. Boca Raton: CRC Press, 2003.

ISBN 978-0-84933512-9.

[6] M. T. Sebastian, R. Ubic, and H. Jantunen, *Microwave materials and applications.* Hoboken, NJ: Wiley, 2017. ISBN 978-1-119-20852-5.

References Chapter 7

[1] C. Kittel, Introduction to solid state physics, 5th ed. New York: John Willey, 1976.

[2] M.E. Lines and A.M. Glass, Principles and application of ferroelectrics and related materials, Clareton Press, Oxford, 1977.

[3] Y.M. Poplavko, Electronic materials. Principles and applied science. ELSEVIER, 2019.

[4] E.N. Dimarova and Yu.M. Poplavko, "Electrical bias field influence on ferroelectrics thermal conductivity," Izvestia AN SSSR, Serial Phys. 31 (11), pp. 1842, 1967 (in Russian).

[5] V.F. Zavorotnii, Yu.M. Poplavko, "Plane temperature waves method for thermal diffusion study," Pribori e Technika Experimenta, Vol. 5, p. 189, 1984 (in Russian).

[6] W.O. Cady, Piezoelectricity, Amazon com, New York, 1946.

[7] I.S. Jeludev, Basics of ferroelectricity, Atomizdat, Moscow, 1973.

References Chapter 8

[1] Yu.M. Poplavko, S.O. Voronov, Yu.I. Yakymenko. Selected problems of materials science. Науковий посібник (in English), 2021, 410 pages; Ukraine, Kiev, NTUU "Igor Sikorsky KPI", Затверджено Методичною радою НТУУ КПІ (протокол №12 від 14.05 2021 р.).

[2]Yu. M. Poplavko. Electronic materials. Principles and applied science. 2019, 683 pages. Edited by ELSEVIER, USA.

[3] Yu.M. Poplavko, Yu.I. Yakymenko. Functional dielectrics for electronics. Fundamentals of conversion properties. 2020, 294 pages. Edited by ELSEVIER, USA.

[4] Yu. M. Poplavko. Dielectric spectroscopy of electronic materials. Applied physics of dielectrics, 345 pages, 2021, Edited by ELSEVIER, USA.

[5] Yu. Poplavko, "Spontaneous Polarization as Polar-Sensitive Structure Manifestation," 2021 IEEE International Symposium on Applications of Ferroelectrics (ISAF), 2021, pp. 1-4, DOI: 10.1109/ISAF51943.2021.9477391.

[6] Yu. Poplavko, "Polar Bonds Self-Ordering and Negative Thermal Expansion," 2021 IEEE International Symposium on Applications of Ferroelectrics (ISAF), 2021, pp. 1-4, DOI: 10.1109/ISAF51943.2021.9477345.

[7] Yu. Poplavko, Yu.V. Didenko. "Spontaneous polarization or manifestation of peculiar internal structure?" The Third International Conference on Information-Telecommunication Technologies and Radio Electronics (UkrMiCo'2018): Proc. of Int. Sci. Conf. (September 10–14, 2018, Odessa, Ukraine). – Kyiv: Igor Sikorsky Kyiv Polytechnic Institute, 2018. pp. 1–6. DOI: 10.1109/UkrMiCo43733.2018.9047562.